DEPERTMENT OF ELECTRONIC AND ELECTRICAL ENGINEERING

FACULTY OF ENGINEERING

LOUGHBOROUGH UNIVERSITY

DEVELOPMENT AND EVALUATION OF VENOUS OXIMETRY

BY

ANGELOS S. ECHIADIS

A Doctoral Thesis

Submitted in partial fulfilment of the requirements for the award of

Doctor of Philosophy of Loughborough University

September 2007

Supervisor: Dr Sijung Hu

Co-supervisor: Dr Vassilios Chouliaras

Department of Electronic and Electrical Engineering

In memory of Peter Richard Smith,

Professor of Photonics Engineering

ABSTRACT

Photoplethysmography, a technique to measure by optical means volume changes, has been known and applied for many years. One of its most popular applications is pulse oximetry, a non-invasive method to measure oxygen content in arterial blood. It is based on the principle of arterial blood volume changes due to heart contractions, known as systoles. Systolic pulsations appear on the arterial vascular system, while blood flow in veins does not normally present pulsations, especially at remote parts of the peripheral vascular system, such as the fingers. Therefore, pulse oximetry is only applicable to arteries as their pulsations allow for separation of the pulsatile components from the rest of the absorbing components. A novel non-invasive technique permits the measurement of venous oxygen saturation by introducing a series of pulsations in the veins thus allowing the separation of venous signal components for calculation of venous oxygen saturation.

This thesis presents a theoretical model describing the mechanical coupling of arteries and veins and its effects in the accuracy of oxygen saturation measurement. Hardware and software design of the prototypes used both in the lab and in the clinical setting is also presented in detail. A clinical feasibility study was carried out, where peripheral venous oxygen measured by Venox was compared to central venous oxygen saturation during cardio-pulmonary bypass. A comparative calibration of Venox versus a commercial pulse oximeter was performed by using a set of light absorbers, a finger phantom and commercially available pulse oximetry probes, in order to investigate the accuracy of the prototype. A laboratory trial using healthy volunteers was performed, in order to investigate venous de-saturation effects and how accurately they can be detected by the venous oximetry method. Other laboratory experiments evaluated and validated the theoretical model describing the arterio-venous coupling.

It is concluded that the venous oximetry method and technology are worthy of further research.

ACKNOWLEDGEMENTS

It is a pleasure to acknowledge the major contribution from my supervisors Professor Peter R. Smith and Dr Sijung Hu. I am grateful for their guidance and support throughout the duration of my research. I would also like to express my deep appreciation to my co-supervisor Dr Vassilios Chouliaras for his invaluable guidance and support right through the course of my work. I would also like to thank all the other members of the Optical Engineering Group for their companionship and numerous scientific discussions. I am very thankful to the collaborating team led by Prof Tomasz Spyt, Cardiothoracic Clinic, Glenfield Hospital, Leicester for their precious efforts, advice and support throughout this project.

I am very thankful to the technicians and other staff from Loughborough University for their advice and assistance in realisation of this project. I would also like to acknowledge the Department of Electronic and Electrical Engineering for the full support of my studentship and BTG plc who have provided financial backing for this project.

Finally, I wish to express my deep appreciation to my wife Niki and to my parents for their continuous support and patience throughout the duration of my research.

CONTENTS

1 INTRODUCTION

Non-invasive measurement of oxygen saturation can be performed on arterial blood only with the current technology. The principal factor limiting the non-invasive measurement of venous oxygen saturation is the lack of pulsations in the peripheral venous flow, although it has been reported that venous pulsations can appear at peripheral sites[1,2]. Pulse oximetry employs the principle of photoplethysmography (PPG) to distinguish the light absorption due to arterial blood by measuring the change of light intensity whenever an arterial pulse is detected in the measured area. The arterial pulsatility helps distinguish the light absorption due to arterial blood by measuring the minimum and maximum light intensity between pulses. Given that other biological structures do not change their light absorption characteristics over this short period of time, the light intensity changes are attributed purely to arterial blood volume changes.

1.1 BACKGROUND CONTEXT

The non-invasive measurement of arterial oxygen saturation is very important and is currently standard procedure in a variety of clinical and ambulatory environments, with the most important application being in anaesthesia, as it provides information about the adequacy of oxygen supply to the tissues. Although the value of arterial oxygen saturation must be interpreted with great attention and in conjunction with other physiological parameters, it is a widely used, rapid assessment tool of oxygen supply to the tissues.

The use of pulse oximeters for the monitoring of arterial oxygen saturation provides information on the oxygen supply but it does not offer information on the demand for oxygen which is consumed in the human body. The poor supply and demand balance is only evident in a pulse oximeter once the cardiovascular system presents serious deterioration because of low cardiac output or in severe pathophysiological conditions which may affect the carriage or binding of oxygen. A more complete image of the oxygen supply and demand would be provided if both arterial and venous oxygen saturations were known, in which case clinicians would have a more powerful tool to assess the oxygen supply and utilisation. For example, high arterial oxygen saturation indicates that there is adequate oxygen in arterial blood to be delivered to tissues and organs, but what is really important is how much oxygen returns to the lungs, that is the venous oxygen saturation. When the venous oxygen saturation drops below certain values which depends on the duration and intensity of physical activities, then oxygen reserve mechanisms are activated. This oxygen reserve may provide compensation for short periods of time, after which the value of venous oxygen saturation can drop to critical levels, often followed by lactic acidosis in the absence of oxygen in the metabolic process.

A novel oxygen assessment technique, capable of measuring arterial and venous oxygen saturation non-invasively, is presented in this thesis. The method allows for the detection and correction of arterial and venous mechanical coupling which may affect the accuracy of pulse oximetry readings under certain conditions. The method

allows not only the real-time monitoring of oxygen consumption in tissues but it also provides a valuable tool for the correction of errors in conventional pulse oximetry, caused by arterio-venous mechanical coupling.

1.2 AIMS AND OBJECTIVES

The aims of this thesis are:

1) To provide an understanding of oxygen supply in the human body, focusing on the cardiovascular system, the oxygen transportation system, and the role of human physiology in the oxygen supply and demand.
2) To introduce the fundamental principles of the Beer-Lambert law as applied to tissue spectroscopy and to further expand it into a novel opto-physiological model.
3) To present the various stages of design and development of the venous oximeter with a particular focus on the acquisition systems, the venous pulse modulation control system and the importance of modulation depth and frequency.
4) To investigate and validate the performance and accuracy of the venous oximeter in a combination of clinical and laboratory environments and to explore the clinical significance of venous oxygen saturation in a variety of pathophysiological conditions.
5) To identify and discuss the potential of venous oximetry in other applications as well as to suggest further work which can be carried out to extend the applicability of the venous oximeter to other sites of the human body.

From these aims, the following objectives become apparent:

1) To describe the current invasive and non-invasive oximetry techniques, what are their advantages and disadvantages, and what is the importance of venous oxygen saturation as a physiological parameter (aim 1).
2) To describe the role of oxygen in the human body and how it is transported from the heart to the tissues and vice-versa, to provide an insight into the human cardiovascular system and to elucidate the role of human physiology in oxygen utilisation and the importance of venous oxygen saturation measurement (aim 1).
3) To provide an overview of the invasive venous oxygen saturation measurement methods in terms of their limitations and underlying risks for

the patient and to introduce the application the Beer-Lambert law, in conjunction with spectroscopy and photoplethysmography, in the non-invasive measurement of arterial and venous oxygen saturation (aim 1).

4) Starting from first principles in fundamentals of light propagation, to develop a theoretical model in order to describe the arterial and venous PPG signals under certain physiological and anatomical conditions. The model will provide the means of defining the optimal operating conditions of the artificial venous modulation system as well as the possibility to introduce a method of correcting arterial oxygen saturation obtained from pulse oximeters (aim 2).
5) The development of three different generations of prototypes will outline the course of functionality improvement, by introducing a digitally controlled pulse modulation board and two generations of photoplethysmographic systems, in order to facilitate the automatic and continuous operation of the venous oximeter, shifting from a manually controlled to an automatic pulse modulation system (aim 3).
6) To validate the arterio-venous coupling model through experimental protocols specifically targeting the variation of the mechanical coupling between arteries and veins (aim 4).
7) A system calibration will be carried out in order to define the performance in terms of measuring the absorbance of haemoglobin and how closely it compares with a commercial pulse oximeter. A finger phantom will be employed in the investigation of the technique's accuracy, in conjunction with a series of light absorbers simulating the light absorbance of blood (aim 4).
8) A venous oxygen de-saturation study will be performed in order to confirm that the device is able to detect the gradual decrease of venous oxygen saturation. The venous oximeter will be compared to a blood gas analyser, after obtaining blood samples from the participants (aim 4).
9) A feasibility study in the clinical setting will investigate the performance and functionality of the device in real-life conditions and from different perspectives. The environmental perspective will test the utility of the device

in its operational surroundings (i.e. the operating theatre); the feasibility perspective will investigate the use of the device with a variety of patients who have a range of physiological conditions; the performance perspective will cross-validate the results taken from the device with the accepted gold standard physiological measurement (aim 4).

10) The mathematical model describing the effects of arterio-venous mechanical coupling will be validated through two different experimental protocols. The first experiment will target the investigation of arterial oxygen saturation variation following venous pressure augmentation, thus providing a way to detect and correct the error when the arterial-to-venous coupling is significant. The second experiment will demonstrate that the effects of mechanical artefact originating from the artificial venous modulation can lead to erroneous values of venous oxygen saturation – although these errors can be corrected (aim 4).

11) Design ideas for new disposable and re-usable probes will briefly be presented, extending the application of venous oximetry to other sites of the body which require the use of a surface-mount probe. In addition, future application ideas are presented, including the potential for arterial calcification assessment by employing the arterio-venous coupling model in a suitable protocol (aim 5).

12) Suggestions for future work will show the path to the next stage of evaluation and optimisation of the venous oximetry system (aim 5).

1.3 PLAN OF THESIS

Chapter 2 starts by introducing the basic principles of oxygen supply to human tissues and organs, presenting briefly the cardiovascular system, the mechanisms of oxygen delivery, as well as the oxygen supply and demand relationship and the role of physiological parameters. Current invasive and non-invasive techniques are also discussed including basic operating principles and limitations of the current technology. Photoplethysmography and pulse oximetry are presented including the operating principles and the techniques used for the calculation of arterial oxygen saturation.

In chapter 3 a novel model is developed to describe the mechanical coupling of arteries and veins and how it can affect the measurement of arterial and venous oxygen saturation using the novel non-invasive venous oxygen saturation method. Whilst physical interpretation of the origin of the arterio-venous coupling is explored theoretically, the effects caused to the measured oxygen saturation values are investigated experimentally. Through the experimental analysis it is confirmed that the mechanical coupling does affect the both arterial and venous oxygen saturation values, hence it is concluded that arterial PPG signals can have venous components that contribute to the calculation of arterial oxygen saturation.

Chapter 4 discusses the engineering design and implementation of a next generation oximeter that measures both arterial and venous oxygen saturations. Starting from a manually-operated prototype device, the latest version of the prototype was developed under a different philosophy than conventionally designed experimental equipment, taking into account the possibility of delivering prototype devices to multiple locations for a fast, large-scale trial to further evaluate the method and if necessary, advance the technology even further. The relatively low-cost, easy to operate portable embedded prototype device does not require any external connections making it a self-contained continuous arterial and venous oxygen saturation monitor.

An experimental investigation into the validity of hypotheses upon which the model was built is presented in chapter 5. The arterial-to-venous effects are investigated separately from the venous-to-arterial effects since they required different experimental protocols. Also presented in this chapter is the comparative calibration of the device against a commercial pulse oximeter when using a finger phantom with a series of light-absorbing solutions. Furthermore, the method was tested on 13 healthy subjects in a venous de-saturation study in order to establish whether the device could detect the gradual decrease of venous oxygen saturation when the arterial blood supply to the arm was stopped. Finally, the results from a clinical feasibility and evaluation study are presented in the last section of the chapter, where the device was employed in 23 patients undergoing a heart operation. Results from this study have previously been published.

A S Echiadis, V P Crabtree, J Bence, L Hadjinikolaou, C Alexiou, T J Spyt and S Hu, 'Non-invasive measurement of peripheral venous oxygen saturation using a new venous oximetry method: evaluation during bypass in heart surgery', in IoP Physiological Measurement, (2007) Vol 28(8), pp.897-911.

V P Crabtree, A S Echiadis, P R Smith, M Boehm, M Oc, J Bence, D Machin, J Swanavelder, C Alexiou, G Doukas, W Pidgeon, L Hadjinikolaou and T J Spyt, 'Prospective Venox Feasibility Study', In: Proceedings of the 27th Annual International Conference of the IEEE Engineering in Medicine and Biology Society, (Shanghai, 2005), pp.1968-1971, ISBN 0-7803-8741-4.

Chapter 6 briefly reiterates the major achievements of the work and provides concluding remarks. Recommendations are also made for further studies in this area.

The references are collected in a common section following the main body of the report. Appendices are included that give technical details about the prototype device, analytical results from the clinical evaluation and copies of the ethics approvals obtained for the studies.

Other publications relating to work carried out in photoplethysmography, pulse oximetry and the development of the prototype device are listed below:

S Xin, S Hu, V P Crabtree, J Zheng, V Azorin-Peris, A Echiadis, P R Smith, 'Investigation of blood pulse PPG signal regulation on toe effect of body posture and lower limb height', in Journal of Zhejiang University – Science A, (2007) Vol 8(6), pp.916-920.

A S Echiadis, V P Crabtree, P R Smith, 'VENOX - a non-invasive method for venous pulse oximetry from the upper limb', Proceedings of the 4th IEEE EMBSS UKRI (Reading, 2005), pp.39-40, ISBN 0-9543-1573-1.

A S Echiadis, V P Crabtree, P R Smith, 'VENOX Technology Implementation', 1st ESC Division Conference (Loughborough, 2005), pp.31-34.

P Y S Cheang, A S Echiadis, P Gibbon, P R Smith, 'Methodology for evaluation of an oximetry foot probe', In: Proceedings of the 3rd IEEE EMBSS UKRI (Southampton, 2004), pp.19-20.

2 PHYSIOLOGY AND OXIMETRY

Oxygen is a vital element for the survival of living organisms and its monitoring is one of the most valuable tools in the hands of clinicians. Monitoring the levels of oxygenation can have a number of different meanings, such as arterial oxygen saturation and venous oxygen saturation or total oxygen supply and demand, all related to each other but each with a particular clinical meaning. In order to make an overall assessment of the oxygenation, a combination of measurements must be performed before a clinician can produce an overall clinical image of a patient. Two of the major parameters in the assessment of oxygenation are arterial and venous oxygen saturations. Arterial saturation can be measured either invasively or non-invasively but current venous saturation measurement techniques are invasive. The introduction of a non-invasive method for the measurement of venous oxygen saturation will constitute an important addition to the existing clinical tools for the continuous assessment of oxygenation.

2.1 OXYGEN SUPPLY IN THE HUMAN BODY

Human living tissues and organs require oxygen (O_2) which is delivered via a transportation system, the cardiovascular circulatory system. The circulatory system serves to transport and distribute essential substances to the tissues and to remove metabolic by-products. The circulatory system also serves in homeostatic mechanisms such as regulation of body temperature and adjustments of oxygen and nutrient supply in different physiologic states. Oxygen delivery to the tissues is achieved with the aid of haemoglobin molecules, contained in the red blood cells, or erythrocytes. In the lungs, oxygen from the inhaled air attaches to haemoglobin molecules and is transported to the cells for aerobic respiration. Carbon dioxide (CO_2) produced by cell respiration is carried by the blood to the lungs for elimination in the exhaled air. The oxygen supply and utilisation depends on a number of parameters which are briefly presented within this section.

2.1.1 The Human Cardiovascular System

The cardiovascular system consists of a pump, a series of distributing and collecting tubes and an extensive system of thin vessels that permit rapid exchanges between the tissues and the vascular channels. The pump of the system is the heart which consists of two pumps in series: the right ventricle to propel de-oxygenated blood through the lungs for exchange of CO_2 and O_2, and the left ventricle to propel oxygenated blood to the human body. Unidirectional flow through the heart is achieved through flap valves which open and close accordingly. Although the blood supply from the heart (cardiac output) is intermittent, continuous flow is achieved by expansion of the aorta and its branches during ventricular contraction (systole) and subsequent elastic recoil of the walls of large arteries that move the blood forward during ventricular relaxation (systole). Blood moves through the aorta and its arterial branches, which become narrower and their walls become thinner and change histologically toward the periphery. The predominantly elastic structure of large arteries such as the aorta becomes more muscular until the muscular layer predominates at the arterioles.

In the large arteries, frictional resistance is relatively small and blood pressure values are relatively close to the aortic blood pressure. However, the resistance increases in smaller arteries and becomes maximal in the arterioles; hence the pressure drop is significant and is greatest in the small arteries and in the arterioles. Tissue blood flow is regulated by the adjustment in the degree of contraction of the circular muscle and aid in the control of arterial blood flow. In addition to a sharp reduction in blood pressure across the arterioles, there is also a change from pulsatile to steady flow as pressure continues to decline from the arterial to the venous ends of the capillaries, where the oxygen extraction happens. Therefore the arterial pulsatile flow caused by the cardiac ejection, is damped at the capillaries by the combination of distensibility of the large arteries and frictional resistance in the arterioles.

From each arteriole, many capillaries arise so that the total cross-sectional area of the capillary bed is very large, despite the fact that the cross-sectional area of each capillary is less than that of each arteriole. As a result blood flow becomes very slow and the ideal conditions in the capillaries permit the effective exchange of diffusible substances between tissues and blood. On its return to the heart from the capillaries, blood passes through venules and then through veins of increasing size with a progressive decrease in pressure until it reaches the right atrium[3].

2.1.2 The Oxygen Transportation Mechanism

Blood consists of red blood cells, white blood cells and platelets suspended in a complex solution (plasma) of various salts, proteins, carbohydrates, lipids and gases. Haemoglobin is the main protein in the erythrocytes and consists of haem, an iron-containing tetrapyrrole. Haem is linked to globin, a protein composed of four polypeptide chains. The iron moiety of haemoglobin binds loosely and reversibly to O_2 to form oxyhaemoglobin.

In the centre of each haem is one atom of iron, which can combine with one molecule of O_2. Thus each haemoglobin molecule can combine with four molecules of O_2. The loading reaction occurs as deoxy-haemoglobin (Hb) and O_2 combine to

form oxy-haemoglobin (HbO_2), which takes place in the lungs. The unloading reaction occurs as oxy-haemoglobin dissociates to yield deoxy-haemoglobin and free O_2, which happens in the systemic capillaries. The reversible reaction of haemoglobin and O_2 is shown in equation 2.1:

$$Hb + O_2 \underset{\text{tissues}}{\overset{\text{lungs}}{\rightleftharpoons}} HbO_2 \qquad [2.1]$$

The extent that the reaction will go in each direction depends on the partial pressure of O_2 in the environment (P_{O_2}) and the affinity between haemoglobin and O_2. High P_{O_2} in the pulmonary capillaries drives the equation 2.1 to the right in order to combine O_2 with Hb, while low P_{O_2} drives equation 2.1 to the left to promote unloading of O_2 in the tissue capillaries. The affinity between haemoglobin and O_2 also influences the reaction and depends on pH, temperature and 2,3-DPG (diphosphoglycerate). The affinity is decreased when the pH is lowered and increased when the pH is raised, called the Bohr Effect. The net effect is that the tissues receive more O_2 when the pH is lowered, which can happen when CO_2 increases (through the formation carbonic acid). Therefore the Bohr Effect helps to provide more O_2 to the tissues when their CO_2 output (due to high metabolism) is increased. The temperature also affects the affinity by decreasing it when the temperature is elevated. Therefore, the net effect at high temperatures (for example in warmed muscles during exercise) is more O_2 being unloaded to the tissues[4].

2.1.3 The Role of Physiological Parameters in Oxygen Supply and Demand

The regulation of blood flow throughout the body is an extremely complex system which requires substantial clinical knowledge and its complete analysis is not in the scope of this thesis. The clinical investigation which was carried out in this work included the study of the effects of temperature, blood flow and oxygen consumption, parameters which are being controlled either directly or indirectly during cardiopulmonary bypass (CPB) in heart surgery. In a typical CPB operation, the blood temperature is reduced in order to reduce the rate of metabolism in tissues, hence protect them from damage[5]. The blood flow is directly proportional

to the oxygen delivery hence a high cardiac output will result in an elevated venous oxygen saturation value. The difference between SaO_2 and SvO_2 (ΔO_2) is attributed to tissue oxygen consumption, which is a function of cardiac output (CO) (the volume of blood pumped by the heart per minute), blood haemoglobin (Hb) concentration and oxygen consumption (VO_2).

The total oxygen consumption depends on a number of physiological and pathological factors. Namely, a physiological factor is the intensity level of exercising muscles and their ability to utilise supplied oxygen, while pathological factors may include dysfunctional haemoglobin, hypothermia and hyperthermia, sepsis and other complications in sick patients, where there is impaired functionality of the metabolic system. The relation between oxygen saturation and oxygen supply and demand is shown in the following modified Fick equation[6]:

$$SvO_2 = SaO_2 - \frac{VO_2}{1.306 \times CO \times Hb} \qquad \textbf{[2.2]}$$

where SvO_2 is the mixed venous oxygen saturation, SaO_2 is the arterial oxygen saturation, VO_2 is the total oxygen consumption, Hb is the haemoglobin concentration and 1.306 is the oxygen combining power of haemoglobin [7]. VO_2 is particularly important in the clinical diagnosis of certain conditions, such as tissue hypoxia which may occur when the cardiac output is low, hence oxygen supply is lower than oxygen demand. The normal cardiovascular response to increasing oxygen consumption is the augmentation of CO which may, or may not fully compensate for the increased metabolic rate. A low value of SvO_2 does not necessarily indicate tissue hypoxia while a normal or high value of SvO_2 may be hiding underlying pathological conditions such as sepsis, where the misdistribution of blood flow and the disturbance of mitochondrial oxygen utilisation may cause anaerobic metabolism even in the presence of normal or high SvO_2. Therefore it is important that VO_2 values are interpreted carefully in the context of a wider clinical and biochemical picture.

The clinical investigation of the method was particularly focussed on the effects of temperature, blood flow and oxygen consumption and results are presented in chapter 5.

2.2 INVASIVE OXIMETRY METHODS

Oximetry is the term used for a range of techniques which are employed for the measurement of oxygen saturation in blood. Oximetry can be divided in two main categories: arterial and venous oximetry. Arterial oximetry measurement is employed in the monitoring of oxygen supply through the arteries while venous oximetry investigates the body's demands for oxygen by measuring the oxygen transported back to the lungs through the venous vascular system.

Venous oxygen measurement can be separated in two major categories: invasive and non-invasive methods which can be continuous or non-continuous. Continuous measurement of oxygen saturation is usually performed with electro-optical catheters while non-continuous monitoring requires blood samples which can be obtained from catheters or by directly drawing a blood sample from the tissue region which needs investigation. Continuous monitoring is much preferred because it constantly measures the oxygen saturation without requiring further tests, such as blood gas analysis. Blood sampling is however used for the calibration of non-invasive oxygen saturation monitors, such as the heart-lung bypass machine used in heart surgery and the electro-optical monitors which use fibre-optic catheters[8], often used during cardiac surgery and post-operatively in the Intensive Care Unit (ICU). Continuous and non-continuous venous oxygen saturation can be separated in three further categories: continuous mixed venous (SvO_2), continuous central venous ($ScvO_2$) and non-continuous peripheral venous oxygen saturation ($SpvO_2$).

2.2.1 Continuous Mixed Venous Oxygen Saturation Monitoring (SvO_2)

Mixed venous oxygen saturation is obtained by inserting an oximetric pulmonary artery catheter (PAC) and indicates the balance between oxygen supply and demand and therefore provides an way to assess the overall tissue oxygenation, since the pulmonary artery carries all venous blood from the right ventricle to the lungs[9,10]. SvO_2 can be directly measured by using a PAC or it can be calculated from other parameters such as the oxygen delivery DO_2, which is a function of cardiac output (CO), haemoglobin (Hb) and arterial oxygen saturation (SaO_2).

Direct measurement of SvO_2 is most often carried out by using a pulmonary artery catheter which was first introduced by Swan and Ganz in the 1960s and became a standard by the 1970s. The current monitoring technique is a variation of the Swan-Ganz catheter and became a standard in the ICU for the post-operative evaluation of heart surgery patients, to monitor the fluid balance in patients with serious burns or for the monitoring of patients with kidney disease. The catheter is a long, thin plastic tube which contains multiple channels within it.

The use of PAC involves high risk for the patient and severe complications, since accessing the pulmonary artery is a highly invasive procedure. Additionally, the requirement for a specially trained clinician to perform the procedure and the elevated cost of the catheter increase the health care cost[11,12,13,14]. Moreover, in a recent overview of the PAC in anaesthesia practice the usefulness of its application was questioned[15]. It was found that among other reasons for the PAC's inability to improve outcome, the blood filling pressures measured from the catheter and particularly the pulmonary artery 'wedge' pressure, have no physiologic value. The wedge pressure has been shown not to correlate with other accepted methods of determining left ventricular filling of intravascular volume while it does not help to generate cardiac function curves. Therefore, knowledge of it may actually lead to incorrect management more frequently than not.

A typical PAC installation procedure[16] is described as shown in figure 2.1: after administration of local anaesthetic, the catheter is fist inserted into a vein usually under the collar bone, in the neck, in the arm or in the leg. The PAC in then advanced through the vein and through the right ventricle and right atrium it reaches the pulmonary artery. It is usually left in place for 24 to 72 hours depending on each individual patient. Its primary use is the monitoring of haemodynamic parameters[17], such as the pumping ability and the chambers' pressures of the heart which are important indicators for the outcome of surgery.

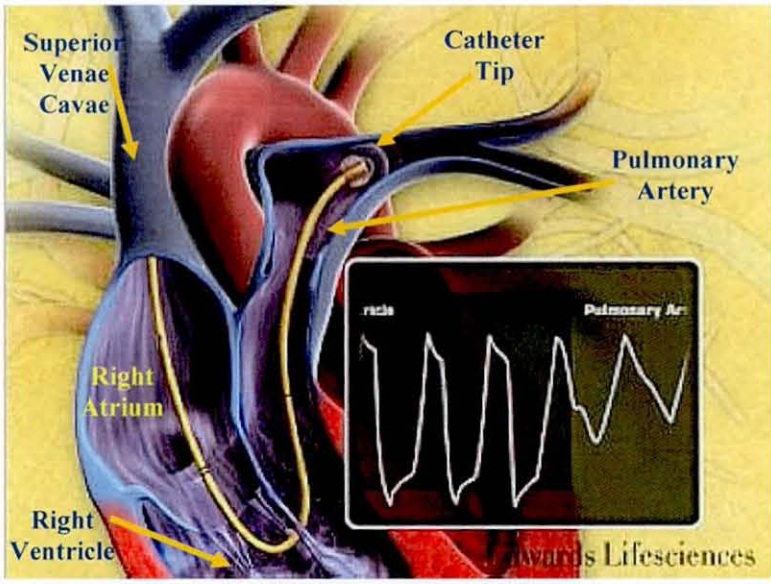

Figure 2.1 – Pulmonary artery catheter installation

A further variation of the PAC was introduced in the late 1980s where two fibre-optic bundles were added to the catheter for the transmission and reception of light at the tip of the catheter[18]. The receiving fibres were then connected to a photodetector which converted the light absorption into venous oxygen saturation, based on the principles of spectrophotometry and on the fact that blood becomes darker as it releases oxygen. Therefore, the darker the colour of blood becomes, the less oxygen it contains. This modified PAC is expensive to use and its potential complications widely limit its use therefore it is still not being used in all haemodynamic monitoring.

2.2.2 Continuous Central Venous Oxygen Saturation ($ScvO_2$)

Central venous oximetry is performed by inserting a catheter in the superior vena cava which carries venous blood from the upper body and it is considered less risky and less painful, easier to insert and less expensive than the PAC[19,20]. Additionally, central venous catheters are routinely used in ICU patients for central venous pressure monitoring, vasoactive and others drugs, parenteral nutrition and fluid resuscitation, therefore measurement of central venous oxygen saturation ($ScvO_2$) can be performed without the need for additional catheterisation. Hence central venous oximetry is a simple and attractive alternative measurement method of SvO_2

for the initial evaluation of critically ill patients, since it is less risky and less costly than PAC[21].

Regarding the similarity of the two parameters (SvO_2 and $ScvO_2$), there is a discordance in literature; some studies suggest that SvO_2 and $ScvO_2$ are interchangeable[22,23,24,25] but other investigators[26,27,28,29,30] reported that there is poor correlation between the two parameters and questioned the usefulness of $ScvO_2$ measurement. However, in the same studies it was found that there is significant correlation between the two parameters only under certain conditions, such as heart failure or when the patient is not in shock.

2.2.3 Non-Continuous Peripheral Venous Oxygen Saturation ($SpvO_2$)

Peripheral venous oxygen saturation ($SpvO_2$) is useful in the assessment of more confined areas of the human body such as in the adult human forearm[31]. Oxygen supply to the peripheral tissues of animals under shock and critically ill patients have been studied by measuring the partial pressure of oxygen (PO_2), where it was found that the measurement of peripheral oxygenation is a sensitive method of studying the progress of shock and resuscitation. Additionally, it was found that the measurement of $SpvO_2$ in conjunction with exercise protocols can help in the diagnosis of peripheral vascular disease (PVD)[32]. Other applications of $SpvO_2$ include measurement of regional blood flow and muscle oxygenation during intense exercise and under physiopathological conditions which present impaired oxygenation, such as cardiovascular disease and septic shock[33].

2.2.4 Limitations and Drawbacks of Invasive Techniques

Although continuous and real-time monitoring offered by these techniques is extremely advantageous, there are certain aspects which limit their use. For example, one of the limitations is the fact that only two wavelengths are used and therefore the accuracy of these monitors is affected by the presence of certain elements in the blood, such as excess lipids or dyes which can adversely affect the perceived redness of blood and therefore obtain false SvO_2 readings[34]. There were however further improvements of the two wavelength system, when Baxter

addressed the problem by modifying the processing methods and further studies support its accuracy[25,35,36,37].

Another limitation is the time and skills required to install a catheter. Many patients require urgent admission to the operating room therefore an immediate assessment of venous oxygen saturation is needed and there might not be sufficient time to carry out catheterisation on these patients. Lack of precision during the insertion procedure could cause severe complications such as perforation of vessels and may prove fatal for the patient. A non-invasive device such as a pulse oximeter to measure venous blood would be extremely useful, especially in cases where there is not very much time to spare or in the ambulatory setting, where during the transportation time paramedics could measure the venous oxygen saturation without delay.

A major drawback of catheterisation is the invasive nature of the measuring probe with severe underlying risks for the patient. Resistant bacteria or superbugs, such as the methicillin-resistant staphylococcus aureus (MRSA), could enter the body through the catheterisation point and cause severe complications which can also be fatal, especially for patients with impaired immune system after surgery or following a prolonged sickness. Therefore a non-invasive monitor would be extremely advantageous in this aspect.

The high cost of the SvO_2 catheters is also a problem for clinical management, as their multi-channel configuration and the addition of optical fibres for the spectrophotometric monitors involve high manufacturing cost, given the fact that they require precision engineering and sterilised environment to produce and deliver safely to hospitals. There are however studies suggesting that early goal directed therapy for patients with severe sepsis, which includes treatment goals for SvO_2, was able to increase survival rate in these patients[38]. Therefore, monitoring the oxygen saturation of venous blood is extremely important and therefore a non-invasive venous oxygen saturation monitor would provide all the advantages of

SvO_2 monitoring without side-effects, risks and cost associated with invasive techniques.

2.3 NON-INVASIVE OXIMETRY METHODS

The aforementioned limitations of invasive oximetry methods have driven the technology towards alternative solutions, minimising the risk factor for the patient. The use of light for diagnostic and therapeutic purposes in the transillumination tissue spectrum window extending from about 600 to 1200 nm has become very attractive because of the light's ability to penetrate tissues in this range. Penetration depth is dependent upon wavelength and ranges from several micrometers to several millimetres also depending on the underlying biological structure[39]. The light-tissue interaction is of great importance in the development of non-invasive monitoring methods since biological tissues are extremely complex with absorption and multiple scattering effects dominating the on-going research.

Over the last few decades there have been several attempts to describe biological tissue and light interaction with mathematical models often leading to complicated and impracticable solutions. Two of the major competitors in the field of non-invasively oximetry are Near Infrared Spectroscopy (NIRS) and Pulse Oximetry. They can be described as neighbouring technologies since they both utilise the near-infrared light spectrum, there is however a fundamental difference between the two: NIRS requires the knowledge of the light path among other parameters, while pulse oximetry is based upon several assumptions which render it more practicable.

2.3.1 Blood Oxygen Measurement Using Near Infrared Spectroscopy

The history of near-infrared radiation dates back in 1800 with Herschel concluding that there was light radiation beyond what we now know as visible spectrum, through his experiments to filter heat from a telescope. After a long period of neglect, near-infrared spectroscopy (NIRS) was applied for the first time in the 1950's by Wilbur Kaye with Beckman Instruments and published two papers which established NIR spectroscopy[40]. More than 20 years later in 1977, Jöbsis published the first paper to investigate the use of NIRS for the purposes of the monitoring cerebral and myocardial oxygen sufficiency and other circulatory parameters[41].

Other studies have followed which investigated cerebral haemodynamics in newborn babies, children and adults[42,43,44].

In NIRS, the light emitted by light sources which are typically laser diodes in the wavelength range between 650 and 900nm, is transmitted into the skin of the subject. During propagation through the biological tissues, the light is attenuated through both absorption and scattering effects[45]. The optical absorption occurs due to a number of structures which constitute tissue, and due to other substances such as water, cytochrome α and α_3, myoglobin, melanin, bilirubin, lipids and haemoglobin which absorb most of the light in the NIR range. Scattering of light occurs primarily in the membranes and organelles, where the refractive index presents discontinuities. A dominant light absorber in the range between 700nm and 850nm is haemoglobin in both oxygenated (oxy-haemoblogin, HbO_2) and reduced format (deoxy-haemoglobin, Hb), with a single isobestic point at approximately 790nm. After propagating through the tissues, a small part of the light will reach the skin through diffusion and scattering effects, where it can be detected at a distance from the light source. The spacing between light emitter and detector is very important for the sensitivity; when the distance from the emitter is large, the detected light will have travelled through a long optical path thus carrying more information about the underlying tissue. There is however a trade-off between sensitivity and signal-to-noise ratio (SNR), since sensitivity also depends on the signal quality but at the same time, in order to achieve a sufficiently high SNR it is necessary to limit the distance between emitter and detector[46].

The mathematical models and algorithms describing NIRS vary with respect to the applied field, for example, a model describing exclusively the concentration changes of the three major absorbing species of blood, otherwise known as chromophores (HbO_2, Hb and cytochrome α_3) is briefly presented.

An algorithm of NIRS based on a modified version of Beer-Lambert Law using three wavelengths[47] is briefly presented, which mathematically relates the

absorbance of a substance with the concentration and effective path length of the light incident through a linear model. The generalised form of the Beer-Lambert Law is expressed as:

$$A = \mu_\lambda \times C \times L \qquad [2.3]$$

where μ_λ is the specific absorption coefficient (l mol^{-1} cm^{-1}) which is wavelength dependent, L is the effective light path length (cm), C is the concentration of the substance (mol l^{-1}) and A is the total light absorbance. Therefore, concentration changes of chromophores result in a change of absorbance. A further modification of the Beer-Lambert Law includes a further parameter G known as the length modifier.

$$A = \mu_\lambda \times C \times L \times G \qquad [2.4]$$

The addition of G compensates for tissue properties and geometrical characteristics of the measurement probe, called the optode. If we assume that L, μ_λ and G remain constant, then the only parameter which can affect the total absorbance is the concentration C.

$$\Delta A = \mu_\lambda \times \Delta C \times L \times G \qquad [2.5]$$

The three chromophores which are taken into consideration are HbO_2, Hb and α_3 and if we consider the absorption of each chromophore separately, the total absorption due to all chromophores will be given by:

$$\frac{A_\lambda}{L \times G} = \mu_\lambda^{HbO_2} \times C_{HbO_2} + \mu_\lambda^{Hb} \times C_{Hb} + \mu_\lambda^{\alpha_3} \times C_{\alpha_3} \qquad [2.6]$$

In order to calculate the concentration change of the chromophores, three light sources of different wavelengths are required in order to form a system with three simultaneous equations. Further discussion of this path length-dependent method is

out of the scope of this thesis, which focuses on a path length-independent photoplethysmographic approach.

There are limitations in the application of the modified Beer-Lambert Law in biological tissues. Their complex structure which not only absorbs but also scatters light is the primary reason for inaccuracies when carrying out measurements in living tissue. As a result of the scattering and the inhomogeneity of tissues, it is not possible to know the exact path of the light incident or the *G* factor in the modified Beer-Lambert equation, since they both vary with different skin types and body characteristics of the subject, such as skin thickness and body fat percentage.

The problem is currently being investigated with light time-of-flight and phase modulation techniques which might turn NIRS into a clinical tool for venous oxygen assessment rather than its present use a research tool. The current main application of NIRS on physiological measurements is the use of spectrometric techniques to measure cerebral oxygenation and perfusion changes.

2.3.2 Blood Oxygen Saturation Measurement Using PPG

PPG stands for photoplethysmography (literal translation "registration of population through light"), originating from the Greek words "phos" and "plethysmos" which translate to light and population, respectively. It was first discovered by Hertzman in 1938[48] and it is known for its ability to non-invasively measure volume changes and more specifically blood volume changes. It is based upon the simple principle of light absorption changes when blood volume changes at the measurement site. The cardio-vascular pulse wave which is caused by the heart's contractions can be detected throughout the human body since it propagates through arteries. There are many different clinical applications of PPG, such as the monitoring of blood volume changes, pressure and heart rate[49], pulse transit time (PTT), with the most important application being pulse oximetry[50].

2.3.2a Application of Photoplethysmography in Human Tissues

The simplicity and the non-invasive nature of this method have resulted in the dominance of optical radiation in biomedical applications. Photoplethysmography was originally described as a photoelectric method for the blood supply measurement in fingers and toes[51] and in various skin areas. PPG signals can be detected by illuminating a tissue region and by placing a photodetector at a nearby position or at the opposite side of the measurement site. Blood volume changes resulting from the arterial pulsations affect the quantity of light reaching the photodetector and result in the formation of a PPG waveform.

Depending on the relative position between light source and detector, PPG probes can be separated in two categories: transmission and reflection mode. Transmission mode probes are in the form of a clip that has the light source and the detector positioned opposite to each other so that when the probe is applied to the measurement site (e.g. the finger), the light source is touching the front side of the tissue while the detector is placed on the back side of it. Therefore, as the arterial blood volume changes through the cardiac cycle, the amount of light reaching the photodetector also varies, hence the light is modulated by the vascular bed. In reflection mode, both the light source and the detector are positioned on the same side of the tissue (similarly to the NIRS optode configuration) and usually a few millimetres apart, in order to achieve the desired SNR with the highest possible path length and without direct light coupling between source and detector. Reflection mode probes allow monitoring on peripheral sites, such as the forehead, limbs and chest[52].

One of the major applications of PPG is pulse oximetry[53], a technique capable of measuring the oxygen content of haemoglobin in arterial blood. It relies on the principle that when two compounds with different absorption spectra are mixed together, the ratio of the two concentrations can be derived by measuring the light absorbance at two different wavelengths.

2.3.2b Photoplethysmographic Components in Human Tissues

Light absorption in human tissue can be due to many different structures such as skin, tissue (fat or muscle) and bone, as well as due to liquids found in the human body such as water and blood. All tissue structures present a static absorption of light, provided that they remain motionless, while light absorption of blood is changing because the heart wave changes the blood volume. There are two principal components in a PPG waveform[54]: the dynamically changing component (called the AC signal) which is due to blood volume changes, and the static component (called the DC signal) which represents the constant absorption of all other tissue components, including blood and other fluids, as shown in figure 2.2. The amplitude of the AC is usually around 1-5%[55] of the amplitude of the DC which however can be accurately measured by filtering and amplification of the PPG signal. The amplitude of the AC signal due to arterial pulsations has been described as a measure of skin blood perfusion[56], while the value of DC is indicative of the venous blood volume when employed in comparison methods[57,58]. Therefore, both AC and DC components of photoplethysmography are employed in different ways which depend on the application, and are of extreme importance.

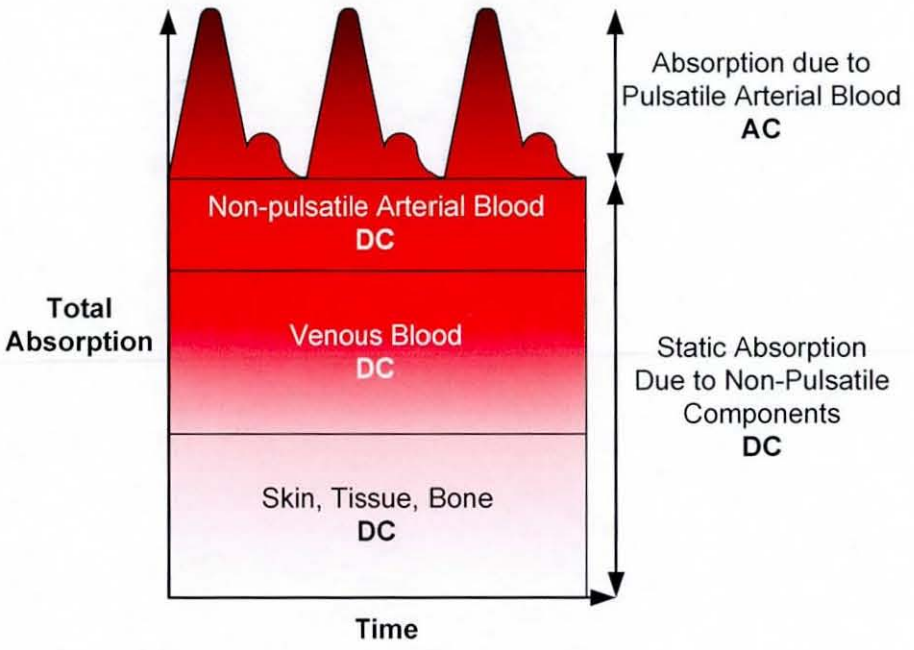

Figure 2.2 – Photoplethysmographic components

2.3.2c Photoplethysmographic Waveform

A typical PPG waveform, as mentioned above, can be obtained by amplifying the received signal from the photodiode. In well-perfused areas it is often possible to observe the changing light intensity just by looking at the DC signal, where small amplitude changes occur upon a heart induced wave. However, it is necessary to remove the DC offset and amplify the dynamic component (AC) in order to achieve high resolution when digitising the AC signal. If the AC component would be digitised without amplification, there would be large errors in the calculation of parameters derived from the plethysmograph. Although it is an implicit assumption that the AC PPG signal is due to blood volume changes, the over simplistic Beer-Lambert law of optical transmission does not allow for quantitative formulation between the observed pulsations and the underlying physiological dynamics. Whilst the received light intensity is dependent on numerous factors (anatomical and physiological), appropriate sensor designs coupled with smart techniques to adjust the transmitted light intensity[59] and the received intensity gain can result in a quasi-static DC component and an amplified AC component suitable for digitisation and further signal processing. The separation of the two signal components is of dual purpose: to isolate the absorption of dynamically-changed blood (arterial) from the absorption of static components, and also to provide a measurement baseline (total absorption in absence of arterial pulsation) and to compensate for different physiological and anatomical conditions. To achieve this, the AC values are divided by the DC values in order to normalise the dynamic component.

The PPG waveform can be used to infer physiological information. For example, it can be used to assess the mechanical properties of the arteries by looking at the amplitude of the AC signal during posture changes or before and after exercise, for example, on diabetics[60]. By comparing the measured response before and after, it is possible to carry out simple screening tests for neuropathy or atherosclerosis before carrying out more complex examinations. Another example is the measurement of Pulse Transit Time (PTT) by placing two PPG probes at locations of known distance; the measurement of transit time between two set points can provide

extremely valuable information about the elasticity of the arteries[61]. A more obvious feature of the PPG waveform is the dichrotic notch which is a small pulse observed immediately after the heart pulse and it is attributed to the pressure wave reflection from the lower body at the bifurcations of the arterial tree[62]. Studies have shown that this feature slowly disappears with age[63] due to reduced wave reflection.

2.3.2d Principle of pulse oximetry operation

The degree to which oxygen is chemically combined with haemoglobin is called functional arterial oxygen saturation (SaO_2)[64]. This quantity is defined as the ratio of concentration of oxy-haemoglobin (oxygenated haemoglobin, or HbO_2) to the sum of deoxy-haemoglobin (de-oxygenated haemoglobin, or Hb) and oxy-haemoglobin Hb + HbO_2, shown in equation 2.7.

$$SaO_2 = \frac{HbO_2}{Hb + HbO_2} \times 100\% \qquad [2.7]$$

SaO_2 is closely related to the fractional arterial oxygen saturation which is the ratio of oxy-haemoglobin to the sum of haemoglobin of all species, including those found in small quantities in blood such as carboxyhaemoglobin and methaemoglobin. However, the do have an effect in the accuracy of pulse oximeter readings[65,66] so they cannot be ignored as part of the calibration process.

The spectroscopic method for measuring the concentration of each species of haemoglobin relies on the fact that oxy-haemoglobin has different absorption characteristics than deoxy-haemoglobin, as shown in figure 2.3.

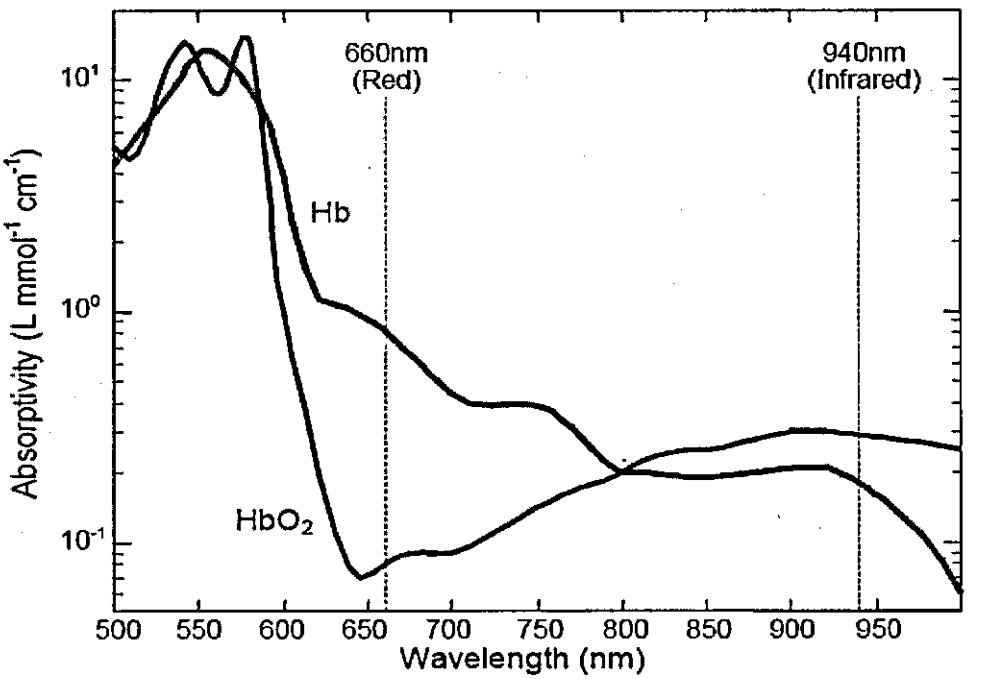

Figure 2.3 – Absorption spectra of haemoglobin species (Hb and HbO_2)

By illuminating the measured area at two wavelengths λ_1 and λ_2, the intensity of light transmitted or reflected (depending on the type of probe used) at the two wavelengths is used to calculate the light absorption for each wavelength and hence, calculate the oxygen saturation. The method is presented more in detail in chapter 3.

2.3.3 The Importance of Venous Oxygen Saturation Measurement

Conventional pulse oximetry provides information about the uptake of oxygen in the lungs and the delivery to the tissues, but it does not provide any indication of how oxygen is utilised or if it is enough to fulfil the oxygen needs. Moreover, if oxygen consumption is to be measured in a particular region, for example to monitor a skin graft or burn, a more localised measurement technique must be employed. A non-invasive venous oximeter can provide extremely valuable information about the oxygen supply and demand balance not only in the clinical setting to monitor patients but also in the ambulatory setting where fast and robust decisions must be made in order to preserve the vital functions of the patient. The importance of continuous venous oxygen saturation monitoring centrally was discussed in section 2.3, but the risks involved clearly show the advantages of a

non-invasive venous oxygen saturation monitor which could be employed in a variety of applications. Apart from the obvious application in critically ill patients, for example during surgery or post-operatively in the intensive care unit, another application could be the long-term monitoring of patients who suffer from heart insufficiency. In this case their long-term venous oxygen saturation could indicate how well the prescription medicines perform by looking at the venous oxygen saturation before and after drug administration, where low values of venous oxygen saturation for example, would indicate insufficiency of oxygen supply to the tissues.

2.4 OVERVIEW

The basic principles of the oxygen supply via the cardiovascular system were presented, in order to provide an overall understanding of the mechanism. A more profound analysis of the parameters involved, would certainly provide a lot more information and grounds for further analysis but with the main focus of this thesis being engineering, the study was confined to the effects of temperature, blood flow and oxygen consumption. These parameters, in fact, provide extremely useful information about the oxygen supply and demand balance, a very important parameter in the clinical management of patients.

The principles of arterial and venous oxygen saturation were introduced stressing the importance of venous oxygen saturation monitoring, especially in critically ill patients. Monitoring techniques were introduced and the advantages/disadvantages, as well as the limitations of each method were discussed. The use of a catheter for the continuous monitoring of venous oxygen saturation was discussed from different perspectives, such as clinical usefulness, risks involved and cost efficiency, stressing the importance for a non-invasive venous oxygen saturation monitor.

Non-invasive methods based on simplified Beer-Lambert models were also introduced with a particular interest in near-infrared spectroscopy, for which the principles of operation were briefly presented, introducing the light absorption in tissues and how chromophores affect the overall absorption of the travelling light. The principles and applications of photoplethysmography were introduced and further discussed in the context of pulse oximetry. The photoplethysmographic waveform and the method of extracting particular components for pulse oximetry were presented briefly, followed by a more detailed discussion in the following chapters. The importance of non-invasive venous oxygen saturation measurement concludes this section by highlighting in brief the potential applications of non invasive venous oximetry.

3 MODELLING

There are numerous photoplethysmographic models for pulse oximetry which were approached from a number of different theoretical perspectives to include motion artefact compensation, scattering effects, probe geometry etc. The development of a photoplethysmographic model for venous oximetry was approached from a physiological and anatomical point of view, in order to investigate the mechanical interaction between arteries and veins. Previous models[67] consider the venous flow to be quasi-static and free from any pulsations and this assumption, in fact, works well in pulse oximetry. However, the non-invasive venous oximetry method requires the introduction of artificial pulsations in the veins by inflating and deflating a cuff which was previously assumed to affect only venous flow. The introduction of arterio-venous mechanical coupling coefficients aims at the more accurate description of the venous photoplethysmographic model which is presented here, investigating both the arterial-to-venous and venous-to-arterial mechanical effects. The experimental protocols are also presented for both the photoplethysmographic model validation and the calibration of the prototype device.

3.1 VENOUS OXYGEN SATURATION MEASUREMENT

Presently available techniques require either the installation of a catheter in a vein or alternatively, collection of a blood sample for gas analysis. Current techniques are invasive, require certain skills and they impose risks to the patient. The method of venous oxygen saturation measurement is considered to be virtually risk-free, as it is non-invasive, and it requires no particular skills to perform a measurement, like with pulse oximetry. The similarity with pulse oximetry does not only lie on the simplicity of application, but also from a theoretical point of view, the method is in a way, an extension of pulse oximetry. The major difference between the two methods is the shape of the captured photoplethysmographic signal; traditionally, a pulse oximetry waveform is similar to figure 3.1 and is attributed to the changing arterial blood volume, which results in changing light intensity captured by the photodiode.

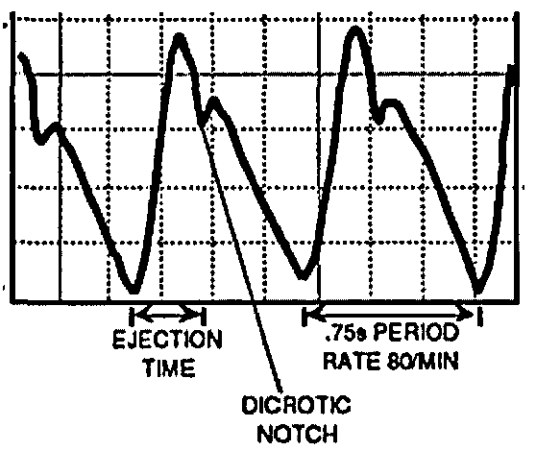

Figure 3.1 - A typical PPG waveform

3.1.1 Artificial Venous Pulsatile Signal

To separate the venous from the arterial signal, the new method introduces an artificial pulsatile signal in the range of 6.5-8Hz into the venous system[65,68], the aim of which is to perturb the venous flow. The modulation frequency was chosen to be distant from the heart's frequencies. The pulsatile signal is created by inflating and deflating a small digit cuff tied around the base of the 1st finger as shown in figure 3.2, at a peak pressure below 40mmHg to avoid interfering with the arterial system, which carries blood at a higher pressure.

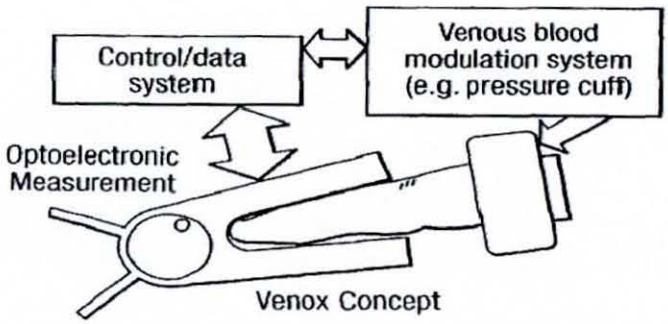

Figure 3.2 - Principle of operation of the method

A miniature air pump provides the air and a pinch valve driven with square pulses controls the inflation and deflation of the cuff (0-40mmHg). Figure 3.3 shows the variation of cuff pressure and the effect it has on the PPG signal. The shape of the pressure sensor signal is similar to a capacitor charging-discharging cycle, which means that the cuff is acting as a capacitor. The characteristics of the pressure variation are lost however, as it can be seen in the PPG signal.

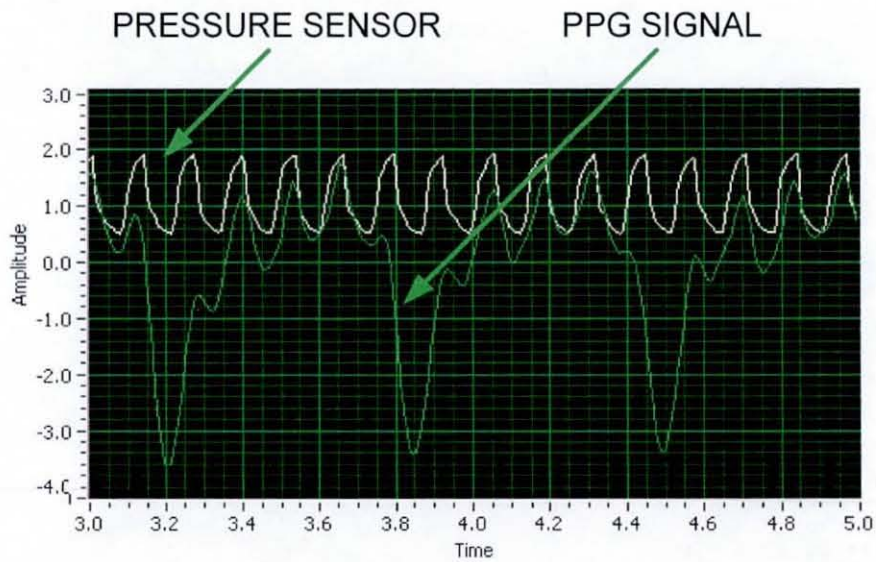

Figure 3.3 - The effect of miniature cuff pressure on the PPG signal

The high-frequency component in the PPG signal is slightly different in shape, because the biological tissues have a certain frequency response and some of the cuff pressure frequency components are essentially being filtered out.

3.1.2 Beer-Lambert Model for Pulse Oximetry

The commonly employed Beer-Lambert model in pulse oximetry, describes the effective optical absorbance of a medium when light travels through a given path length. In pulse oximetry, the Beer-Lambert law describes the relation between incident and transmitted light which has travelled through the medium, in this case, the finger. The transmission of light is a logarithmic function of the density or concentration of the absorbing solution, and is also dependent on the path length of the absorbing medium. The law can be expressed with the following equation:

$$I(\lambda) = I_0(\lambda) \exp[-\mu(\lambda)\, l] \qquad [3.1]$$

Where $\mu(\lambda)$ is the absorption coefficient and l is the path length, in other words the distance between the light emitter and the collector. $I_o(\lambda)$ is the light intensity of the light source and $I(\lambda)$ is the received intensity, which is dependent on the wavelength of the illuminated light, since the absorption coefficient varies with wavelength. The Beer-Lambert law is valid in pure absorbing mediums which have a certain range of concentration (molarity) and its accuracy gets reduced when either the concentration is very high or if there is a significant scattering component in the medium. Additionally, for the law to be valid the path length must be known exactly and no other absorbers must exist in the measured solution. It has been shown however, that certain assumptions and approximations in pulse oximetry can give a reasonable first order solution[69].

Since living biological tissues and structures are too complex to directly describe, it is impossible to know the exact path length of the measured site; there is however an important feature which helps take the law one step further and that is the arterial blood pulsation. Upon every heart contraction, the arterial blood volume varies and therefore the light absorption is different between the systolic and diastolic phases of the cardiac cycle. This allows for the dynamic component of the arterial blood to be expressed separately from the rest of the absorbers, such as baseline arterial

blood, venous blood, tissue, bone etc. The absorption coefficient can therefore be expressed as:

$$\mu(\lambda)\, l = \mu_{dyn}(\lambda)\, r(t) + \mu_{static}(\lambda)\, d \qquad [3.2]$$

where $\mu_{dyn}(\lambda)$ is the absorption coefficient of the changing arterial blood volume and $\mu_{static}(\lambda)$ is the absorption coefficient of the static components such as baseline arterial and venous blood, tissue, bone etc. $r(t)$ is the time changing path length of the dynamic component which is the arterial blood variation, and d is the path length of the static components.

The absorption coefficient of the dynamic component can be further analysed in the sense that oxygenated blood has a different absorption curve than reduced-oxygen blood. Therefore for a given wavelength of illuminating light, the path length of the dynamic component can be expressed as:

$$\mu_{dyn}(\lambda) = S\, \mu_{HbO_2}(\lambda) + (1\text{-}S)\, \mu_{Hb}(\lambda) \qquad [3.3]$$

where S is the proportion of haemoglobin that is oxygenated, in other terms, the arterial saturation SaO_2, μ_{HbO_2} and μ_{Hb} are the extinction coefficients of oxy-haemoglobin and deoxy-haemoglobin respectively. This equation allows expressing the received light intensity at a wavelength λ, as a function of oxygen saturation and time:

$$I(t,\lambda) = I_0(\lambda) \exp\{-[(S\, \mu_{HbO_2}(\lambda) + (1\text{-}S)\, \mu_{Hb}(\lambda))\, r(t) + \mu_{static}(\lambda)\, d]\} \qquad [3.4]$$

Therefore it is possible to create instances of the above equations at different wavelengths to form a system of equations which can be solved to calculate the oxygen saturation SaO_2. There are different approaches regarding the calculation of SaO_2 utilizing light intensities, namely the linear peak and valley method and the differential method. The new method employs the latter and is described in detail in the following sections.

Applying the linear differential method, the derivative of the received light intensity is given by:

$$\frac{d[I(t,\lambda)]}{dt} = -I_o(\lambda)\exp\{-[(S\mu_{HbO2}(\lambda)+(1-S)\mu_{Hb}(\lambda))r(t)+\mu_{static}(\lambda)d]\} \times[S\mu_{HbO2}(\lambda)+(1-S)\mu_{Hb}(\lambda)]\frac{d[r(t)]}{dt} \quad [3.5]$$

Assuming that the time variant optical path length change *r(t)* is not wavelength-dependent, the ratio of two instances of equation 3.5 eliminates the path length dependence.

$$\frac{\left(\frac{d[I(t,\lambda_1)]}{dt}\right)\Big/I(t,\lambda_1)}{\left(\frac{d[I(t,\lambda_2)]}{dt}\right)\Big/I(t,\lambda_2)} = \frac{S\mu_{HbO2}(\lambda_1)+(1-S)\mu_{Hb}(\lambda_1)}{S\mu_{HbO2}(\lambda_2)+(1-S)\mu_{Hb}(\lambda_2)} = R \quad [3.6]$$

In discrete time,

$$\frac{d[I(t,\lambda_1)]/dt}{I(t,\lambda_1)} = \frac{I(t_2,\lambda_1)-I(t_1,\lambda_1)}{I(t_3,\lambda_1)} = \frac{AC(\lambda_1)}{DC(\lambda_1)} \quad [3.7]$$

where t_1 and t_2 are the maximum and the minimum of the waveform (*AC* value) and $t_1<t_3<t_2$, t_3 is some point in time between t_1 and t_2 (*DC* value)[70]. Therefore the ratio-of-ratios *R* is given by:

$$R = \frac{AC(\lambda_1)/DC(\lambda_1)}{AC(\lambda_2)/DC(\lambda_2)} \quad [3.8]$$

The calculation of oxygen saturation from *R* is presented in chapter 5, where calibration methods are presented in detail.

3.2 EXTENSION OF BEER-LAMBERT MODEL FOR VENOUS OXIMETRY

In section 3.1.1 the artificial pulsation of the venous system was described, which permits the further break down of the absorbing components. The artificial venous pulsation helps distinguishing the venous blood from the rest of the absorbing components, thus enabling the possibility of calculating venous oxygen saturation by employing an algorithm similar to conventional pulse oximetry. The Beer-Lambert law will be discussed in detail, with particular attention to effects arising from the natural arterial pulsations and the artificial venous pulsations.

Recalling equation 3.1, the Beer-Lambert law combines the physical path length and the medium's absorbance into a single definition of optical density, which is employed in conventional pulse oximetry. The new model is an extension of the Beer-Lambert law, and will consider separately the path length of pulsatile arterial blood and artificially pulsatile venous blood, as well as the mechanical interaction between the modulating cuff, the arterial and the venous compartments. The model has more than one dynamic component: the natural arterial pulsatile blood and the artificially generated pulsatile venous blood, as well as three more dynamic terms which arise from the cross-coupling of the two blood compartments and the modulating cuff.

3.2.1 Model Hypotheses

The model is based upon a sequence of initial hypotheses. Figure 3.4 shows a simplified structure of the measured site, which is the 1st digit. Human anatomy defines two pairs of main blood vessels which run along the sides of the finger, with the veins being close to arteries, primarily for heat exchange[71], as this is one of the thermoregulatory mechanisms of the human body.

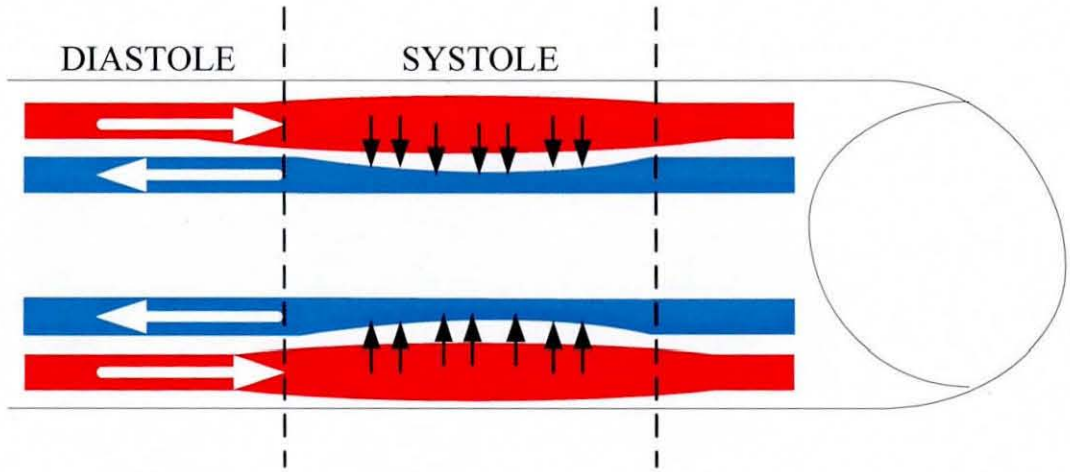

Figure 3.4 - Simplified representation of blood flow in the finger

The first hypothesis of the model is regarding the mechanical coupling of arteries and veins. More specifically, the arterial expansion during systole introduces mechanical stress to the adjacent vein. With the venous vascular system running at very low pressure (<20mmHg) the highly-pressurised arterial system (between 80mmHg and 120mmHg in a healthy adult) affects surrounding tissues upon expansion, and therefore introduce a change in venous blood flow by momentarily distorting the walls of the adjacent vein, therefore the arterial pulse transfers to a neighbouring vein[72]. This arterio-venous coupling is, in fact, one of the venous return mechanisms. The coupling will have an effect in the dynamic components' path length and the received light intensity will have a dynamic component which will not be purely due to arterial blood volume change, but part of it will be due to venous blood volume change. As a result, the pulse oximeter will be measuring a mixture of arterial and venous blood oxygen saturation and to be more precise, the calculated saturation will be lower than the actual value, since the venous oxygen saturation is lower that the arterial saturation.

The second hypothesis is concerning the breakthrough of the artificial pulsation in the venous system either by direct induction of the cuff's pressure pulse or by coupling of the venous pulses to the arterial compartment. Although there is no literature for venous-to-arterial coupling, the arteriovenous coupling[70] implies that there is mechanical coupling arteries and veins, and the artificially generated venous

pulsation could in principle transfer to neighbouring veins. Hence, when the cuff is inflated to a maximum pressure that is higher than the diastolic pressure, the artificial pulses will not only cause change in venous blood flow, but will also affect arterial blood flow; on the other hand, when the cuff pressure is smaller than the arterial pressure, the cuff pulsations will break through to the veins with possible coupling of the pulse from the venous to the arterial compartment. As a result of the appearance of artificial pulsations in the arterial flow, the measured venous oxygen saturation will be higher than the real value, since the venous dynamic signal component will in reality be due to a mixture of venous and arterial blood being modulated by the cuff. Figure 3.5 illustrates the hypothesis, where the finger is divided in three sections A, B and C. Section B is where the cuff is positioned and light is illuminated and collected in section C.

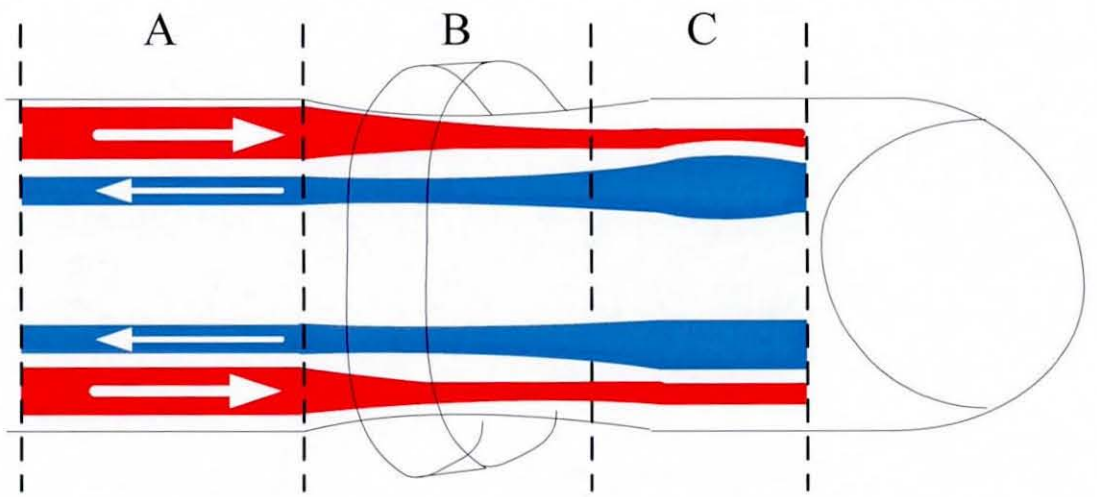

Figure 3.5 - Simplified representation of blood flow in the finger

There are two scenarios during the inflation phase:

i) The cuff pressure is small and unable to cause any direct disturbance to the arterial system: in this case, there is a change in venous blood flow and more specifically, the blood volume increases in section C, while it decreases in section A. This is because the venous flow is from the periphery towards the heart, therefore referring to figure 3.5, from right to left. The partial occlusion of the vein (the degree of which depends on

the cuff pressure) causes venous blood pooling in section C resulting in a variation of received light intensity, since the additional venous blood volume changes the optical path length. On the other hand, venous blood volume in section A decreases, as blood continues to flow towards the left, through the non-return venous valves. Additionally, there is the possibility of venous pulsation transfer to neighbouring arteries based on the arterio-venous coupling[70], although is it assumed that the venous-to-arterial effect is small or insignificant because of the large pressure difference between arterial and venous systems, with the latter being lower.

ii) The cuff pressure exceeds the arterial pressure: in this case, there is a change in venous and arterial blood flow and more specifically, arterial blood volume will decrease and venous blood volume will increase in section C upon cuff inflation. This is because the arterial flow is from the heart towards the periphery (left to right in figure 3.5) and venous flow is from right to left, as described previously. During inflation there is probably total occlusion of the vein, since the cuff pressure is a lot higher than the venous pressure, but the level of arterial occlusion depends on the cuff pressure. On the other hand, venous blood volume decreases and arterial blood volume increases in section A. At the measured site (section C), the light intensity will change because both arterial and venous path lengths change either because of direct break through of the cuff pressure to the artery, or indirectly by coupling of the venous pulsation into the arterial compartment.

3.2.2 Arterio-Venous Cross-coupling Modelling

Starting from first principles, the arterial-to-venous coupling model considers the natural arterial pulsations and the mechanical coupling to the venous vasculature. Figure 3.6 shows the variation of path length during diastole and systole.

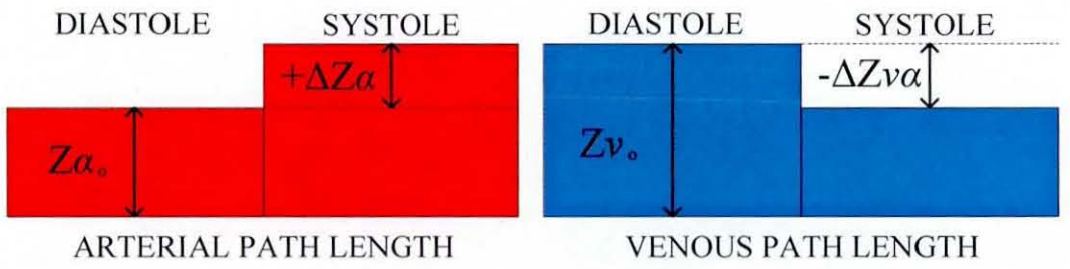

Figure 3.6 - Path length changes due to arterial pulsations

$Z\alpha$ is the varying arterial optical path length, $Z\alpha_0$ is the baseline arterial path length (during diastole) and $\Delta Z\alpha$ is the variation of the path length due to the arterial pulsation. Similarly, Zv is the varying venous optical path length, Zv_0 is the baseline venous path length (when the cuff is deflated) and $\Delta Zv\alpha$ is the variation of the path length due to the arterial pulsation.

The initial hypothesis is the existence of mechanical coupling which originates from the natural arterial pulsations and breaks through to neighbouring veins[70]. There are connective tissues between arteries and veins therefore part of the mechanical force originating from the artery is absorbed by the connective tissues, as they undergo a degree of compression before mechanical energy is transferred to the vein. At this point a coefficient to describe the degree of arterial-to-venous coupling is introduced, called the coupling coefficient ε.

The arterial and venous path lengths considering the artery-to-vein effect can be expressed as following (with reference to figure 3.6):

$$Z\alpha = Z\alpha_0 + \Delta Z\alpha \qquad \textbf{[3.9]}$$

and

$$Zv = Zv_0 - \Delta Zv\alpha \qquad \textbf{[3.10]}$$

The opposite signs in equations 3.9 and 3.10 are due to the opposite variations of path lengths. In the artery, the natural pulsation is causing expansion of the artery, therefore an increase in path length (positive sign), while in the vein, the arterial

expansion causes compression of the vein and therefore the venous path length decreases (negative sign). While $\Delta Z\alpha$ only depends on the arterial pulsation α, $\Delta Zv\alpha$ depends on the following three parameters: the coupling coefficient ε, the baseline venous perfusion level having path length Zv_o, and the arterial pulsation α. Therefore the venous path length may be expressed as follows:

$$Zv = Zv_o - \varepsilon Zv_o \alpha \qquad \textbf{[3.11]}$$

Considering the second part of the model where the venous-to-arterial effects are described, figure 3.7 shows the variation of the path lengths during the inflated and deflated states of the cuff.

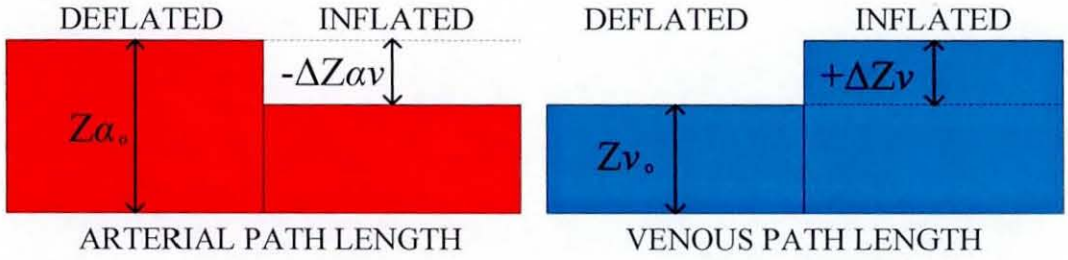

Figure 3.7 Path length variations due to artificial venous pulsations

The path lengths in equations 3.9 and 3.11 can now be expressed as:

$$Z\alpha = Z\alpha_o + \Delta Z\alpha - \Delta Z\alpha v \qquad \textbf{[3.12]}$$

and

$$Zv = Zv_o - \varepsilon\, Zv_o\, \alpha + \Delta Zv \qquad \textbf{[3.13]}$$

Again, the opposite signs in equations 3.12 and 3.13 are due to the opposite variations of path lengths upon inflation/deflation. Upon inflation, the arterial flow will be decreased due the cuff's mechanical stress applied to the arterial walls, causing a drop of arterial blood volume in section C (referring to figure 3.5) and therefore the arterial optical path length will decrease. On the other hand, as a result of the occlusion of the vein, the venous path length will increase in section C (figure 3.5), since there will be venous blood pooling. $\Delta Z\alpha v$ will depend on three

parameters: the coupling coefficient δ, the baseline arterial perfusion level having path length $Z\alpha_o$, and the artificial venous pulsation v introduced through the inflation and deflation of the cuff. Therefore the arterial path length may be expressed as follows:

$$Z\alpha = Z\alpha_o + \Delta Z\alpha - \delta\, Z\alpha_o v \qquad \textbf{[3.14]}$$

Coupling coefficients ε and δ essentially describe the same coupling effect but with different nature and origin. Since the structure between arteries and veins is the same when considering the model, then the two coupling coefficients would be numerically equal if the mechanical effects originating from the artery to the vein and vice versa. However, due to the differences of the mechanical effects, both in nature and origin, the arterio-venous coupling coefficient was separated to arterial-to-venous (ε) and venous-to-arterial (δ), since they are independent of each other.

3.2.3 Path Length Elimination from the Model[68]

Calling Io the light source intensity, I the received light intensity and T the transmittance of the light absorbing medium (the finger), I can be expressed as:

$$I = T \times I_0 \qquad \textbf{[3.15]}$$

For the case of n identical absorbing mediums, equation 3.15 may be rewritten as:

$$I = T^n \times I_0 \qquad \textbf{[3.16]}$$

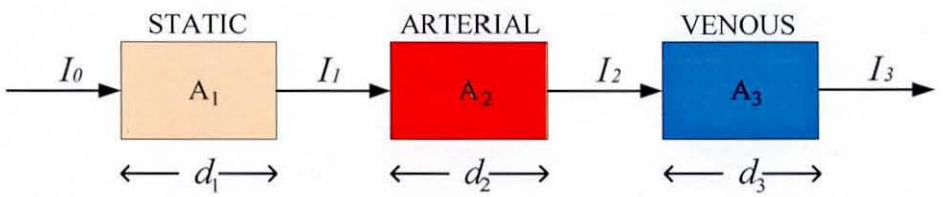

Figure 3.8 - Block diagram illustrating the transmittance of light through different components of the finger

Figure 3.8 illustrates the light path as it travels through different components inside the finger. The static components have absorbance A_1 and they include tissue, bone, skin, and arterial (during diastole) as well as venous blood, in baseline conditions. The dynamic components having absorbances A_2 and A_3 and path lengths d_2 and d_3 are the arterial and venous pulsatile blood, respectively. The received light intensity I_1 emerging from the static components can be written as a function of the incident light I_0 based on equation 3.1:

$$I_1 = I_0 \exp(-A_1 d_1) \qquad \textbf{[3.17]}$$

Likewise, the intensity of light I_2 emerging from the pulsatile arterial component is a function of its incident light intensity I_1 and can be expressed as follows:

$$I_2 = I_1 \exp(-A_2 d_2) \qquad \textbf{[3.18]}$$

Similarly, the light intensity emerging from the pulsatile venous component is a function of its incident light I_2 and can be written as follows after substitution of I_2 from equation 3.18:

$$I_3 = I_2 \exp(-A_3 d_3) = I_1 \exp(-A_2 d_2 - A_3 d_3) \qquad \textbf{[3.19]}$$

Substituting the expression of I_1 (equation 3.17) in the expression for I_3, the light emerging from the finger as a function of the incident light intensity I_0 is as follows:

$$I_3 = I_0 \exp[-(A_1 d_1 + A_2 d_2 + A_3 d_3)] \qquad \textbf{[3.20]}$$

The effect of light variation produced by the arterial and venous blood volume changes is given by the relationship between I_3 and I_1. Defining the change in transmittance produced by the arterial and venous components as ΔT, we have:

$$\Delta T = I_3 / I_1 \qquad \textbf{[3.21]}$$

Substituting equations 3.17 and 3.20 into 3.21, yields:

$$\Delta T = \frac{I_0 \exp[-(A_1 d_1 + A_2 d_2 + A_3 d_3)]}{I_0 \exp[-(A_1 d_1)]} \quad \textbf{[3.22]}$$

The term I_0 in the numerator and the denominator, as well as the term $A_1 d_1$ can be eliminated, therefore ΔT will be independent of the light source intensity and the static components. As a result, the change of arterial and venous transmittance can be expressed as:

$$\Delta T = \exp[-(A_2 d_2 + A_3 d_3)] \quad \textbf{[3.23]}$$

Hence, this principle renders the method self-calibrating, since it does not depend on the incident light intensity or the particular structure of the finger, since change in transmittance is independent of the static components.

3.2.4 Introduction of Time in the Model

The next step is to introduce the 'real life' representation of the absorbance and path length in the form of blood absorbance and arterial and venous path lengths. Recalling equations 3.14 and 3.13, the arterial and venous path lengths are given by

Arterial path length: $Z\alpha = Z\alpha_0 + \Delta Z\alpha - \delta\, Z\alpha_0\, v$
Venous path length: $Zv = Zv_0 + \Delta Zv - \varepsilon\, Zv_0\, a$

$Z\alpha_0$ and Zv_0 are the baseline path lengths of the arterial and the venous blood, respectively. $\Delta Z\alpha$ and ΔZv are the changes in the path length, due to the natural arterial pulsations and the artificial venous pulsations respectively. δ and ε are the arterial-venous and venous-arterial coupling coefficients respectively. The path lengths will now be expressed as functions of time, since they are time variant. $\alpha(t)$ is the time variant natural arterial pulsations and $v(t)$ are the time variant external venous pulsations. At this point it is assumed that arterial pulsations have a frequency range of 0.7Hz to 3Hz (42 to 180 beats/min as a guide), however the

minimum and maximum heart rate varies significantly between persons, depending on age, level of fitness, and generally by the autonomic nervous system[3]. The external venous modulation frequency is set higher at 8Hz, in order to make possible the separation of the arterial from the venous signal through signal processing techniques[66]. The arterial and venous optical path length changes can now be expressed in the time domain:

$$\Delta Z\alpha = \alpha(t)\, Z\alpha_o \qquad [3.24]$$

$$\Delta Zv = v(t)\, Zv_o \qquad [3.25]$$

The time variant arterial and venous path length changes due to arterial and venous cross-coupling can also be expressed in the time domain:

$$-\delta\, Z\alpha_o\, v = \delta\, Z\alpha_o\, v(t) \qquad [3.26]$$

$$-\varepsilon\, Zv_o\, a = \varepsilon\, Zv_o\, a(t) \qquad [3.27]$$

The time variant arterial and venous path lengths can be expressed in the time domain by substituting 3.24, 3.25, 3.26 and 3.27 into 3.14 and 3.13:

$$Z\alpha(t) = Z\alpha_o[1 + \alpha(t) - \delta\, v(t)] \qquad [3.28]$$

$$Zv(t) = Zv_o[1 + v(t) - \varepsilon\, a(t)] \qquad [3.29]$$

At this stage equation 3.20 is recalled from the development of the generalized model. The intensity I_3 of light emerging from the finger was given by:

$$I_3 = I_0 \exp[-(A_1 d_1 + A_2 d_2 + A_3 d_3)] \qquad [3.20]$$

Introducing comprehensive notations for the absorption coefficients and the path lengths, table 3.1 can be constructed.

Table 3.1a – Extinction coefficients of measured biological structures

Static Components	Dynamic Components	
A_1	Arterial A_2	Venous A_3
Tissue, bone, skin and other finger structures. μ_{static}	Arterial blood. μ_α	Venous blood. μ_v

Table 3.1b – Effective path lengths of measured biological structures

Static Components	Dynamic Components	
d_1	Arterial d_2	Venous d_3
-Tissue, bone, skin and other finger structures. Z_{static} -Baseline arterial blood. $Z\alpha_0$ -Baseline venous blood. Zv_0	Pulsating arterial blood. $Za(t)$	Pulsating venous blood. $Zv(t)$

Equation 3.20 can now be expressed similarly to equation 3.4 in terms of time, introducing also the wavelength λ as a parameter.

$$I(t,\lambda) = I_0 \exp[-(\mu_\alpha Z\alpha_0 + \mu_v Zv_0 + \mu_{static} Z_{static}) - (\mu_\alpha Z\alpha_0\, \alpha(t) - \delta\, \mu_\alpha Z\alpha_0\, v(t)) - (\mu_v Zv_0\, v(t) - \varepsilon\, \mu_v Zv_0\, \alpha(t))] \quad [3.30]$$

Rearranging 3.30 yields:

$$I(t,\lambda) = \underbrace{I_0 \exp[-(\mu_\alpha Z\alpha_0 + \mu_v Zv_0 + \mu_{static} Z_{static})]}_{\text{STATIC TERM}} \times \underbrace{\exp[-(\mu_\alpha Z\alpha_0 - \varepsilon\, \mu_v Zv_0)\, \alpha(t)]}_{\text{ARTERIAL TERM}} \times \underbrace{\exp[-(\mu_v Zv_0 - \delta\, \mu_\alpha Z\alpha_0)\, v(t)]}_{\text{VENOUS TERM}} \quad [3.31]$$

The static term is essentially the light intensity in baseline conditions, in other words, the *DC* component of the PPG signal. At this point, the origin of the cross-coupling can be seen by expanding equation 3.31 to second order. The Taylor expansion of e^{-x} is:

$$e^{-x} = 1\text{-}x + \frac{x^2}{2} - \ldots \qquad \textbf{[3.32]}$$

Therefore by approximating the dynamic term (arterial + venous) to second order, equation 3.31 becomes:

$$I(t,\lambda) \cong I_0(\lambda)\exp[-\mu_a Za_0 - \mu_v Zv_0 - \mu_{static} Z_{static}]\times$$
$$\left[\begin{array}{l} 1-(\mu_a Za_0 - \varepsilon\mu_v Zv_0)a(t) - (\mu_v Zv_0 - \delta\mu_a Za_0)v(t) + \frac{1}{2}(\mu_a Za_0 - \varepsilon\mu_v Zv_0)^2 a^2(t) \\ +\frac{1}{2}(\mu_v Zv_0 - \delta\mu_a Za_0)^2 v^2(t) + (\mu_a Za_0 - \varepsilon\mu_v Zv_0)(\mu_v Zv_0 - \delta\mu_a Za_0)a(t)v(t) \end{array}\right] \qquad \textbf{[3.33]}$$

In the absence of pulsations, $a(t) = v(t) = 0$. Hence the static term (*DC*) is given by:

$$I(t,\lambda) = I_0 \exp[-(\mu_\alpha Za_0 + \mu_v Zv_0 + \mu_{static} Z_{static})] \qquad \textbf{[3.34]}$$

The dynamic terms (*AC*) normalised by the static term (*DC*) can be expressed as:

$$\frac{\Delta I(t,\lambda)}{I(t,\lambda)} \cong \overbrace{-(\mu_a Za_0 - \varepsilon\mu_v Zv_0)a(t)}^{\text{ARTERIAL}} \overbrace{-(\mu_v Zv_0 - \delta\mu_a Za_0)v(t)}^{\text{VENOUS}} \overbrace{+\frac{1}{2}(\mu_a Za_0 - \varepsilon\mu_v Zv_0)^2 a^2(t)}^{\text{ARTERIAL}}$$
$$\underbrace{+\frac{1}{2}(\mu_v Zv_0 - \delta\mu_a Za_0)^2 v^2(t)}_{\text{VENOUS}} \underbrace{+(\mu_a Za_0 - \varepsilon\mu_v Zv_0)(\mu_v Zv_0 - \delta\mu_a Za_0)a(t)v(t)}_{\text{MULTIPLICATIVE TERM}} \qquad \textbf{[3.35]}$$

Equation 3.35 shows the origin of light intensity components in the signal, including the previously described multiplicative term[65], which is:

$$(\mu_a Za_0 - \varepsilon\mu_v Zv_0)(\mu_v Zv_0 - \delta\mu_a Za_0)a(t)v(t) \quad \textbf{[3.36]}$$

It is worth noting that even if there is no mechanical coupling between arteries and veins ($\varepsilon = \delta = 0$), the cross coupling term is always finite. This makes physical sense as the 'multiplication' of the arterial and venous light intensities can either be optical or mechanical (or both) in origin. For example, some of the light will only be modulated by arterial blood (ARTERIAL in equation 3.31), by venous blood (VENOUS in equation 3.31) and part of it will be modulated by both arterial and venous blood, as shown in equation 3.36.

Equation 3.35 can be further simplified, in order to investigate how the cross coupling between arteries and veins can be mitigated. By approximating e^{-x} to (1-x), considering x (the dynamic term) to be a very small value (1-5% of the overall intensity signal[53]) the normalised dynamic term in equation 3.35 is further simplified to first order, yielding:

$$\frac{\Delta I(t,\lambda)}{I(t,\lambda)} \cong -(\mu_a Za_0 - \varepsilon\mu_v Zv_0)a(t) - (\mu_v Zv_0 - \delta\mu_a Za_0)v(t) \quad \textbf{[3.37]}$$

According to the model, the arterial and venous path length variations are a function of the arterial and venous pulsations. *a(t)* is the function which describes the arterial pulsations and *v(t)* describes the venous pulsations. Equation 3.37 can be expressed in terms of path length variation, since functions *a(t)* and *v(t)* are unknown.

$$\frac{\Delta I(t,\lambda)}{I(t,\lambda)} = -(\mu_a \Delta Za_0 - \varepsilon\mu_v \Delta Zv_0) - (\mu_v \Delta Zv_0 - \delta\mu_a \Delta Za_0) \quad \textbf{[3.38]}$$

Equation 3.38 is still dependent on the path length. A common technique in pulse oximetry is the use of two wavelengths to obtain a ratio of signals, and with the assumption that the path length is the same at both wavelengths, oxygen saturation calculation becomes independent of the path length. A method of deriving the ratio-

of-ratios using the separated *AC* and *DC* parts of the PPG waveform is presented here[73].

In this method the ratio-of-ratios is determined using derivatives, the instantaneous change in path length due to arterial pulsation must also be the same for both wavelengths. Recalling equation 3.1:

$$I(\lambda) = I_o(\lambda) \exp[-\mu(\lambda)\, l] \qquad \textbf{[3.1]}$$

Then the derivative will be:

$$\frac{dI(t,\lambda)}{dt} = I_o(\lambda)\exp[-\mu(\lambda)l]\left(-\mu(\lambda)\frac{dl}{dt}\right) \qquad \textbf{[3.39]}$$

Dividing by $I(t,\lambda)$ yields:

$$\frac{dI(t,\lambda)/dt}{I(t,\lambda)} = \left(-\mu(\lambda)\frac{dl}{dt}\right) \qquad \textbf{[3.40]}$$

Using two wavelengths λ_1 and λ_2 and taking the ratio of the two equations:

$$\frac{\left(\frac{d[I(t,\lambda_1)]}{dt}\right)\Big/ I(t,\lambda_1)}{\left(\frac{d[I(t,\lambda_2)]}{dt}\right)\Big/ I(t,\lambda_2)} = \frac{-\mu(\lambda_1)\frac{dl}{dt}}{-\mu(\lambda_2)\frac{dl}{dt}} \Rightarrow Ratio = \frac{-\mu(\lambda_1)}{-\mu(\lambda_2)} \qquad \textbf{[3.41]}$$

Equation 3.40 can be expressed in discrete time between two instances t_1 and t_2. If t_1 and t_2 are the minimum and the maximum of the waveform respectively (*AC* PPG component), and a point in time t_3 between t_1 and t_2 (*DC* PPG component)[68], then equation 3.40 yields:

$$\frac{dI(t,\lambda)/dt}{I(t,\lambda)} = \frac{\Delta I(\lambda)}{I(\lambda)} = -\mu(\lambda)\Delta l \Rightarrow \frac{I_{t1}(\lambda) - I_{t2}(\lambda)}{I_{t3}(\lambda)} = \frac{AC(\lambda)}{DC(\lambda)} = -\mu(\lambda)\Delta l \qquad \textbf{[3.42]}$$

Applying equation 3.42 to two wavelengths λ_1 and λ_2 and taking the ratio, yields:

$$\frac{\left(\frac{d[I(t,\lambda_1)]}{dt}\right)\Big/ I(t,\lambda_1)}{\left(\frac{d[I(t,\lambda_2)]}{dt}\right)\Big/ I(t,\lambda_2)} = \frac{\Delta I(\lambda_1)/I(\lambda_1)}{\Delta I(\lambda_2)/I(\lambda_2)} = \frac{-\mu(\lambda_1)}{-\mu(\lambda_2)}\frac{\Delta l}{\Delta l}$$
$$\Rightarrow \frac{AC(\lambda_1)/DC(\lambda_1)}{AC(\lambda_2)/DC(\lambda_2)} = \frac{-\mu(\lambda_1)}{-\mu(\lambda_2)} = R \qquad \textbf{[3.43]}$$

From equation 3.42, $\frac{\Delta I(\lambda)}{I(\lambda)}$ is essentially equal to $-\mu(\lambda)\Delta l$, which is equal to the ratio $\frac{AC(\lambda)}{DC(\lambda)}$. Therefore equation 3.38 can be written as:

$$\frac{\Delta I(t,\lambda)}{I(t,\lambda)} \cong -[A(\lambda) - \varepsilon V(\lambda)] - [V(\lambda) - \delta A(\lambda)] \qquad \textbf{[3.44]}$$

where $A(\lambda) = \frac{AC(\lambda)^{Art}}{DC(\lambda)}$ is the normalised arterial peak-to-peak signal and $V(\lambda) = \frac{AC(\lambda)^{Ven}}{DC(\lambda)}$ is the normalized venous peak-to-peak signal. Since the artificial venous pulsation is applied at a different frequency (8Hz) than the arterial frequency, arterial and venous signals can easily be separated by applying band-pass filtering. Equation 3.44 may be applied to two different wavelengths, after arterial and venous signals have been separated:

$$\left\langle \frac{\Delta I(t,\lambda_1)/I(t,\lambda_1)}{\Delta I(t,\lambda_2)/I(t,\lambda_2)} \right\rangle_{arterial} = \frac{A(\lambda_1) - \varepsilon V(\lambda_1)}{A(\lambda_2) - \varepsilon V(\lambda_2)} = R_a \qquad \textbf{[3.45]}$$

$$\left\langle \frac{\Delta I(t,\lambda_1)/I(t,\lambda_1)}{\Delta I(t,\lambda_2)/I(t,\lambda_2)} \right\rangle_{venous} = \frac{V(\lambda_1) - \delta A(\lambda_1)}{V(\lambda_2) - \delta \mathrm{A}(\lambda_2)} = R_v \qquad \textbf{[3.46]}$$

At this stage ε, δ are unknown and therefore R_a and R_v cannot be evaluated. Nevertheless, equations 3.45 and 3.46 may be used to write the explicit relations:

$$\varepsilon = \frac{A(\lambda_2)R_a - A(\lambda_1)}{V(\lambda_2)R_a - V(\lambda_1)} \quad \textbf{[3.47]}$$

$$\delta = \frac{V(\lambda_2)R_v - V(\lambda_1)}{A(\lambda_2)R_v - A(\lambda_1)} \quad \textbf{[3.48]}$$

In conventional pulse oximetry it is assumed that there the PPG signal is purely arterial, therefore $\varepsilon=0$. Hence equation 3.45 describing the arterial *ratio-of-ratios R* becomes consistent with equation 3.8:

$$R_a = \frac{A(\lambda_1)}{A(\lambda_2)} \quad \textbf{[3.49]}$$

where $A(\lambda)=\frac{AC(\lambda)}{DC(\lambda)}^{Art}$.

The model is validated experimentally in chapter 5, where the interpretation and experimental protocol are described in detail.

3.3 CALIBRATION MODEL

Since the venous oximetry method employs pulse oximetry principles, it was anticipated that pulse oximetry calibration curves for arterial blood would extend to venous blood. Calibration curves are derived empirically and are usually different between manufacturers of pulse oximeters due to particular signal processing techniques, different probes, different light source wavelengths and other parameters which affect signals. The empirical calibration of a pulse oximeter is carried out by the manufacturer in a controlled environment where oxygen content in air is reduced slowly, in order to introduce mild de-saturation of the arterial blood. More specifically, the way this works is by 'starving' the lungs in terms of oxygen, rendering difficult for the lungs to completely re-saturate venous blood. Hence, the smaller the inspired oxygen volume is, the smaller the percentage of haemoglobin that carries oxygen in arterial blood will be. During the gradual reduction of the oxygen volume, arterial blood samples are taken from the calibration volunteers while PPG signals are being recorded with the pulse oximeter which undergoes calibration, and the result is an X-Y plot which relates the measured oxygen saturation of the blood sample with the signals recorded during the sampling period[74]. This plot is the *calibration curve* which is stored in the pulse oximeter memory and serves as a lookup table when PPG signals are captured from a measured subject.

The calibration procedure described involves a certain risk and ethics approval which must be obtained prior to testing. Furthermore, due to health risks involved it is not permitted to carry out the de-saturation below 60%[68] of measured arterial saturation, as oxygen insufficiency might result in tissue damage or organ failure.

An alternative approach was decided to be followed, which was an *in-vitro* calibration using a finger phantom and light absorbing solutions with different absorption characteristics at certain wavelengths. A comparative calibration against a commercial pulse oximeter (Nonin 8600) was performed by employing a simple finger phantom, similar to a commercially available calibration phantom (Nonin

Phantom, Nonin Medical Inc)[73]. Part of a Nonin Finger Phantom shown in figure 3.9 was used as a scattering medium, and a set of light absorbers inside the phantom shown in figure 3.10 simulated the changing absorbance of blood against differing oxygen saturation values. The simulation of blood absorption was done by preparing absorption solutions of Methylene Blue (otherwise known as India Ink) and Cupric Sulphate Pentahydrate ($CuSO_4 \cdot 5H_2O$). Methylene blue is a strong absorber in the red region (peak absorption around 660nm) and cupric sulphate absorbs strongly in the near-infrared region. By mixing the two solutions at different proportions, specific absorption ratios can be achieved at the desired wavelengths[75].

Figure 3.9 - Nonin Finger Phantom light diffuser

The finger model shown in figure 3.10 was constructed from a pair of 1mm thick glass slides cut 16mm x 76mm x 3mm (width × height × depth). A chamber was formed between the two slides using double-sided high density sponge tape of 1mm thickness, following the contour of the glass to form a watertight container of 1mm thickness.

Figure 3.10 - Finger phantom constructed from microscope glass slides (left)

The entry to the container was kept open to administer the light absorbing solutions and the glass container was then inserted in the Nonin light diffuser to form the optical phantom. The experimental results are presented in chapter 5.

3.4 OVERVIEW

The new developed model for non-invasive venous oximetry has facilitated a way to detect and correct erroneous values of arterial and venous oxygen saturation when mechanical coupling occurs between arterial and venous compartments. The first section of the model, where the arterial-to-venous mechanical effects are introduced, is useful in the case the arterial expansion causes mechanical effects to veins, which would result in lower values of arterial oxygen saturation. The second section of the model, where the venous-to-arterial mechanical effects are introduced, is useful when a large cuff pressure is required in order to obtain a venous signal. Especially in poor peripheral perfusion conditions, the model can indicate whether the cuff pressure is large enough to create arterial volume changes and therefore cause a higher venous oxygen saturation value which could lead to false diagnosis. The finger phantom model has been developed as close as possible to the commercially available version and has been successfully used to perform a sequence of comparative calibration measurements which are discussed in chapter 5.

4 ENGINEERING DEVELOPMENT

Over the past few years the prototype device of the venous oximetry method has been under continuous improvements in terms of functionality, safety, robustness and portability. Functionality was improved to make the device operable by non-technical persons, such as nurses and doctors when the device would undergo clinical testing. The second generation system was designed with a higher functionality, since the method required a clinical evaluation in order to identify the response and sensitivity to different physiological parameters. Five second-generation prototypes were built (2004-2005) and used successfully in a pilot study, where the feasibility of the method was examined in the clinical setting. In this version a photoplethysmographic board was used (DISCO4, Dialog Devices Ltd) and a control board was designed and built. The control board along with the photoplethysmographic board were both connected to a laptop computer via a single USB connection, making the system more versatile and convenient to use. The real-time processing and control software was written on the Labview platform and its functionality is described in detail later in this chapter. The system was subsequently updated again (2006) to form the third generation prototype which is a fully embedded device without the need for an external computer. The added value to the third generation prototype was the high portability and the simplicity of the system, capable to be operated by non-experts. This chapter presents in detail the development stages of the hardware and software used for the experimental and clinical evaluation of venous oximetry. Appendix II includes the schematic diagrams of the control board, as well as the software written for the μ-controllers.

4.1 FIRST GENERATION – PRIOR TECHNOLOGY

The first generation system which was split in two enclosures required an experienced operator, since all controls were manually set, such as the LED intensity, the amplifier gain, the cuff pressure level and other parameters. Additionally, an external connection to the parallel port of a computer was required therefore overall, it was difficult to transfer the system from one location to another; for example, from the operating theatre to the intensive care unit if the device were to be used in a clinical study. It was built around a Programmable Logic Device (PLD) which was controlled in software via a computer's parallel port. An important feature which was missing at this stage was real-time control and display of raw data, and signal processing was performed in Matlab (Mathworks Inc) after the end of the recording. Additionally, the setup of the system was performed via a script written in Matlab, without any means of control while recording data. The lack of this feature was one of the major tasks for the newer prototypes developed, since the real-time display of signals (raw and processed) and the ability to control certain parameters are important to ensure the correct setup of the acquisition and pressure control systems.

4.1.1 PPG System

The first generation system is shown in figure 4.1, where the photoplethysmographic system was in a separate box from the artificial pulse generator. The PPG system was built in-house and it was designed to operate with commercially available pulse oximetry probes, as shown in figure 4.1. LED intensity and amplifier gain were controllable via the PC through the execution of a script in Matlab.

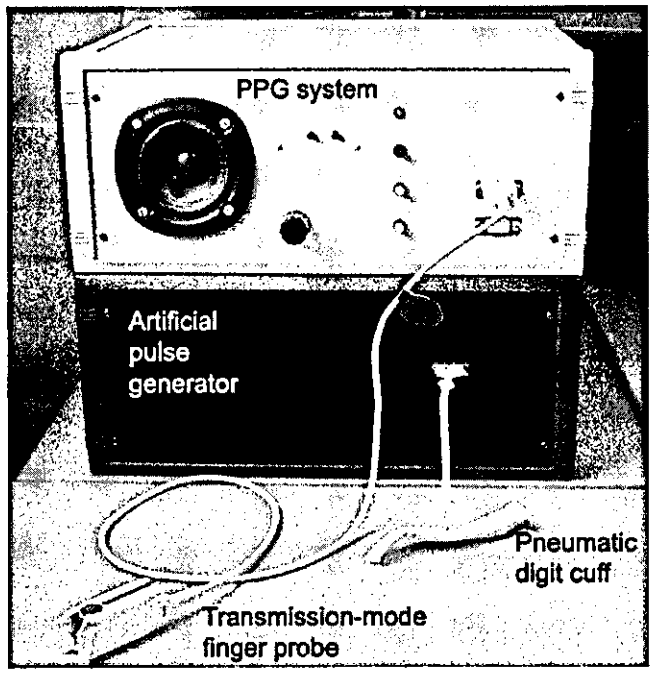

Figure 4.1 - First Generation System

4.1.2 Pressure Modulation Control

The pressure modulation control system was enclosed in a separate container as shown in figure 4.1 and it was controllable via a PLD by execution of a script in Matlab, similarly to the PPG system. The pressure modulation was created with an air pump and a pinch valve, which was driven with a series of square pulses, at a fixed frequency of 6.5Hz.

4.1.3 Data Acquisition System and Software

The data acquisition system of the first generation system only allows recording of data but not real-time display of the raw signals. Therefore, recorded raw data are processed in Matlab after the device has finished recording; the lack of real-time processing and display posed a problem should the device be used in a clinical trial. Signal quality can degrade over the course of a measurement due to hypoperfusion or other physiological responses of the cardiovascular system. The software was written in C programming language and LED, gain and pressure parameters were controlled from Matlab through Dynamic Data Exchange (DDE).

4.2 SECOND GENERATION PROTOTYPE - LABORATORY TESTS AND CLINICAL STUDIES

In order to address the lack of functionalities in the first generation prototype, a new system was designed around three main axes: functionality, safety and portability. A new PPG board (DISCO4) supplied by Dialog Devices Ltd was employed in the new prototype allowing the real-time control of parameters, while raw signals were amplified and filtered before fed into an external data acquisition board (DAQ) for analogue-to-digital conversion. Additionally, a pressure control board was designed which allowed an air pump and a pinch valve to be connected and controlled via a USB connection from the computer. Another important feature was the addition of means of modulation frequency selection from software, while the previous prototype required the removal and re-programming of the modulation frequency control IC. The second generation prototype also featured an LCD display on the front panel of the enclosure, which displayed messages sent from the control software. The purpose of the screen was to display status information and for debugging purposes, should the communication between the system and the computer be lost. The analogue-to-digital conversion of raw data was performed in a 14-bit DAQ (USB-6009, National Instruments), which sampled and streamed data in real-time to the computer with a 128Hz sampling rate. The software was also re-designed from scratch and it was built in LabView (National Instruments Inc) with a friendly graphics user interface in order to provide easy operation of the device by non-experts. Data logging included both raw and processed data, with time stamp in both data sets in order to have a point of reference when analysing simultaneous recordings from other devices. Additionally, two temperature sensor inputs were added to provide a means of comparison between central with peripheral skin temperatures which can provide information about blood perfusion[76]. Furthermore, signal quality indices were added for both arterial and venous signals, in order to provide a fast and easy way of assessing whether the current PPG and pressure configurations are satisfactorily set. Regarding safety, the second generation prototype had a medically approved power supply which was initially installed inside the enclosure, but at a later version, an external type was used in order to

comply with the latest medical device safety regulations. The overall size and weight of the device was reduced vastly, with the final device weighing approximately 2kg (dimensions: W27cm x D27cm x H10cm). The second generation prototype was designed in three phases which are shown in figure 4.2.

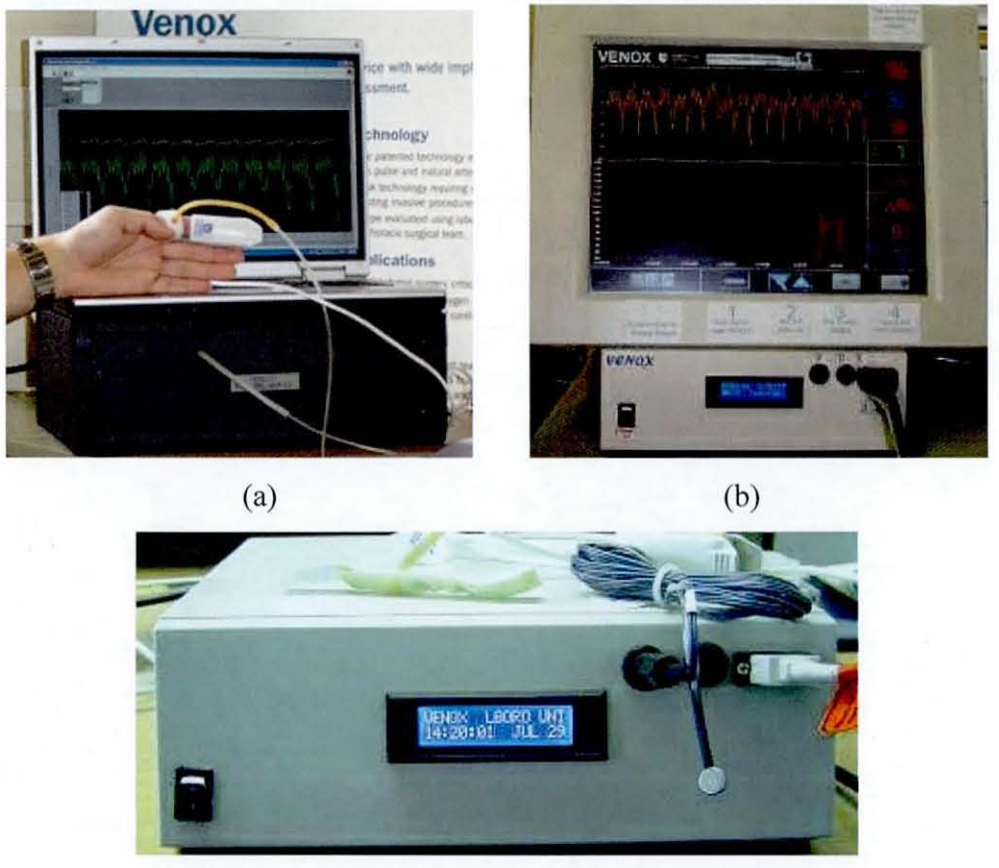

(a) (b)

(c)

Figure 4.2 - Second generation prototypes: (a) was employed in a clinical study, (b) was designed for the second phase study and (c) was used for laboratory tests

The system comprises of the following components:

- An air pump and a pinch valve which are controllable from the computer.
- A data acquisition board (DAQ USB-6009, National Instruments Inc) converts all the PPG board signals to digital data at 14-bit resolution.
- A serial-to-USB converter along with the USB hub provide a communication channel to the PPG board, the control board and the DAQ connect via a single cable to the computer.

- A switch mode power supply provides +/- 15V to the PPG board and +15V to the linear power supply (PCM50UT05, XP Power Ltd).
- A custom designed linear power supply provides +5V to the control board and +12V to the pump, the valve and the opto-isolators. Additionally, it features two MOSFETs which help to drive the air pump and the valve from the PIC.

A dual-µcontroller control board communicating with the computer, drives the LCD screen, the air pump and the valve and digitises the output signal of the pressure sensor. Furthermore, there is a level translator on-board to convert TTL to RS232 levels and vice-versa. Figure 4.3 illustrates the block diagram of the prototype.

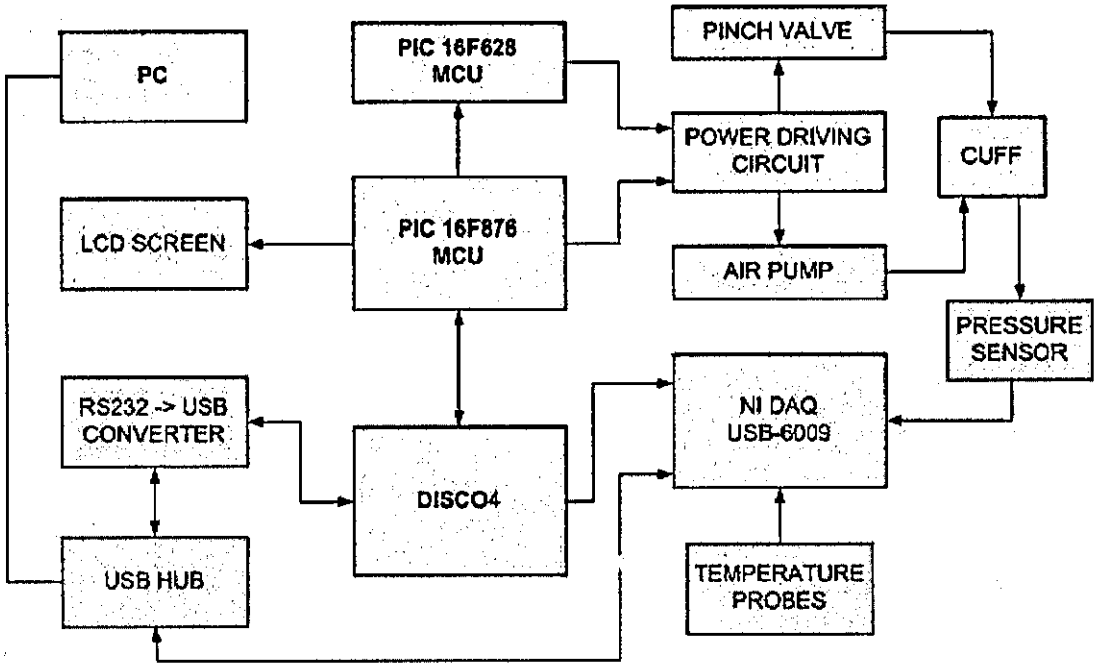

Figure 4.3 - Second generation prototype system block diagram

4.2.1 DISCO4 PPG System

The DISCO4 PPG board is a four-wavelength photoplethysmographic system that provides all the necessary analogue signal-processing to perform multi-channel photoplethysmography or pulse oximetry. Whilst the primary outputs of this board

are analogue signals, the majority of system functions are configurable digitally, using an RS232 serial communications interface. The board requires a dual power supply of ±15V and it can operate with standard pulse oximetry probes. The LED intensities are controllable digitally (8 bit resolution, 30mA or 100mA selectable current), as well as the photodiode amplifier gain (5 bit resolution with linear dB scale, 15dB ≤ Gain ≤ 77dB, 2dB step). The board provides two output channels for each wavelength which contain the raw and the processed output signals. The raw signal is essentially the *DC* signal, if a low frequency low-pass filter is applied to it, while the processed signal is the *AC* signal. The LEDs are pulse-driven by the board and signals are de-multiplexed, in order to provide a clean signal, free from ambient light artefacts. This system works by switching LEDs sequentially on and off, so the ambient light registered during the LED-off period can be subtracted from the signal. The switching speed can be set to either 1 kHz or 2 kHz, depending on the probe, and attention must be paid to the photodiode's frequency response since a large photodiode will have a certain amount of capacitance which will slow down its response. The DISCO4 PPG board is shown in figure 4.4.

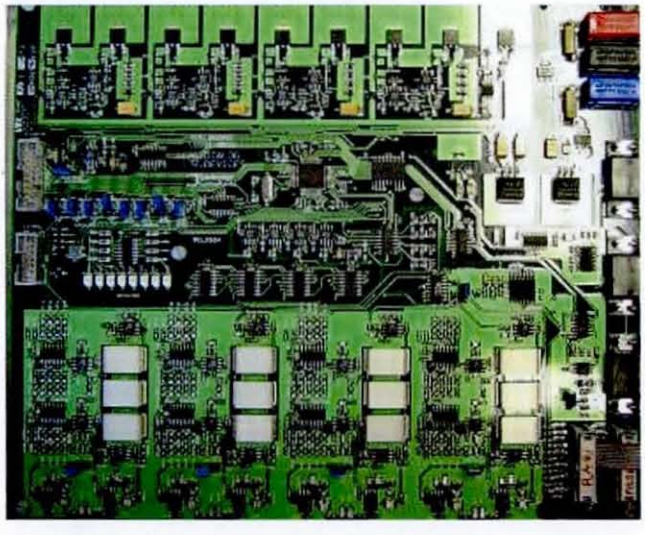

Figure 4.4 - DISCO4 PPG system board

4.2.2 Digital Pressure Modulation Control

The pressure modulation depth and frequency are important for the proper use of the artificial venous pulsation in two ways:

1) The pressure modulation depth (pressure of the cuff) must be below the arterial systemic pressure otherwise the modulation will also appear in arteries, resulting in higher venous oxygen saturation values, as described by the model in chapter 3. At the same time, the modulation depth should be large enough to introduce artificial pulsations in the venous flow.
2) The pressure modulation frequency must be away from the heart frequency in order to make the artificial venous pulsations distinguishable via conventional filtering techniques. Furthermore, according to signal theory, the arterial signal will present harmonic components at multiples of the heart's frequency, e.g. if the heart beats at 60 beats per minute, that means that there will be one beat per second. In arterial signal terms, there will be a change of light intensity at the PPG probe every one second, therefore in the frequency domain there will be a signal component at 1Hz. The harmonics of the arterial signal will therefore appear at 2Hz, 3Hz, 4Hz and so on. Although harmonics become smaller and smaller as they become more distant from the fundamental frequency of the heart, they can be significant in terms of amplitude and possibly comparable to the amplitude of the pressure modulated venous signal. The amplitude of the harmonics depends on the morphology of the PPG signal, and more specifically most of the harmonics are due to the dichrotic notch[77]. Therefore, the modulation frequency should lie between harmonics, in order to avoid overlapping of the venous signal with harmonics of the arterial signal, which would lead to false readings.

4.2.2a Pressure System Configuration

The method of creating the pressure modulation was designed in a similar way to the first generation system by employing a miniature air pump and a pinch valve. The air pump provides the air which inflates the cuff and a two-way pinch valve controls the flow of air in and out of the finger cuff, in order to create pulsations of the cuff which in turn, are transmitted mechanically to veins and other biological structures. The arrangement of the pressure modulation system is shown in figure 4.5. The diaphragm air pump (NMP50KNDC-12V, KFN Neuberger GmbH) is

driven from a pulsed voltage source, which is controlled in a microcontroller. The air pump can provide up to 4 l/min and can reach a maximum pressure of 0.5bar (or 375mmHg). The output air flow of the air pump is proportional to the rotation speed of the air pump motor hence the cuff's pressure is partially controlled by the air pump's air flow. The other parameter that affects the cuff pressure is the length of the pinch valve pulse which is driven from a pulsed voltage source, controlled by a dedicated microcontroller.

There are infinite combinations of air pump speed and pinch valve pulse length in order to achieve the desired cuff pressure during a full cycle. However, not all combinations are practicable as one must also consider the length of the tubing between the device and the cuff which will need some certain time before pressure can be built up. After extended experimentation in order to find the right pinch valve pulse width, it was concluded that a square pulse waveform with a 50% duty cycle was the most appropriate for the given application and for the range of tubing length used with the device, which can be up to approximately 4m long.

The pressure modulation is created through the switching of a two-way pinch valve (075P3MP12-02B, Bio-Chem Valve Inc) as shown in figure 4.5. The valve has two ports which open and close in anti-phase. When port one is open, port two is closed and vice-versa, allowing air in and out of the modulation cuff.

Starting from the top left corner of figure 4.5, air is supplied by the miniature air pump and fed to an expandable reservoir which has dual purpose: a) to dampen any air pulsations originating from the membranes of the air pump, and b) to build up pressure during the deflation phase of the cuff.

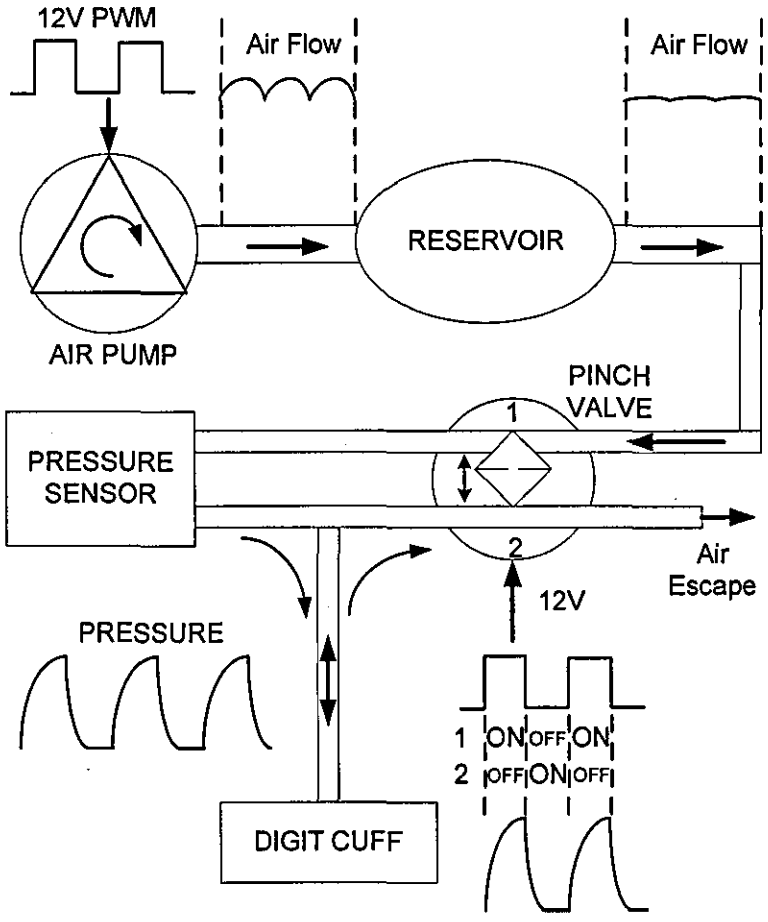

Figure 4.5 - Pressure modulation system

The following sequence describes the principle of operation:

1) This phase is applicable when the modulation is first switched on. The air pump is operating and supplying air. Port 1 of the pinch valve is closed therefore air supplied by the pump is stored in the reservoir. Port 2 of the pinch valve is open therefore the digit cuff is deflated.
2) The air pump continues to supply air, port 1 opens allowing air into the cuff and at the same time port 2 closes restricting outflow from the cuff. The digit cuff builds up pressure and exercises force around the finger, altering the venous flow, thus creating an artificial pulse in the venous system.
3) The air pump still supplies air, port 1 closes allowing the reservoir to build up pressure, and port 2 opens allowing air out of the digit cuff. The cuff has

now completed a full inflate-deflate cycle which caused a full cycle of the venous signal.

Phases 2 and 3 occur continuously one after the other providing a continuously changing venous waveform, similar to the natural pulsatile waveform found in the arteries but different in frequency. For example when the venous modulation is set at 8Hz, then a full inflation-deflation cycle would last 1/8 s, hence at 50% duty cycle of the valve driving pulses, each phase would last 1/16 s.

4.2.2b Control Board Communication Protocol

In contrast to the first generation prototype, the second generation prototype has real-time control of the modulation system allowing the setting of the cuff pressure and the modulation frequency to the desired values. The heart of the system is the electronic control board which provides serial communication (RS232 protocol) with a computer and controls the air pump and the pinch valve digitally. The core components are two PIC μcontrollers (16F876A and 16F628A, MicroChip) both driven via a 20 MHz crystal oscillator. The 16F876A provides the serial communication, digitises the pressure sensor signal, and controls the LCD message screen and the air pump via PWM (Pulse Width Modulation) and drives the second μcontroller (16F628A) which in turn, controls the pinch valve.

The control board is connected through the PPG DISCO4 board to the computer via a single USB connection and communicates bi-directionally via the RS232 protocol. The control board communication protocol was designed in the same way as the PPG board protocol in the sense that the computer can send commands to either change or read a value, such as air pump speed or pinch valve operating frequency. Furthermore, the command syntax is the same allowing for easy software implementation and modification. In order to distinguish whether a command is destined to the PPG or the control board, each one was assigned an ID, with the PPG board being ID1 and the control board ID2. Therefore, each time there is a valid packet with ID=2, the control board reads and executes the command;

otherwise the command is ignored. The communication protocol is described in Table 4.1.

Table 4.1 - Control board communication protocol

Command description	Command PC to Board	Reply Board to PC	Value Range
Set air pump speed	=2AXX<CR>	2A:0XXOK<CR>	00≤XX≤FF
Read air pump speed	?2A<CR>	2A:XX<CR>	00≤XX≤FF
Set valve frequency	=2BXX<CR>	2B:0XXOK<CR>	00≤XX≤07
Read valve frequency	?2B<CR>	2B:XX<CR>	00≤XX≤07
Read pressure value (HN)	?2C<CR>	2C:XX<CR>	00≤XX≤03
Read pressure value (LN)	?2D<CR>	2D:XX<CR>	00≤XX≤FF
Send LCD Control command	=2EXX<CR>	2E:0XXOK<CR>	00≤XX≤FF
Read LCD Control command	?2E<CR>	2E:XX<CR>	00≤XX≤FF
Send LCD Data command	=2FXX<CR>	2F:0XXOK<CR>	00≤XX≤FF
Read LCD Data command	?2F<CR>	2F:XX<CR>	00≤XX≤FF

The packet handling is briefly outlined with a flow chart in figure 4.6.

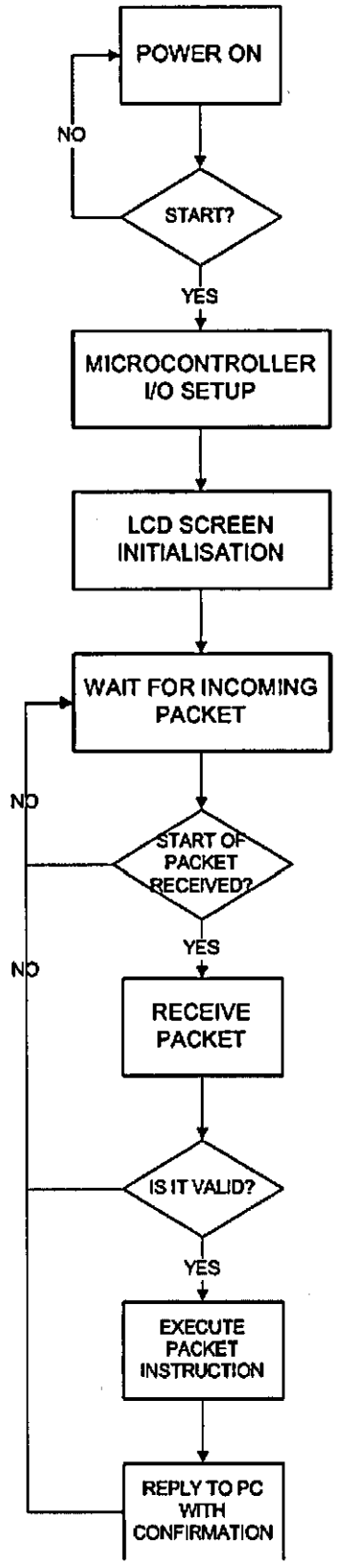

Figure 4.6 – Flowchart of the control board packet handling

Referring to figure 4.6, as soon as the μcontroller receives the first character, it checks if it is the "start of packet" which is either character '=' (set command) or '?' (read command). If the received character is neither of the two, it goes back to the beginning and waits for the next "start of packet", otherwise it proceeds to the next step which is to check if the next character is equal to the control board ID, which is set to '2'. If the character is not equal to '2' it exits and returns to the beginning, else it continues to the next step which is to check which register is to be set or enquired. Register 'A' is for air pump speed, 'B' for valve frequency, 'C' and 'D' for pressure sensor value (read-only), 'E' for LCD screen control and 'F' for LCD screen data. After the μcontroller has read which register needs reading or writing it proceeds to the next step which is either to retrieve the current value from the corresponding register (if it is a 'read' command), or to update the value of the corresponding register (if it is a 'set' command). In either case, the μcontroller will reply back to the computer to acknowledge that the command has been read and executed properly, by sending back a similar packet with the ID number, the register which has been set or read and the new value of the register. If the packet values are out of range or if characters are missing from the packet, the board replies back with the word 2:ERR.

Through this simple procedure the computer can check whether the new register value was properly updated. This method of data packet hand-shaking makes the use of hardware hand-shaking redundant, since the computer can detect problems in the communication channel or in the control board by checking if the sent and the received values are matching. Therefore the serial connection channel only requires three wires: RX (receive), TX (transmit) and ground reference. Since the embedded RS232 hand-shaking facilities are not being used the transmission speed has been set to 9,600bps in order to maintain data integrity, although it has been successfully tested up to 115,200bps without errors, given that the cable length is very short.

4.2.2c Control Board System Architecture

The control board was built to provide means of digital control of the air pump and the pinch valve, as well as to be able to record the cuff pressure waveform. The board has two μcontrollers which provide serial communication, analogue-to-digital conversion (ADC), and digital control of the air pump and pinch valve, as well as general function input/output (I/O) ports which are provided for future use. The heart of the board is the PIC16F876A which belongs to the 8-bit PIC μcontroller family of MicroChip. It can be considered the master μcontroller of the board, as it performs the following tasks:

- Serial communication with the computer
- Encoding and decoding of data packets
- Analogue-to-digital conversion of the pressure sensor signal
- Air pump speed control
- LCD screen driver
- Communication with PIC16F628A

The second μcontroller (16F628A) can be considered as the slave μcontroller and drives the pinch valve at an adjustable operation frequency set by the master μcontroller. Referring to Table 4.1, the valve frequency set command may take values between hex'00' and hex'07' and this is because the frequency can be set at seven different levels. The method in which the frequency value is sent from the master to the slave μcontroller is shown in figure 4.7. The master μcontroller sets port outputs RC3, RC4 and RC5 (which are connected to RB5, RB6 and RB7 of the slave μcontroller respectively) according to the desired frequency and subsequently, the slave μcontroller reads inputs RB5, RB6 and RB7 and sets the valve frequency to the corresponding value.

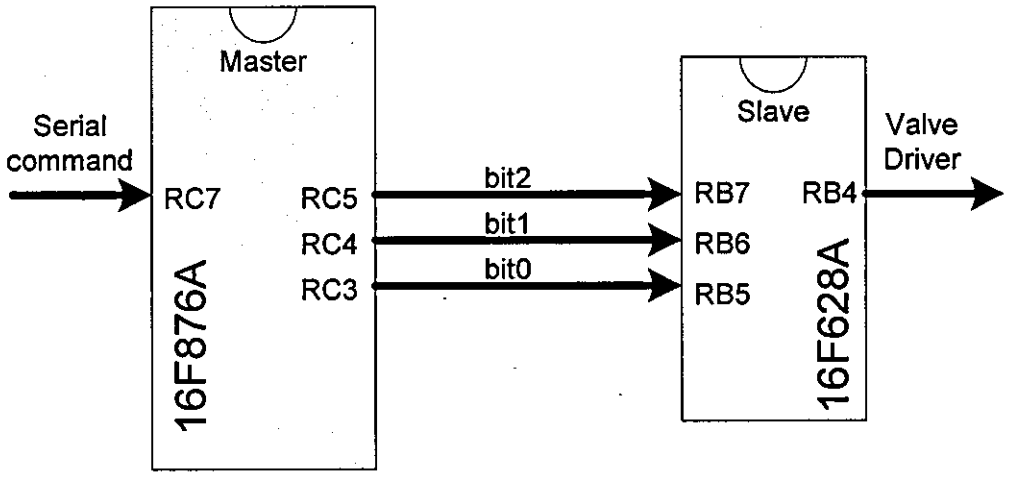

Figure 4.7 - Communication between master and slave µcontrollers

Table 4.2 outlines the range of frequencies and the relevant commands. The maximum frequency is set to 8Hz because beyond this point the frequency response of the tissues is poor, acting as a low-pass filter, hence the artificial pulsations cannot reach efficiently the actual blood vessels. The minimum frequency of 6.45Hz was set to be as far away as possible from the harmonics of the heart, in order to avoid overlapping with significant arterial frequency components.

Table 4.2 - List of valve frequencies and corresponding serial commands

Frequency Selection (Hz)	Serial Set Command	Configuration Bits	On-Off Cycle Time (s)
OFF	=2B00<CR>	000	0
6.45	=2B07<CR>	111	0.155
6.67	=2B06<CR>	110	0.150
6.90	=2B05<CR>	101	0.145
7.14	=2B04<CR>	100	0.140
7.41	=2B03<CR>	011	0.135
7.69	=2B02<CR>	010	0.130
8.00	=2B01<CR>	001	0.125

The importance of frequency configurability lies in the fact that when harmonics of the heart overlap with the fundamental artificial venous components, the result is false venous oxygen saturation readings. Figure 4.8 illustrates a case where the heart rate is 60 beats/min (1Hz) with the artificial venous modulation being set at 7Hz. If the PPG signal is analysed to its frequency components it can be made clear that the 6th harmonic of the arterial signal will overlap with the artificial venous modulation signal. This will cause implications in the accuracy of the venous oxygen saturation value, since part of the signal at 7Hz will be originated from the arterial signal.

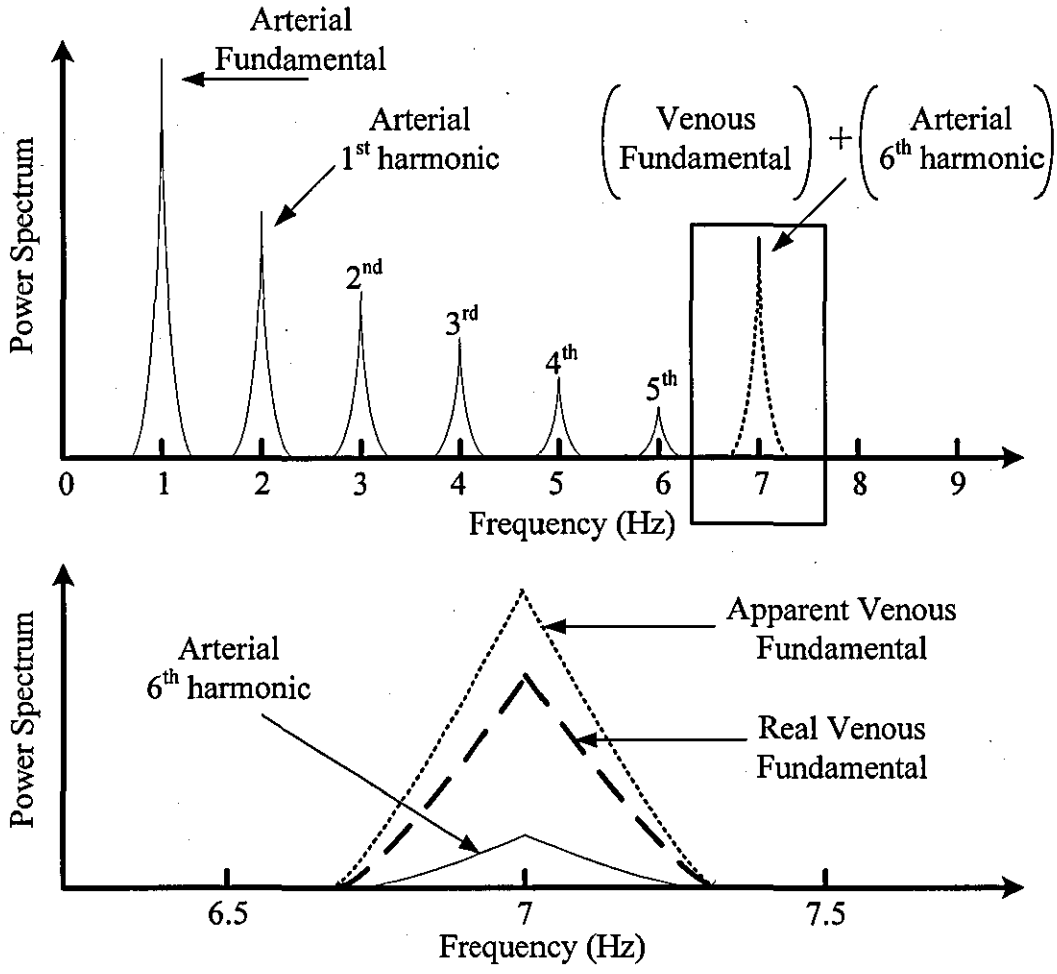

Figure 4.8 - Arterial harmonic overlapping with the fundamental venous

By constantly measuring the heart rate, the system can adjust the frequency of the artificial venous modulation in order to avoid this unwanted effect. Figure 4.9

shows how the overlapping can be avoided by shifting the modulation frequency to the right by 0.5Hz. Hence, by applying a narrow band-pass filter to the PPG signal, the venous signal component can be safely recovered.

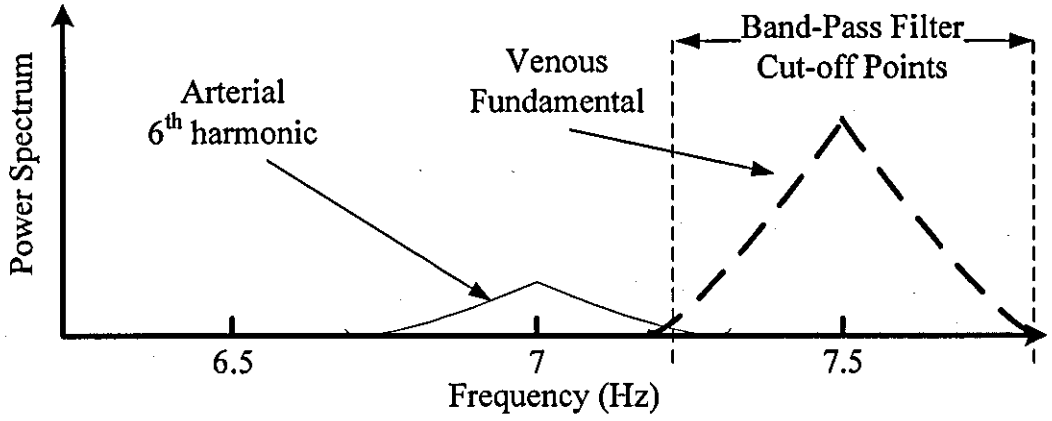

Figure 4.9 - Avoiding overlapping effects by shifting the modulation frequency

Although the modulation frequency is extremely important to the accuracy of venous oxygen saturation values, attention must also be paid to the strength of the modulating pulse. The previously explained effects of inflating the modulating cuff at high pressures can be overcame by controlling the air pump speed. Although there is a large difference between arterial and venous blood pressure in normal physiological conditions, it is sufficient to keep the cuff pressure close to the venous pressure. However, in non-clinical environments it can be difficult or time-consuming to obtain venous and arterial blood pressures therefore it is not entirely safe to assume that arterial modulation does not occur at a low cuff pressure, since arterial pressure in critically ill patients can drop dramatically. On the other hand, a higher modulation pressure will be needed should the venous pressure raises above normal levels. Given the fact that the complex human cardio-vascular systemic governed by the sympathetic and parasympathetic nervous system is extremely dynamic, certain parameters such as venous blood pressure could diverge from normal values and hence require particular attention when performing measurements.

The level of cuff pressure (modulation depth) is configurable digitally via the serial communication of the control board with the computer, in 255 steps. The master μcontroller drives the mosfet which powers the air pump with PWM, which is a continuous train of square pulses with a fixed frequency of 2.46kHz but with different duty cycles. Examples of PWM are shown in figure 4.10.

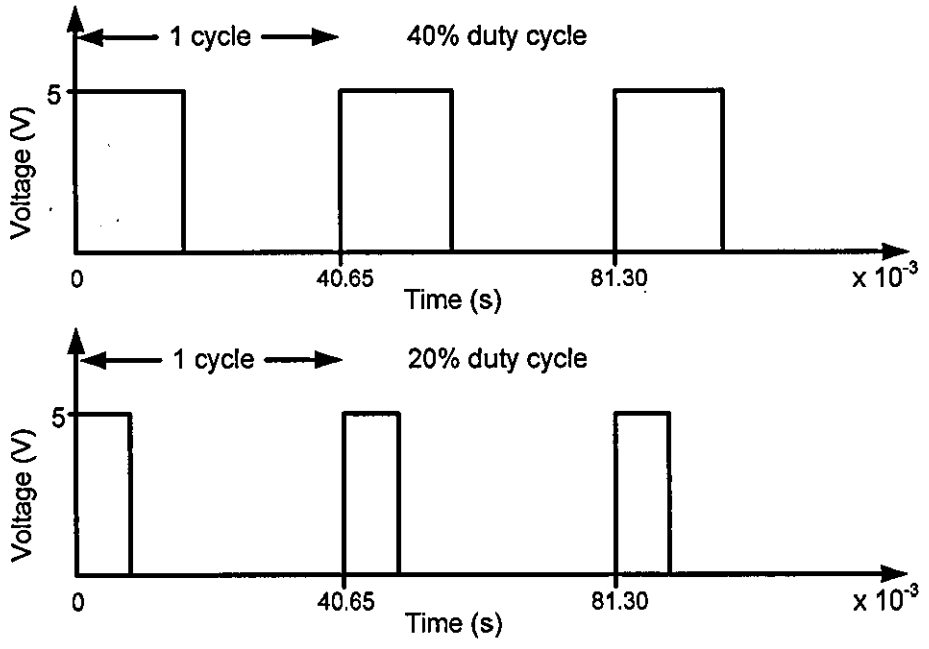

Figure 4.10 - Examples of PWM provided to the air pump driver

The air pump response is linear therefore in the first example shown in figure 4.10, the air pump provides double the volume of air in comparison with the second example. Altering the length of the pulses essentially changes the average voltage applied to the air pump. The master μcontroller's PWM signal drives a mosfet (IRF520) via an opto-coupler (TPL250) in order to avoid back-EMF induced by the air pump's motor, as shown in figure 4.11. The opto-coupler's LED is driven through a current limiting resistor from the master μcontroller's PWM output. The signal is optically coupled to the receiver end and then fed into the MOSFET's Gate. Diode D1 is forward biased in order to suppress back-EMF coming from the air pump's inductive load and capacitor C1 reduces dV/dt in order to reduce the magnitude of the air pump's back-EMF. The pinch valve, operated through an

identical driver, is a solenoid operated valve and applies an inductive load to the MOSFET, therefore a similar design to the air pump was implemented.

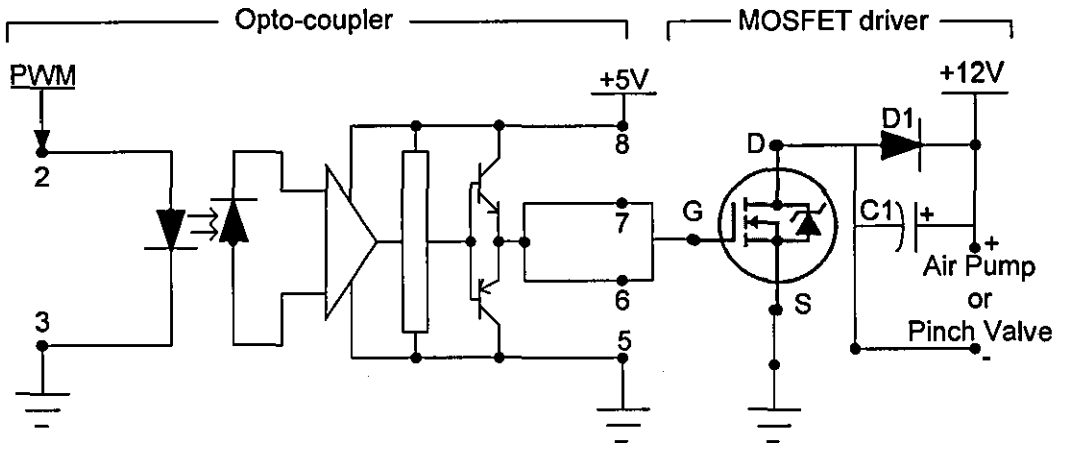

Figure 4.11 - Air pump and pinch valve opto-coupled MOSFET driver

When the control board is first switched on, the master μcontroller runs through the initialisation routine, part of which is the default setting 'OFF' of the pinch valve by setting RC3, RC4 AND RC5 outputs to logic '0'. The PWM generator is also switched off initially, which means both the pressure modulation system is switched off. In order to set the air pump speed to the desired level, a serial command must be sent from the computer, as in Table 4.2. For example, to set the air pump to maximum speed (therefore maximum cuff pressure) the following command must be sent:

=2AFF<CR>

which results in a PWM of 100% duty cycle, or in other terms, it provides a DC voltage. If the desired duty cycle were 50%, then the nearest hexadecimal value required would be:

50% × decimal'255' ≈ decimal'128' = hex'80'

Therefore, the serial command would be:

=2A80<CR>

The control board provides 8-bit resolution for the cuff pressure setting. The current configuration of the pressure system can provide up to 130-150mmHg of pressure depending on the size of tubing, hence a pressure resolution of approximately 0.5mmHg is achieved with the current system.

The most important functions of the control board were described in this section, with a particular interest in the management of the air pump and the pinch valve to drive the digit cuff with proper pressure at the right frequency. Other tasks performed by the board are the control of the LCD message screen and monitoring of the cuff pressure by digitising the pressure sensor output signal. The master µcontroller performs 10-bit analogue-to-digital conversion and stores the pressure value in a memory register, which is continuously compared to a software configurable threshold value stored in the µcontroller, in order to provide a fail-safe mechanism in the case something should go wrong in the system; i.e. the air pump will be immediately switched off, if the cuff pressure supersedes the threshold value.

In terms of the configurability, the control board was designed in such a way to provide expansion ports for future experiments, such as generic digital I/O ports, analogue comparators and analogue I/O ports. Moreover, the master µcontroller firmware incorporates a boot-loader (Tiny Bootloader), providing an easy way to quickly update the function of the control board via USB, without having to remove the chip from the circuit board for programming. Hence the second generation prototype, a fully configurable system via a single USB connection, provides versatility and expandability.

4.2.3 Data Acquisition System and Software

The control software is based on the LabView (National Instruments Inc) software platform, which provides a fast way to interface a computer with external systems as well as to design virtual instruments. The control application has been designed

with a simple user interface to allow operation of the system by non-experts. Additionally, the touch-screen provides easy operation without the need for a mouse or keyboard adding more versatility to the system. The control software can control the artificial venous modulation in real time and raw signals along with processed values are displayed on the screen. Additionally, processed values are logged and displayed on a history window which can display all the processed parameters by selecting the corresponding button on the user interface.

Raw data are acquired by a data acquisition board (DAQ) which provides 14-bit resolution. Logged data include:

- Red and Infrared *AC* and *DC* PPG signals
- Pressure sensor signal
- 2x Temperature probe signals
- Control board supply voltage

The PPG signals are separated into *AC* and *DC* signals. The *DC* signals represent the static components of the finger and the *AC* signals represent dynamic light absorbing components such as arterial blood, and venous blood when the pressure modulation operates. Figure 4.12 shows a typical set of PPG signals and the pressure sensor signal, when the pressure modulation operates. The correlation between the pressure sensor signal and the *AC* signals is noticeable, while the presence of small amplitude changes in the *DC* signals as highlighted is attributed to the arterial pulsations. The *AC* signals are essentially extracted from the *DC* signals, after removal of the offset and subsequent amplification. The raw signals are filtered in software and subsequently stored in the computer's hard disk, while they are also used in real-time to calculate arterial and venous oxygen saturation values, heart rate and signal quality indices.

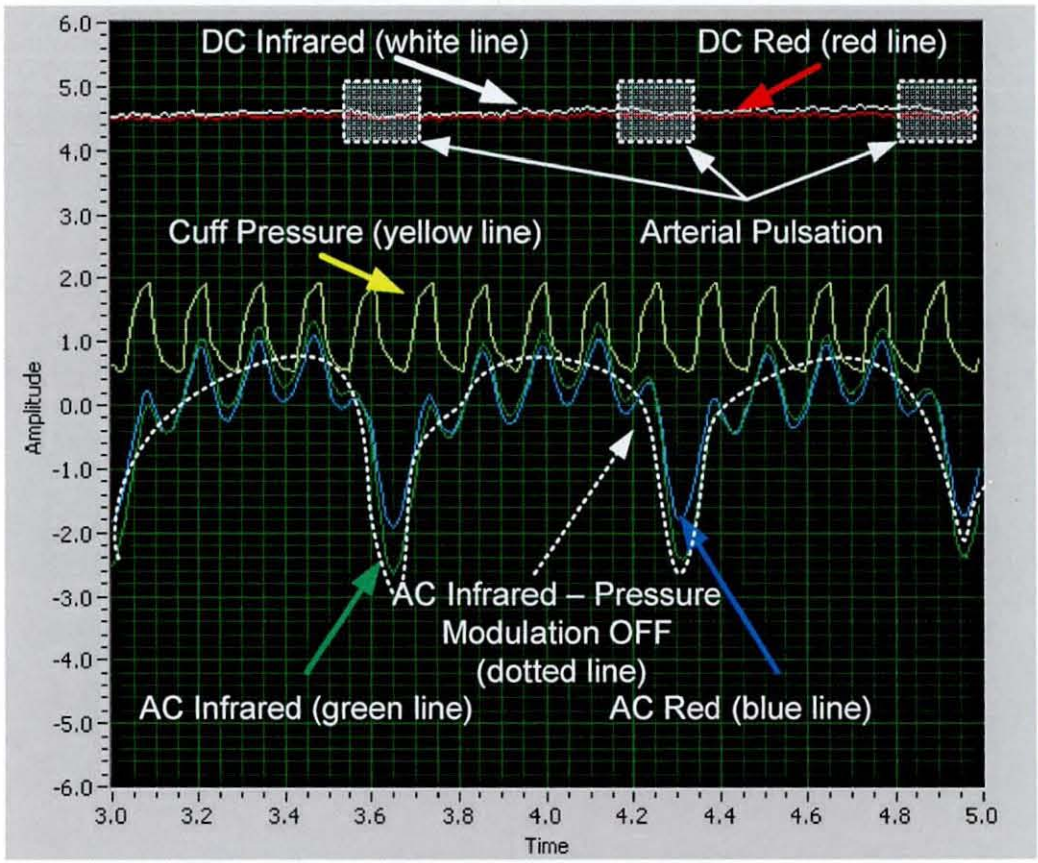

Figure 4.12 - Typical raw signals

The DAQ performs analogue-to-digital conversion of the PPG signals, the pressure sensor signal output and the two temperature probe signals. The analogue PPG signals have a range of values between -10V and +10V, therefore the DAQ's 14-bit resolution can provide

$$resolution = \frac{\text{Voltage Range}}{\text{Conversion Levels}} = \frac{10-(-10)}{2^{14}-1} = \frac{20}{16384-1} \cong 1.22\text{mV}$$

In a typical configuration of the system, $AC_{pk\text{-}pk}$ and DC_{avg} values are ideally set between 4V and 6V therefore the resolution of the digitised signals is approximately 5mV. The pressure sensor signal is also connected to an analogue input of the DAQ, as well as the two temperature probes, the purpose of which is to monitor the temperature at two different sites of the body, for example centrally in the armpit and peripherally on the measured finger. The change of temperature peripherally

will most likely indicate change in blood perfusion[74]. Figure 4.13 illustrates the basic processing path of the signals.

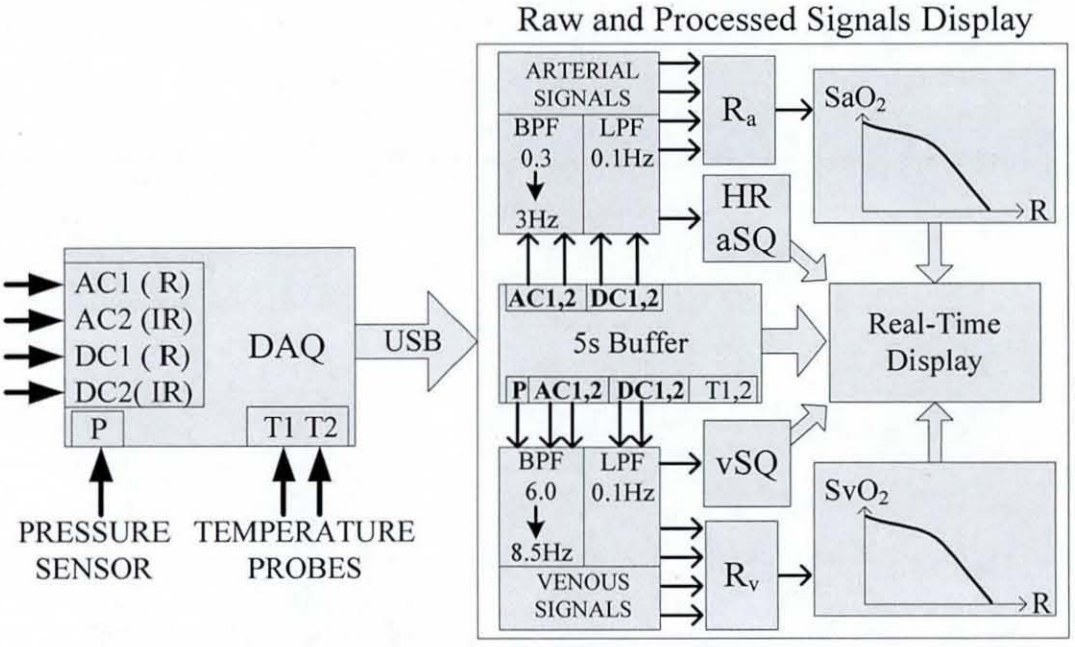

Figure 4.13 – Block diagram of signal processing path. Both arterial and venous signal filters are 10th order IIR Butterworth.

The graphic user interface design was based on commercial clinical monitors in an attempt to provide a comparable simplicity. The interface provides real-time display and history of calculated parameters (updated every 5s) as well as continuously plotted raw PPG signals. Additionally, the FFT of the raw signals is also available to provide detection of modulation sidebands, which indicate the modulation of arterial blood besides venous blood. Figure 4.14 shows the graphic user interface and the following parameters are shown on the right hand side of the screen:

- SaO_2 – Arterial oxygen saturation %.
- SvO_2 – Venous oxygen saturation %.
- HR – Heart rate in beats/min.
- P – Average cuff pressure in mmHg.
- Tm, Tp – Central and peripheral temperature in °C, respectively.
- aSQ and vSQ – Arterial and venous signal quality index, respectively.

Figure 4.14 - Control software graphic user interface

SaO_2 and SvO_2 are calculated from an empirical calibration formula, after the ratio-of-ratios R has been obtained from the AC and DC signals at two wavelengths. The relation between SaO_2, SvO_2 and R is given by equation 4.1[78]:

$$Sa(v)O_2 = \frac{1000 - 550R}{900 - 350R}\% \qquad \textbf{[4.1]}$$

HR is calculated by detecting the peaks and troughs of the AC signals and subsequently measuring the time t between two successive pulsations. The heart rate[79] is given by equation 4.2:

$$HR = \frac{60}{t} \qquad \textbf{[4.2]}$$

Pressure is calculated from the pressure sensor signal and is an average value. The sensor's output is fully conditioned and temperature compensated, providing a calibrated value with a maximum error of ±2%. The output signal has a 0.5V offset and it provides 0.8V/PSI (pounds of force per square inch, 1 PSI = 51.7149mmHg), therefore in order to obtain a reading in mmHg the following formula must be applied:

$$P_{\text{mmHg}} = \frac{V_{out} - V_{offset}}{0.8} = \frac{V_{out} - 0.5}{0.8} \times 51.7149 \qquad \textbf{[4.3]}$$

The temperatures are calculated from the calibration curve of the temperature probe's datasheet (adult temperature skin probe 37904, Viamed Ltd). The resistance of the probe is converted to voltage in a voltage divider configuration. Figure 4.15 shows the connection method of a temperature probe:

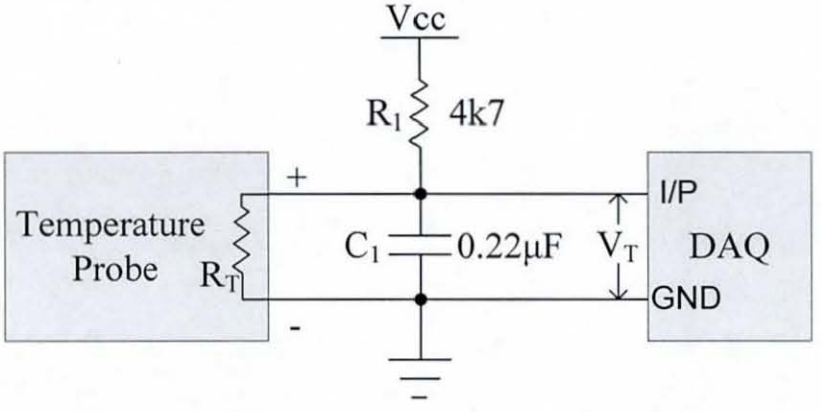

Figure 4.15 - Temperature probe configuration

From Ohm's Law[80], the voltage across the temperature probe is given by:

$$V_T = \frac{R_T}{R_T + R_1} \times Vcc \qquad \textbf{[4.4]}$$

The temperature probe's resistance response (from the datasheet) to temperature is shown in figure 4.16, while a calibration curve relating V_T and temperature can be produced from equation 4.4, as shown in figure 4.17.

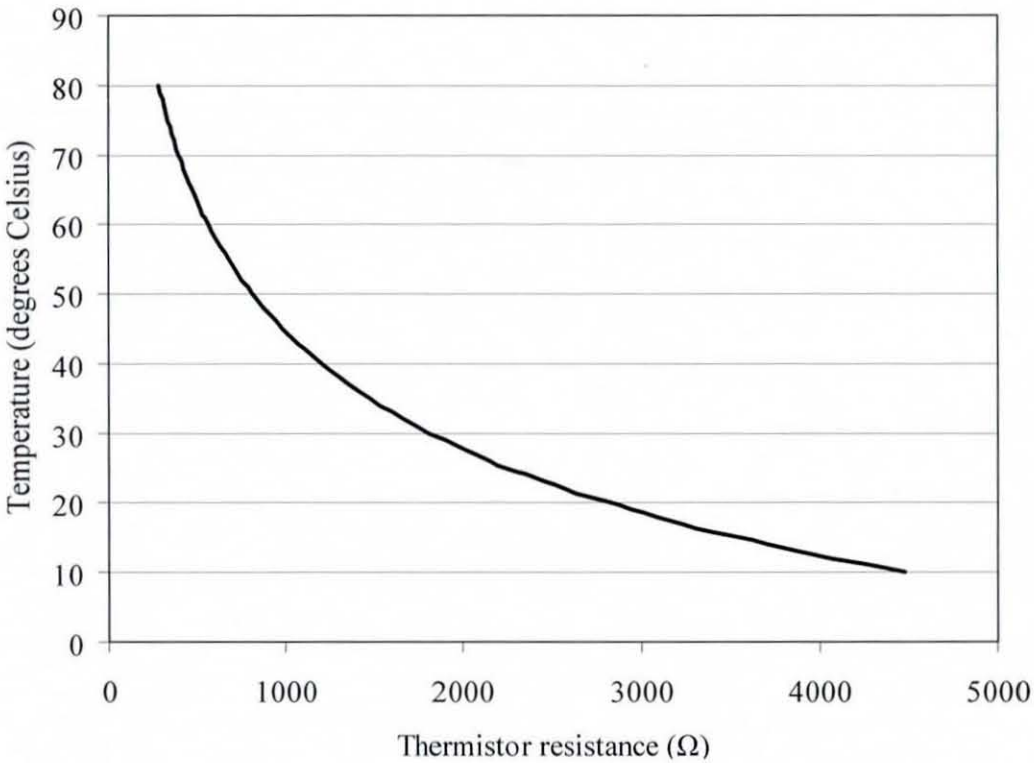

Figure 4.16 - Temperature probe resistance response to temperature

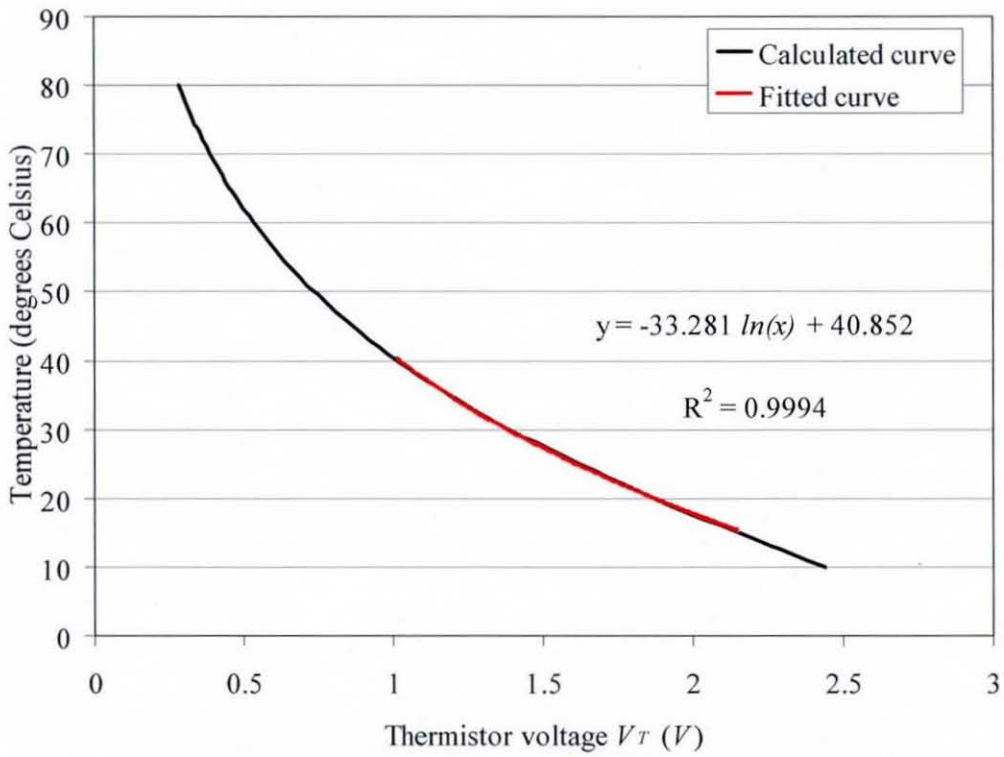

Figure 4.17 - Temperature probe calibration curve

Furthermore, the voltage-temperature curve in the range of interest (15°C-40°C) can fairly accurately (R^2=0.9994) be fitted to logarithmic equation 4.5, which can be used to convert the probe's voltage to temperature (°C) :

$$T = -33.281 \times \ln(V_T) + 40.852 \ ^{\circ}\mathrm{C} \qquad \textbf{[4.5]}$$

The arterial and venous signal quality indices are correlation coefficients; in the case of arterial signal, the signal quality index is the correlation coefficient between the band-pass filtered (0.3Hz-4Hz) red and infrared AC signals, while the signal quality index for the venous signal is calculated from the correlation between the band-pass filtered (6.0Hz-8.5Hz) infrared signal and the pressure sensor output signal, processed through the same filter.

The top waveform chart displays the raw PPG signals providing visual indication of the signal quality, while the bottom window displays the history of each parameter. For example, to see the history graph of SvO_2, a touch on the SvO_2 value would show the graph and highlight the SvO_2 box in grey colour. The same window is used to display the FFT plot of the infrared AC signal upon activation from a hidden button, for a more technical representation of the signals. The history chart has control buttons to zoom into specific parts of the history chart or to move the chart forwards or backwards in time.

The control of the pressure modulation is made via three buttons; one button activates/deactivates the modulation and sets the pressure to a default value (10mmHg), and two buttons are used to increase or to decrease the modulation depth, which is the digit cuff pressure. The maximum pressure permitted can be configured in software in order to avoid excessive pressure levels, which would lead to erroneous venous oxygen saturation values.

Data logging can be initiated by pressing a button on the screen, after entering identification data for the recording, which are subsequently logged as a header in

the data files. Data are stored in real-time instead to keeping them in the memory and purging them in a file at the end of the recording, hence providing virtually unlimited logging capacity. Logged data are stored in two separate files; one file contains all the raw data sampled at 128Hz for further processing if required, and the second file contains all the processed data as shown in figures 3.18 and 3.19.

Patient's Name: test-2-1
This is the Raw Data Logger
Acquisition Started at: 14:51:28 on: 21/05/2007
Ended at: 14:55:31 on: 21/05/2007
Sample rate in samples/second: 128

IR DC	IR AC	R DC	R AC	Press
2.319	1.273	2.341	0.916	0.982
2.329	0.902	2.346	0.714	1.008
2.337	0.567	2.366	0.469	0.852
2.26	0.199	2.341	0.153	0.638
2.334	-0.159	2.364	-0.181	0.581
2.332	-0.428	2.351	-0.419	0.538
2.4	-0.492	2.308	-0.439	0.52
2.321	-0.272	2.397	-0.227	0.507
2.372	0.229	2.343	0.112	0.495

Figure 4.18 - Raw data file layout

Patient's Name: test-2-1
This is the Processed Data Logger
Acquisition Started at: 14:51:28 on: 21/05/2007
Ended at: 14:55:31 on: 21/05/2007
Refresh Time : 5

HR	SaO2	SvO2	Press	vSQ	aSQ	Tc	Tp	IrLED	RLED	Gain
99.9	96.6	91.7	12.7	95.2	98.6	0	0	255	255	9
104.8	96.5	93	12.8	95.7	98.7	0	0	255	255	9
94.8	96.4	91.1	12.7	95.6	98.5	0	0	255	255	9
94.5	96.7	92.6	12.7	97	98.5	0	0	255	255	9
99.2	96.5	92	12.9	95.8	98.3	0	0	255	255	9
102.3	96.5	90.9	12.9	95.5	98.5	0	0	255	255	9

Figure 4.19 - Processed data file layout

4.3 THIRD GENERATION PROTOTYPE– CURRENT VERSION

The third generation prototype was built as an embedded system without depending on external systems or computers. Apart from adopting the approach of designing a self-contained device, other significant improvements were implemented within the prototype device. An automatic pressure modulation algorithm was implemented, the PPG board was replaced by a miniature-sized board providing digital data without requiring a DAQ, and a mini-ITX computer system with a touch screen was installed within the custom designed enclosure. The result is a small-sized system powered from an external medically approved switch-mode power supply, virtually ready to go into the clinical setting for further evaluation of the non-invasive venous oxygen saturation measurement method.

4.3.1 Miniature PPG System

The PPG board previously employed in the second prototype was replaced by a miniature PPG board (Venox PPG, Shanghai Berry Medical), which supports up to four different wavelengths and provides all raw data in a digital format via a RS232 serial port. The communications protocol was designed in a similar way to the control board, while the implemented raw data packet syntax provides simple collection and storage and packet integrity check.

The PPG board is based on a PSoC Mixed Signal Array (CY8C27443-24PVXI, Cypress MicroSystems), which performs analogue-to-digital conversion (14-bit), digital signal filtering, LED driver control with ambient compensation and serial communication via the RS232 protocol. Its small size factor (80mm × 50mm) compared to the previously used PPG board (250mm x 210mm), as well as the low power consumption (0.5W) and its ability to operate from a single voltage supply rail (+5V), have permitted the design of a small-sized prototype. Additionally, the built-in analogue-to-digital converter has replaced the previously required DAQ resulting in a more straightforward system design. Figure 4.20 illustrates the miniature PPG board's basic operation principles and figure 4.21 shows the circuit board.

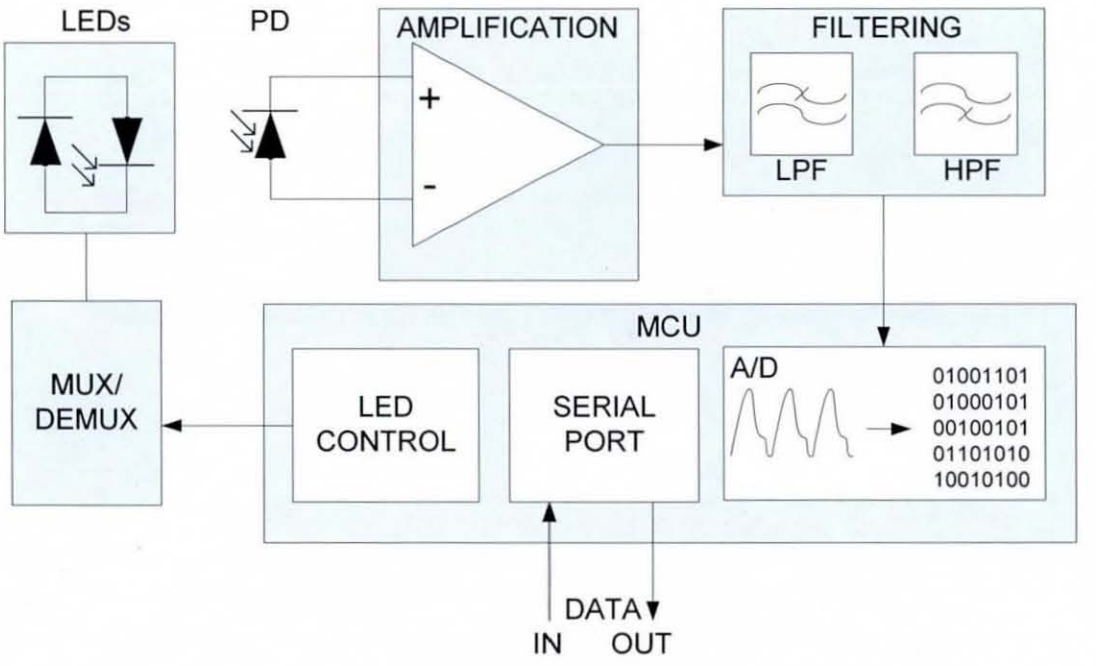

Figure 4.20 - Miniature PPG board operation block diagram (LPF is 3rd order $f_{cut\text{-}off}$= 0.1Hz; HPF is 3rd order $f_{cut\text{-}off}$= 0.5Hz)

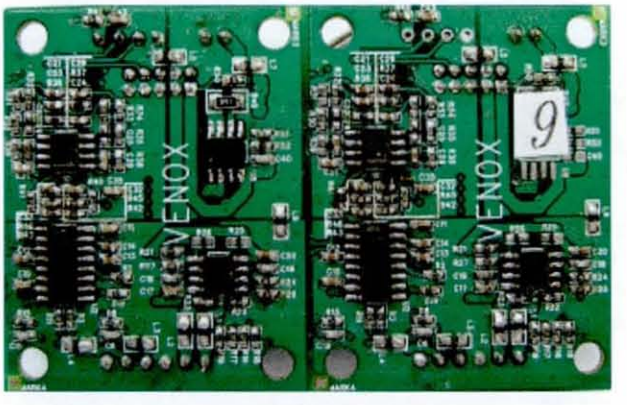

Figure 4.21 - Miniature PPG circuit board in real size (front side)

4.3.2 Automatic Digital Pressure Modulation Control

One of the targets of the third generation prototype design was automation therefore an improved pressure modulation system was designed which allows for automatic frequency selection of the artificial pulsations. The aim of the algorithm is to prevent the artificial modulation frequency from overlapping with the heart's

harmonics, as shown in figures 3.8 and 3.9. The software algorithm based upon the average heart rate calculated every 5s, checks the condition of equation 4.6[66].

$$f_{\mathrm{mod}\,ulation} \neq n \times f_{heart}\,,\ n \in \mathbb{N} \qquad \textbf{[4.6]}$$

Therefore by measuring the heart rate every 5s, the system calculates the harmonics and chooses the best modulation frequency possible, in terms of distance from the adjacent harmonics. For example, if the heart rate is 60 bpm, then f_{heart}=1Hz and its harmonics will be at 2Hz, 3Hz, 4Hz, 5Hz, 7Hz, 8Hz etc. Table 4.3 shows how the modulation frequency is selected.

Table 4.3 - Selection of best modulation frequency for heart rate = 60 bpm

Frequency Selection (Hz)	Left Harmonic (Hz)	Right Harmonic (Hz)	min(f_{mod}-$f_{harmonic}$) (Hz)
6.45	**6.00**	**7.00**	**0.45 (max)**
6.67	6.00	7.00	0.33
6.90	6.00	7.00	0.10
7.14	7.00	8.00	0.14
7.41	7.00	8.00	0.41
7.69	7.00	8.00	0.31
8.00	7.00	8.00	0.00

Hence, the best modulation frequency when the heart rate is 60bpm would be 6.45, since it will be as distant as possible from the nearby harmonics. A software algorithm calculates the heart's harmonics in the range between 6-8Hz and compares them with the available modulation frequencies (6.45, 6.67, 6.90, 7.14, 7.41, 7.69 and 8.00Hz), thus selecting the modulation frequency with the maximum value of the function $min(f_{mod} - f_{harmonic})$, as shown in table 4.3.

4.3.3 Embedded Acquisition System

The second generation prototypes required the use of data acquisition board in order to convert PPG analogue signals into digital data. The third generation prototype employs a miniature PPG board which features on-board filtering and analogue-to-digital conversion. The PPG board transmits data packets via a RS232 serial port to the computer, which is embedded with the rest of the system.

The data protocol was designed in such a way to provide data integrity check by means of checksum, while packets are clearly separated from each other with square brackets.

The PPG board outputs packets in HEX format, containing a single 12 bit value (3 HEX characters) for each of 8 output channels followed by an 8 bit checksum value (2 HEX characters). Each packet starts and ends with square brackets:

[AAABBBCCCDDDEEEFFFGGGHHHXX][AAABBB…]

where the signals are in the following order:

[$DC_1AC_1DC_2AC_2DC_3AC_3DC_4AC_4$XX]

XX is the data integrity segment (CHECKSUM), which will be calculated in the PPG board and then sent within the packet (XX). For a data packet, for example [1352F74E43B65FFAB1DA384B--] the checksum would be calculated as follows by the PPG board:

- Step 1: 13+52+F7+4E+43+B6+5f+FA+B1+DA+38+4B = 60Ah.
- Step 2: Drop carry nibble: 0Ah.
- Step 3: Get the two's complement of 0Ah = F6h. This is the checksum.

Therefore the packet will look like:

[1352F74E43B65FFAB1DA384BF6]

Data integrity can be checked in software in the following steps:

- Step 1: 13+52+F7+4E+43+B6+5f+FA+B1+DA+38+4B = 60Ah.
- Step 2: Add the Checksum byte (F6) to the sum (60A) to yield 700h.
- Step 3: Drop the carry nibble to get 00h.

Since the result is 00h, the packet has reached the computer without errors.

Regarding the control of LEDs and photodiode gain, the board accepts commands in the following format:

*Xnnn<CR> (<CR>=carriage return)

where X is the parameter to be changed and nnn is a number between 000 and 063 for the LEDs, and between 000 and 031 for the gains. The board confirms that it has received and executed the command by replying:

XnnnOK

Table 4.4 shows the registers for each parameter:

Table 4.4 - Control registers of the miniature PPG board

Register	Parameter	Register	Parameter
A	LED1	B	Gain1
C	LED2	D	Gain2
E	LED3	F	Gain3
G	LED4	H	Gain4

For example, to set Gain1=10 (decimal), the command would be:

*B010<CR>

The board acknowledges receipt of the command by replying between packets:

[…]B010OK[…]

Therefore the board is fully controllable via a serial connection with the computer, set at 115,200 bps.

4.4 OVERVIEW

Over the course of investigating this non-invasive venous oximetry method, a number of changes have been made to both, software and hardware. The first generation design was a large and very heavy prototype (figure 4.1), lacking real time control, display and signal processing, all of which had to be done off-line. Additionally, the complexity of the system required the assistance of someone familiar with the technology in order to operate the system. One of the most important issues when recording is the signal quality and the strength of the modulation depth, both very important in the degree of accuracy of the method.

Figure 4.22 - Third generation prototype

After several stages of development, the third generation prototype is easy to be operated by clinicians, facilitating the fast data acquisition on a large scale clinical trial. Moreover, by providing real-time processed data such as oxygen saturation, heart rate, temperature and signal quality index, it is extremely fast to produce statistical numbers from the automatically generated log files using standard statistics software packages. Hence, clinicians and medical statisticians can produce

results from a clinical trial without the need for post-processing of the raw data. While a large-scale trial would previously take long periods to complete, it can now be completed in a fraction of the time by providing more prototypes to be operated by clinicians.

5 EXPERIMENTAL INVESTIGATION

The non-invasive method for measuring venous oxygen saturation has been evaluated in four different ways:

- With an in-vitro experimental setup to perform a comparative calibration with a commercial pulse oximeter.
- In the laboratory with a series of experiments in order to investigate the hypotheses of the theoretical model.
- In the laboratory setting with 13 volunteers participating in venous oxygen de-saturation study, with blood gas analysis facilities.
- In the clinical setting, with 23 patients undergoing heart surgery and the heart-lung machine monitor employed as the gold standard.

All data have been post-processed with functions written in Matlab, although real-time signals and values of processed parameters were available during data recording. Results from the experiments are presented in separate sections further in this chapter.

5.1 IN-VITRO COMPARATIVE CALIBRATION

A comparative calibration against a commercial pulse oximeter (Nonin 8600, Nonin Medical Inc) was performed by employing a simple finger phantom. A Nonin Finger Phantom diffuser shown in figure 3.9 was used as a scattering medium, and a set of light absorbers inside a custom-made cuvette shown in figure 3.10 simulated the changing absorbance of blood against different oxygen saturation values.

5.1.1 Experimental Purpose, Protocol and Setup

The finger model was constructed from a pair of 1mm thick glass slides cut 16mm x 76mm x 3mm (width × height × depth). A chamber was formed between the two slides using double-sided high density sponge tape of 1mm thickness, following the contour of the glass to form a watertight container of 1mm thickness, figure 3.10. The entry to the container was kept open to administer the light absorbing solutions and the glass container was then inserted in the Nonin light diffuser shown in figure 3.9 to form the optical phantom. The aqueous solutions were prepared with Methylene Blue (MB, or India Ink) and Cupric Sulphate Pentahydrate ($CuSO_4.5H_2O$) which have different light absorption properties. Figure 5.1 illustrates the stock solutions' absorption curves.

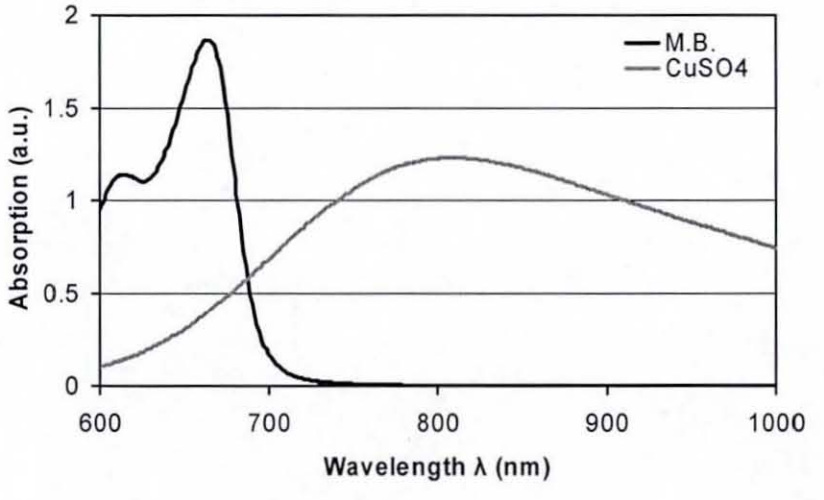

Figure 5.1 – Absorption curves of Methylene Blue and Cupric Sulphate Pentahydrate in water

A total of 11 different solutions were prepared in order to simulate varying values of oxygen saturation. The high concentrations of the solutions ($0.033x10^{-3}$M for MB, and 0.1M for $CuSO_4.5H_2O$) as well as the significant scattering properties of MB have not permitted the agreement between calculated and measured absorptions. The non-negligible scattering of MB can cause errors in optical phantom work if the ink is assumed to be a pure absorber, due to overestimation of the absorption if this is determined using spectrophotometry[81]. This was also confirmed when measuring the calibration solutions with a spectrophotometer (UV-1650PC Shimadzu, Japan). Hence, the calibration solutions were made empirically by starting with a 0.1M solution of $CuSO_4.5H_2O$ and gradually adding MB until the required reading on the Nonin oximeter was reached.

Since the method employs a 6.5-8Hz artificial venous pulsation, it would be preferable to squeeze the phantom at this frequency range but the mechanically induced motion artefacts and the fact that the commercial oximeter is designed to operate within the human heart rate range, could raise questions about the accuracy of SpO_2 readings. The method processes the high-frequency pulsations (6.5-8Hz) in the same way as heart pulsations to obtain *AC* and *DC* levels with different filters (BPF 0.3-4Hz for arterial pulsations, BPF 6-8.5Hz for venous pulsations), hence a "low-frequency" calibration (1Hz phantom pulsations) was assumed to be sufficient to investigate the level of agreement between the commercial oximeter and the proposed method when measuring oxygen saturation, in general.

The phantom was mounted upright in a pulse oximetry finger probe, then the top part of the watertight container was lightly squeezed rhythmically once per second to mimic the pulsatile blood signal by creating small liquid displacements, emulating a typical pulse oximetry signal. The oximeter saturation values (SpO_2) were recorded every 10 seconds for a period of 2 minutes, and this experiment was repeated five times to investigate repeatability. The proposed method's probe was then connected to the finger phantom and the above procedure was repeated; recorded R values were converted to SpO2 values by using the empirical calibration equation 5.1 with $\alpha=1000$[76].

$$SpO_2 = \frac{\alpha - 550R}{900 - 350R} x100\% \qquad \textbf{[5.1]}$$

5.1.2 Experimental Results

The comparative calibration results have shown excellent repeatability with no significant deviation and a very close correlation between the prototype device and the Nonin oximeter. Figure 5.2 illustrates the calibration curves based on equation 5.1 before (VENOX U) and after (VENOX C) comparative calibration.

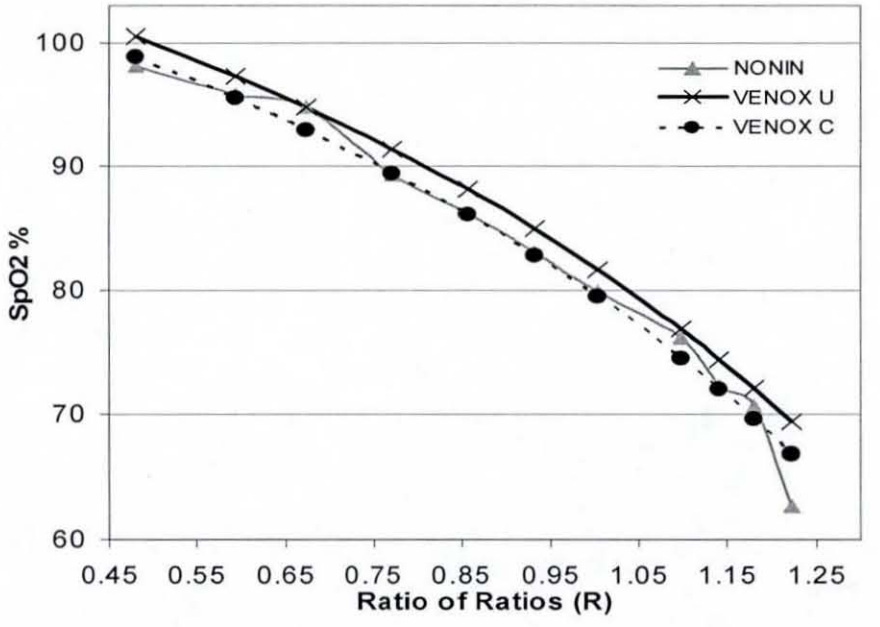

Figure 5.2 - Nonin and Venox (the proposed method) calibration curves (VENOX U=before calibration, VENOX C = after calibration)

All percentage O_2 values are compared against the R values recorded by the prototype device for a given solution. For example, for the first solution the Nonin oximeter has shown an average of 98.10% while the prototype device has measured an average ratio of 0.48. By using equation 5.1, the corresponding SpO_2 was 100.50%. After measuring all the samples it was clear that there was an almost constant average offset of 2% between Nonin and the prototype device (Nonin and Venox U respectively). The calibration equation 5.1 was then adjusted so that the re-calculated values of the prototype device (Venox C) would fit the Nonin curve (Nonin), by adjusting α=1000 to α=988. Table 5.1 illustrates averages and range of

values from the Nonin oximeter and the prototype device, as well as the average ratios recorded by the latter.

Table 5.1 Measurement results before comparative calibration.

NONIN		VENOX U (Uncalibrated)		
Average (%)	Range (%)	Average (%)	Range (%)	Average R
98.1	98.0-99.0	100.5	99.8 - 101.6	0.481
95.9	95.0-96.0	97.3	95.7 - 98.3	0.594
94.8	94.0-95.0	94.8	93.4 - 95.3	0.674
89.3	89.0-90.0	91.4	90.7 - 92.0	0.772
86.2	86.0-87.0	88.1	87.2 - 89.4	0.856
83.0	83.0-83.0	84.9	84.3 - 86.9	0.932
79.9	79.0-80.0	81.7	81.1 - 83.1	1.003
76.2	76.0-77.0	76.9	75.8 - 77.6	1.097
72.3	72.0-73.0	74.5	71.9 - 76.0	1.140
70.7	70.0-71.0	72.1	70.2 - 73.6	1.179
62.7	62.0-63.0	69.4	68.4 - 71.6	1.222

5.1.3 Discussion and Analysis

Recalling the fundamentals of PPG from chapter 2, arterial blood absorbs more infrared than red light and as oxygen saturation decreases, red light absorption becomes stronger than infrared light absorption. Hence, the arterial system had a mixture of MB and CS solutions which provided a stronger infrared than red absorption and this was achieved by increasing the concentration of CS (the infrared absorber) in the solution. On the other hand, in order to simulate venous blood the red absorption must become stronger and as soon as it matches the infrared absorption, then according to the standard calibration curve (equation 5.1) the saturation becomes 82% (for an absorption ratio $R = 1$).

The purpose of the experiment was fundamentally to test whether the electronics of the prototype were providing the same ratio of red and infrared signals. For example, if a band-pass filter on the circuit board would fail, there would be an imbalance of gain between red and infrared channels, which would lead to false readings. It was proven however that the prototype device was close to the commercial oximeter with only a quasi-constant 2% difference between them. This was attributed to the wavelength difference between probes which varies between manufacturers. Figure 5.3 shows the light spectra of the Nonin probe and the

Viamed P861RA probe in the 800nm-1000nm region. The red light output peaks at 664nm in both probes. Data were captured with a PCI spectrophotometer (ADC2000, Ocean Optics). The jitter in figure 5.3 is due to electrical noise in the spectrophotometer.

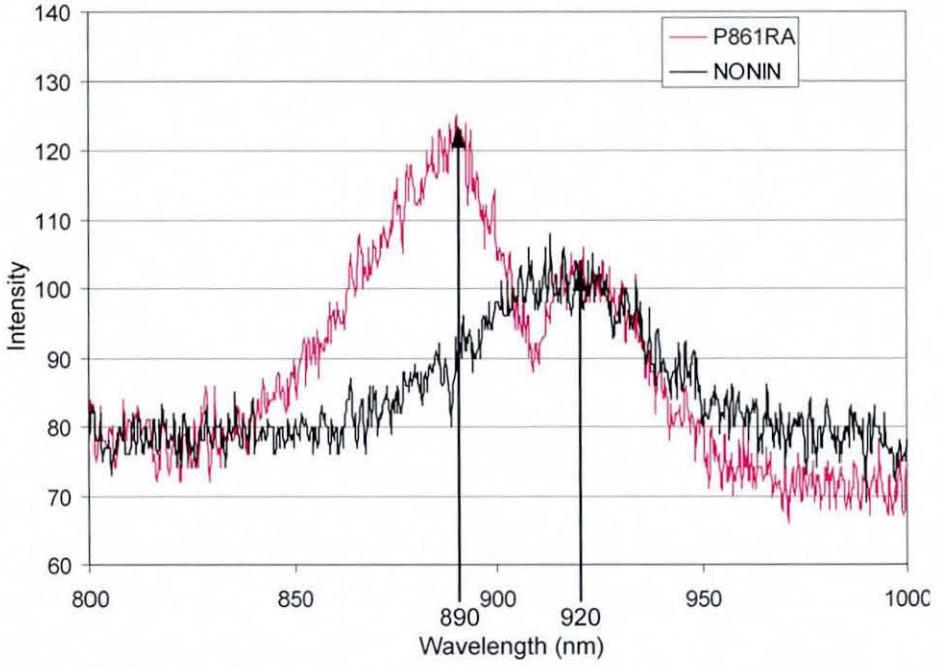

Figure 5.3 - Infrared light output of Nonin and Viamed (P861RA) probes

Figure 5.4 shows the absorption curve of cupric sulphate pentahydrate in the region between 880nm and 930nm.

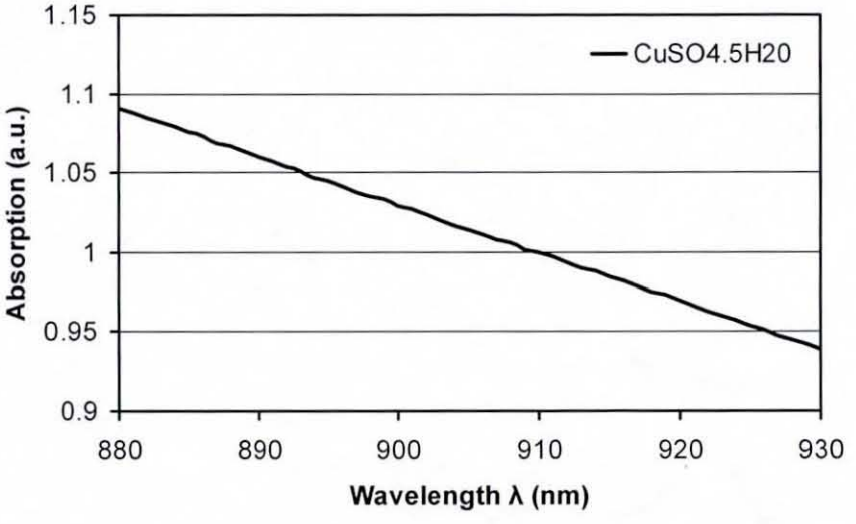

Figure 5.4 - Absorption curve of $CuSO_4.5H_2O$ in the 880-920nm region

The reason for the 2% difference between the Nonin and the Viamed probes can be explained through figures 4.3 and 4.4. Referring to figure 5.3, the infrared emitter of the Nonin probe has a maximum peak at 920nm, while the Viamed probe's infrared light intensity peaks at 890nm. Moving to figure 5.4, it can be seen that the light absorption of $CuSO_4.5H_2O$ is different between 890nm and 920nm. In fact there is a stronger absorption at 890nm than at 920nm. Recalling that the ratio of red/infrared signal essentially gives the oxygen saturation, the 920nm emitter will give a stronger infrared signal during a pulsation, than the 890nm emitter. This results in a smaller ratio which yields a higher saturation value when the 920nm is used; hence the average measured difference of 2%.

Regarding the preparation of the absorbing solutions of MB and CS, the initial approach was the theoretical calculation of absorption based on the Beer-Lambert law. After preparation of concentrated solutions of MB and CS in water, the concentration-absorption curves (Beer's curves) were prepared by diluting the solutions with distilled water. For CS, the initial concentration of 0.5M was reduced to 0.25M, 0.125M, 0.0625M and 0.03125M. For MB, the initial concentration of 4.47×10^{-4}M reduced to half upon every dilution with water, until it was reduced to 6.98×10^{-6}M. Figure 5.5 shows the Beer's curves of MB at 664nm and CS at 905nm.

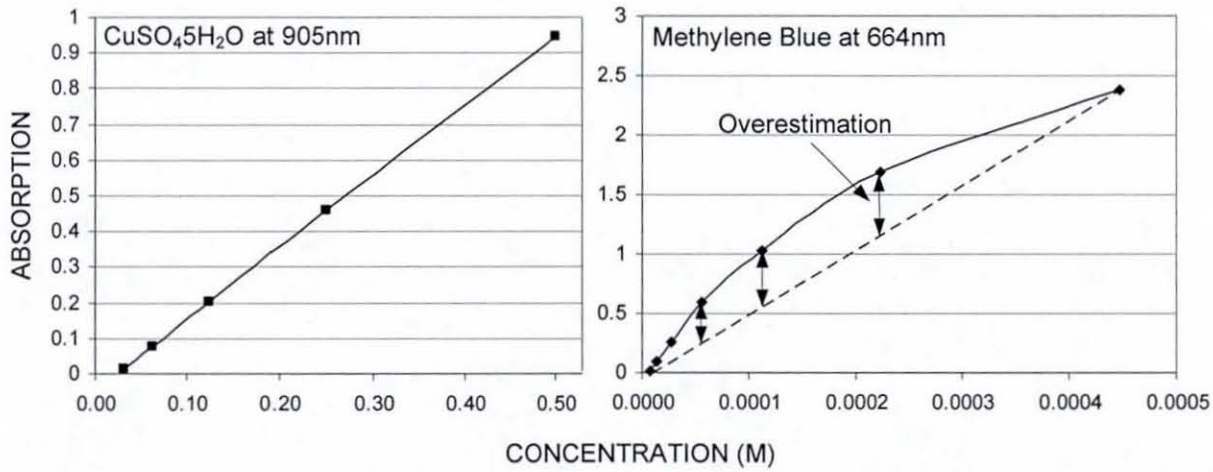

Figure 5.5 Beer's curves of CS at 905nm and MB at 664nm

It can be seen that CS has a linear concentration-absorption curve but MB does not follow Beer-Lambert's law due to the significant scattering effects. The use of MB in optical phantoms is discussed in a study[79] where it was concluded that the significant scattering effects of MB can lead to the overestimation of absorption when this is measured by spectrophotometry, which was also confirmed through the experiments as shown in figure 5.5. Further experiments were carried out by using a buffer solution (phthalate) as a solute instead of distilled water, but similar results were obtained. To resolve this problem chemometrics[82] is often used, but further investigation was out of the scope of this experiment. The disagreement between values obtained from the spectrophotometer and from the pulse oximeter has led to the empirical preparation of the absorbing solutions and the scope of the experiment was successfully fulfilled.

Recalling that the aim of the comparative calibration experiment was to establish whether the PPG circuit board of the experimental prototype provided similar values to a standard pulse oximeter, it was concluded that the use of a standard pulse oximetry calibration curve was appropriate after modification of the parameter α in equation 5.1, from α=1000 to α=988.

5.2 EXPERIMENTAL INVESTIGATION OF THE THEORETICAL MODEL

The theoretical model describing the non-invasive method for the measurement of venous oxygen saturation presented in chapter 3 investigated the following two aspects relating to anatomical and physiological effects:

- The mechanical coupling between arteries and veins arising from the expansion of arteries when an arterial pulsation is present, and how this affects the venous optical path length.
- The mechanical coupling between veins and arteries arising either from the expansion of veins when an artificial venous pulsation is present or from the direct modulation of the arteries when the modulation cuff pressure is high and sufficient to cause changes in the arterial optical path length.

A series of laboratory experiments were carried out in order to investigate whether these effects exist and how they influence the arterial and venous oxygen saturation readings.

5.2.1 Experimental Purpose, Protocol and Setup

The purpose of the experiments is to investigate the validity of the model. The investigation was separated into two sections; the first section investigates the arterial-to-venous effects described in the first part of the theoretical model, while the second section investigates the direct and indirect effects of the artificial venous modulation. Each section includes two sub-sections which describe the validation of the model through experiments and simulations with a clear interpretation of the model for each experiment.

5.2.1a Arterial-to-Venous Coupling

Recalling the first part of the theoretical model which focuses on the mechanical effects introduced to the venous system by the arterial contraction, the validation experiment can be carried out by creating two contrasting measurement conditions. In normal physiological conditions the arterial circulatory system has a pressure of

120mmHg during systole and 80mmHg during the diastole phase, while the venous vascular system carrier a far lower pressure which varies between 20mmHg and 0mmHg depending on the location and size of the venous vessel. Generally, the venous pressure is higher in veins which are away from the heart and becomes smaller in proximal areas of the heart; this pressure difference is one of the driving forces of venous circulation.

Therefore the validation experiment was carried in the following two physiologically different conditions:

(a) When the arm is in horizontal position rested on a flat surface, arterial and venous pressures will have physiological values. According to the hypothesis, veins will be vulnerable to external mechanical forces applied by the arterial expansion. Hence the venous optical path length, which in principle should remain steady over a short period of time, will be affected by arterial expansion. As a result the arterial PPG signal will not only originate from the arterial path length change, but also from the venous path length change.

(b) Install an inflatable cuff around the arm and inflate to a pressure of 80mmHg. This will cause no significant effect to the arterial inflow but it will cause total venous occlusion during the first few seconds during which the venous pressure will keep on rising until it reaches approximately half the pressure of the cuff[83], hence 40mmHg. After this point, venous blood will start flowing towards the heart but the pressure will be maintained. With a higher venous pressure, veins will be less prone to compression originating from the arterial expansion. If the hypothesis is valid then there will be a difference in the PPG signals, since the venous path length will now be different.

Recalling equation 3.45 from chapter 3, the arterial-to-venous coupling is described by the following equation:

$$\left\langle \frac{\Delta I(t,\lambda_1)/I(t,\lambda_1)}{\Delta I(t,\lambda_2)/I(t,\lambda_2)} \right\rangle_{arterial} = \frac{A(\lambda_1) - \varepsilon V(\lambda_1)}{A(\lambda_2) - \varepsilon V(\lambda_2)} = R_a$$

where $\Delta I(t,\lambda)/ I(t,\lambda)$ is the apparent arterial normalised peak-to-peak signal which includes the real arterial normalised peak-to-peak signal ($A(\lambda)$) and the venous normalised peak-to-peak signal ($V(\lambda)$).

During part (a) of the experiment it is assumed that there is some level of coupling between arteries and veins, therefore the enumerator and denominator of equation 3.45 will be a mixture of arterial and venous blood. Given that the venous oxygen saturation is lower than the arterial oxygen saturation, the ratio-of-ratios R of venous blood is greater than the arterial R. Therefore, R_α will be greater when there is coupling than when there is no coupling. Calling R_1 the ratio-of-ratios when there is coupling (part (a) of the experiment) and R_2 the ratio-of-ratios when there is no coupling (no coupling is assumed in part (b) of the experiment). R_1 is given by equation 3.45 while R_2 is given by:

$$R_2 = \frac{A(\lambda_1)}{A(\lambda_2)} \qquad \textbf{[5.2]}$$

because it is assumed that there is no coupling between arteries and veins, hence ε=0. For the purposes of demonstrating the numerical accuracy of the model, the maximum oxygen saturation during part (b) of the experiment is used as the "correct value" based upon the assumption that no arterio-venous coupling exists at that specific time. Hence the coupling coefficient ε will be calculated based upon this value. Recalling equation 3.47 from chapter 3, ε is given by:

$$\varepsilon = \frac{A(\lambda_2)R_a - A(\lambda_1)}{V(\lambda_2)R_a - V(\lambda_1)}$$

Where R_α will be the minimum value recorded during part (b) (maximum oxygen saturation), $A(\lambda)$ the normalised arterial AC peak-to-peak values and $V(\lambda)$ the normalised venous AC peak-to-peak values.

The experimental protocol divided in parts (a) and (b) was carried out continuously without interrupting the data recording in order to show clearly the effect of occluding the venous outflow and it was repeated one more time during the same recording. The subject was a healthy male, age 29 with no history of cardiovascular related diseases. The prototype device recorded data at a sample rate of 128Hz using a standard pulse oximetry probe (P861RA, Viamed UK), while the modulation digit cuff was installed on the same finger with the pulse oximetry probe in order to create venous pulsations. Recorded data were processed off-line in Matlab.

5.2.1b Venous-to-Arterial Coupling

Recalling the second part of the theoretical model focusing on the mechanical effects introduced to the arterial system by the artificial venous pulsations, the validation experiment can be carried out in a similar way to the arterio-venous experiment, by creating the following two contrasting measurement conditions:

(a) When the arm is in horizontal position rested on a flat surface, arterial and venous pressures will have physiological values. The venous modulation system operates at a low pressure of 15mmHg hence the modulating cuff will be unable to cause high frequency modulation of the arterial flow, since the arterial blood pressure is normally above 80mmHg. In this case the high frequency signal will only be due to venous optical path length changes.

(b) Increasing of the modulation cuff pressure to a value higher than the arterial systolic pressure, according to the hypothesis, will cause the introduction of venous pulsations into the arterial blood. If the hypothesis is true, then the venous oxygen saturation value during this part of the experiment will be higher that in part (a). This is due to the high frequency signal originating not only from the venous but also from the arterial optical path length change. The highly-pressurised cuff operating at a pressure higher than the

systolic pressure will cause a local partial restriction of arterial flow during inflation, hence decreasing the arterial path length. During deflation, the arterial path length will be restored to its original state, therefore this difference in the arterial path length between the inflation and deflation phases will introduce a high frequency signal component originating from arterial blood. As a result, the overall high frequency signal will be a combination of arterial and venous signals.

Recalling equation 3.46 from chapter 3, the venous-to-arterial coupling is described by the following equation:

$$\left\langle \frac{\Delta I(t,\lambda_1)/I(t,\lambda_1)}{\Delta I(t,\lambda_2)/I(t,\lambda_2)} \right\rangle_{venous} = \frac{V(\lambda_1) - \delta A(\lambda_1)}{V(\lambda_2) - \delta \mathrm{A}(\lambda_2)} = R_v$$

where $\Delta I(t,\lambda)/ I(t,\lambda)$ is the apparent venous normalised peak-to-peak signal which includes the real venous normalised peak-to-peak signal ($V(\lambda)$) and the arterial normalised peak-to-peak signal ($A(\lambda)$).

During part (b) of the experiment it is assumed that there is some level of coupling between veins and arteries, therefore the enumerator and denominator of equation 3.46 will be a mixture of arterial and venous blood. Given that the arterial oxygen saturation is higher than the venous oxygen saturation, the ratio-of-ratios R of arterial blood is lower than the venous R. Therefore, R_v will be smaller when there is coupling than when there is no coupling. Let's call R_1 the ratio-of-ratios when there is no coupling (part (a) of the experiment) and R_2 the ratio-of-ratios when there is coupling (part (b) of the experiment). R_2 is given by equation 3.46 while R_1 is given by:

$$R_1 = \frac{V(\lambda_1)}{V(\lambda_2)} \qquad \textbf{[5.3]}$$

because it is assumed that there is no coupling between arteries and veins, hence δ=0. Parts (a) and (b) of the experiment are consecutively repeated every 20s (10s for each part). During part (a) of the experiment the venous ratio-of-ratios R_I is calculated and subsequently used in equation 3.48 (as the "correct value") in order to calculate the coupling coefficient δ during part (b). Recalling equation 3.48 from chapter 3, δ is given by:

$$\delta = \frac{V(\lambda_2)R_v - V(\lambda_1)}{A(\lambda_2)R_v - A(\lambda_1)}$$

Where R_v will be the average value recorded during part (a) (correct venous oxygen saturation), $A(\lambda)$ the normalised arterial AC peak-to-peak values and $V(\lambda)$ the normalised venous AC peak-to-peak values.

The experimental protocol divided in parts (a) and (b) was carried out continuously without interrupting the data recording and it was repeated 7 times during the same recording (10s low cuff pressure, 10s high cuff pressure, total recording duration 140s). The subject was a healthy male, age 29 with no history in cardiovascular related diseases. The prototype device was recording data at a sample rate of 128Hz using a standard pulse oximetry probe (P861RA, Viamed UK), while the modulation digit cuff was installed on the same finger with the pulse oximetry probe in order to create venous pulsations. The peak cuff pressure in part (a) was 45mmHg and 260mmHg in part (b). Recorded data were processed off-line in Matlab.

5.2.2 Experimental Results

The hypotheses upon which the model was developed, divide the experiments in two sections; the first section describes the coupling between arteries and veins and how the arterial expansion during the systole phase may affect the venous flow, while the second section describes the effect of the artificial venous modulation on the arterial flow. The model was demonstrated through experimental tests which are presented further on.

5.2.2a Arterial-to-Venous Coupling Results

The coupling coefficient ε gives the indication that there is a venous component in the arterial signal when it is not equal to zero. This part of the model is based upon the hypothesis that in part (b) of the first experiment (highlighted areas in figure 5.7) arterio-venous coupling is not significant. For the purposes of demonstrating the model, the maximum value of oxygen saturation obtained during this part was assumed to be the correct arterial value. This assumption was based upon the hypothesis that the prolonged venous occlusion would cause an increase of the venous blood pressure in the lower arm, therefore the expansion of the arteries will have a smaller or no effect on the high-pressure veins. Hence, the 'low-frequency' signal (natural arterial pulsations) will originate from arterial blood only when the veins are minimally disturbed, resulting in a higher saturation value compared to the baseline measurement, where the venous pressure was normal and was assumed that arterial pulsations affected the venous flow. The results of this experiment are shown in figure 5.6.

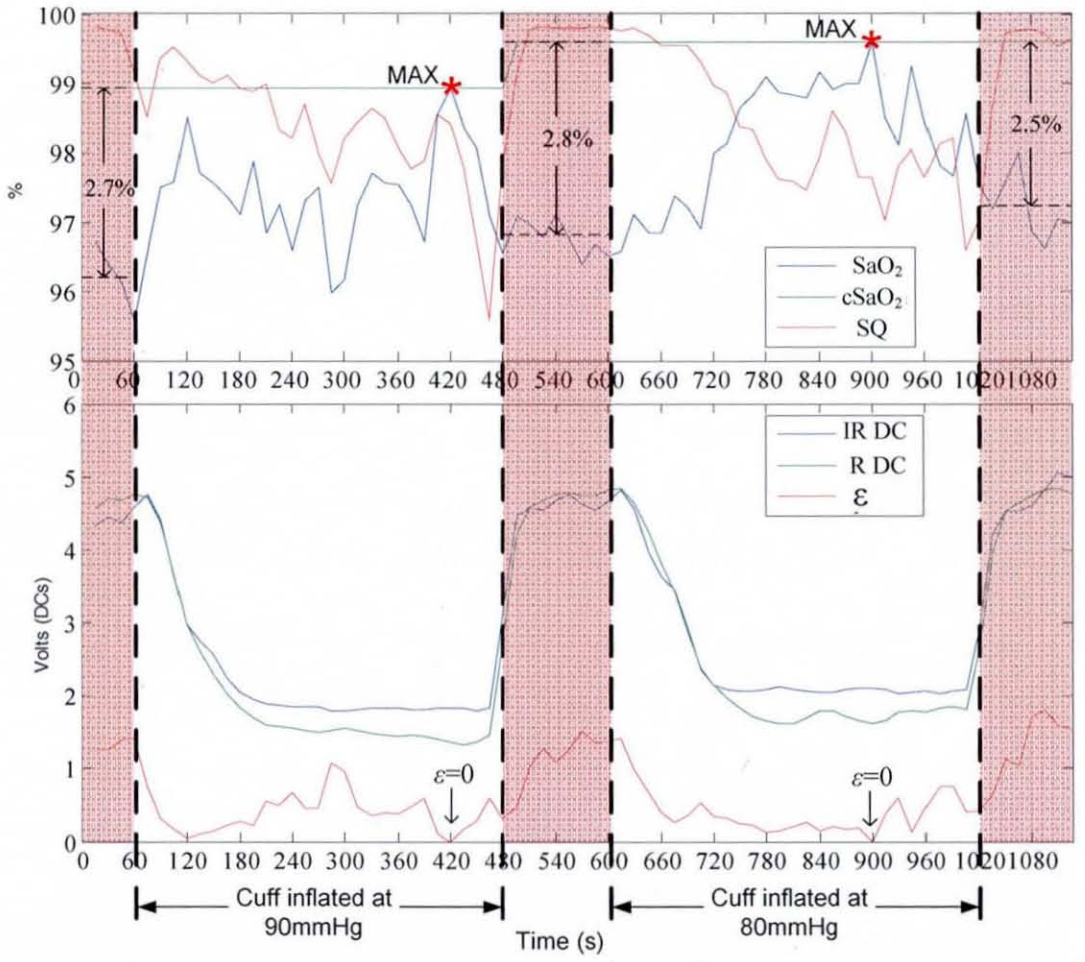

Figure 5.6 - Results of experiment 1: arterial-to-venous coupling

The experiment started with the measurement of arterial blood pressure which was found to be 132/85mmHg. The occlusion cuff was placed around the upper arm while the artificial venous modulation operated throughout the duration of the experiment. Parts (a) and (b) were carried out twice as it can be seen in figure 5.6 and more specifically the following protocol was implemented:

1) The pulse oximetry probe and the modulating digit cuff were attached to the 1st digit of the left hand. The left arm was positioned on a flat surface and PPG signals were observed in order to establish steady-state PPG signals.
2) Recording was initialised with the arm cuff deflated and continued until t=60s.

3) At t=61s the occluding cuff was inflated to 90mmHg and continued recording for 420s until t=480s, when the occlusion cuff pressure was deflated.
4) The occluding cuff remained deflated for 120s until t=600s. At t=601s the occluding cuff was inflated to 80mmHg and continued recording for 420s until t=1020s, when the cuff was deflated. Recording stopped at t=1140s.

The different phases of the protocol were selected after multiple experiments were carried out, in order to establish the average time required for the DC values to be stabilised. A constant DC value indicates a state of equilibrium between blood inflow and outflow. Hence with the arm cuff inflated at 80mmHg the venous pressure is closer to the arterial pressure and as a result the veins will be less susceptible to compression during the arterial expansion. The level of pressure at the arm cuff was set just below the arterial diastolic pressure in order to avoid interfering directly with the arterial inflow.

Data were processed in 30s long windows, sliding by 15s each time. The model was interpreted in Matlab through the following algorithm:

1) Read the recorded file, place *AC* and *DC* values in vector variables.
2) Filter *AC* signals and separate arterial from venous frequency components.
3) Resample from 128Hz by applying a 30s sliding window (4 values per minute) and calculate signal quality SQ (red trace on top graph) by correlating the arterial red and infrared AC signals.
4) Normalise the *AC* values by dividing them by the *DC* values and calculate the ratio-of-ratios R_1 hence the oxygen saturation SaO_2 (blue trace on top graph) using equation 5.1 (with α=988). These are the "un-corrected" values of SaO_2.
5) Calculate the arterial ratio-of-ratios (R_2) using equation 5.2 for the occlusion periods and find the minimum values (maximum SaO_2). These are assumed to be the correct arterial values since they occur after venous pressure was built-up and denoted by the two asterisks in figure 5.8.

6) Calculate ε using equation 3.47 separately for periods $0<t<480$s and $481<t<1140$s (red trace on bottom graph).
7) Calculate R_I using equation 3.45, hence the corrected oxygen saturation $cSaO_2$ (green trace on top graph) from equation 5.1 (with α=988).

Although it cannot be concluded whether the occlusion has raised the venous pressure high enough in order to prevent the compression of veins whenever arteries expanded (which was assumed for the purposes of the experiment), there was a difference of 2.5-2.8% between SaO_2 and $cSaO_2$ (the latter being greater) which is in agreement with the initial hypothesis. It is worth noting the variation of the DC values during occlusion which confirms that the total blood volume in the measured area was increased vastly, since the light intensity had decreased from $4.5V$ to less than $2V$. The value of ε depends on the level of venous oxygen saturation as well as the relative amplitude of arterial and venous red and infrared signals, hence the absolute value of ε does not offer any information unless it approaches zero ($\varepsilon<0.1$), which means that the arterio-venous coupling is minimal.

5.2.2b Venous-to-Arterial Coupling Results

The coupling coefficient δ gives the indication that there is an arterial component in the venous signal when it is not equal to zero. This part of the model is based upon the hypothesis that in part (a) of this experiment, venous-arterial coupling is not significant. For the purposes of demonstrating the model, the average venous oxygen saturation during part (a) was assumed to be the correct venous value. Figure 5.7 illustrates the results from the experiment.

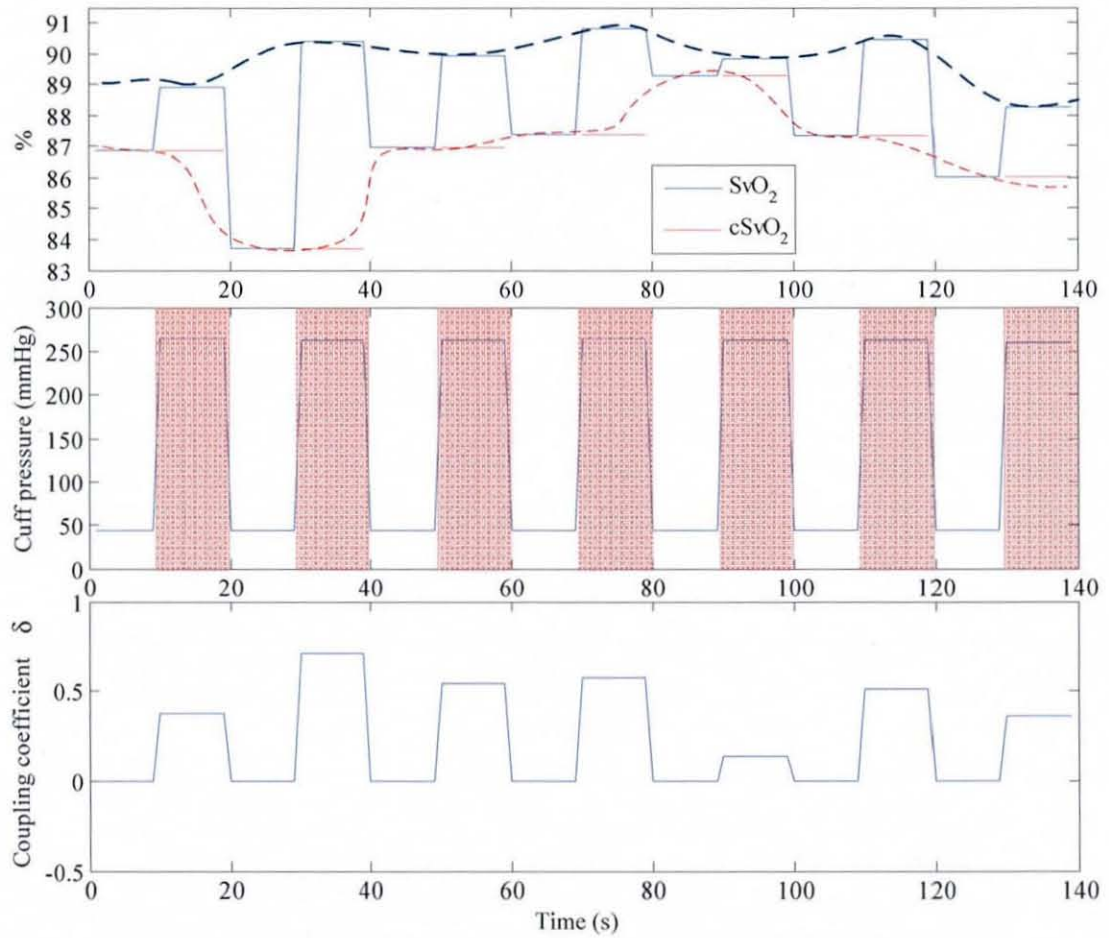

Figure 5.7 - Results of experiment 2: venous-to-arterial coupling

The experiment started with the measurement of arterial blood pressure which was found to be 125/78mmHg. The artificial venous modulation operated throughout the duration of the experiment, while the modulation depth was changed from 45mmHg to 260mmHg and back to 45mmHg, allowing 10s of data recording for each pressure level. Parts (a) and (b) were carried out seven times as it can be seen in figure 5.7 and highlighted areas are the high modulation depth period. The following procedure was implemented:

1) The pulse oximetry probe and the modulating digit cuff were attached to the 1st digit of the left hand. The left arm was positioned on a flat surface and PPG signals were observed in order to establish steady-state PPG signals.

2) Recording was initialised with the modulation cuff operating at P=45mmHg between $0<t<10$s.
3) At t=10s the modulation depth was increased to 260mmHg and continued recording for 10s until t=20s, when the modulation depth was set back to 45mmHg.
4) Steps 1-3 repeated seven times.

The pressure level of the modulation cuff was set between two different values, in order to achieve two contrasting conditions: in the low pressure level (45mmHg) the cuff pressure is sufficient to only modulate venous blood flow without affecting the highly-pressurised arterial system (>80mmHg), while the high pressure level (260mmHg) was selected in order to intentionally introduce maximal disturbance to both the arterial and venous blood flow. Therefore, in the low pressure condition the modulated signal originated from veins only, while in the high pressure condition there was a combination of arterial and venous components. The purpose of this protocol is to determine the level of coupling between the modulated signal and the arteries, when the pressure exceeds the arterial diastolic pressure. This allows for the application of high pressure modulation in poor peripheral blood perfusion conditions, where a stronger mechanical stimulation of the area is required to produce a sufficient venous signal.

Data were processed in 1s long windows and values were averaged every 10s in order to provide a single value for each part of the experiment. The model was interpreted in Matlab through the following algorithm:

1) Read the recorded file, place AC and DC values in vector variables.
2) Filter AC signals and separate arterial from venous frequency components.
3) Resample from 128Hz to 1Hz by applying a 1s moving window with no overlapping.
4) Normalise the AC values by dividing them by the DC values and calculate the ratio-of-ratios R hence the venous oxygen saturation SvO_2 (blue trace on

top graph) using equation 5.1 (with α=988). These are the "un-corrected" SvO_2 values.

5) Calculate the venous ratio-of-ratios (R_1) using equation 5.3 for the low modulation depth periods (part (a)) and calculate the average values. These are assumed to be the correct venous values because of the low modulation depth.
6) Calculate δ using equation 3.44 for the high modulation depth periods of the experiment, shown in the bottom graph of figure 5.7.
7) Calculate the average maximum pressure (modulation depth) for each 10s data segment, shown in the middle graph of figure 5.7.
8) Calculate R_2 using equation 3.42, hence the corrected venous oxygen saturation $cSvO_2$ (red trace on top graph) from equation 5.1 (with α=988).

It is evident from experiment 2 that when the modulation depth is high, venous oxygen saturation values are greatly affected because of the resulting arterial modulation. The results have confirmed the initial hypothesis of the model's second part, where high venous oxygen saturation was expected in high modulation depth conditions.

5.2.3 Discussion and Analysis

The aims of experiments 1 and 2 were to confirm the hypothesis that there is mechanical arterio-venous coupling, which were both confirmed. The first experiment investigated the mechanical coupling of the arterial pulses when the venous pressure has physiological values which are significantly lower than the arterial blood pressure. According to the model this coupling effect would be minimised upon increment of the venous pressure, which was confirmed by inflating an arm cuff at a pressure of 80-90mmHg, creating venous occlusion. The arterial flow was assumed to be unaffected since the cuff pressure was lower than the diastolic pressure. In the second experiment, the modulation depth was changed between low and high values in order to investigate the presence of arterial signal in high modulation depth conditions, due to arterial optical path length variations.

5.2.3a Arterial-to-Venous Coupling

Referring to figure 5.6, during the first 60s the arm cuff was deflated and according to the model hypothesis the arterial PPG signal comes from both the changes of arterial and venous path lengths $\Delta Z\alpha$ and $\Delta Zv\alpha$ respectively, as shown in figure 3.6, chapter 3. The average arterial oxygen saturation during this period was $SaO_2^{(0\text{-}60s)}$=97.2%. During the next 420s the arm cuff was inflated to 90mmHg in order to cause venous blood pooling, which in turn would increase the venous pressure. Referring to the bottom graph of figure 5.6, the *DC* signals show how the received light intensity was gradually decreased over a period of several minutes. This proves essentially that there was blood pooling after inflation of the arm cuff, since the light absorption was increased. Moreover, it is worth noting that not only the IR *DC* and the R *DC* values had changed dramatically but their difference had also changed significantly. While initially (0<t<60s) the R *DC* was greater than the IR *DC*, after inflation of the arm cuff and upon gradual venous blood pooling the R *DC* became smaller than the IR *DC*, hence Δ(IR *DC*) < Δ(R *DC*). Recalling that reduced-haemoglobin (venous blood) absorbs stronger than oxygenated-haemoglobin (arterial blood) in the red range, it can safely be concluded that venous blood pooling had caused the change in the difference between the R *DC* and the IR *DC* signals. In simple terms, more venous blood had caused more red absorption which in turn caused less red light intensity.

At t=420s the maximum arterial oxygen saturation was measured, which also happened to be towards the end of the occlusion period and after the *DC* values had settled. During this time, it was assumed that $\Delta Zv\alpha$ was zero or insignificant, therefore the measured value of 98.9% was considered to be the real arterial oxygen saturation value because no venous component was involved in the arterial signal. Hence, ε was calculated from equation 3.47 and had a maximum value at the maximum difference between SaO_2 and $cSaO_2$. It is important to note that the experiment was based upon the assumption that the real arterial oxygen saturation had remained the same throughout the length of the recording. At t=421s the same procedure was repeated and the same effects were observed, with the particularly

interesting observation that the difference between SaO_2 and $cSvO_2$ has remained quasi constant between 2.5% and 2.8% which shows the consistency of the experimental protocol.

5.2.3b Venous-to-Arterial Coupling

Referring to figure 5.7, during the first 10s the low modulation depth does not cause any mechanical effects to arterial flow hence according to the model hypothesis the venous PPG signal comes purely from the changes of venous path length. On the other hand, when the modulation depth was set high, according to the hypothesis the venous PPG signal originated from both venous and arterial optical path length changes ΔZv and ΔZav respectively, as shown in figure 3.7. The average venous oxygen saturation during this period was $SvO_2^{(0\text{-}10s)}$=86.9%. During the next 10s the modulation depth was increased to 260mmHg (peak pressure) in order to introduce pulsations in arterial blood and according to the model hypothesis, the venous oxygen saturation value would be greater than when the modulation depth is low, because the venous PPG signal would be a "mixture" of arterial and venous signals. The same experiment was repeated seven consecutive times and the hypothesis was confirmed in all cases, as it can be seen in figure 5.9. The continuous blue line is the continuously measured SvO_2 both at low and high modulation depth conditions. In low modulation depth conditions (0-10s, 21-30s, 41-50s, 61-70s, 81-90s, 101-110s, 121-130s), SvO_2 was lower than in high modulation depth conditions (11-20s, 31-40s, 51-60s, 71-80s, 91-100s, 111-120s, 131-140s) as predicted by the model.

At this point the coupling coefficient δ was calculated from equation 3.48 and subsequently the "corrected" venous oxygen saturation values $cSvO_2$ (red lines in figure 5.9) were calculated from equations 3.46 and 4.1. It is important to note that the experiment was based upon the assumption that the venous oxygen saturation had remained the same throughout the length of each 20s-long section, however it appears that the venous oxygen saturation had changed quite significantly over the experiment. Nevertheless, $cSvO_2$ values during high modulation depth, match with the SvO_2 values from the low modulation depth periods hence the model can

accurately detect and correct the presence of arterial components in the venous signal.

5.3 VENOUS OXYGEN DE-SATURATION INVESTIGATION

Venous oxygen saturation (SvO_2) is a function of oxygen supply and demand, in other words it depends on a number of parameters, such as:

- Arterial blood supply from the heart (Cardiac Output).
- Arterial Oxygen Saturation (SaO_2).
- Regional blood flow depending on the nervous system.
- Local tissue oxygen extraction according to demand for oxygen.
- Other physiological effects triggered by secondary parameters, such as environmental changes or pathological conditions which may affect any of the above.

This series of experiments were carried out with healthy volunteers in normal temperature conditions (21-23°C) in order to minimise environmental effects to blood supply and oxygen consumption.

5.3.1 Experimental Purpose, Protocol and Setup

The aim of the experiment is to investigate two aspects of the method:

- The validation of a standard pulse oximetry calibration curve in venous oximetry.
- The accuracy of the method when compared to blood gas analysis.

In order to obtain a series of different values of venous oxygen saturation a de-saturation experiment was set up after consultation with collaborating clinicians. Subsequently ethics approval was obtained from the Loughborough University Ethical Advisory Committee (Ref No R07-P12) and tests were carried out in Glenfield Hospital, UHL. 13 volunteers were recruited in the study, all of whom completed a health questionnaire, and were informed both verbally and in writing through an information sheet about the purpose and the protocol of the study. Participants were asked to sign a written informed consent form.

The protocol was designed around the hypothesis that total occlusion of arterial blood supply would cause gradual venous oxygen de-saturation, because even though there would be no blood flow, stationary blood would continue to release oxygen to the tissues in order to satisfy the needs for oxygen, hence venous oxygen saturation would gradually decrease. The following procedure describes the experimental protocol:

- Allow the subject to relax for 2 min, seated with the right arm resting on a desk.
- Arterial blood pressure measurement by a qualified clinician.
- Installation of finger probe and modulation cuff on the 1st digit, and occlusion arm cuff on the upper arm.
- Initialise recording with modulation depth set at 12mmHg, without blood occlusion for 1 min.
- Inflate the arm cuff until a pressure of approximately 200mmHg is reached.
- Continue recording while monitoring the venous oxygen saturation.
- Draw a venous blood sample from a proximal metacarpal dorsal vein, as soon as venous saturation drops below 80% approximately.
- Release the arm cuff air slowly to restore circulation and stop recording data.

The experimental setup included a mercury pressure meter with an arm cuff, the prototype system for pressure modulation and signal acquisition, a pulse oximetry probe (P861RA, Viamed UK) and a digit cuff (DC-1.6, Hokanson USA) and consumables for blood collection and analysis. Blood sampling and gas analysis were performed by qualified clinicians by following hygienic practices.

5.3.2 Experimental Results

The initial hypothesis was that occlusion of the upper arm would infer gradual drop of venous oxygen saturation due to continuing release of oxygen to the tissues, despite the fact blood flow was stopped. This was confirmed in all cases but with

different time delays between subjects due to the different physiological response of each individual. From a total of 13 data sets collected, one had to be excluded from the study due to insufficient blood sample volume. Although the blood gas analyser only required 200-300μl of blood volume, it can often fail to report results due to insufficient volume therefore it is usually preferred to introduce larger volumes of blood. Although the blood sample volume for this particular case was nearly 1ml, the analyser did not produce any results.

Each case is presented separately, in order to demonstrate clearly the oxygen de-saturation of venous blood as well as to display how quickly the venous blood sample was drawn (within the indicated window), as prolonged blood drawing might have introduced errors. For example, if it took 90s to draw the sample, it is unknown whether most volume came from the initial period (0-30s) or from the last period (60-90s), which makes it difficult to make a direct comparison with the non-invasively obtained venous oxygen values. Moreover, in cases where the oxygen rate of change was fast, the error can be large, as there was a case where the rate of change was as high as -60%/min.

Non-invasively measured values are average values extracted from a data window corresponding to the blood sampling time period. Venous oxygen de-saturation occurs almost immediately after the arterio-venous occlusion (at 60s), initially at a small negative slope and as time progresses, the negative rate of change increases in most cases. In the following figures, the following parameters are presented in different colours and formats:

- SvO_2 (blue line) – Venous oxygen saturation (%).
- IR x P (green line) – Correlation coefficient (%) of the infrared raw signal with the pressure sensor signal, which is high when the 'high frequency' component (6.5-8Hz) is strong (high SNR) and in phase with the pressure sensor. Low values indicate the possible presence of a heart harmonic overlapping with the artificial venous pulsation, or small SNR.

- R x P (red line) – Correlation coefficient (%) of the red raw signal with the pressure signal, similar to IR x P.
- R x IR (cyan) – Correlation coefficient (%) of the red and infrared signals. Low values indicate low SNR.
- Blood sample (red asterisk) – Venous oxygen saturation (%) measured by blood gas analysis, invasively.
- Calculated (blue asterisk) – Venous oxygen saturation (%) measured by the non-invasive method, averaged over the blood sampling time period.

Because the arterial flow was completely occluded there was no arterial pulse therefore no harmonic components, hence the modulation frequency was fixed to 8Hz.

Case 1: male, age 46, height 172cm, weight 90kg, arterial blood pressure 135/85mmHg. Blood sample data: 13/03/2007 16:02, Sample No. 14451, Gas analyser ID. 348-3353

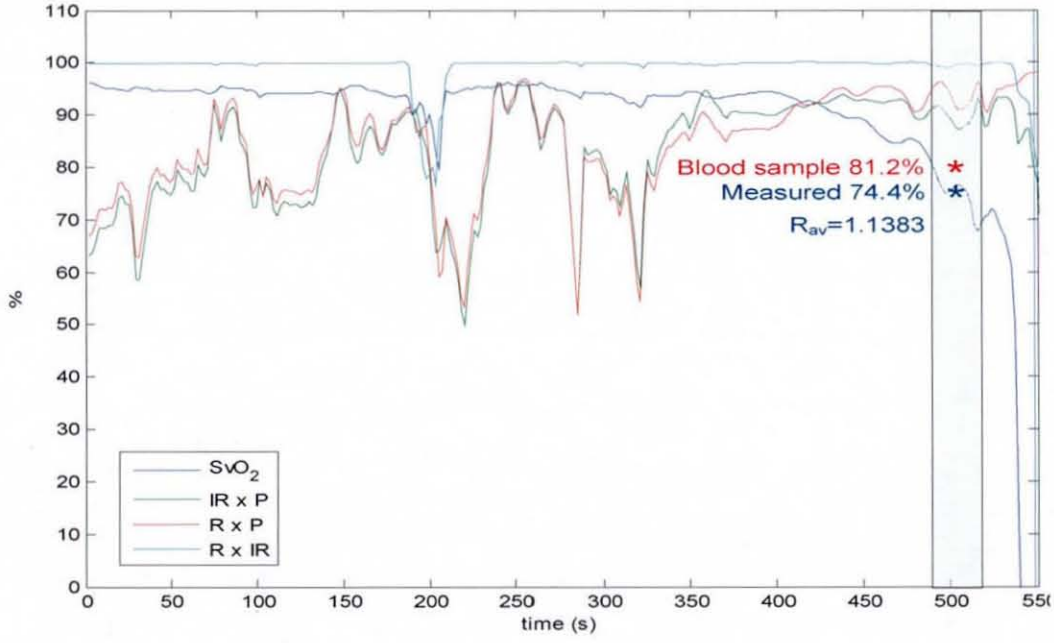

Figure 5.8 - Case study no.1

Case 2: male, age 47, height 170cm, weight 78kg, arterial blood pressure 110/75mmHg. Blood sample data: 13/04/2007 12:23, Sample No. 14604, Gas analyser ID. 348-3353

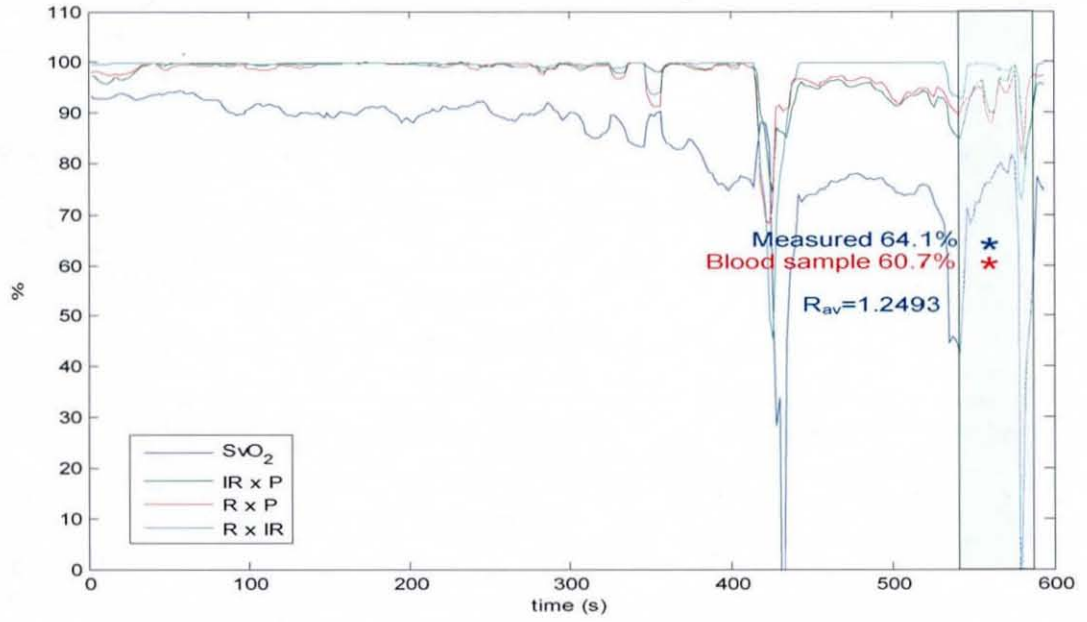

Figure 5.9 - Case study no.2

Case 3: male, age 32, height 175cm, weight 84kg, arterial blood pressure 130/85mmHg. Blood sample data: 13/04/2007 14:00, Gas analyser ID. CICU2/5081

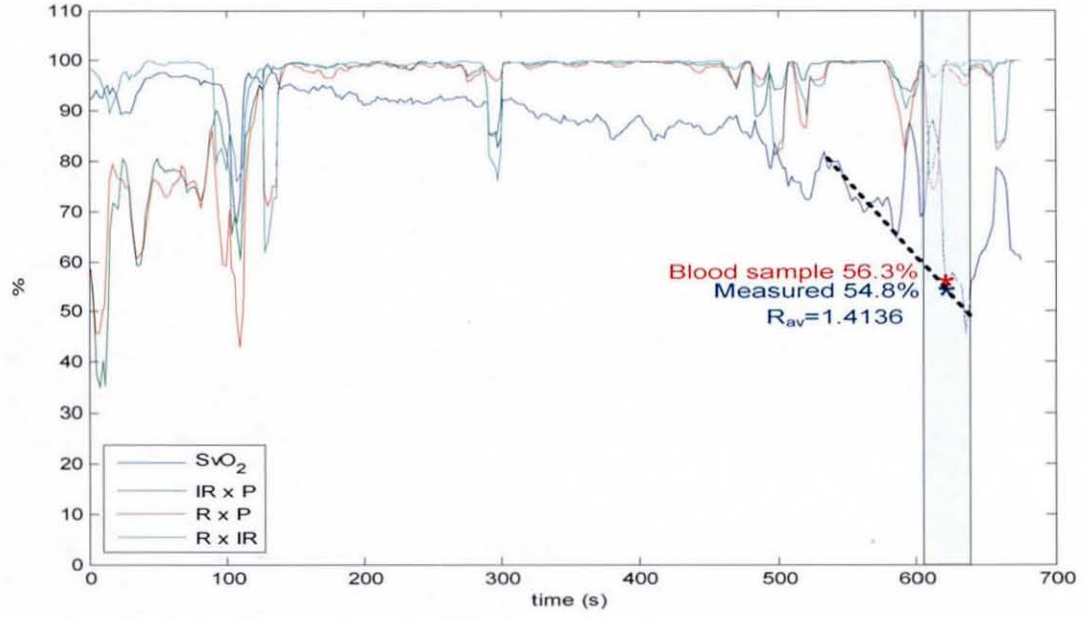

Figure 5.10 - Case study no.3

Case 4: male, age 29, height 183cm, weight 100kg, arterial blood pressure 135/85mmHg. Blood sample data: 13/04/2007 14:48, Gas analyser ID. CICU2/5081

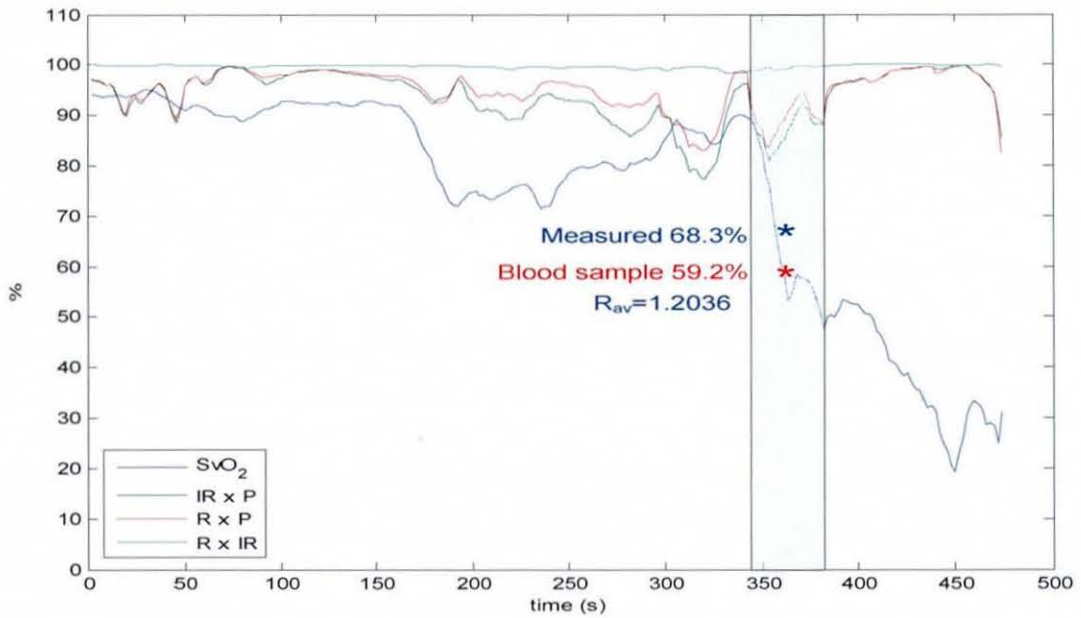

Figure 5.11 - Case study no.4

Case 5: male, age 54, height 181cm, weight 83kg, arterial blood pressure 120/75mmHg. Blood sample data: 13/04/2007 15:31, Gas analyser ID. CICU2/5081

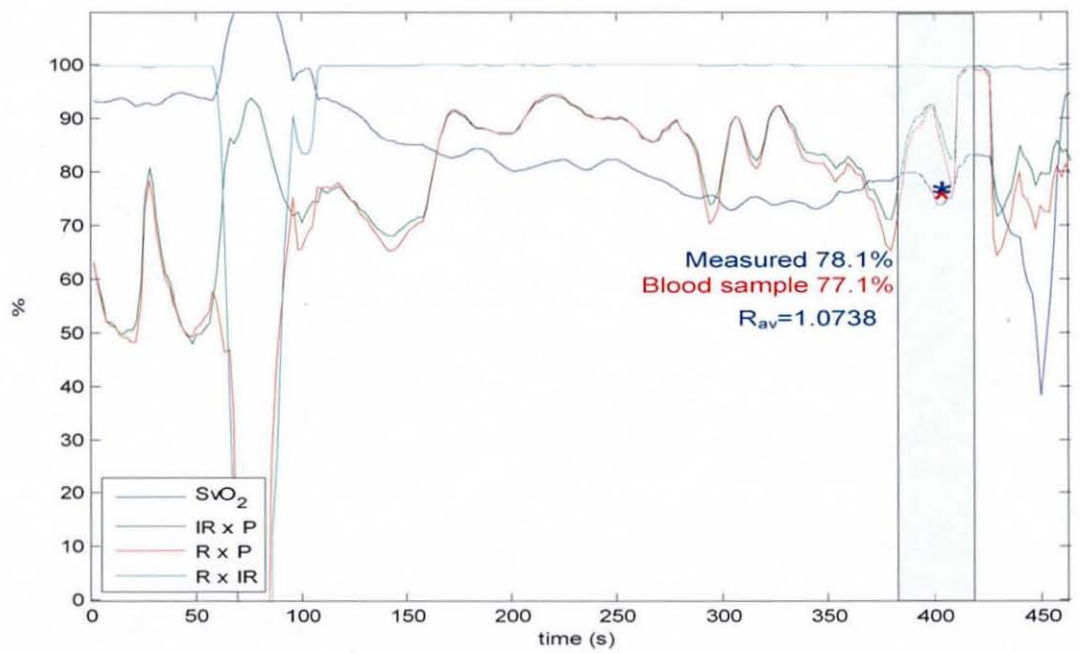

Figure 5.12 - Case study no.5

Case 6: female, age 65, height 178cm, weight 79kg, arterial blood pressure 128/78mmHg. Blood sample data: 16/04/2007 13:50, Gas analyser ID. CICU2/5081

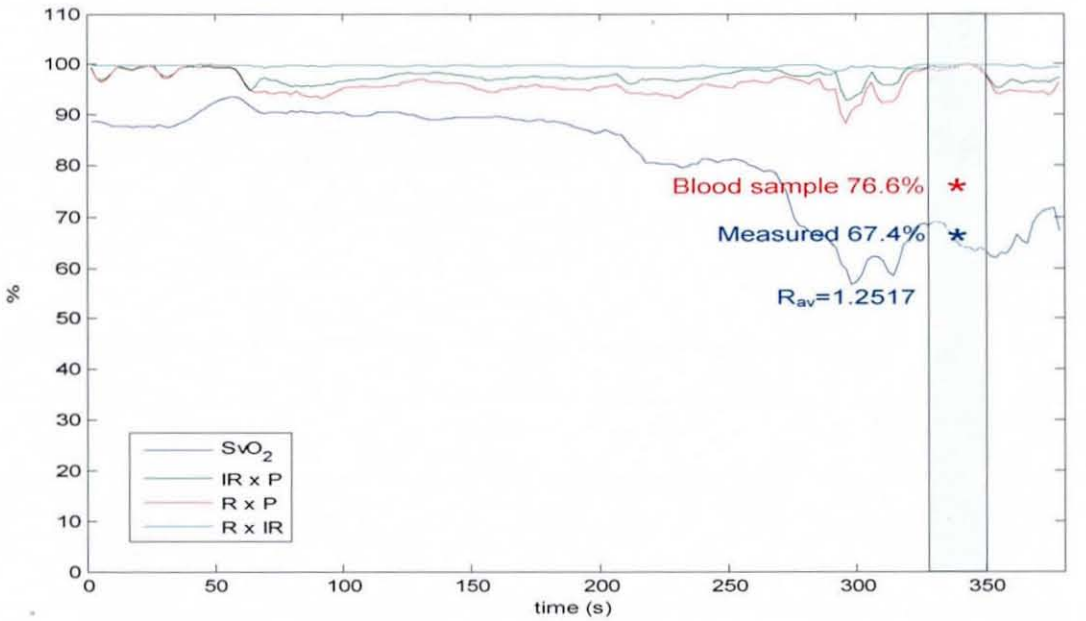

Figure 5.13 - Case study no.6

Case 7: female, age 30, height 165cm, weight 90kg, arterial blood pressure 144/94mmHg. Blood sample data: 16/04/2007 14:36, Gas analyser ID. CICU2/5081

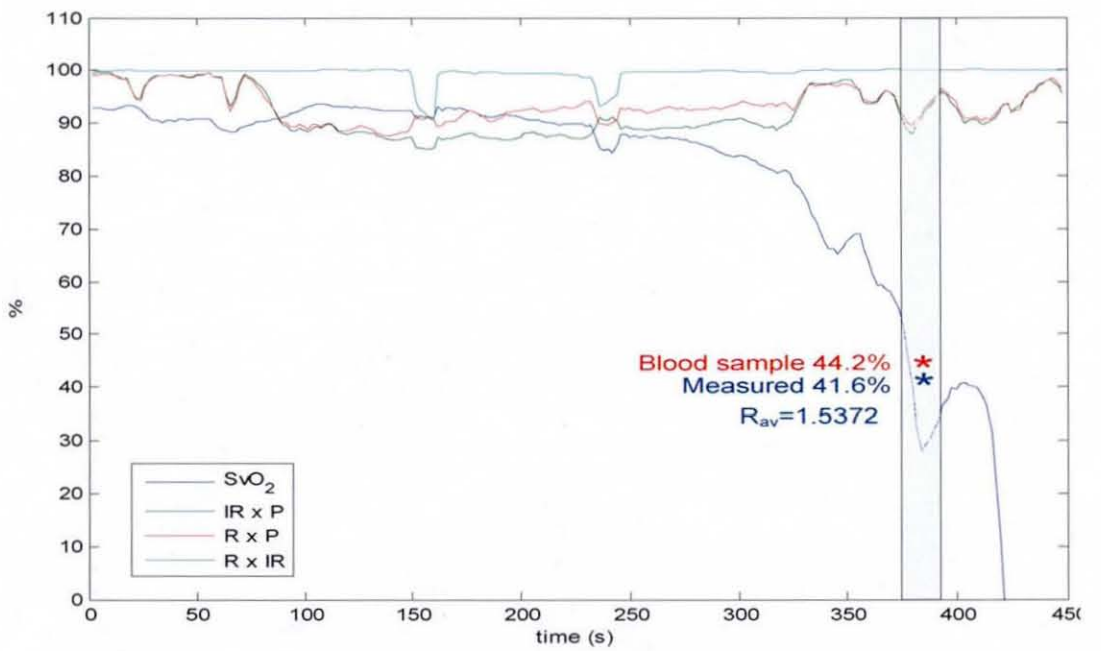

Figure 5.14 - Case study no.7

Case 8: female, age 52, height 172cm, weight 60kg, arterial blood pressure 115/70mmHg. Blood sample data: 16/04/2007 15:11, Gas analyser ID. CICU2/5081

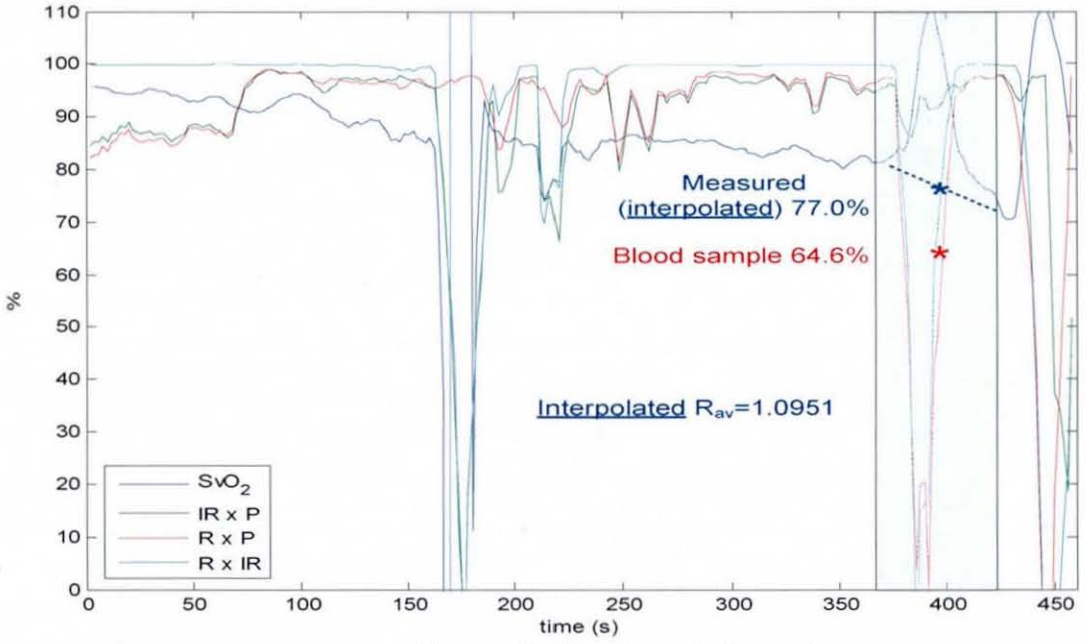

Figure 5.15 - Case study no.8

Case 9: male, age 32, height 179cm, weight 89kg, arterial blood pressure 132/85mmHg. Blood sample data: 16/04/2007 15:58, Gas analyser ID. CICU2/5081

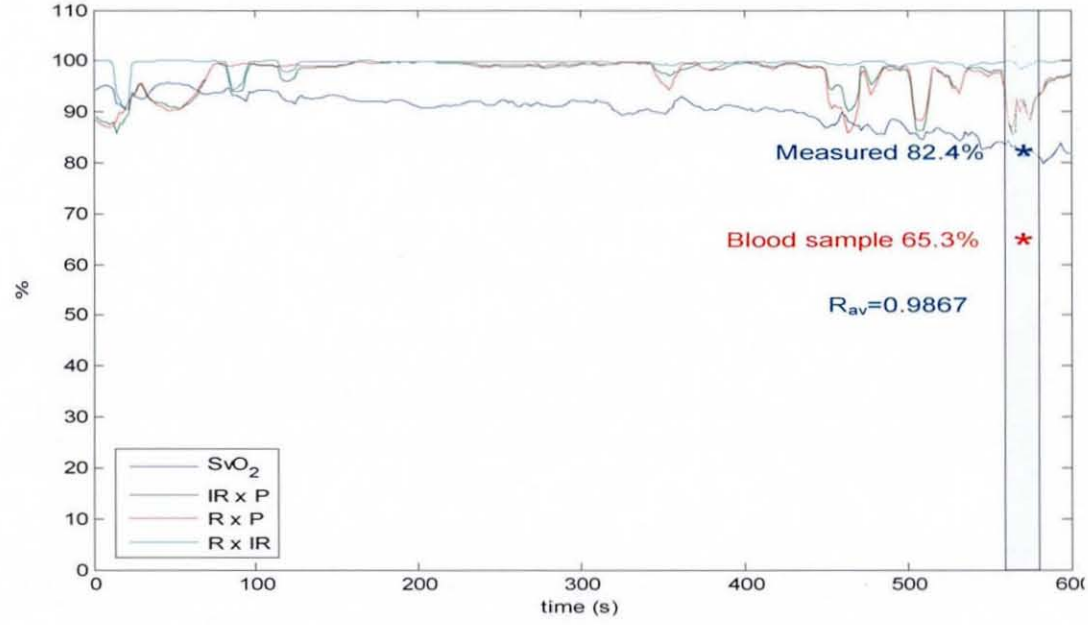

Figure 5.16 - Case study no.9

Case 10: male, age 30, height 175cm, weight 70kg, arterial blood pressure 110/70mmHg. Blood sample data: 16/04/2007 16:41, Gas analyser ID. CICU2/5081

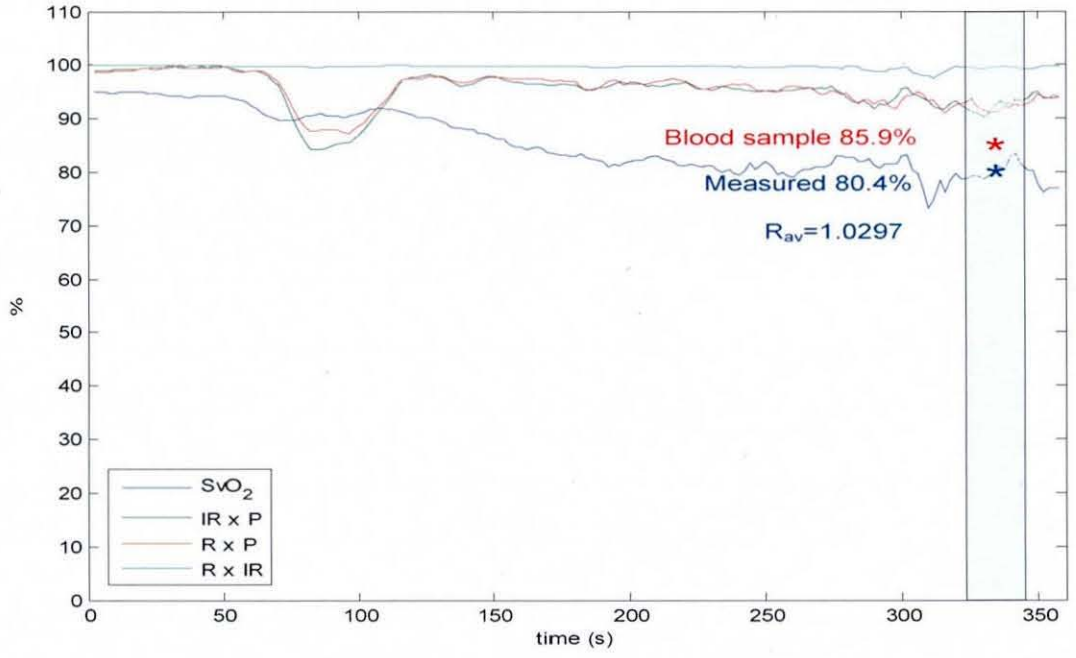

Figure 5.17 - Case study no.10

Case 11: male, age 27, height 175cm, weight 85kg, arterial blood pressure 125/75mmHg. Blood sample data: 17/04/2007 12:54, Sample No. 14625, Gas analyser ID. 348-3353

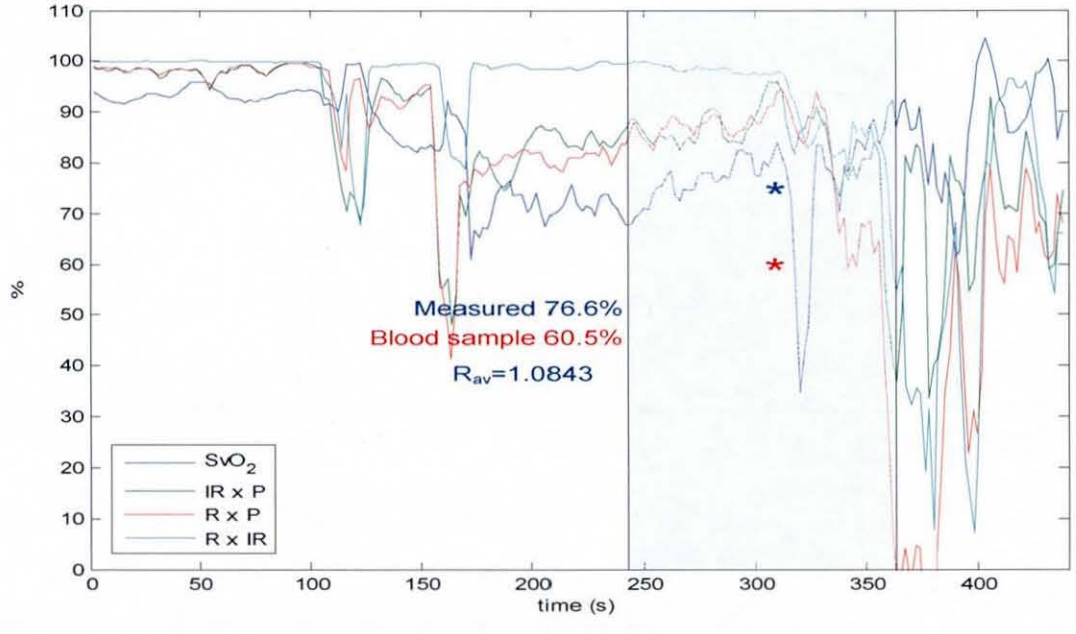

Figure 5.18 - Case study no.11

Case 12: female, age 45, height 173cm, weight 70kg, arterial blood pressure 120/75mmHg. Blood sample data: 17/04/2007 13:34, Sample No. 14627, Gas analyser ID. 348-3353

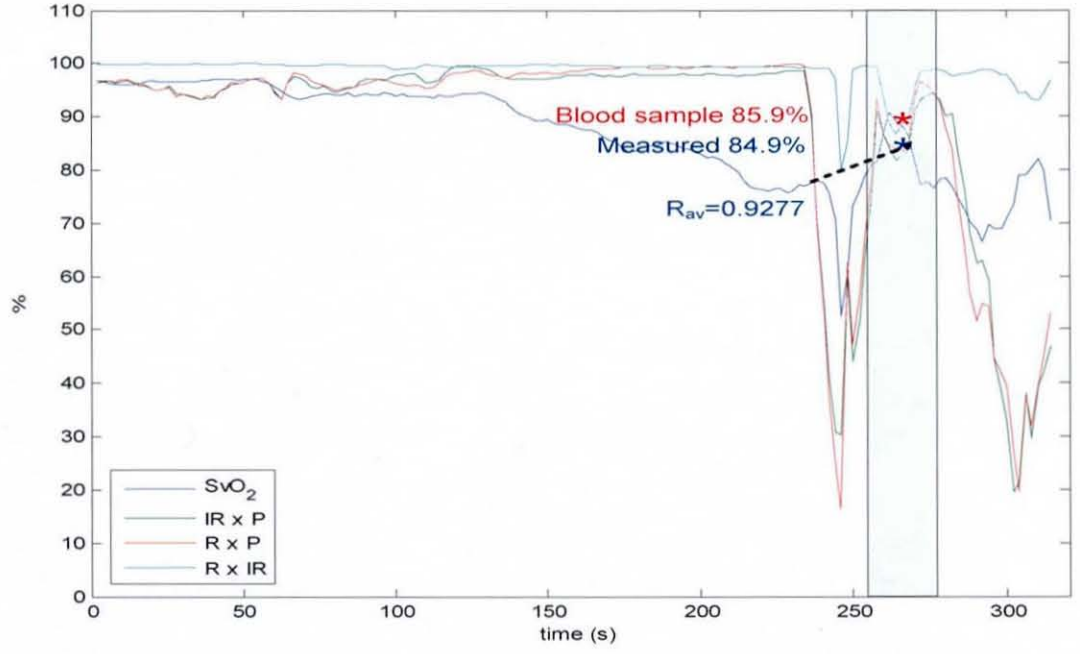

Figure 5.19 - Case study no.12

5.3.3 Discussion and Analysis

Although some values are closely related with a difference smaller than 4%, there are large differences in some paired values and the source of errors is discussed in each case separately, with a particular attention on signal quality indices (IR x P, R x P, IR x R) which provide the following indications in the presence of arterial and venous pulsations:

1) Good quality venous signal – no overlapping with heart harmonics: IR x R high (high SNR) and IR x P, R x P high (high frequency PPG signal well correlated with the pressure sensor signal).
2) Good quality venous signal – overlapping with heart harmonics: IR x R high (high SNR) and IR x P, R x P low (venous signal not very well correlated with the pressure sensor signal because of potential phase difference between high frequency PPG signal and pressure sensor signal). This does

not apply to this experiment, as arterial pulses and therefore arterial harmonics are not present.

3) Low quality venous signal: IR x R low (low SNR) and IR x P, R x P low (either because of the low SNR or overlapping with heart harmonics). It can be distinguished whether low IR x P, R x P are due to overlapping with heart harmonics, but the heart rate must be known. In this experiment, the heart rate is unknown due to arterio-venous occlusion, therefore poor signal quality indices can only be attributed to noisy signals.

Each case is separately discussed in the following section, where the time stamps represent the time interval after commencement of the study.

- Case 1: blood sample was drawn over a period of 30s, between 490s and 520s. During this period, all three signal quality indicators were high, therefore the source of the error cannot be attributed to poor signal (high IRxR). During the fist few seconds of sampling ($490s < t < 500s$) the non-invasive measurement was showing values around 80% (compared to 81.2% obtained from the blood sample) therefore if most of the sample volume was drawn during the first few seconds, then there is a close match between invasive and non-invasive methods.
- Case 2: blood sample was drawn over a period of 50s, between 540s and 590s. During most time in this period, all three signal quality indicators were high, therefore the source of the error cannot be attributed to poor signal (high IRxR). Furthermore, the non-invasive values seem to vary mainly between 70% and 80%, apart from short periods of dropping to lower values which are most likely contributed to low signal quality, as indicated by low values of IR x R, IR x P and R x P. Therefore no conclusion can be made about the difference between the two methods.
- Case 3: blood sample was drawn over a period of 35s, between 605s and 640s. During the first half of the blood sampling period, signal quality was low and non-invasive values went unexpectedly high, however, during the

second half of the sampling period signal quality indicators returned to high values and non-invasive values went down to 55%, following the interpolated slope shown in figure 5.10. Therefore it can be concluded that there was a close match between the two methods.

- Case 4: blood sample was drawn over a period of 40s, between 340s and 380s. During the blood sampling period, the venous oxygen saturation was dropping rapidly from 90% to 50% therefore since the blood sample volume was drawn over this period, the source of the error cannot be described. If it was known that most blood volume was drawn during the middle 15s of the sampling period, there would be a close match between the invasive and non-invasive methods.
- Case 5: blood sample was drawn over a period of 40s, between 380s and 420s. During the blood sampling period, the venous oxygen saturation has only changed by a few percentage units, while the signal quality indices were high, especially the IR x R which defines the SNR. The invasive and non-invasive methods have given closely matched values in this case.
- Case 6: blood sample was drawn over a period of 40s, between 380s and 420s. During the blood sampling period, the venous oxygen saturation has only changed by a few percentage units, while the signal quality indices were high. In this case it was difficult to obtain enough blood hence the surrounding tissues where rubbed in order to cause displacement of venous blood towards the punctured vein. The 9% difference between the two methods could be attributed to the fact that drawn venous blood originated from a different area, which although was proximal, it may have consumed less oxygen than the measured area, hence the higher venous oxygen value obtained from the blood sample.
- Case 7: blood sample was drawn over a period of 20s, between 370s and 390s. During the blood sampling period, the venous oxygen saturation has changed rapidly from 54% to 35%, while the signal quality indices were high. The blood sample was quickly and easily drawn and the invasive and non-invasive methods have given closely matched values.

- Case 8: blood sample was drawn over a period of 60s, between 365s and 425s. During the blood sampling period, the venous oxygen saturation seems to have changed by approximately 10% if non-invasive values were interpolated. It was difficult to obtain a blood sample and rubbing of surrounding vessels was required in order to obtain enough blood volume. The large difference between invasive and non-invasive methods could be attributed to the blood sample originating from a different area where more oxygen was extracted.
- Case 9: blood sample was drawn over a period of 20s, between 560s and 580s. The blood sample was quickly and easily drawn but there was a large difference between the two methods, hence due to the good signal quality indices no conclusions can be made.
- Case 10: blood sample was drawn over a period of 20s, between 325s and 345s. The blood sample was quickly and easily drawn and the small value difference shows that there is a close match between the two methods.
- Case 11: blood sample was drawn over a period of 120s, between 240s and 360s. It was extremely difficult to obtain a blood sample and repeated rubbing of surrounding vessels was required in order to obtain enough blood volume. The large difference between invasive and non-invasive methods could be attributed to the blood sample originating from a different area where more oxygen was extracted, but it can also be due to poor signal quality.
- Case 12: blood sample was drawn over a period of 20s, between 255s and 275s. The blood sample was quickly and easily drawn and the small value difference shows that there is a close match between the two methods however it is questionable whether the low signal quality contributed to the increase of measured venous oxygen saturation. If the non-invasive values were interpolated during the low signal quality period, then the average non-invasive value would rather be at the high 70's to low 80's region.

All data have been processed in Matlab and a reasonable agreement was observed between the invasive and the non-invasive methods, although is has to be said that the major source of error is likely to be the difficulty of obtaining blood samples. Peripheral perfusion can be poor at times therefore it is not always possible to easily draw a blood sample, especially from veins which are essentially thin collapsible tubes. Figure 5.20 shows paired values of invasively and non-invasively obtained values of venous oxygen saturation. Cases 8 and 11 denoted with '▲' in figure 5.20 were not taken into account when calculating the trend line, the mean error and the standard deviation because of the long blood sampling periods (60s and 150s respectively). The mean error was 0.4%, the standard deviation between the two measurement methods was ± 7.8% and the 95% confidence interval was ± 4.87%. If case 9 denoted with '♦' was also discarded because of the substantially larger error among paired values, then the mean error, the standard deviation and 95% confidence interval would be -1.4%, ± 5.5% and ± 3.63% respectively, while the correlation coefficient would change from 0.7 to 0.86.

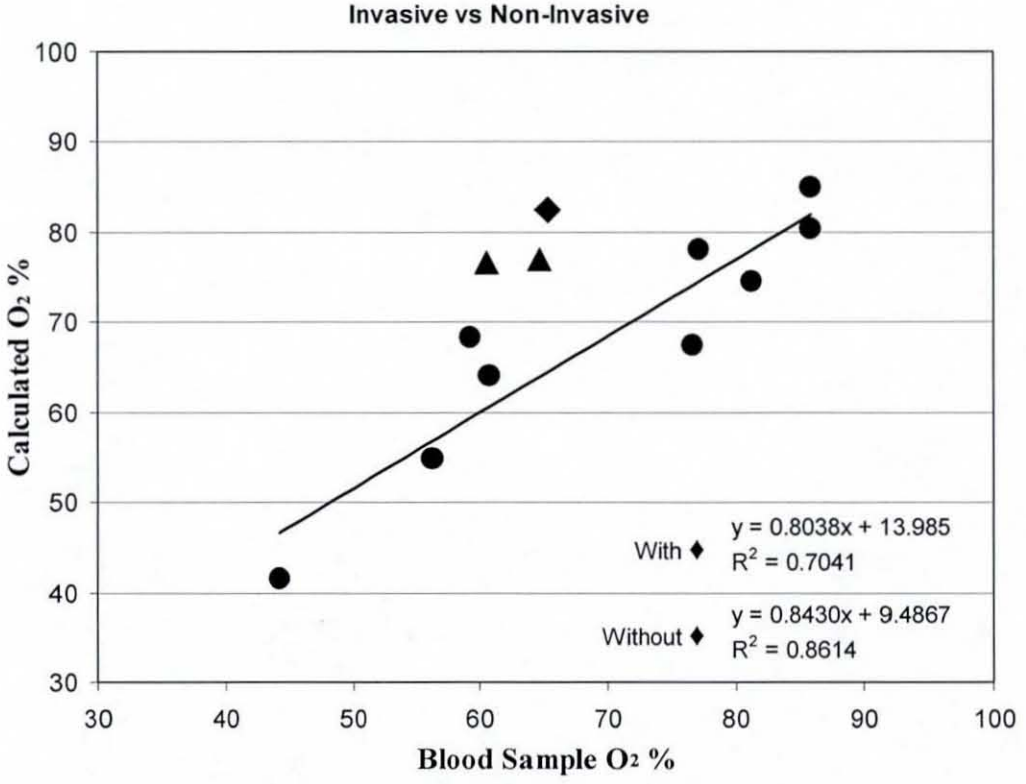

Figure 5.20 - Paired values of venous oxygen saturation

An important conclusion from this study was that the method of obtaining blood samples with fine-needled syringes, although it is the less painful solution, it could be less efficient than the method of cannulisation, where a cannula-operated needle would be inserted before the start of the experiment to provide blood samples without having to puncture a vein during measurement. However, collaborating clinicians have advised against it due to increased pain involved, as well as because it was anticipated that the blood filling the needle upon insertion of the cannula would affect the accuracy of the results. More specifically, the blood which would occupy the cannula would not lose any oxygen, therefore the drawn blood sample would contain a mixture of blood before and during the experiment.

It is still questionable thought if the use of a cannula would actually decrease the degree of difficulty to obtain enough blood volume from proximal veins, due to collapsing of the vessel. Depending on the particular vascular structure of each subject, in some cases it was reasonably easy and quick (<30s) to draw a venous blood sample but in other cases there was not enough venous blood, which required the rubbing of the surrounding area in order to move some more venous blood towards the punctured vein resulting in prolonged periods of sampling.

5.4 FEASIBILITY STUDY IN HEART SURGERY PATIENTS

The technique underwent various stages of laboratory tests in order to identify a reliable protocol which would infer venous oxygen saturation changes. One method which has shown consistent results during preliminary tests was the total occlusion of the arm (arm cuff pressure higher than systolic pressure), where gradual decrease of venous oxygen saturation was observed. It was not feasible to reliably obtain venous blood samples from the 1st digit (the measurement site of the proposed method) and hence direct comparison of blood gas analysis and readings from the proposed technique was not tenable. However, the study presented in section 5.3 where blood samples from large proximal veins were obtained has shown good agreement in some cases but there have been other cases where there was a large difference when comparing the oxygen values obtained invasively and non-invasively. A study carried out with patients undergoing various heart operations is presented in this section.

5.4.1 Experimental Purpose, Protocol and Setup

The pilot study presented in this section was designed under the hypothesis that in patients undergoing heart surgery where blood volume and temperature are both being controlled in the bypass machine during CPB, it would be possible to observe synchronised changes of peripheral ($SxvO_2$) and mixed (SvO_2) oxygen saturations. The bypass machine employs an optical fluorescence and reflectance-based in-line system to perform blood measurements and is been as the gold standard for this study. Ethical approval was given by the Leicestershire NHS Health Authority Research Ethics Committee (Appendix III). Each case is presented separately in Appendix I.

After patient anaesthetic induction and before final preparation for surgery, the pulse oximetry probe and pressure cuff were applied to the 1st digit of the left hand. The system then logged raw PPG data for the full length of the procedure. The cuff pressure was set to inflate/deflate at a maximum pressure of 40mmHg (baseline value 0mmHg) and the modulation frequency was initially set at 7.85Hz which was

re-adjusted when necessary in order to avoid overlapping with the heart's harmonics. At the end of each inflation/deflation cycle, the cuff completely deflates to avoid unwanted effects, such as venous stasis.

As part of the standard surgical procedure and anaesthetic process, arterial blood samples for blood gas and acid-base status were taken besides venous blood samples which were taken from a peripheral cannula inserted in a vein in the dorsum of the left hand. Venous blood sampling was not included in this study, as poor peripheral perfusion precluded the collection of sufficient blood quantity for analysis. Also the heart-lung bypass machine monitoring system was used to continuously monitor critical blood parameters, i.e. flow, pH, PCO_2 (Partial Pressure of CO_2), PO_2 (Partial Pressure of O_2), K^+, temperature, SO_2 (O_2 saturation), haematocrit and haemoglobin, while HCO_3^- (bicarbonate), BE (Base Excess) and VO_2 (O_2 consumption) were calculated values. Flow, blood temperature, SO_2 (venous) and VO_2 were considered in this study. Arterial oxygen saturation was not included in results and discussion, as no variations were observed in all patients (98% - 99%).

The heart-lung machine monitor logged all available blood parameters every 5 minutes and all data recorded by the prototype device were sampled at the same rate. SvO_2 and $SxvO_2$ were expressed in a "self-normalized" format as a percentage of the variation for a given patient, in order to compensate for different variations. For example, if $\max(SvO_2)=90$ and $\min(SvO_2)=50$ respectively, then $SvO_2=70$ expressed as a percentage of the variation, would be $nSvO_2=50\%$.

During the course of the operation all important events and critical changes in the haemodynamic status of the patient were logged for post-operative data analysis. As part of the surgical protocol in certain operation procedures, the blood temperature was dropped to extreme hypothermic levels (24°C) resulting in poor perfusion of the periphery, hence a trained operator was monitoring the venous signal quality index to improve signal quality when necessary; i.e. increase the photodiode's amplifier gain, should AC was too small due to hypoperfusion. In a typical CPB procedure,

body temperature is gradually decreased to reduce the metabolic rate and to avoid tissue damage; the heart is arrested after aortic cross-clamping with a cardioplegic solution. During the cooling phase, VO_2 drops dramatically resulting in increased SvO_2 due to low metabolism. When the surgery is completed, the aortic cross-clamp is released and the patient is warmed up to a body temperature of approximately 37°C; during the rewarming phase, rapid changes of VO_2 cause dramatic variations of SvO_2. The body's increasing demands for oxygen during this phase are compensated for, by increasing the blood flow, which in turn increments SvO_2. The main focus of this study is to observe the response of the proposed method under similar conditions of supply/demand balance changes.

The values and signals displayed on the prototype device were not used during surgery and no changes were made to the patient treatment plan as a result of participating in this study. The study setup included the bypass machine monitor (CDI-500, Terumo USA) which measured the parameters described above, a prototype device to measure peripheral venous oxygen saturation from the 1st digit of the left hand, including a pulse oximetry probe (P861RA, Viamed UK) and a digit cuff (DC-1.6, Hokanson USA) which introduces artificial pulsations in the venous system.

5.4.2 Experimental Results

The primary aim was to observe the performance of the non-invasive technique during cardiopulmonary bypass where major physiological parameters are kept under control, such as temperature and flow. Data analysis has shown positive correlation between central and peripheral oxygen saturation in certain conditions, which implies that the proposed method applied in the periphery, can detect central venous oxygen saturation changes[84]. These changes are more pronounced when there is an increasing or decreasing demand for oxygen. All patient data were grouped according to blood temperature, blood flow and VO_2 in order to show the overall responses of both the proposed method and the bypass machine in a compact format (Box-Whisker plots).

5.4.2a Venous Oxygen Saturation and Blood Temperature as a Function of Overall Oxygen Consumption

Box-Whisker figures 5.21, 5.22 and 5.23 show $nSvO_2$, $nSxvO_2$ and blood temperature for all patients plotted against total oxygen consumption measured by the bypass machine, normalized to body surface area (BSA) by using the Mosteller formula[85]. Therefore the normalised oxygen consumption units are ml O_2 $min^{-1}m^{-2}$.

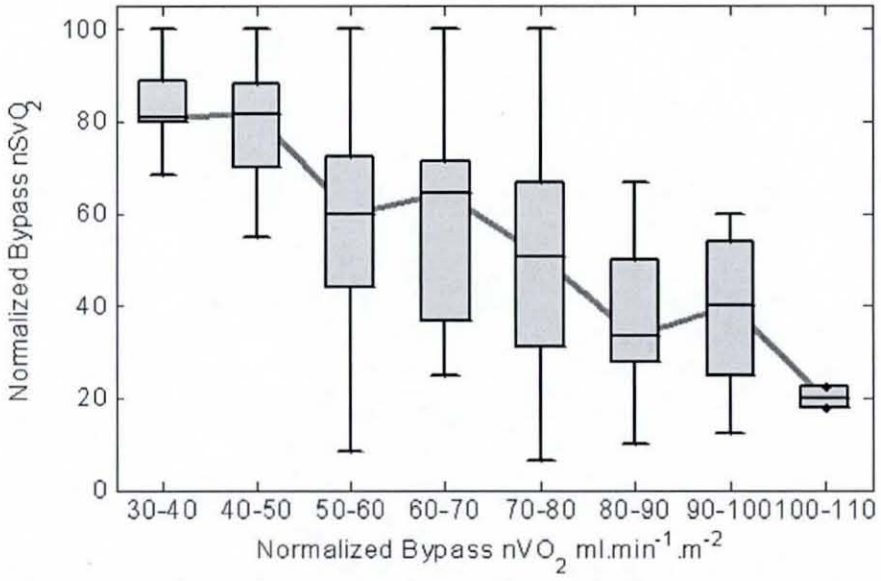

Figure 5.21 - Box and Whisker plot: negative correlation between $nSvO_2$ and nVO_2

The values of $nSvO_2$, $nSxvO_2$ and blood temperature were grouped according to their corresponding VO_2 values. For example, the first box in figure 5.21 shows all values of $nSvO_2$ when $30 \leq VO_2 < 40$ ml min^{-1} m^{-2}. For each time instance, all three parameters were present; in order to achieve this, some data reduction has been performed. From 23 patients which took part in the study, 3 patient data sets were excluded due to insufficient data. From the remaining 20 data sets, there is a total number of n=466 5-minute measurements before data reduction; for each patient, mean=23.3 +/- SD=9.98. Regarding the data reduction, the total number of samples discarded for all patients was n=134 and for each patient, mean=6.70 +/- SD=11.86, mainly because in two long operations (81 samples in total) the bypass machine unexpectedly failed to record VO_2 along with some other parameters.

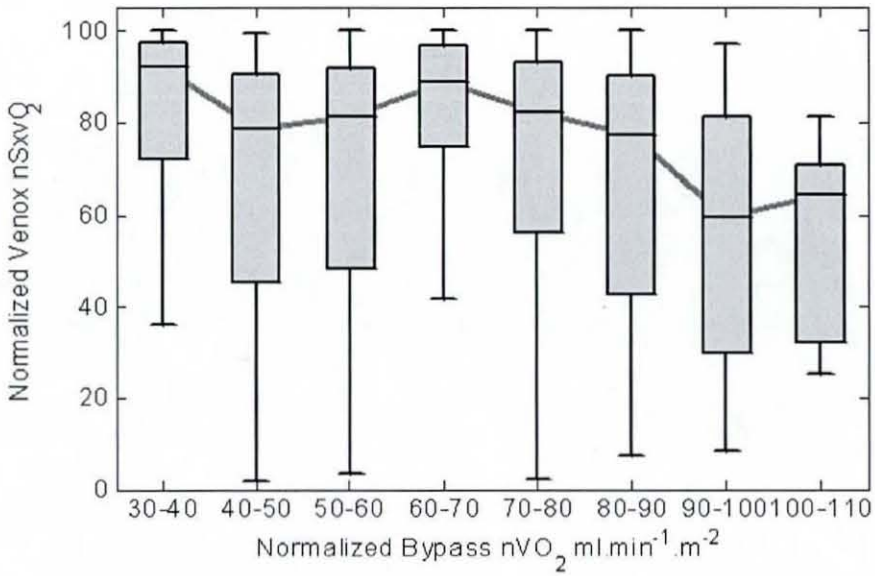

Figure 5.22 - Box and Whisker plot: negative correlation between $nSxvO_2$ and nVO_2

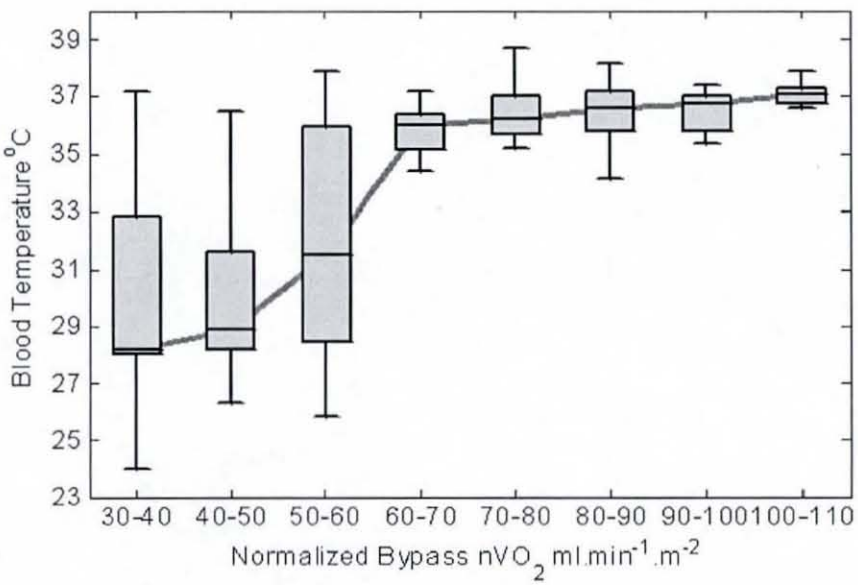

Figure 5.23 - Box and Whisker plot: positive correlation between blood temperature and nVO_2

5.4.2b Venous Oxygen Saturation as a Function of Blood Temperature

Figures 5.24 and 5.25 illustrate the variation of venous oxygen saturation centrally and peripherally respectively, where each box corresponds to a range of 1°C. Similarly to the previous section, some data reduction has been performed to ensure all three values ($nSvO_2$, $nSvO_2$ and blood temperature) were present for each time

instance. Before reduction, total number of samples n=466; for each patient, mean=23.3 +/- SD=9.98 samples. Data reduction: the total number of samples discarded for all patients was n=44 and for each patient, mean=2.20 +/- SD=1.15.

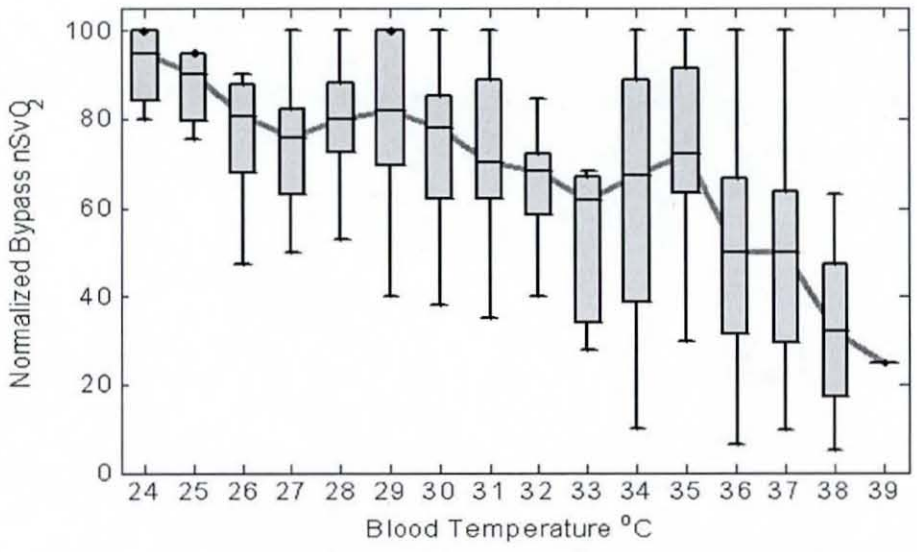

Figure 5.24 - Box and Whisker plot: negative correlation between $nSvO_2$ and blood temperature

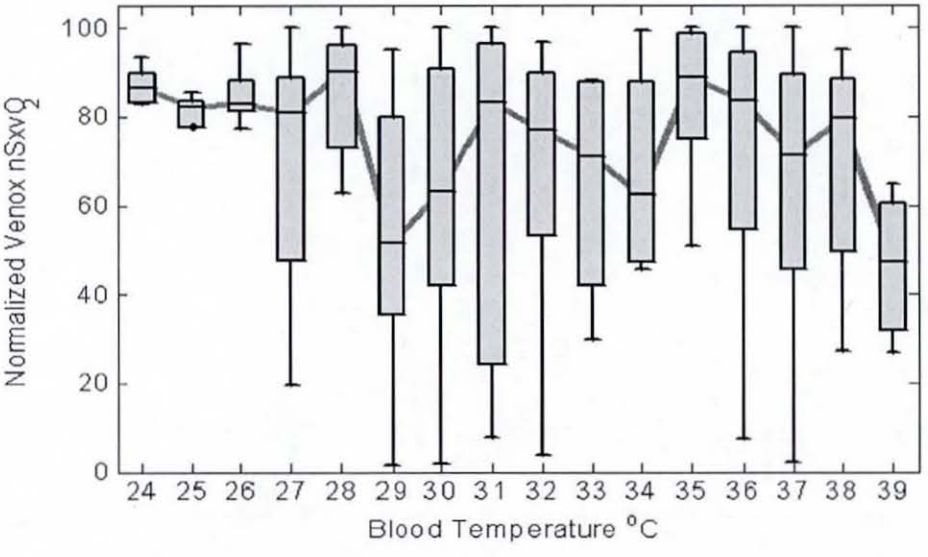

Figure 5.25 - Box and Whisker plot: relationship between $nSxvO_2$ and blood temperature

5.4.2c Venous Oxygen Saturation as a Function of Cardiac Index

The cardiac index (CI in l min^{-1} m^{-2}) was calculated from the cardiac output (CO in l min^{-1}) by dividing it with the BSA of each subject. The CO value is essentially the blood flow of the heart-lung machine pump. Similarly to previous sections, data reduction has been performed to ensure values for all three parameters ($nSvO_2$, $nSxvO_2$ and CI) were present for each time instance in figures 5.26 and 5.27. Before reduction, total number of samples n=466; for each patient, mean=23.3 +/- SD=9.98 samples. Data reduction: the total number of samples discarded for all patients was n=131 and for each patient, mean=6.55 +/- SD=11.90.

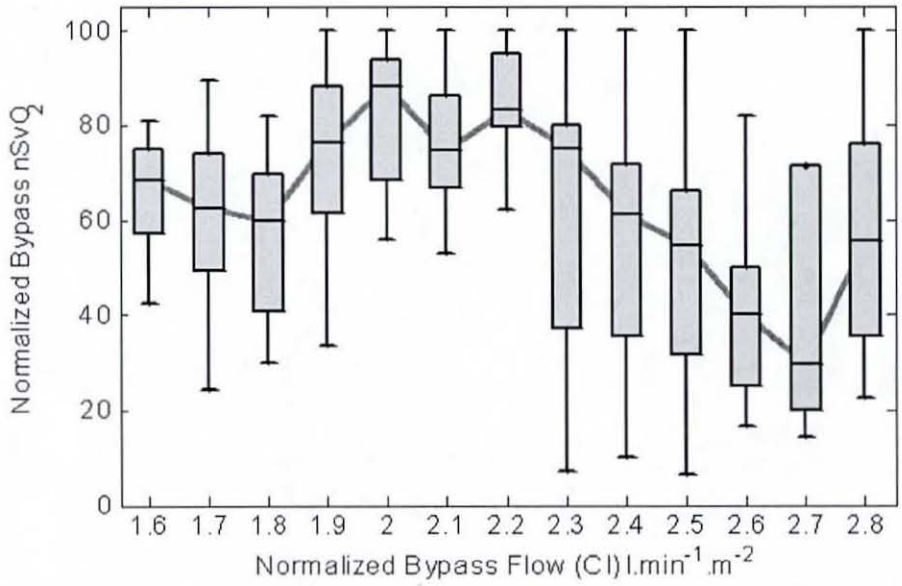

Figure 5.26 - Box and Whisker plot: relationship between $nSvO_2$ and Cardiac Index

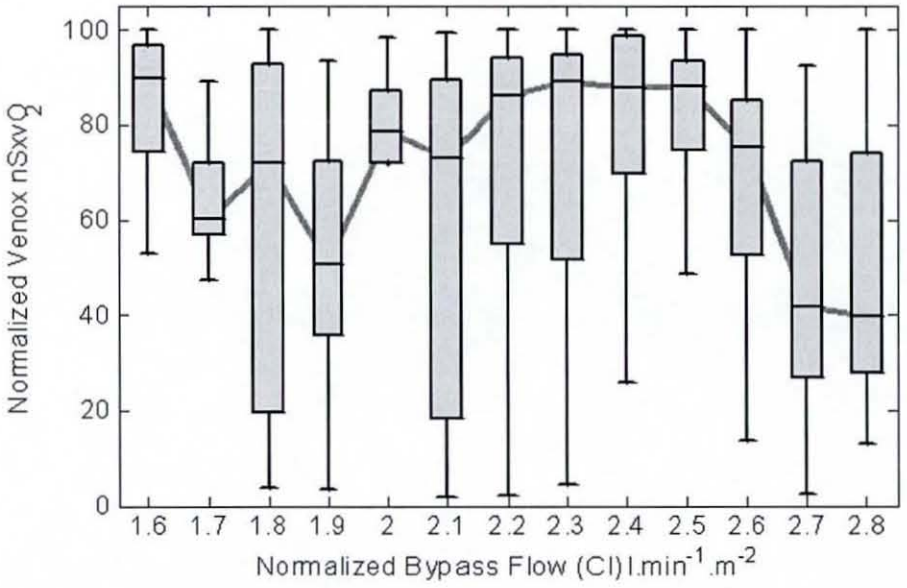

Figure 5.27 - Box and Whisker plot: relationship between $nSxvO_2$ and Cardiac Index

5.4.3 Discussion and Analysis

The data recorded by the prototype device have been converted to oxygen saturation values by using a standard empirical calibration curve - equation 5.1, and then each value was expressed as a percentage of variation for a given patient, as a means of 'self-normalization'. Figure 5.21 shows the relation between normalized $nSvO_2$ and VO_2 normalized to BSA. $nSvO_2$ decreases when the total oxygen consumption increases which shows that when there is an increasing demand for oxygen, $nSvO_2$ drops because more oxygen was released to the tissues.

Figure 5.22 presents the relation between $nSxvO_2$ and normalized VO_2, where a trend similar to figure 5.21 is shown. Vasodilator and/or vasoconstrictor administration during CPB may affect the body oxygen metabolism and worsen the complications induced by hypoperfusion during CPB[86]. Therefore, although these effects render difficult the direct comparison between central and peripheral venous oxygen saturation, the significant trend similarity between figures 4.21 and 4.22 may be an indication of relative agreement between the bypass machine and the proposed method.

Figure 5.23 shows that the main effect of low blood temperature is the decrease of the rate of metabolism and therefore the reduction of oxygen extraction compared to normothermic conditions. The primary purpose of reducing the blood temperature in CPB is to reduce the rate of oxygen metabolism in order to protect organs and tissues. However, a later study[87] has concluded that an immediate decrease in VO_2 caused by the initiation of deep hypothermic CPB could not be simply due to a decrease in the metabolic rate but also due to disturbances in oxygen utilization, one of which seemed to be caused by the impaired oxygen release from haemoglobin. Other studies[88] have investigated the relationship between SvO_2 and temperature and concluded that change of body temperature is the most important factor that affects SvO_2.

The positive correlation between oxygen utilization and blood temperature which can be concluded from figure 5.23 implies the negative correlation between normalized venous oxygen saturation and blood temperature (figure 5.24). Whether the oxygen extraction is a function of metabolism or impaired oxygen release there is negative correlation between oxygen consumption and normalized venous blood saturation. Figure 5.24 illustrates the reduction of $nSvO_2$ as the blood temperature approaches normal values while figure 5.25 shows the normalized oxygen saturation measured peripherally by the proposed method. In figure 5.24, $nSvO_2$ is negatively correlated with blood temperature in accordance with a previous study[85]. There is also a decreasing trend between $nSxvO_2$ and blood temperature in figure 5.25, however the variations of $nSxvO_2$ for a given temperature range are larger than those of SvO_2, especially between 30°C and 31°C. In fact, most patients in this study were cooled down to 28°C-30°C and therefore the rewarming phase for those patients was initiated in this temperature region, hence metabolic acidosis or hypoperfusion during CPB may have caused this large variation of venous oxygen saturation. In the same study[85] it was found that SvO_2 was markedly decreased after rewarming, therefore high peripheral venous oxygen variations will occur after rewarming was initiated. It is important to emphasize that the majority of venous oxygen variations were observed during rapid changes in oxygen consumption (VO_2) which closely followed blood temperature changes; hence the rewarming

temperature region has the largest venous oxygen variation observed. In the temperature region between 35°C and 38°C, $nSxvO_2$ clustered in higher values, which was almost certainly due to the recovery of peripheral perfusion which implies a higher supply/demand fraction. On the other hand, at low temperatures (24°C-26°C) both $nSvO_2$ and $nSxvO_2$ have unusually high values. In fact the study[85] concluded that hypothermia reduces the oxygen consumption and increases the oxygen in physical solution; therefore, most of the metabolic need for oxygen can be met from the dissolved oxygen without using the haemoglobin transport system, hence the high values of $nSvO_2$ and $nSxvO_2$.

Figure 5.26 illustrates the relation between central venous oxygen and flow while peripheral venous oxygen is shown in figure 5.27. The increasing trends of $nSxvO_2$ (between 1.7 and 2.4 l min^{-1} m^{-2}) and $nSvO_2$ (between 1.7 and 2.0 l min^{-1} m^{-2}) are in agreement with the previously referenced study[85], where it was observed that an adequate SvO_2 was found when the flow was greater than 2.4 l min^{-1} m^{-2}. No direct conclusions can be made, since the supply/demand balance is also a function of blood temperature affecting the venous oxygen saturation. More in particular, in the "high flow" region (between 2.3 and 2.7 l min^{-1} m^{-2} for $nSvO_2$ and between 2.6 and 2.8 l min^{-1} m^{-2} for $nSxvO_2$) both peripheral and central normalized venous oxygen values decrease. This could be attributed to the increased oxygen consumption at high flow rates (usually set towards the end of the operation) which are more often accompanied by blood temperature shifts towards normothermic conditions, resulting in higher oxygen consumption.

The present observation study indicates that continuous monitoring of peripheral venous oxygen saturation can be feasible with the proposed method in the clinical care. Direct correlation of central and peripheral venous oxygen saturation values is viable in certain cases where the supply or demand balance changes rapidly, however it is not anticipated that it is presently possible to infer mixed venous oxygen saturation from the periphery. This study showed that the proposed method can detect VO_2 changes even under low perfusion conditions which are common in CPB hypothermia. During hypothermia both $nSxvO_2$ and $nSvO_2$ values were found

to be elevated while during re-warming and upon rapid changes of VO_2, the proposed method was sensitive to surges of oxygen extraction, indicating that the supply/demand balance had changed rapidly. There is also a similar sensitivity to changes of CI under normal temperature conditions. This feature can be extremely useful in pathological conditions which can cause similar effects, such as sepsis[89,90].While this observation study describes the response of the proposed method to changes of oxygen consumption, blood temperature and blood flow, it cannot be concluded whether the proposed method can accurately measure venous oxygen saturation.

5.5 OVERVIEW

This chapter describes the evaluation of the non-invasive method for venous oximetry which was carried out from four different perspectives:

- The in-vitro experiment for the comparative calibration with a commercial pulse oximeter was aiming to the investigation of the PPG board's signal quality and accuracy, which was found to be comparable to the commercial pulse oximeter. Without knowing the performance of the signal capturing device in controlled in-vitro conditions it would be impossible to evaluate its functionality and performance in real-life experiments.
- The model evaluation experiments aimed at the investigation of the hypotheses relating to anatomical and physiological effects which can affect the accuracy of the method, when measuring arterial and venous oxygen saturation. Although the non-invasive method of measuring blood oxygen is an in-vivo method based on numerous assumptions, the modelling experiments have successfully provided a certain level of understanding some basic anatomical and physiological effects of the vascular system.
- The venous oxygen de-saturation study aimed at the confirmation of the method's capacity to measure venous oxygen saturation. Although the results when comparing the method with the gas-analysed blood samples are partly satisfactory, there are still questions about the method of blood sampling and whether adjacent veins actually have comparable oxygen saturation values. Nevertheless, the device was able to register the gradual decrement of venous oxygen saturation in every single case, which shows that the method is capable of measuring venous oxygen saturation.
- The feasibility study in the clinical setting aimed at the investigation of the method's performance and functionality in real-life conditions. Not only from an environmental point of view (the operating theatre) but also from a feasibility point of view (severe clinical conditions) in order to test the overall performance of the device in a variety of pathophysiological conditions arising in major operating procedures, such as heart surgery.

Moreover, this study has confirmed the robustness of the system in long recording conditions in an electrically-noisy environment such as the operating theatre.

Conclusively, the overall performance has proven that the method is worthy of further investigation and is discussed in chapter 6.

6 CONCLUSIONS / FUTURE WORK

Continuous monitoring of venous oxygen saturation currently requires the installation of a catheter, a complicated and time-consuming procedure which is highly invasive and involves severe risks for the patient. Although attempts have been made to address the lack of a non-invasive venous oximeter, no existing technology is suitable for the continuous, non-invasive measurement of simultaneous arterial and venous oxygen saturation. The importance of having both these parameters available lies in the fact that oxygen consumption can be calculated, hence other physiological parameters may be extracted with the aid of a haemodynamic physiological model, or even by using known models such as the Fick principle, relating the cardiac output with oxygen consumption, arterial and venous oxygen saturations. These parameters can be for example, cardiac output currently requiring the use of an invasive thermodilution technique, or oxygen consumption through the use of a spirometer.

6.1 CONCLUSIONS

a. Human physiology of oxygen supply and demand (aim 1): The underpinning physiological concepts were introduced in chapter 2. These concepts have provided the minimum content necessary to provide the context for the development of a device to measure venous oxygenation.

b. Theoretical modelling and its validation (aim 2 and aim 4): The model developed to describe the arterial and venous PPG signals under certain physiological and anatomical conditions is consistent with the predominantly contemporary model of Beer-Lambert law, and has clarified the optimal operating conditions of the artificial venous modulation system as well as the possibility to introduce a method of correcting arterial oxygen saturation obtained from widely used pulse oximeters. Although the difference between uncorrected and corrected arterial oxygen saturation values (SaO_2 and $cSaO_2$) was measured in the region of 3% it is unknown whether such a difference might have a significant clinical meaning in the assessment of adequacy of oxygen supply. Nevertheless, keeping in mind that measurements were carried out on a healthy subject, it cannot be concluded whether similar differences would be observed in a clinical condition. On the other hand, the second part of the model has provided the means of understanding the mechanical coupling of the artificial pulsation into the arteries, which means the optimal modulation depth, is now known and can actually be measured.

c. Development of venous oximetry (aim 3): Through the development of three different generations of prototypes it was shown that close collaboration between engineers and clinicians can lead to the successful design and realisation of innovative methods and devices which can contribute to better clinical monitoring facilities. Moreover, the easy-to-use final prototype device was designed and built in an embedded format, starting from a complicated, large and non-versatile design and through this prototyping experience, valuable expertise on medical device design and construction was gained.

d. Comparative calibration (aim 4): The calibration results have confirmed that the system performance in terms of measuring the absorbance of haemoglobin is closely matched with a commercial pulse oximeter, although it would be preferable to perform the calibration in a circulatory calibration system with real blood. The 2% offset between the prototype device and the commercial oximeter was successfully eliminated by adjusting equation 5.1 and the next step for calibration is to use real blood as the light absorber.

e. Venous oxygen de-saturation study (aim 4): Through the venous oxygen de-saturation study it was confirmed that the device detects the gradual decrease of venous oxygen saturation, although the comparability with blood gas analysis remains inconclusive because of the difficulty to obtain blood samples in certain cases. This problem may be eliminated by performing a study at a more central area where venous blood supply is higher, by employing a reflection mode probe and a patch-type cuff which are briefly presented in section 6.2.

f. Feasibility study in cardiac surgery patients (aim 4): The method was evaluated in a number of different haemodynamic conditions which may occur in the course of a heart surgery, such as low blood flow (cardiac index), vasoconstriction and low oxygen consumption during hypothermia, or vasodilatation and increased oxygen consumption. The device was able to detect changes of blood flow and oxygen consumption, especially during the periods of patient rewarming which accompanied by increased oxygen consumption, therefore a further investigation in a larger scale study is worthwhile.

The evaluation of the method and the device from four different points of view has demonstrated the capability to measure venous oxygen saturation, although further evaluation is necessary in a large number of subjects in order to establish the full potential of the technology. According to the collaborating clinicians, a continuous monitor capable of indicating cardiac output trends, even without absolute values, would be extremely useful post-operatively in heart surgery patients, as it would

provide another way of assessing the successfulness of the operation. Moreover, if absolute values of cardiac index would be possible then the device would make an excellent non-invasive tool for the long-term monitoring of patients suffering from cardiovascular diseases, in which case the doctor would be able to assess the efficacy of drugs administered.

6.2 SUGGESTIONS FOR FUTURE WORK

This section responds to aim 5 of the study and presents suggestions for future work in this area, highlighting both speculative applications empowered by the use of the artificial pulsations and possible studies that could be used to investigate further and develop more sophisticated models taking into account important physiological parameters, such as local and central blood temperatures.

6.2.1 Design of a Disposable Venous Oximetry Probe

Although the current finger probe and modulation cuff configuration was sufficient to obtain reliably PPG signals, the use of a disposable probe would provide multiple benefits, with the most obvious one being hygiene. The existence of highly contagious and life-threatening pathogens like the MRSA has been known for many years, disturbing the smooth operation of hospitals and clinics and subjecting patients to high risk. A re-usable pulse oximetry probe could be one of the contaminating sources if not properly sterilised. Another benefit of single-use probes, especially when used with the non-invasive venous oximetry method, is the mechanical difference with the re-usable probe. More specifically, the re-usable probe has a spring in order to clip around the finger which is tight enough to keep the probe in place, without constricting arterial flow which can be caused by excessive pressure applied to the clip. On the other hand, with the venous system operating at a very low pressure and given the collapsibility of veins due to their particular structure, it was found that the venous PPG signal was a lot stronger when the probe's spring tension was reduced. This observation has lead to the conclusion that arterial pulse oximetry probes may not be fully compliant with the low venous pressure. In an attempt to reduce the spring tension by modifying its steady-state dimensions it was noted that the probe became more susceptible to motion artefacts,

given that the spring tension was not enough to hold the probe tightly around the finger. Moreover, at high modulation depth conditions, the inflation/deflation of the digit cuff can result in finger movement. Considering the weight and inertia of the probe, it is more than likely that the coupling coefficient between the probe and the finger will change, leading to erroneous readings. If a disposable probe was used instead, neither problems would exist because the tightness can be adjusted and the small weight of the probe would solve the problem of motion artefacts. Figure 6.1 shows a typical disposable pulse oximetry probe, while figures 5.2 and 5.3 illustrate an example of the proposed disposable venous oximetry probe.

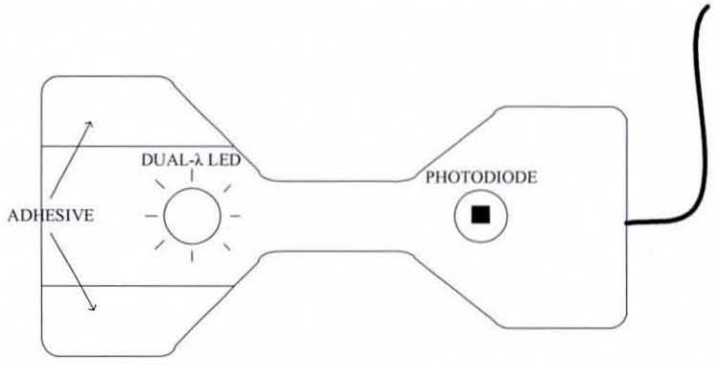

Figure 6.1 - Typical disposable pulse oximetry probe design

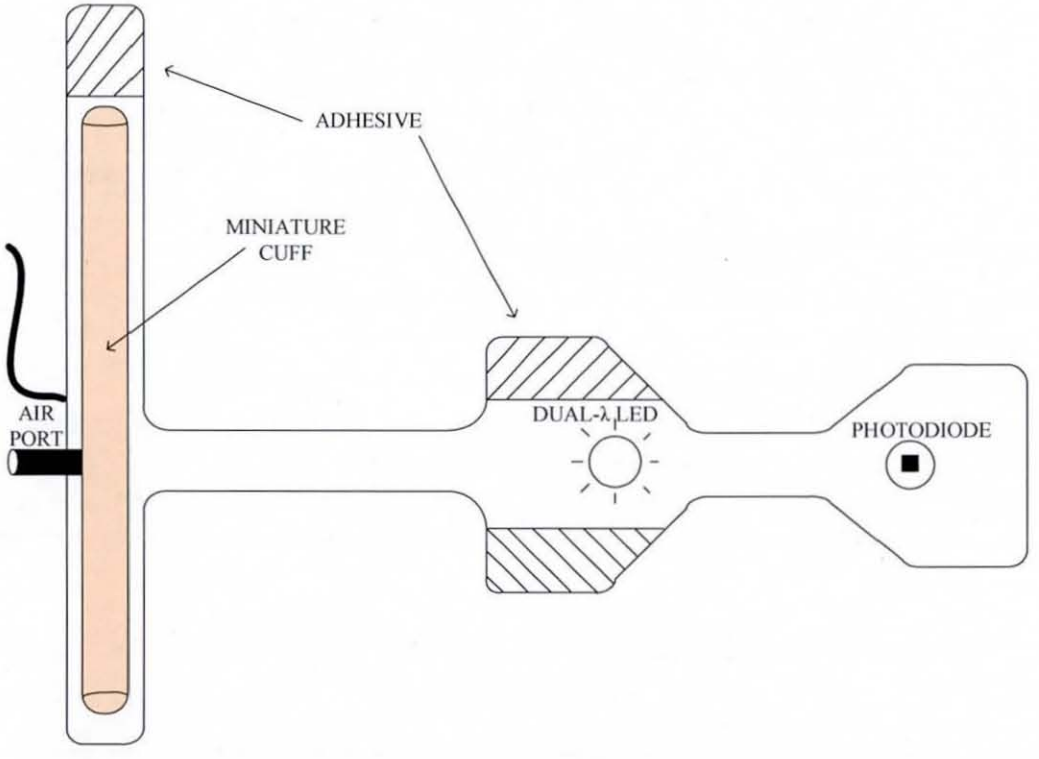

Figure 6.2 - Disposable venous oximetry probe design (bottom view)

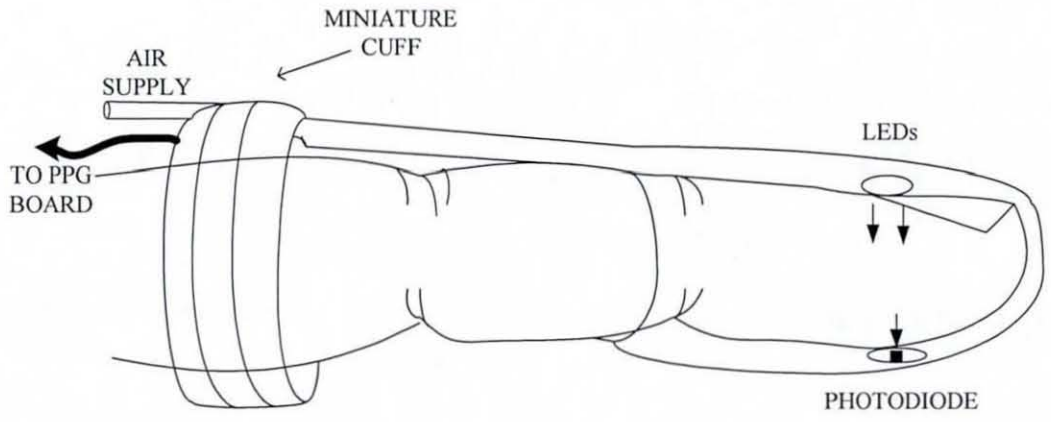

Figure 6.3 - Disposable venous oximetry probe application

6.2.2 Design of a Reflection-Mode Probe

It was demonstrated that it is possible to measure venous oxygen peripherally by applying a pulse oximetry probe and a digit cuff on a finger and it was also shown that there is some relation between cardiac output, oxygen consumption and peripheral venous oxygen saturation. But an important question that still remains is whether peripheral venous oxygen saturation will help in the overall assessment of a clinical condition. One of the important targets for improving the method was to construct a reflection-mode oximetry probe in order to apply the venous oximetry technique as close as possible to the heart in an attempt to measure central venous oxygen saturation, a very important parameter in the assessment of overall oxygen utilisation. One of the problems associated with this approach was the small penetration depth of conventional leds which emit incoherent light, resulting to poor signal quality because of the low SNR. A new probe was designed using newer technology light emitters called RCLEDs, which stands for Resonant Cavity Light Emitting Diodes and provide laser-like performance with narrow light beams and more importantly, narrow output bandwidth. Although they are known for a few years, they have not been used yet in pulse oximetry; they are mainly used in telecommunications and more specifically in optical fibre networks. Their narrow beam means higher penetrations depth, while the narrower output bandwidth means that RCLEDs are likely to provide oxygen saturation values more accurately, since in practice they could almost be considered as monochromatic light sources. Figure

6.4 shows a single-wave (870nm) reflection-mode PPG probe, which was built to test the performance of RCLEDs in photoplethysmography, and it was found that it can pick up PPG signals from areas where it was previously impossible, like from the spine or the back of the head. Therefore it may now be possible to perform measurements in areas which require a greater light penetration depth. Furthermore, the probe has been successfully tested in non-contact experiments where it was shown that arterial photoplethysmographic signals can be captured from a distance of several centimetres. Such a potential could in fact lead to non-contact pulse oximetry which has not been previously achieved.

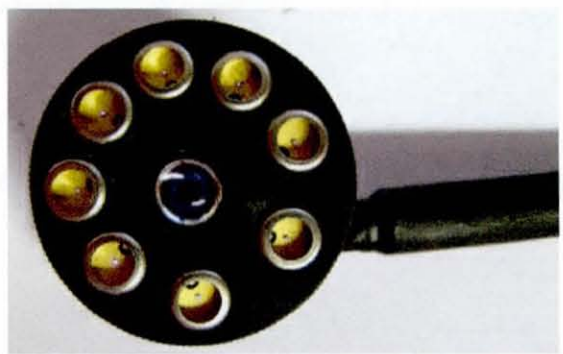

Figure 6.4 - Single-wavelength RCLED reflection-mode PPG probe

6.2.3 Application of Venous Oximetry to Other Areas

Due to the lack of an appropriate probe the method was so far limited to application on a finger. However, after the successful testing of the new reflection-mode probe, the method can now be applied to other areas with a particular interest in the neck. The internal (main return of venous blood from brain[91,92]) external jugular veins carry de-oxygenated blood from the head and descend on each side of the neck. Both veins present pulsations being close to the heart and provide extremely valuable haemodynamic information about the function of the right atrium of the heart. Although there are standard tests to assess jugular veins, the design of a protocol to continuously measure venous oxygen saturation non-invasively from the jugular veins will provide a means of monitoring cerebral venous oxygen saturation. Furthermore, the jugular venous oxygen saturation can provide other important

indications, such as the prediction of short-term postoperative neurologic dysfunction in elderly cardiopulmonary bypass patients[93].

6.2.4 Assessment of Arterial Calcification

Referring to the first part of the model developed in chapter 3 and evaluated in chapter 5, it was found that there was a difference of 2.5%-2.8% between low and high venous pressure, attributed to elasticity of the arteries. When the venous pressure was high (40-45mmHg) the arterial expansion did not affect the venous flow in the same degree as when the venous pressure was at physiological levels. This leads to the conclusion that the level of arterial expansion could be assessed by implementing the test protocol of the first part of the model in the sense that if there is no difference between the two phases of the protocol, then it could indicate the reduced arterial elasticity, a common symptom of the atheromatous plaque which causes arterial hardening[94].

6.2.5 Calibration at a More Central Area

Recalling the problems of obtaining peripheral blood samples in both the venous de-saturation study and the clinical evaluation, as well as the differences between the invasive and non-invasive values of the venous de-saturation study, it was concluded that it would be a better solution to perform measurements on a larger veins where blood sampling would be easier. The main problem was the acquisition of PPG signals from areas other than the finger, where the method is currently limited to. However, previous tests on the forearm and preliminary tests of the reflection-mode RCLED probe have shown that it can be possible to apply the technique to other parts of the body, hence perform a calibration study on well-perfused areas. The investigation of applying the technique on the forearm has shown that it is possible to obtain PPG signals using a normal reflection-model PPG probe on the cephalic vein of the left forearm. The only limitation at this point is the generation of artificial venous pulsations in areas where a cuff cannot be installed. However, a custom-designed patch-cuff could be applied in areas where superficial veins exist. An example of such a cuff is shown in figure 6.5.

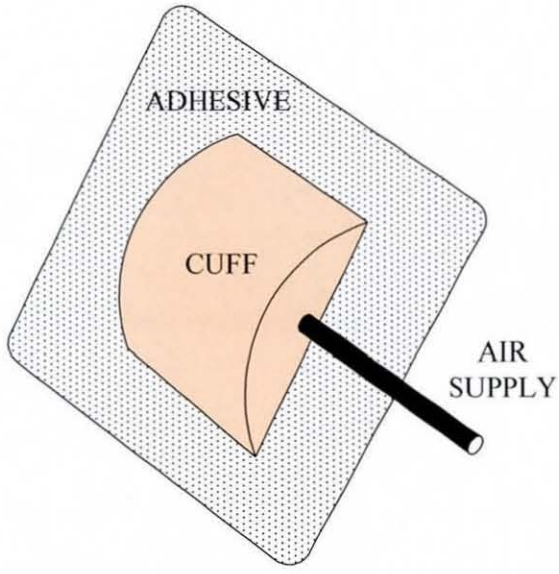

Figure 6.5 - Patch cuff for use with a reflection-mode probe (bottom view)

Therefore, with the use of a reflection mode probe similar to the one in figure 6.4 and a patch-cuff shown in figure 6.5, a more accurate calibration of the method could be implemented in a central area of the body.

6.2.6 In-Vitro Circulatory Calibration System

The first approach for the comparative calibration involved the construction of a finger phantom model with silicone tubing of different sizes and characteristics which was connected in a simple circulatory system, with a peristaltic pump (505S, Watson-Marlow Bredel Pumps Inc) replicating the function of the heart. A set of light absorbing mixtures combined in several different volume ratios was prepared, in order to mimic the light absorption of arterial blood. Figure 6.6 illustrates the arrangement of the circulatory model.

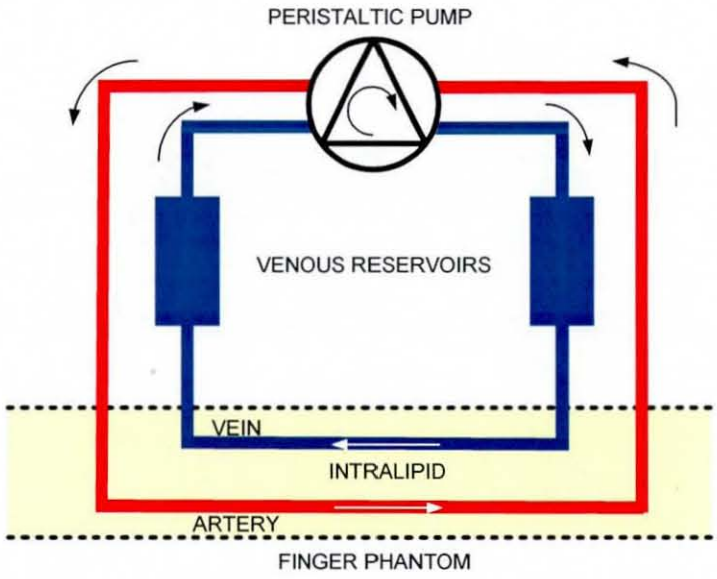

Figure 6.6 - Circulatory model for comparative calibration

The finger phantom was created around a silicone tube with inner diameter of 12mm and wall thickness of 1mm, which contained two smaller latex tubes with 3mm inner diameter and 1mm wall thickness, representing an artery and a vein. The 12mm tube representing the finger was filled with intralipid emulsion 10% diluted in distilled water, a popular diffusion and scattering medium for biological phantoms, since its diffusion and scattering effects are closely matched with biological tissues[95,96]. The finger model is shown in figure 6.7.

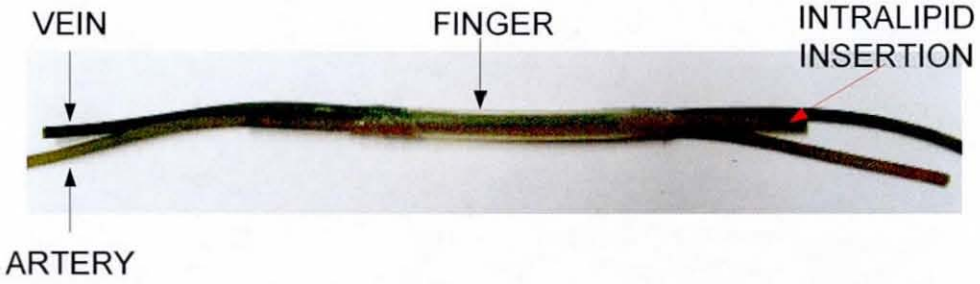

Figure 6.7 - Finger phantom constructed from thin flexible tubing

The 'arterial' and 'venous' circulatory systems were separate systems driven by the same peristaltic pump but in opposite directions, like the real human circulation. The venous system was also connected to two expandable reservoirs in order to minimise the pulsations of the pump by as much as possible; the two venous

reservoirs dissipate the pumping and suction effects by expanding and shrinking in size, respectively.

Tests have shown that there were excessive motion artefacts in the finger model originating from the peristaltic pump's action, causing displacement of the artery and vein, therefore altering significantly the light path, leading to erroneous readings. This was first noted when the pump was set to operate clockwise and afterwards anti-clockwise, where different readings were obtained from the pulse oximeter.

Although the comparative calibration with the design and construction of a static finger phantom has produced very good results, the realisation of an in-vitro circulatory system using real blood would most likely provide more information, not only about the accuracy of the method in terms of oxygen saturation measurement, but with an accurately designed finger phantom, a novel fluid-dynamic study could lead to a mathematical model for major haemodynamic effects, such as vasoconstriction and vasodilatation. By addressing the problem of lack of a physiology model to describe these effects, it could be possible to infer peripheral venous oxygen saturation, to values of central venous oxygen. Such an achievement would introduce a medical device with an enormous number of applications, from GP offices and ambulatory settings to operating theatres and intensive care units, to the same extent as conventional pulse oximetry.

REFERENCES

[1] Shelley K. H, Tamai D, Jablonka D, Gesquiere M, Stout R. G, Silverman D. G. "The effect of venous pulsation on the forehead pulse oximeter wave form as a possible source of error in SpO_2 calculation", Anesth. Analg., **100**, pp.743-747 (2005)

[2] Shelley K, Dickstein M, Shulman S. "The detection of peripheral venous pulsation using the pulse oximeter as a plethysmograph", J. Clin. Monit., **9**, pp.283–7 (1993)

[3] Levy M.N, Pappano A.J. "Cardiovascular physiology" 9th edition, Mosby Elsevier, Philadelphia, pp.1-4 (2007)

[4] Van De Graaff K.M, Fox S.I. "Concepts of human anatomy and physiology" 3rd edition, WCB, Dubuque, pp.673-677 (1992)

[5] Holden M, Makic M.B. "Clinically induced hypothermia: why chill your patient?", AACN Adv. Crit. Care, **17(2)**, pp.125-132 (2006)

[6] Stock M. C, Ryan M. E. "Oxygen consumption calculated from the Fick Equation has limited utility", Crit Care Med., **24(1)**, pp.86-90 (1996)

[7] Gregory I. C. "The oxygen and carbon monoxide capacities of fetal and adult blood", J. Physiol., **236(3)**, pp.625-634, Feb. (1974)

[8] Mark J. B, FitzGerald D, Fenton T, Fosberg A. M, Camann W, Maffeo N, Winkelman J. "Continuous arterial and venous blood gas monitoring during cardiopulmonary bypass", J. Thorac. Cardiovasc. Surg., **102(3)**, pp.431-439 (1991)

[9] Bennett D, Boldt J, Brochard L, Coriat P, Dhainaut J. F, Edwards D, Feihl F, Groeneveld J, Lamy M, Lemaire F, Payen D, Perret C, Rouby J. J, Scheidegger D, Singer M, Suter P, Thijs L, Vincent J. L. "Expert panel: Use of the pulmonary artery catheter" Intensive Care Med., **17**, pp. I-VIII (1991)

[10] Nelson L.D. "The new pulmonary artery catheters: Continuous venous oximetry, right ventricular ejection fraction, and continuous cardiac output", New Horiz., **5**, pp.251–258 (1997)

[11] Weil M.H. "The assault on the Swan-Ganz catheter", Chest, **113**, pp.1379–1386 (1998)

[12] Kelso L.A. "Complications associated with pulmonary artery catheterization", New Horiz., **5**, pp.259–263 (1997)

[13] Roizen M. F, Berger D. L, Gabel R. A et al. "Practice Guidelines for pulmonary artery catheterization. A report by the American Society of Anesthesiologists task force on pulmonary artery catheterization" Anesthesiology, **78**, pp.380-394 (1993)

[14] Chalfin D. B. "The pulmonary artery catheter: Economic aspects", New Horiz., **5**, pp.292–296 (1997)

[15] Leibowitz A. B, Oropello J. M. "The pulmonary artery catheter in anesthesia practice in 2007: an historical overview with emphasis on the past 6 years", Semin. Cardiothorac. Vasc. Anesth., **11(3)**, pp.162-176 (2007)

[16] Scales K, Collie E. "A practical guide to using pulmonary artery catheters", Nurs. Stand., **21(43)**, pp.42-48 (2007)

[17] McGee W. T, Mailloux P, Jodka P, Thomas J. "The pulmonary artery catheter in critical care", Semin. Dial., **19(6)**, pp.480-491 (2006)

[18] Pond C. G, Blessios G, Bowlin J, McCawley C, Lappas D. G. "Perioperative evaluation of a new mixed venous oxygen saturation catheter in cardiac surgical patients", J. Cardiothorac. Vasc. Anesth., **6(3)**, pp.280-282 (1992)

[19] Harry M. H, Rackow E. C. "Critical care medicine", Arch. Intern. Med., **143**, pp.1391–1392 (1983)

[20] Reinhart K, Rudolph T, Bredle D. L, Hannemann L, Cain S. M. "Comparison of central venous to mixed venous oxygen saturation during changes in oxygen supply/demand" Chest, **95**, pp.1216–1221 (1989)

[21] Pinsky M. R. "Hemodynamic monitoring over the past 10 years", Crit. Care., **10(1)**, pp.117 (2006)

[22] Goldman R. H, Braniff B, Harrison D. C, Spivac A. P. "The use of central venous oxygen saturation measurements in a coronary care unit", Ann. Intern. Med., **68**, pp.1280–1287 (1968)

[23] Goldman R. H, Klughaupt M, Metcalf T, Spivack A. P, Harrison D. C. "Measurement of central venous oxygen saturation in patients with myocardial infarction", Circulation, **38**, pp.941–946 (1968)

[24] Berridge J. C. "Influence of cardiac output on the correlation between mixed venous and central venous oxygen saturation", Br. J. Anaesth., **69**, pp.409–410 (1992)

[25] Ladakis C, Myrianthefs P, Karabinis A, Karatzas G, Dosios T, Fildissis G, Gogas J, Baltopoulos G. "Central venous and mixed venous oxygen saturation in critically ill patients", Respiration, **68(3)**, pp.279-285 (2001)

[26] Scheinman M. M, Brown M. A, Brown B. A, Rapaport E. "Critical assessment of use of central venous oxygen saturation as a mirror of mixed venous oxygen saturation in severely ill cardiac patients", Circulation, **40**, pp.165–172 (1969)

[27] Martin C, Auffray J. P, Badetti C, Perrin G, Papazian L, Gouin F. "Monitoring of central venous oxygen saturation versus mixed venous oxygen saturation in critically ill patients", Intensive Care Med., **18**, pp.101–104 (1992)

[28] Vincent J. L. "Does central venous oxygen saturation accurately reflect mixed venous oxygen saturation? Nothing is simple, unfortunately", Intensive Care Med.,**18**, pp.386–387 (1992)

[29] Lee J, Wright F, Barber R, Stanley L. "Central venous oxygen saturation in shock: A study in man", Anesthesiology, **36**, pp.472–478 (1972)

[30] Faber T. "Central venous versus mixed venous oxygen content", Acta. Anaesth. Scand., **39**, pp.33–36 (1995)

[31] Yoxall C. W, Weindling A. M. "Measurement of venous oxyhaemoglobin saturation in the adult forearm by near infrared spectroscopy with venous occlusion", Med. Biol. Eng. Comput., **35(4)**, pp.331-336 (1997)

[32] Casavola C, Paunescu L. A, Fantini S, Franceschini M. A, Lugara P. M, Gratton E. "Application of near-infrared tissue oximetry to the diagnosis of

peripheral vascular disease", Clin. Hemorheol. Microcirc., **21(3-4)**, pp.389-393 (1999)

[33] Boushel R, Piantadosi C. A. "Near-Infrared spectroscopy for monitoring muscle oxygenation", Acta. Physiol. Scand., **168**, pp.615-622 (2000)

[34] Kama G. D, Starr J. M, Symreng T. "Continuous, in vivo pulmonary venous admixture from fiberoptically measured hemoglobin saturations", Crit. Care Med., **18**, pp.1419-1422 (1990)

[35] Armaganidis A, Dhainaut J. F, Billard J. L, Klouche K, Mira J. P, Brunet F, Dinh-Xuan A. T, Dall'Ava-Santucci J. "Accuracy assessment for three fiberoptic pulmonary artery catheters for SvO_2 monitoring", Intensive Care Med., **20**, pp.484 – 488 (1994)

[36] Müller M, Löhr T, Scholz S, Thul J, Akintürk H, Hempelmann G. "Continuous SvO2 measurement in infants undergoing congenital heart surgery--first clinical experiences with a new fiberoptic probe", Paediatr. Anaesth., **17(1)**, pp.51-55 (2007)

[37] Goodrich C. "Continuous central venous oximetry monitoring", Crit Care Nurs Clin North Am., **18(2)**, pp.203-209 (2006)

[38] Reinhart K, Bloos F. "The value of venous oximetry", Curr. Opin. Crit. Care., **11(3)**, pp.259-263 (2005)

[39] Eichler J, Knof J, Lenz H. "Measurements on the depth of penetration of light (0.35-10μm) in tissue", Rad. And Environm. Biophys., **14**, pp.239-242 (1977)

[40] Barton F. E "Theory and principles of near infrared spectroscopy", Spectroscopy Europe, **14(1)**, pp.12-18.(2002)

[41] Jöbsis F. F. "Noninvasive, infrared monitoring of cerebral and myocardial oxygen sufficiency and circulatory parameters", Science, **198**, pp.1264–1267 (1977)

[42] Wyatt J. S, Cope M, Delpy D. T, Richardson C. E, Edwards A. D, Wray S, Reynolds E. O. R. "Quantitation of cerebral blood volume in human infants by near infrared spectroscopy", J. Appl. Physiol., **68(3)**, pp.1086-1091 (1990)

[43] Yoxall C. W, Weindling A. M, Dawani N, Peart I. "Measurement of cerebral venous oxyhemoglobin saturation in children with near infra red spectroscopy and partial jugular venous occlusion", Pediatr. Res., **38**, pp.319-323 (1995)

[44] Miccormick P. W, Stewart M, Goetting M. G, Balakrishnan G. "Regional cerebral oxygen saturation measured by optical spectroscopy in humans", Stroke, **22**, pp.596-602 (1991)

[45] Longini R. L, Zdrojkowski R. "A note on the theory of backscattering of light by living tissue", IEEE Trans. Biomed. Eng., **15**, pp.4-10 (1968)

[46] Feng W, Haishu D, Fenghua T, Jun Z., Qing X, Xianwu T. "Influence of overlying tissues and probe geometry on the sensitivity of a near- infrared tissue oximeter", Physiol. Meas., **22**, pp.201-208 (2001)

[47] Wray S, Cope M, Delpy D. T, Wyatt J. S, Reynolds E. O. R. "Characterization of the near infrared absorption spectra of cytochrome aa3

and haemoglobin for the non-invasive monitoring of cerebral oxygenation", Biochim. Biophys. Acta., **933(1)**, pp.184-192 (1988)

[48] Hertzman A. B. "The blood supply of various skin areas as estimated by photo-electric plethysmograph", Am. J. Physiol., **124**, pp.328-340 (1938)

[49] Gu Y. Y, Zhang Y. T. "Reducing the influence of contacting force applied on photoplethysmographic sensor on heart rate variability estimation", Proc. Conf. IEEE. EMBS., **3**, pp.2718-2620 (2003)

[50] Allen J. "Photoplethysmography and its applications in clinical physiological measurement", Physiol. Meas., **28(3)**, pp. R1-39 (2007)

[51] Hertzman A. B. "Photoelectric plethysmograph of the fingers and toes in man", Proc. Soc. Exp. Biol. Med., **37**, pp.529-534 (1937)

[52] Yelderman M, New W. "Evaluation of pulse oximetry", Anesthesiology, **59**, pp.349-352 (1983)

[53] Yoshiya I, Shimada Y, Tanaka K. "Spectrophotometric monitoring of arterial oxygen saturation in the finger tip", Med. Biol. Eng. Comput., **18**, pp.27-32 (1980)

[54] Teng X. F, Zhang Y. T., "The effect of contacting force on photoplethysmographic signals", Physiol. Meas., **25**, pp.1323-1335 (2004)

[55] Hurch A, Hurch R, Kourg V. "Limitations of pulse oximetry [letter]", Lancet, **1**, pp.357-359 (1988)

[56] De Trafford J, Lafferty K. "What does photoplethysmography measure? [letter]", Med. Biol. Eng. Comput., **22**, pp.479-480 (1984)

[57] Abramowitz H. B, Queral L. A, Flinn W. R, Nora P. F. "The use of photoplethysmography in the assessment of venous insufficiency: a comparison to venous pressure measurement", Surgery, **86**, pp.434-441 (1979)

[58] Barns R. W. "Noninvasive diagnostic techniques in peripheral vascular disease", Am. Heart J., **97**, pp.2-9 (1979)

[59] Fronek A, Blažek V. "Automatic calibration of the D-PPG: its meaning and effectiveness", Report by Third Annual of Congress of NASP, Phoenix USA, (1990)

[60] Williams D. T, Harding K. G, Price P. E. "The influence of exercise on foot perfusion in diabetes", Diabet. Med., Online Early Articles (2007)

[61] Allen J, Oates C. P, Lees T. A, Murray A. "Photoplethysmography detection of lower limb peripheral arterial occlusive disease: a comparison of pulse timing, aplitude and shape characteristics", Physiol. Meas., **26**, pp.811-821 (2005)

[62] O'Rourke M. F. "Principles of arterial hemodynamics" in Mechanics of the Circulation, H. E. D. J. Ter Keurs and J.V. Tyberg, Martinus Nijhoff, Dordrecht, pp.240 (1987)

[63] Sherebrin M. H, Sherebrin R. Z. "Frequency analysis of the peripheral pulse wave detected in the finger with a photoplethysmograph", IEEE Trans. Biomed. Eng., **37**, pp.313-317 (1990)

[64] Wukitsch M W, Petterson M. T, Tobler D. R, Pologe J. A. "Pulse oximetry: Analysis of theory, technology and practice", J. Clin. Monit. Comput., **4(4)**, pp.290-301 (1988)

[65] Reynolds K. J, Moyle J. T. B, Sykes M. K, Hahn C. E. W. "Responses of 10 pulse oximeters to an in vitro test system", Brit. J. Anaesthesiol., **68**, pp.265-269 (1993)

[66] Reynolds K. J, Palayiwa E, Moyle J. T. B, Sykes M. K, Hahn C. E. W. "The effects of dyshaemoglobins on pulse oximetry", J. Clin. Monit., **9**, pp.81-90 (1993)

[67] Chan F. C. D. "Non-invasive venous oximetry through venous blood volume modulation", Doctoral Thesis, Loughborough University (2002)

[68] Chan F. C. D, Hayes M. J, Smith P. R. "Venous pulse oximetry", International Patent WO/2003/063697 (2003)

[69] Steinke J. M, Shepherd A. P. "Role of light scattering in whole blood oximetry", IEEE Trans. Biomed. Eng., **33(3)**, pp.294-301 (1986)

[70] Webster J. G. "Design of pulse oximeters", IoP Publishing, London (1997)

[71] Dul'nev G. N, Korotkevich M. M, Pilipenko N. V, Sigalov A. V. "Mathematical modelling of heat-echange processes in the human body", J. Eng. Phys. Thermophys., **46(1)**, pp.117-125 (1983)

[72] Liapis C. D, Balzer K, Benedetti-Valentini F, Fernandes e Fernandes J. "Vascular Surgery (European manual of medicine)", Springer-Verlag, Berlin, Heidelberg, pp.539 (2007)

[73] Yorkey T. J. "Two 'rat rat' derivation", Personal communication, Hayward, Nellcor Inc.

[74] Moyle J. T. B. "Pulse oximetry", BMG, London (1994)

[75] Volgyesi G. A. "Method of testing the accuracy of pulse oximeters and device therefor", US patent 5,166,517 (1992)

[76] Jing L, Xu L. X. "Estimation of blood perfusion using phase shift in temperature response to sinusoidal heating at the skin surface", Trans. IEEE. Biomed. Eng., **46(9)**, pp.1037-1043 (1999)

[77] McDonald D. A. "Blood flow in arteries", Edward Arnold, London (1974)

[78] Flewelling R. "The Biomedical Engineering Handbook 1st Edition, vol 1", CRC Press, Boca Raton, pp.86-6 (2000)

[79] Barros A. K, Wisbeck J, Ohnishi N. "Extracting the heart rate variability from an electrocardiogram sampled at a very low frequency", Comput. Cardiol., **26**, pp.335-338 (1999)

[80] McKenzie-Smith I, Hughes E. "Hughes Electrical Technology". Longman Group Ltd (7^{th} ed), Essex (1995)

[81] Madsen S. J, Patterson M. S, Wilson B. C. "The use of India ink as an optical absorber in tissue simulating phantoms", Phys. Med. Biol., **37(4)**, pp.985-993 (1992)

[82] Kramer R. "Chemometric Techniques for Quantitative Analysis" , Dekker, New York (1998)

[83] Seagar A. D, Gibbs J. M, Davis F. M. "Interpretation of venous occlusion plethysmographic measurements using a simple model", Med. Biol. Eng. Comput., **22(1)**, pp. 12-18 (1984)

[84] Echiadis A S, Crabtree V P, Bence J, Hadjinikolaou L, Alexiou C, Spyt T J and Hu S. "Non-invasive measurement of peripheral venous oxygen saturation using a new venous oximetry method: evaluation during bypass in heart surgery", Physiol. Meas., **28(8)**, pp.897-911 (2007)

[85] Mosteller R. D. "Simplified calculation of body-surface area", N. Engl. J. Med., **317(17)**, pp.1098 (1987)

[86] Sato K, Sogawa M, Namura O, Hayashi J. "Deterioration of body oxygen metabolism by vasodilator and/or vasoconstrictor administration during cardiopulmonary bypass", Asaio J., **52(1)**, pp.96-99 (2006)

[87] Irita K, Kai Y, Takahashi S. "Impaired oxygen utilisation during rapid cooling on cardiopulmonary bypass", Fukuoka Acta Medica, **90(1)**, pp.14-22 (1999)

[88] Baraka A, Baroody M, Haroun S, Nawfal M, Dabbous A, Sibai A, Jamal S, Shamli S. "Continuous venous oximetry during cardiopulmonary bypass: influence of temperature changes, perfusion flow, and hematocrit levels", J. Cardiothorac. Anesth., **4(1)**, pp.35-38 (1990)

[89] Boushel R, Piantadosi C. A. "Near-Infrared spectroscopy for monitoring muscle oxygenation", Acta. Physiol. Scand., **168**, pp.615-622 (2000)

[90] Quaresima V, Colier W N, van der Sluijs M, Ferrari M. "Nonuniform Quadriceps O2 Consumption Revealed by Near Infrared Multipoint Measurements", Biochem. Biophys. Res. Commun., **285(4)**, pp.1034-1039 (2001)

[91] Huber P. "Cerebral angiography", Thieme, Stuttgart (1982)

[92] Mueller H.R, Hinn G, Buser M.W. "Internal jugular venous flow measurement by means of a Duplex scanner", J. Ultrasound. Med., **9**, pp.261–265 (1990)

[93] Kadoi Y, Saito S, Goto F, Fujita N. "Decrease in jugular venous oxygen saturation during normothermic cardiopulmonary bypass predicts short-term postoperative neurologic dysfunction in elderly patients", J. Am. Coll. Cardiol., **38**, pp.1450-1455 (2001)

[94] Nicita-Mauro V, Maltese G, Nicita-Mauro C, Basile G. "Vascular aging and geriatric patient", Minerva Cardioangiol., **55(4)**, pp.497-502 (2007)

[95] van Staveren H. J, Moes C. J. M, van Marle J, Pral S. A, van Gemert M. J. C. "Light scattering in intralipid-10% in the wavelength range of 400–1100 nm", Appl. Opt., **30**, pp.4507–4514 (1991)

[96] Flock S. T, Jacques S. L,Wilson B. C, StarW. M, van Gemert M.J. C. "Optical properties of intralipid: a phantom medium for light propagation studies", Lasers Surg. Med., **12**, pp.510–519 (1992)

APPENDIX

I. CLINICAL FEASIBILITY STUDY PLOTS

This appendix presents the results from the feasibility study which was carried out in heart surgery, and was presented in chapter 5. Each case in presented on a separate figure which shows the studied variables (mixed venous oxygen saturation SvO_2, peripheral venous oxygen saturation $SxvO_2$, blood flow, blood temperature and oxygen consumption VO_2, plotted against time. These individual plots aim at the better understanding of the device's response to changes of blood flow, blood temperature and oxygen consumption. In certain cases, the bypass machine failed to record certain parameters, therefore in some plots blood flow and oxygen consumption are not present.

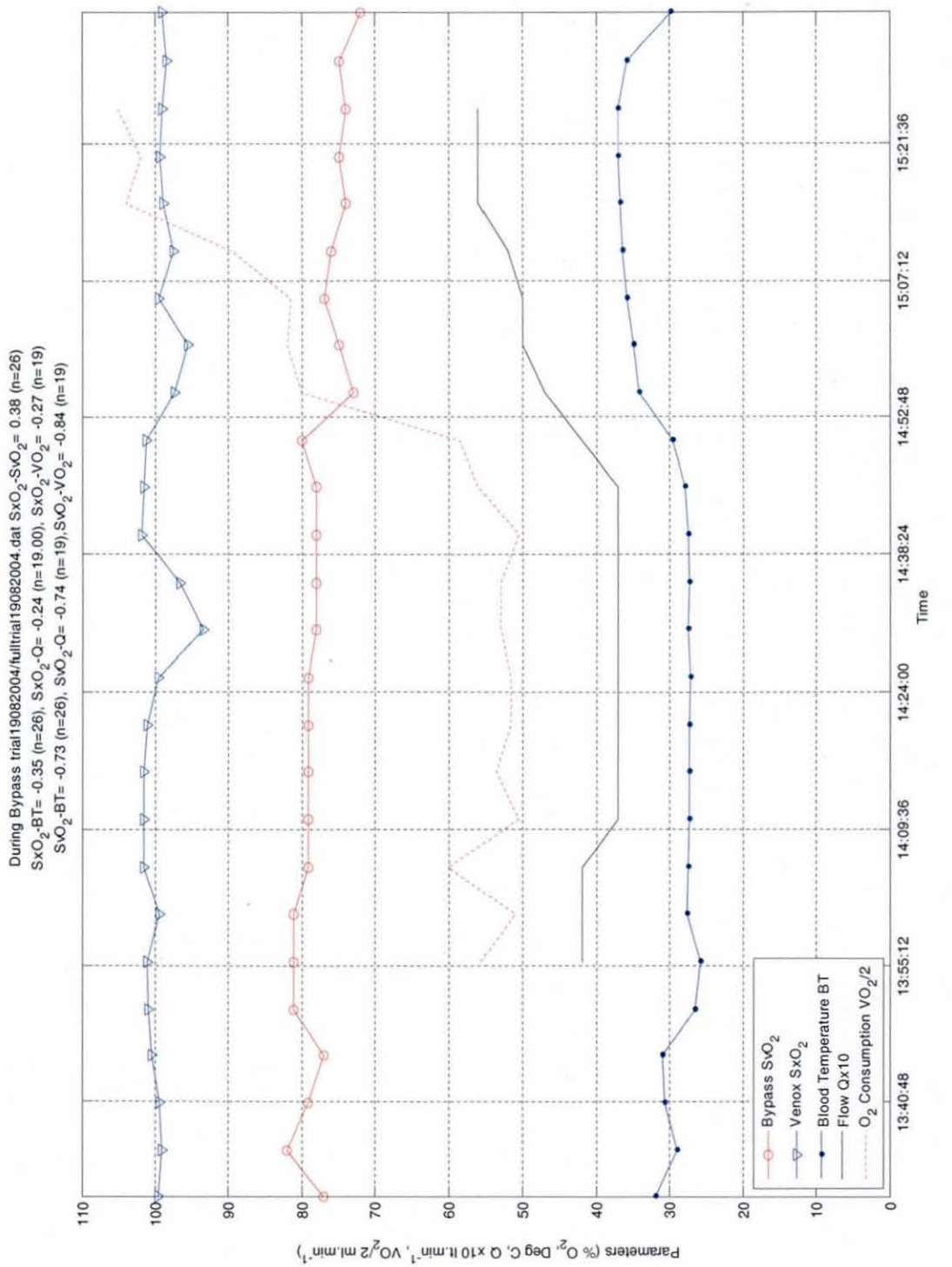

Figure I.1 – Clinical case study 1

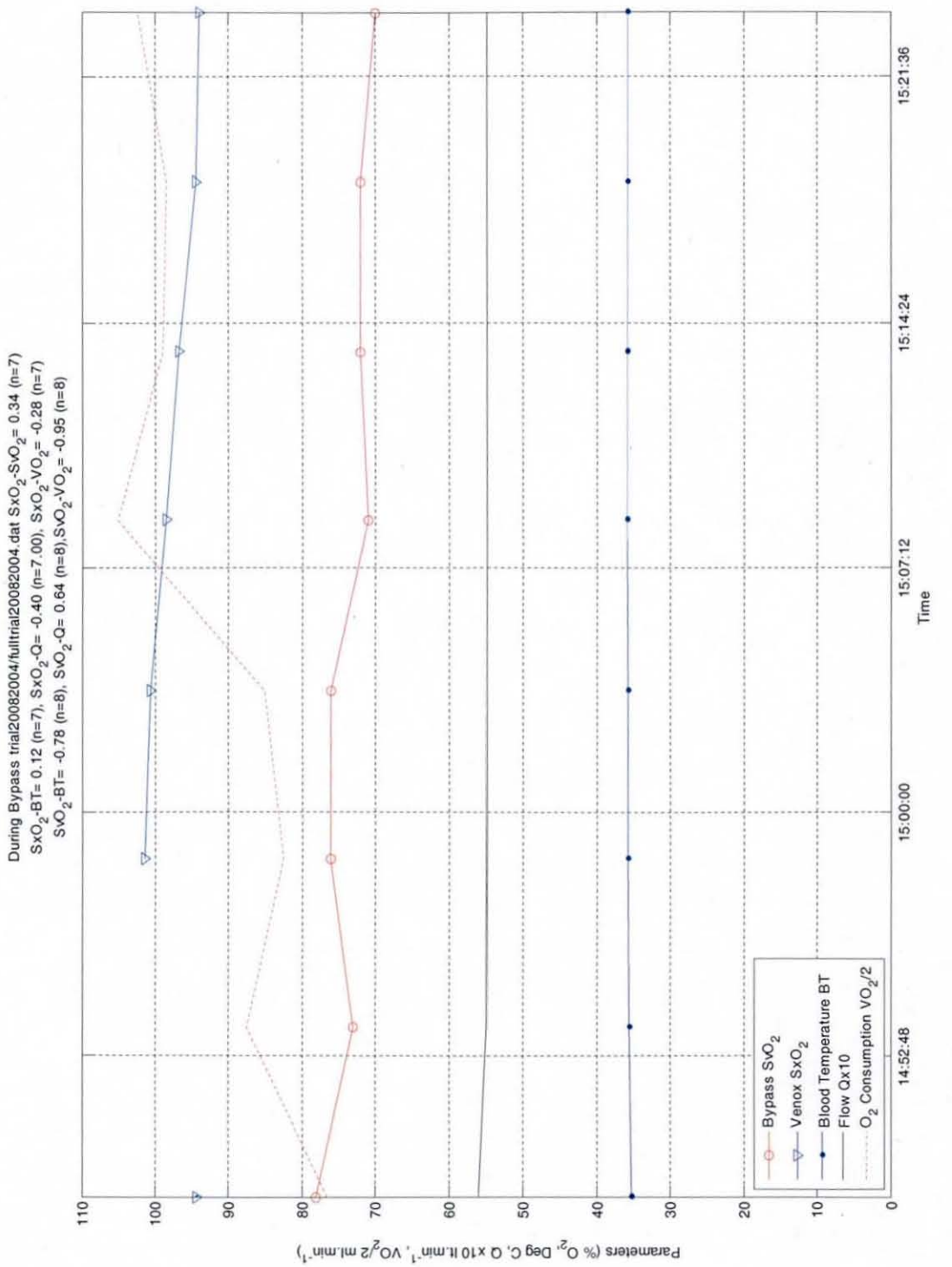

Figure I.2 – Clinical case study 2

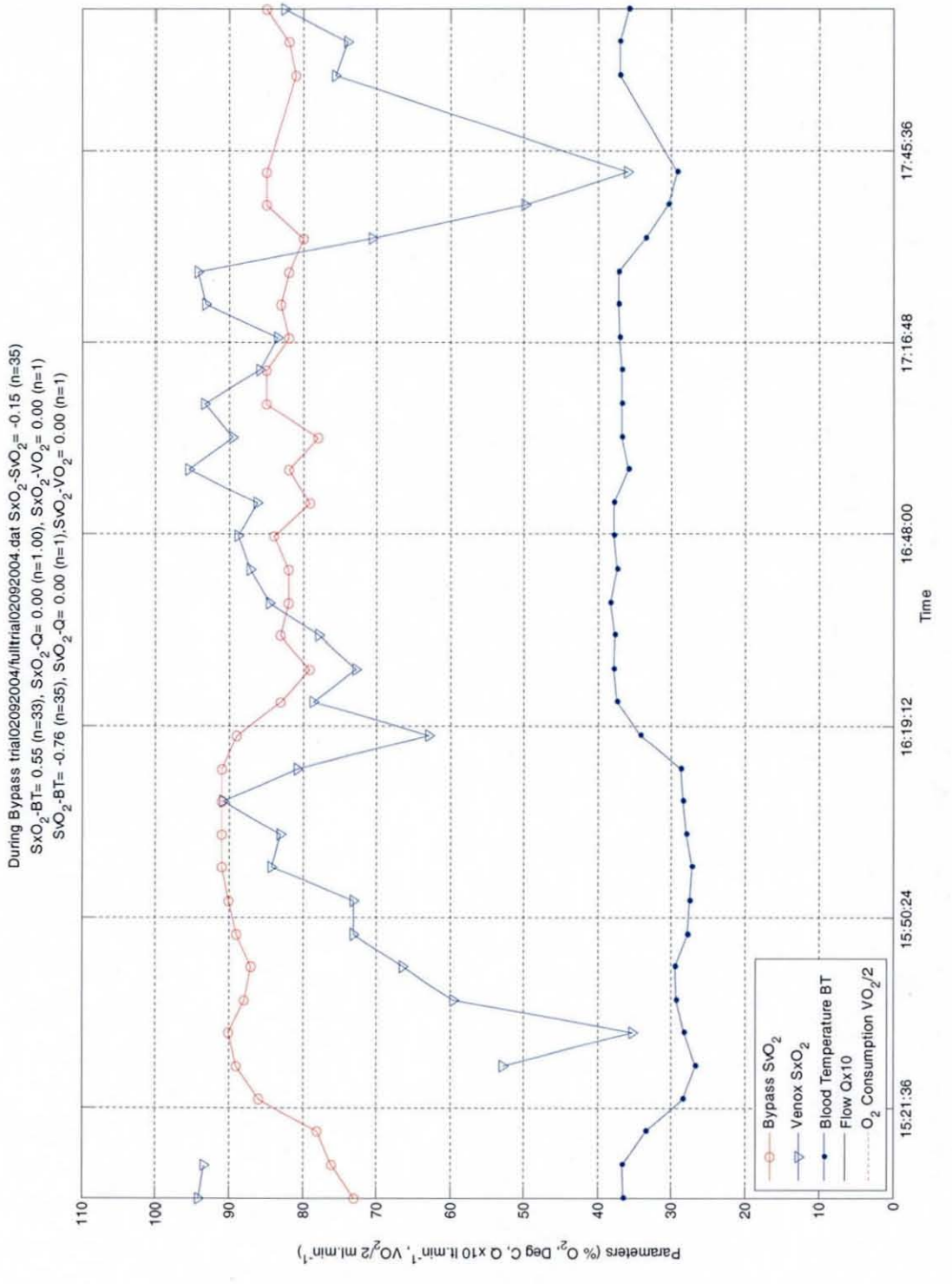

Figure I.3 – Clinical case study 3

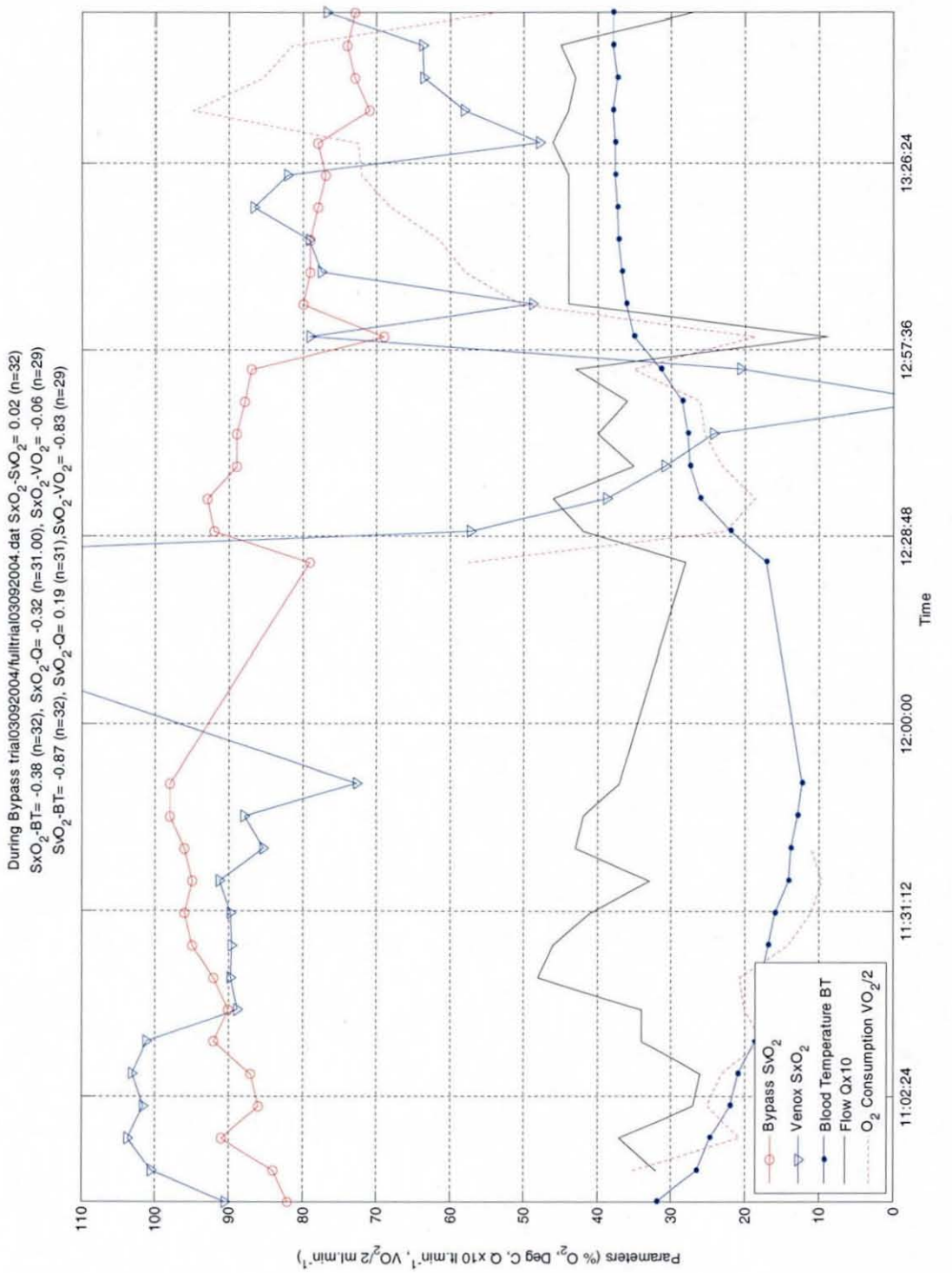

Figure I.4 – Clinical case study 4

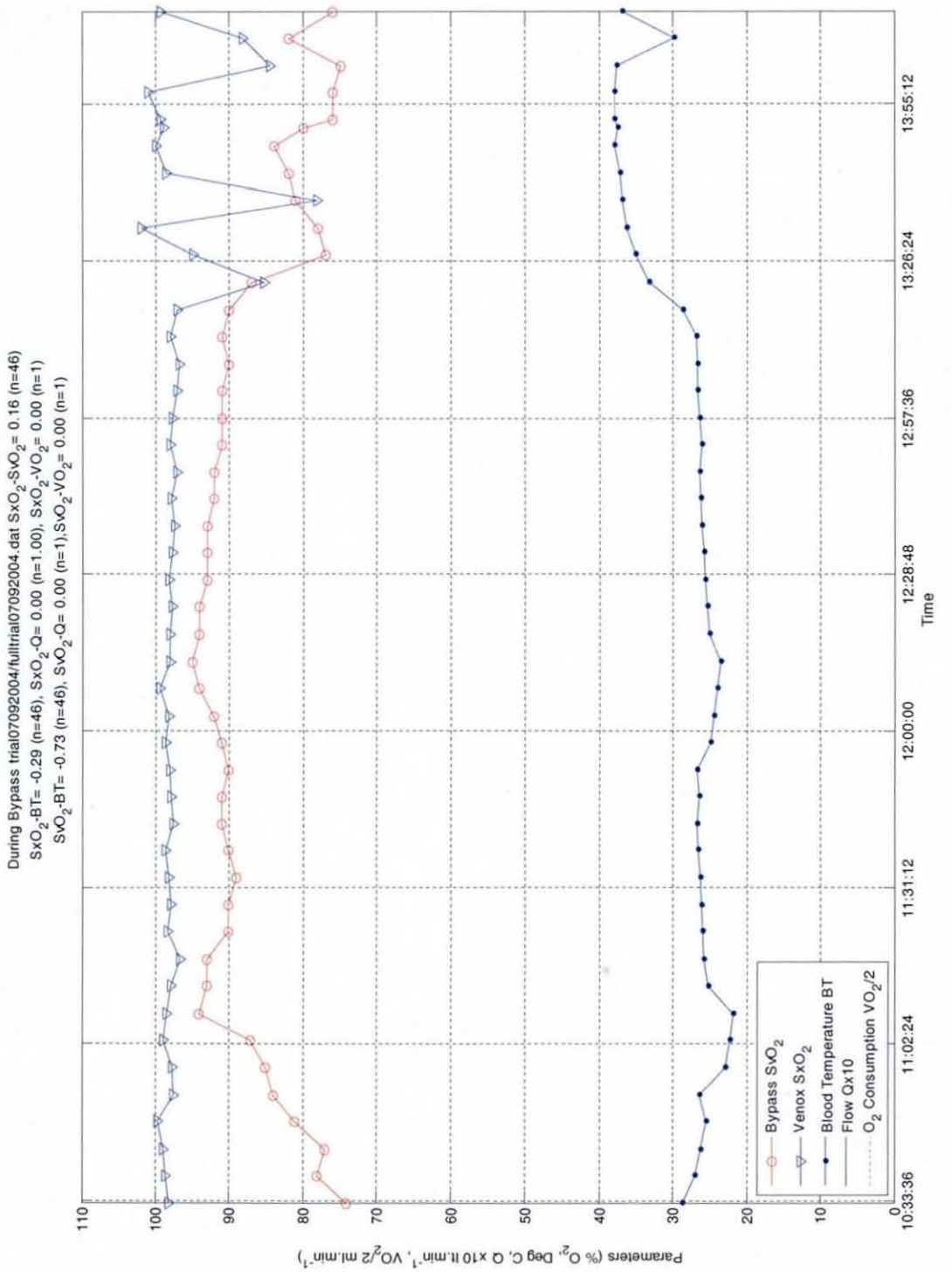

Figure I.5 – Clinical case study 5

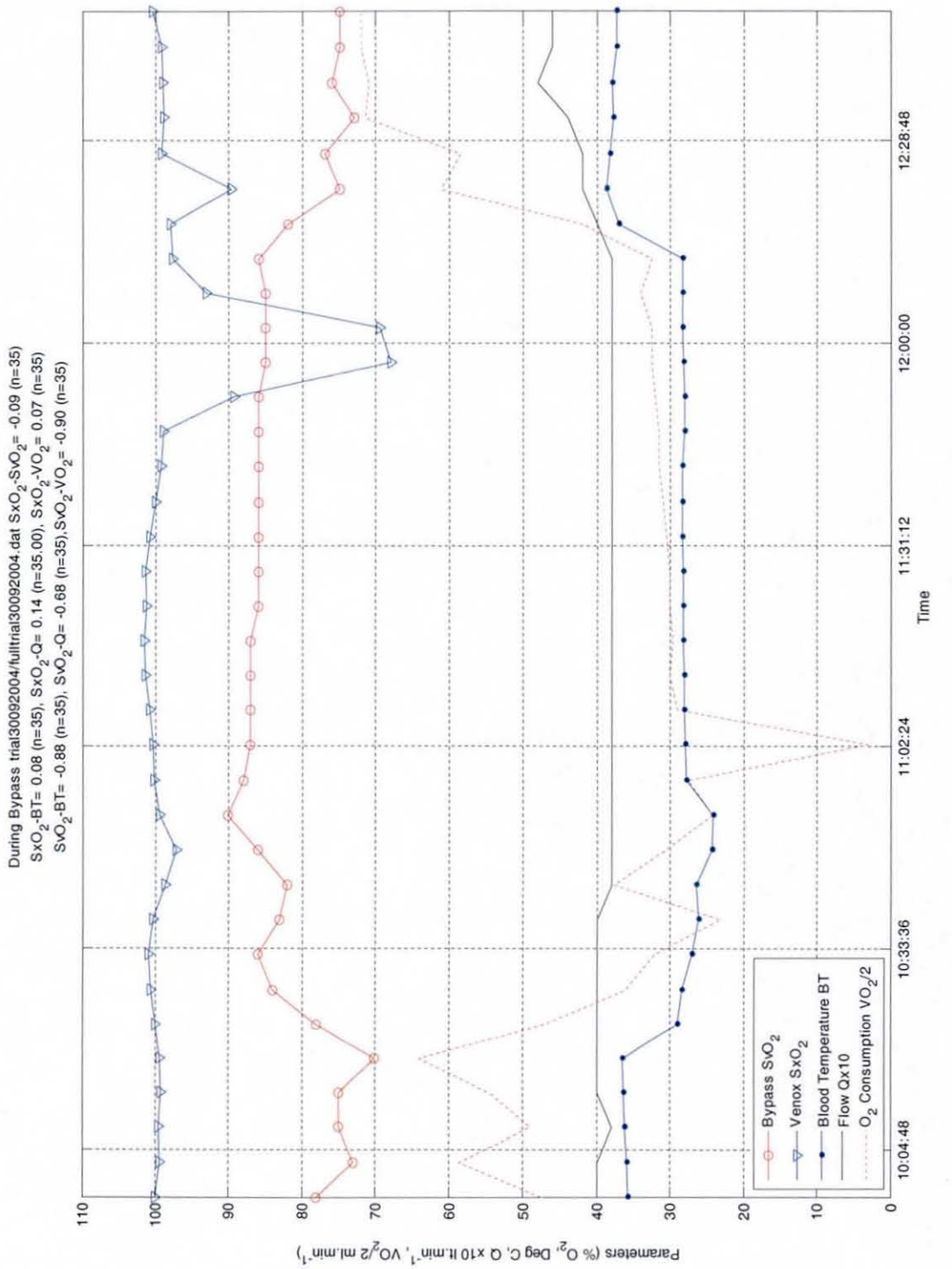

Figure I.6 – Clinical case study 6

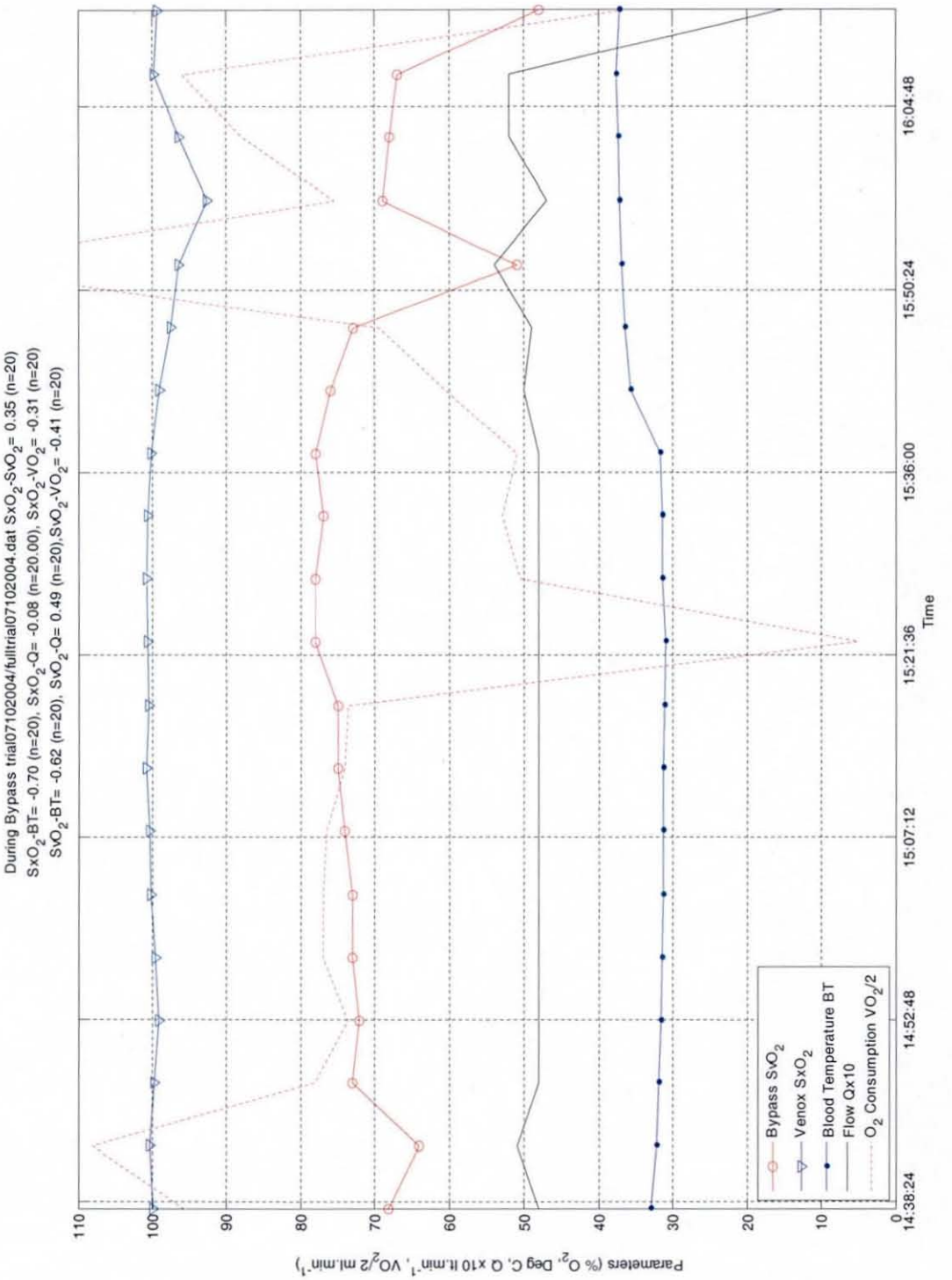

Figure I.7 – Clinical case study 7

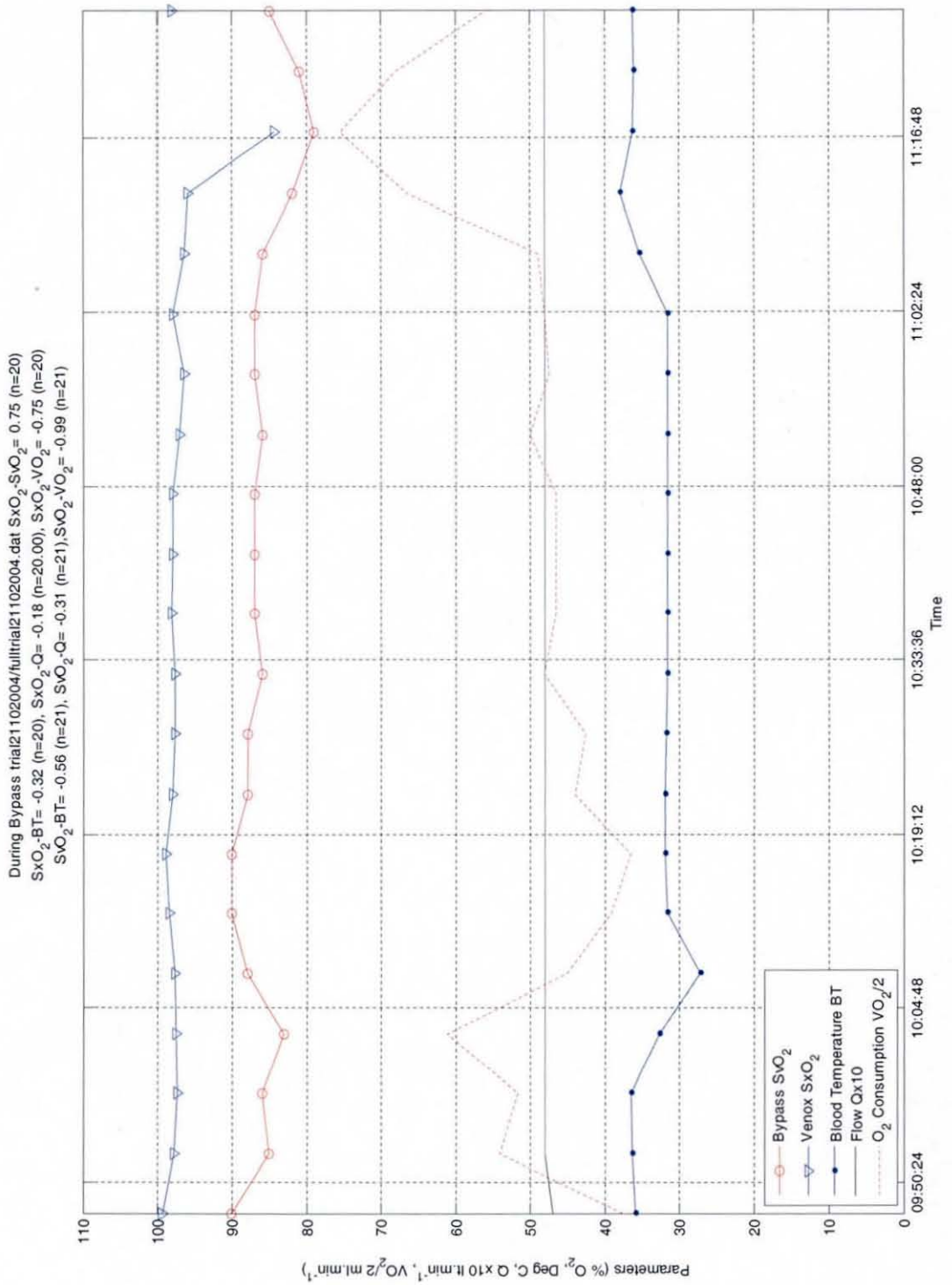

Figure I.8 – Clinical case study 8

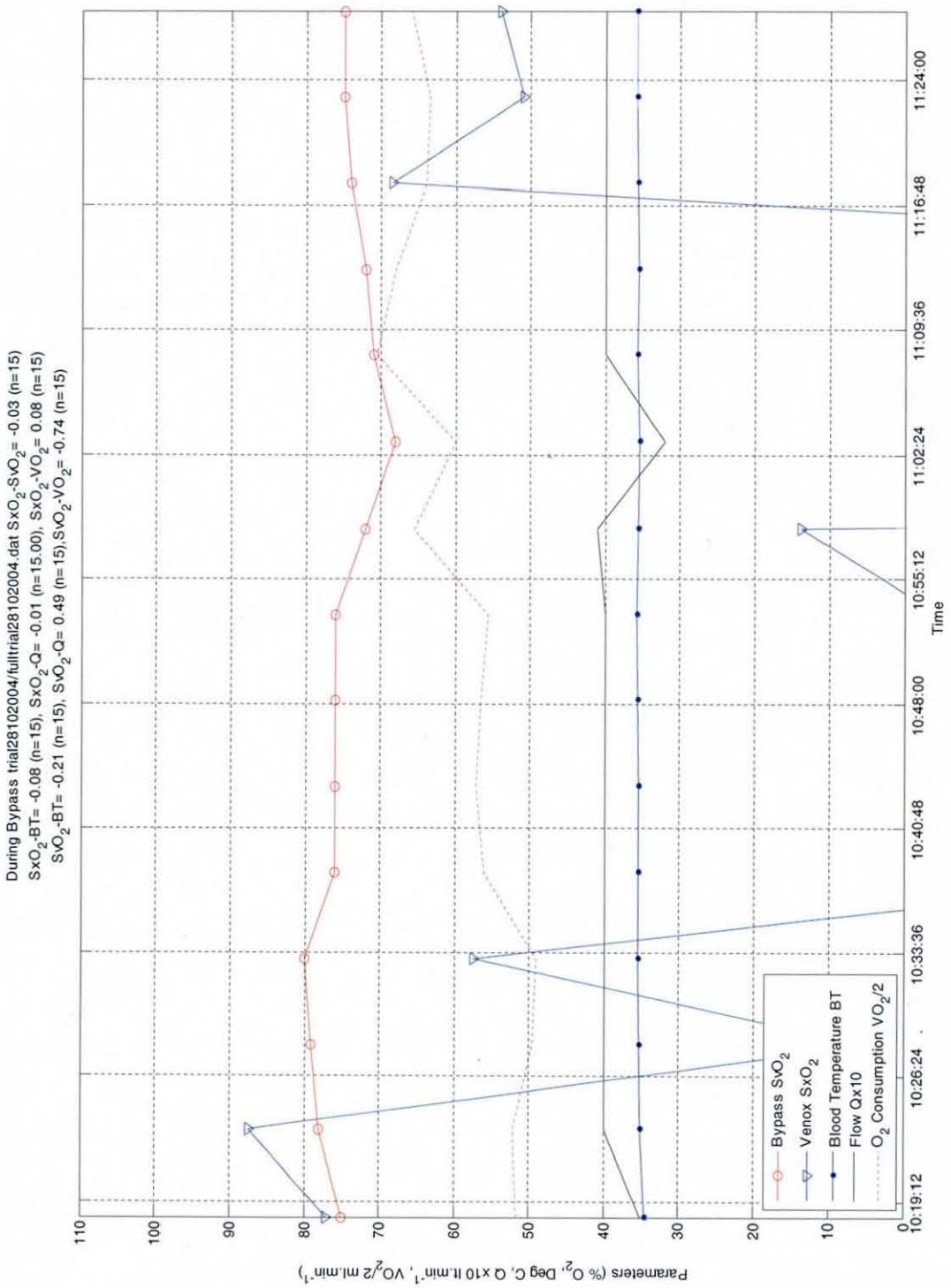

Figure I.9 – Clinical case study 9

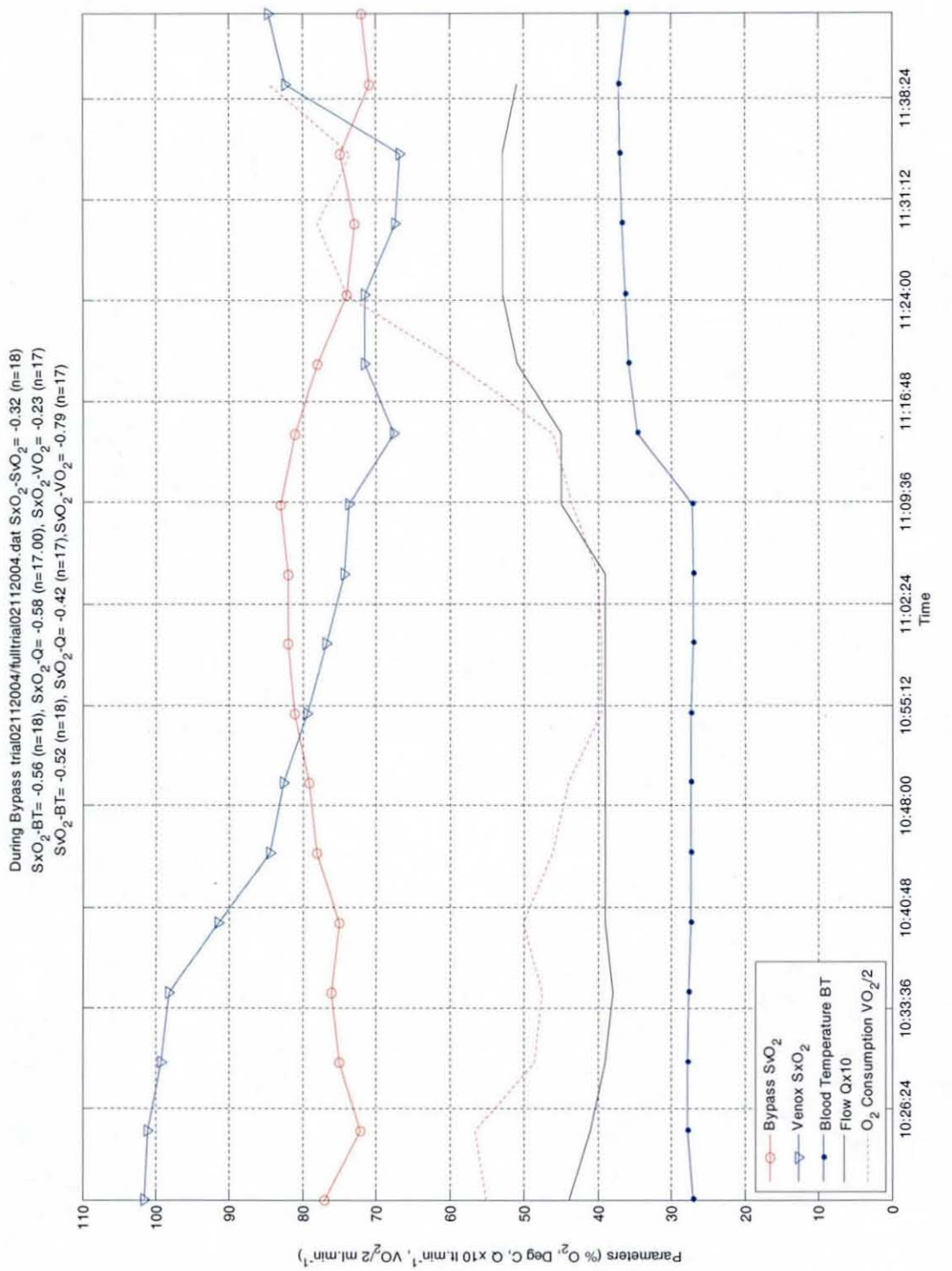

Figure I.10 – Clinical case study 10

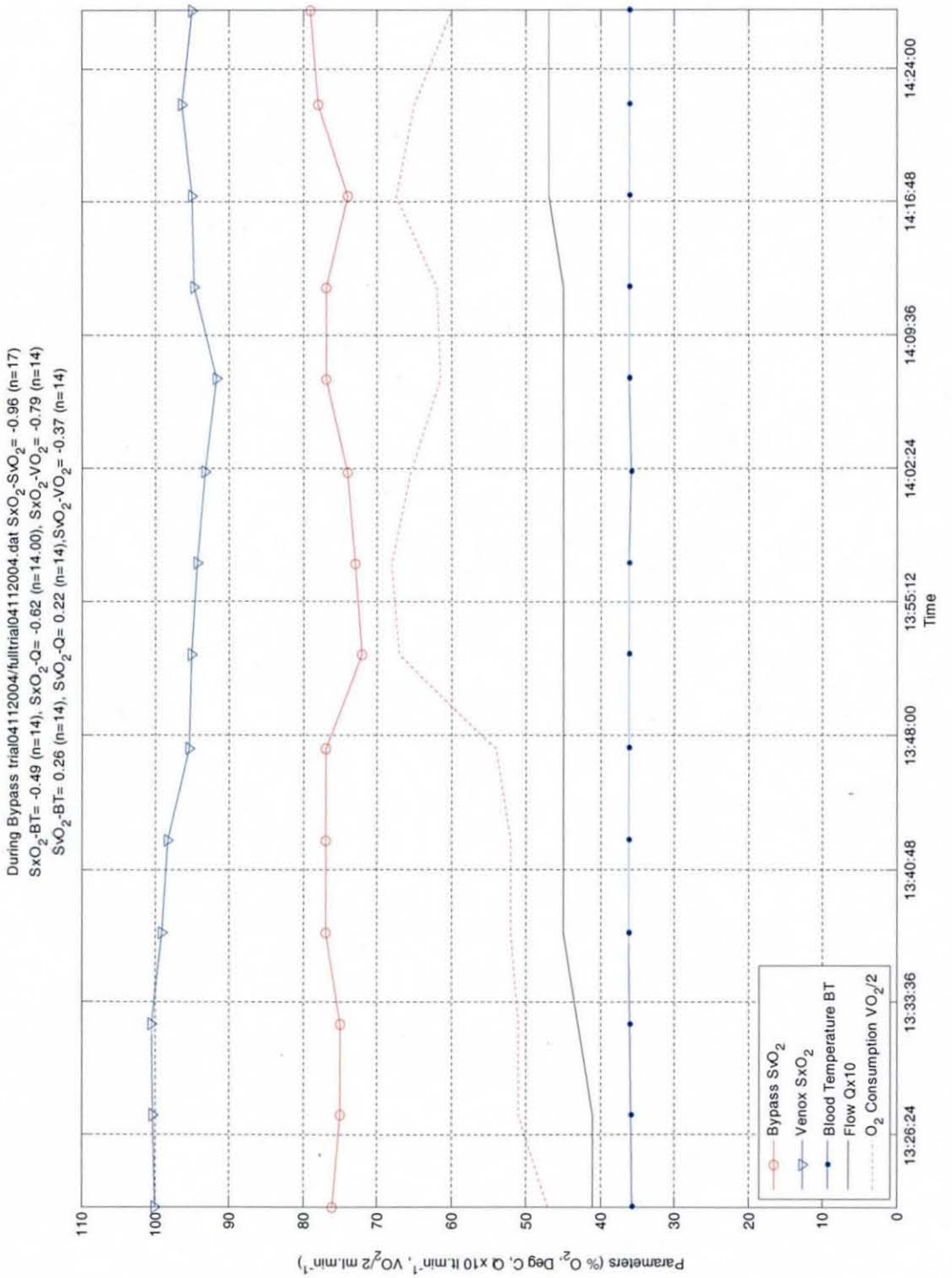

Figure I.11 – Clinical case study 11

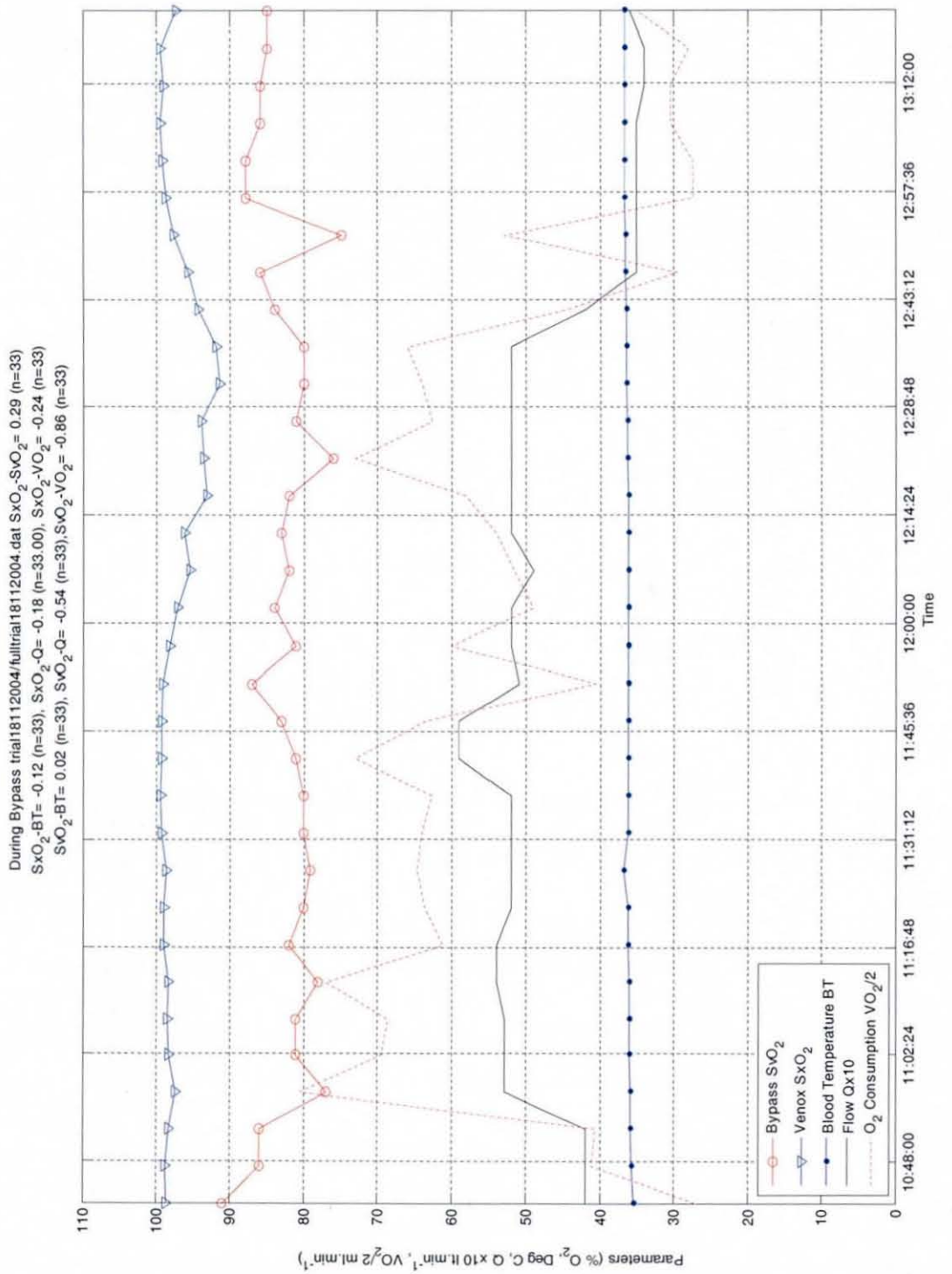

Figure I.12 – Clinical case study 12

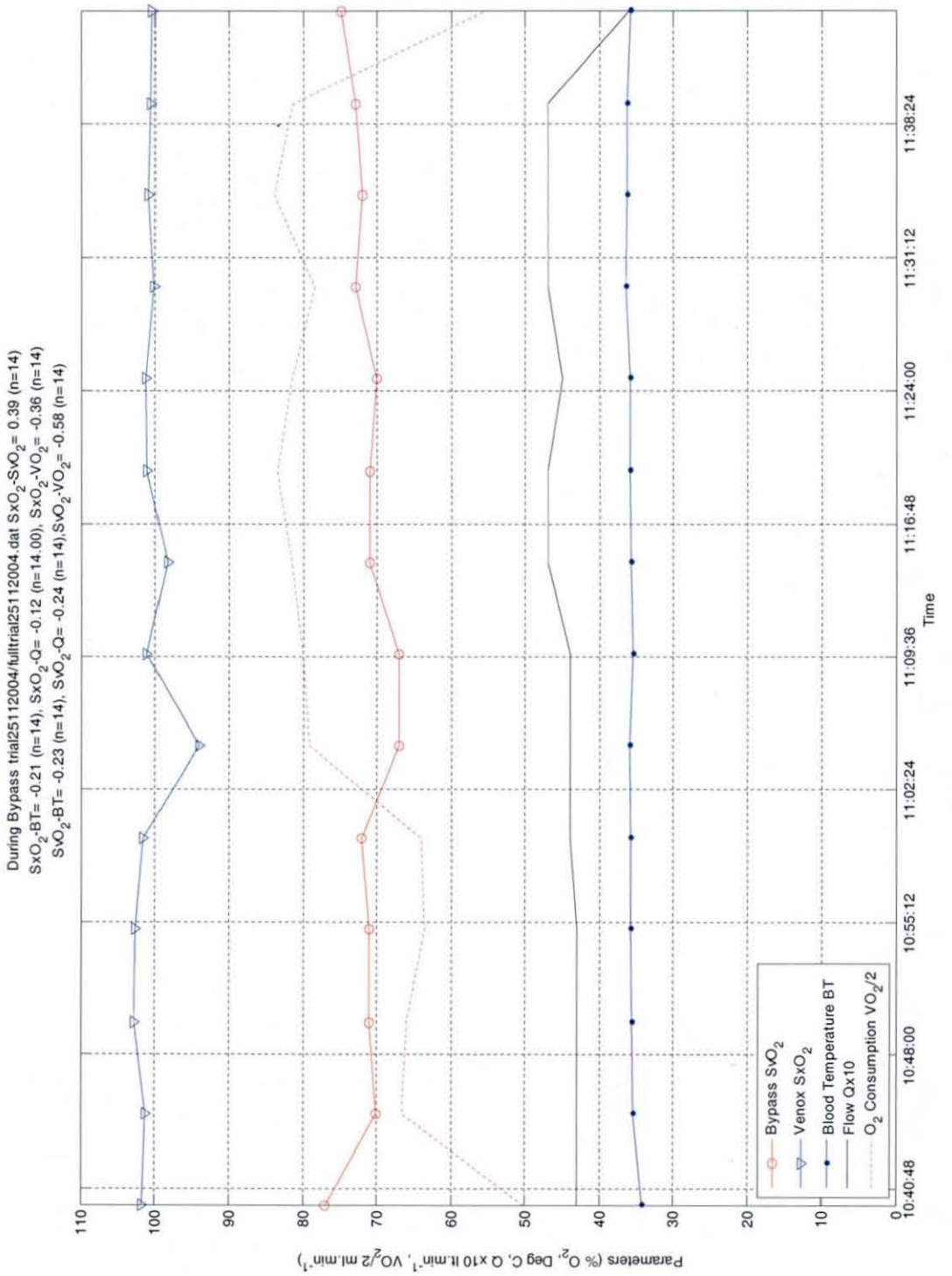

Figure I.13 – Clinical case study 13

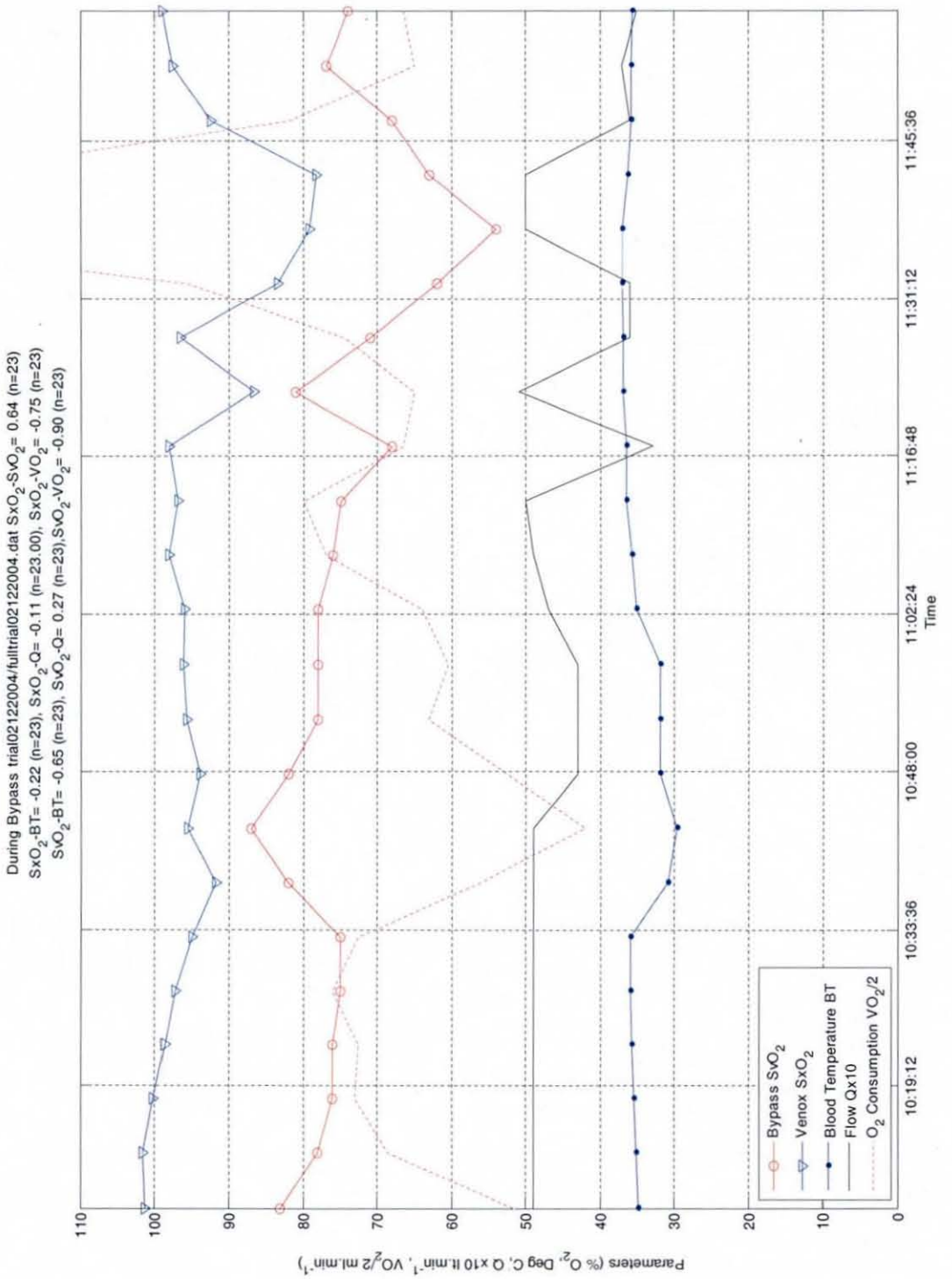

Figure I.14 – Clinical case study 14

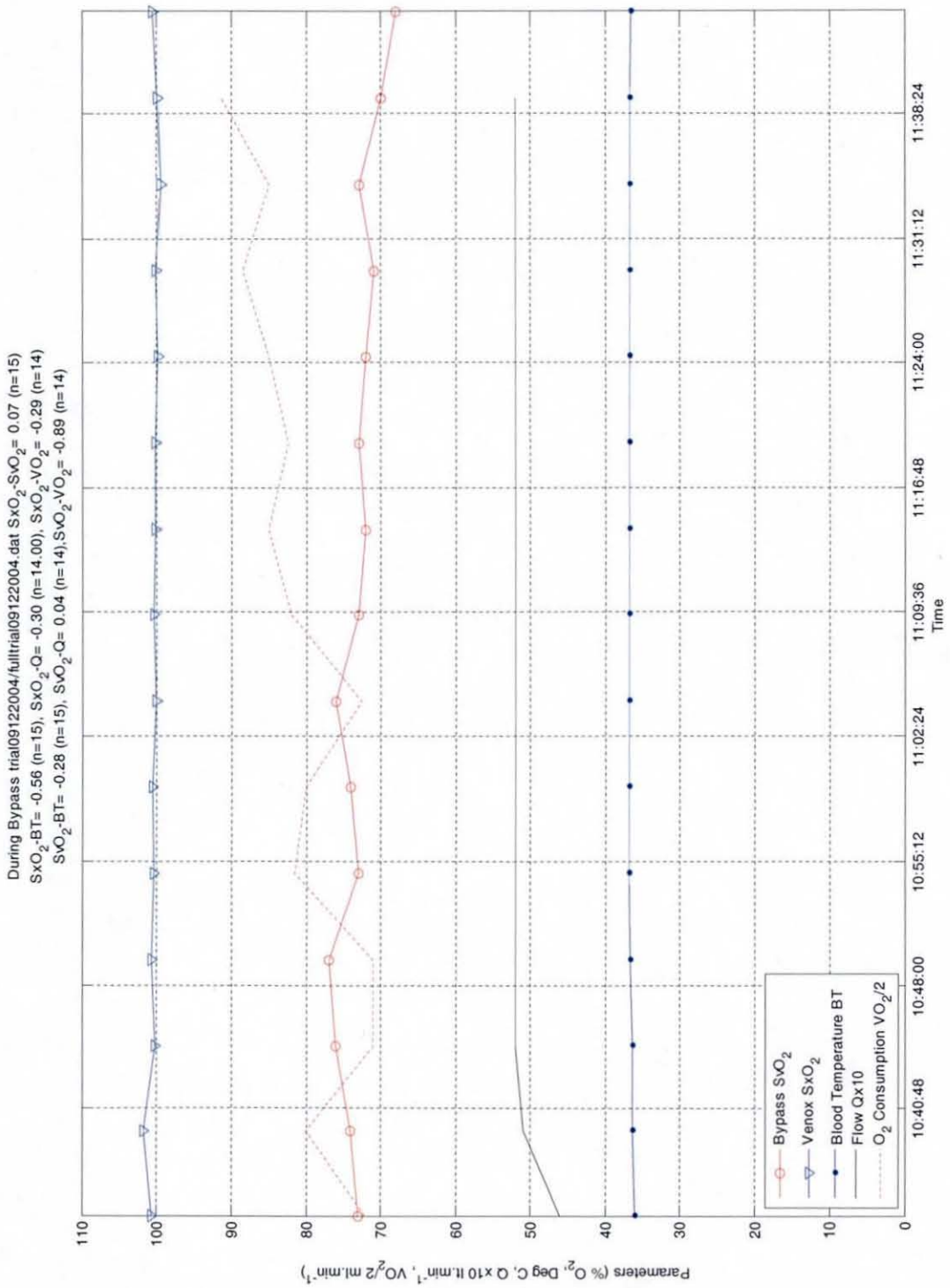

Figure I.15 – Clinical case study 15

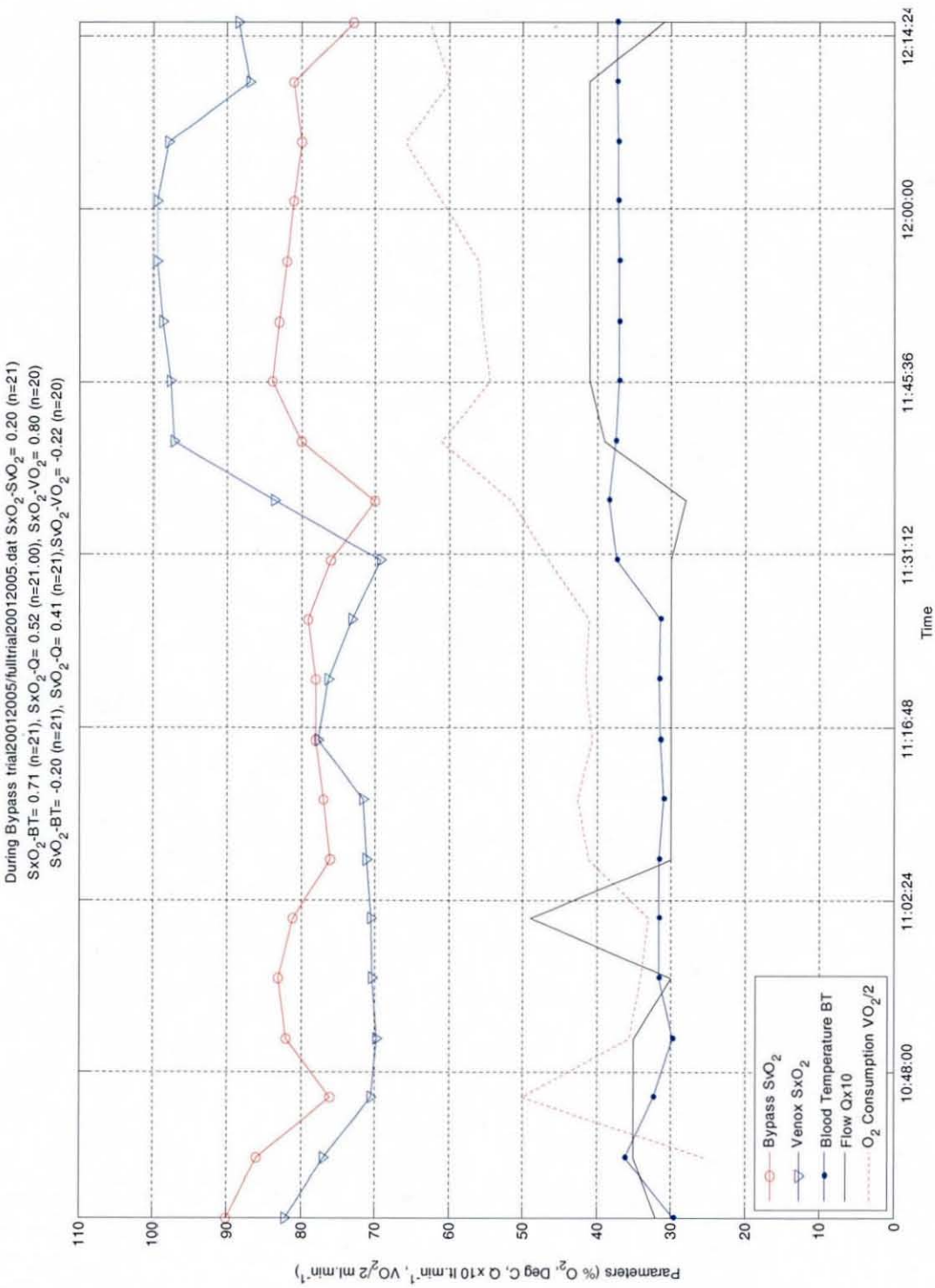

Figure I.16 – Clinical case study 16

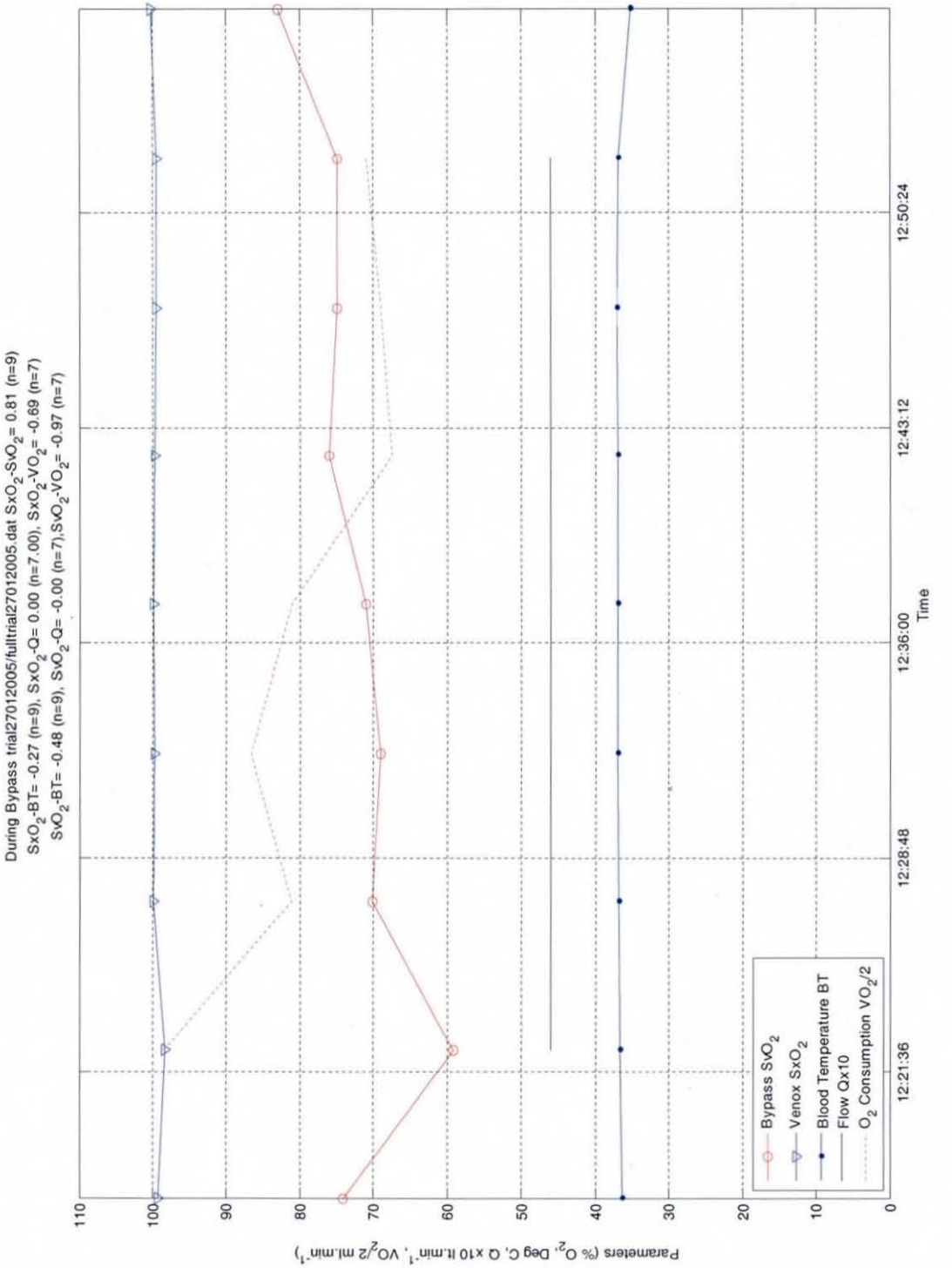

Figure I.17 – Clinical case study 17

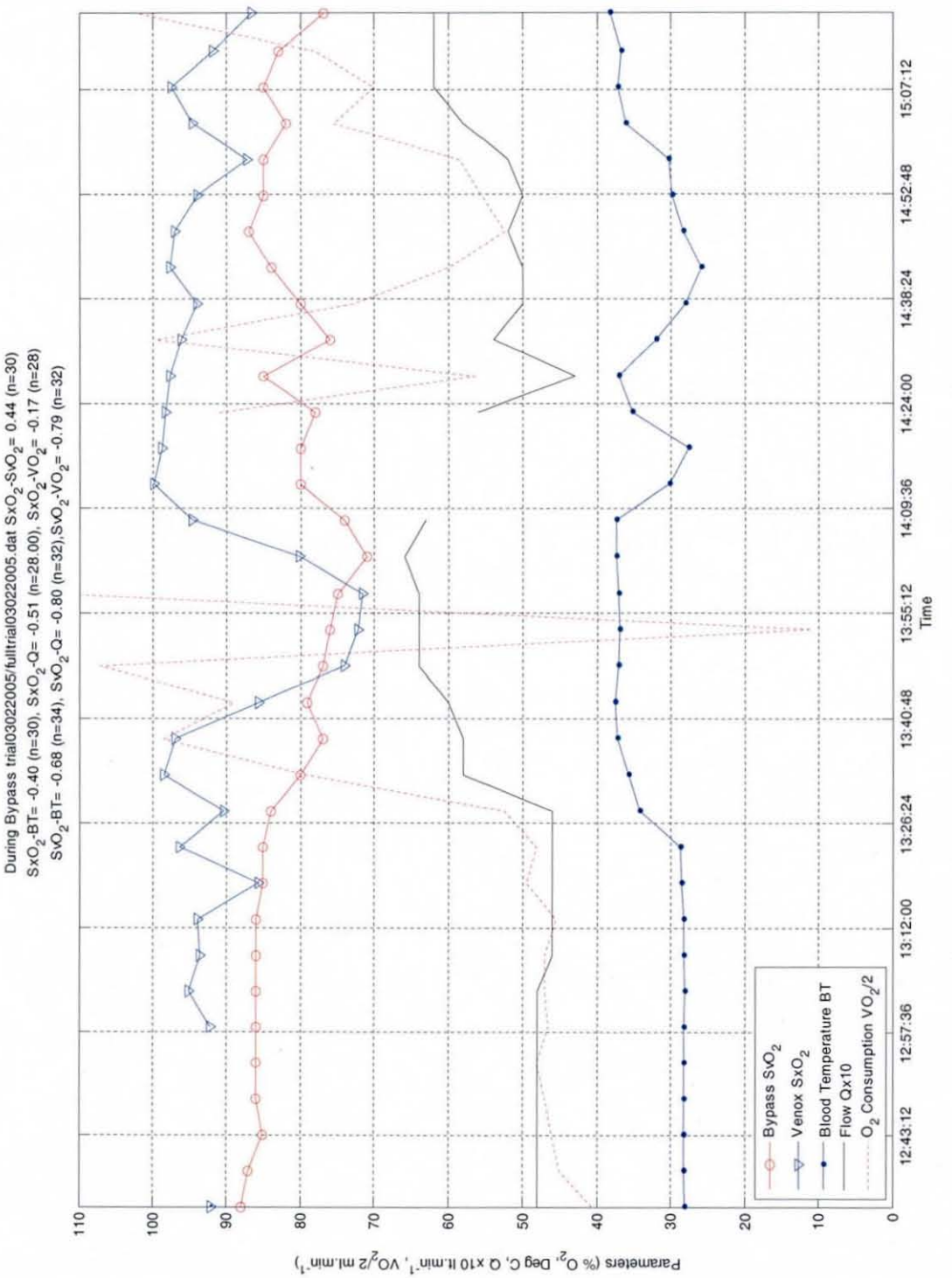

Figure I.18 – Clinical case study 18

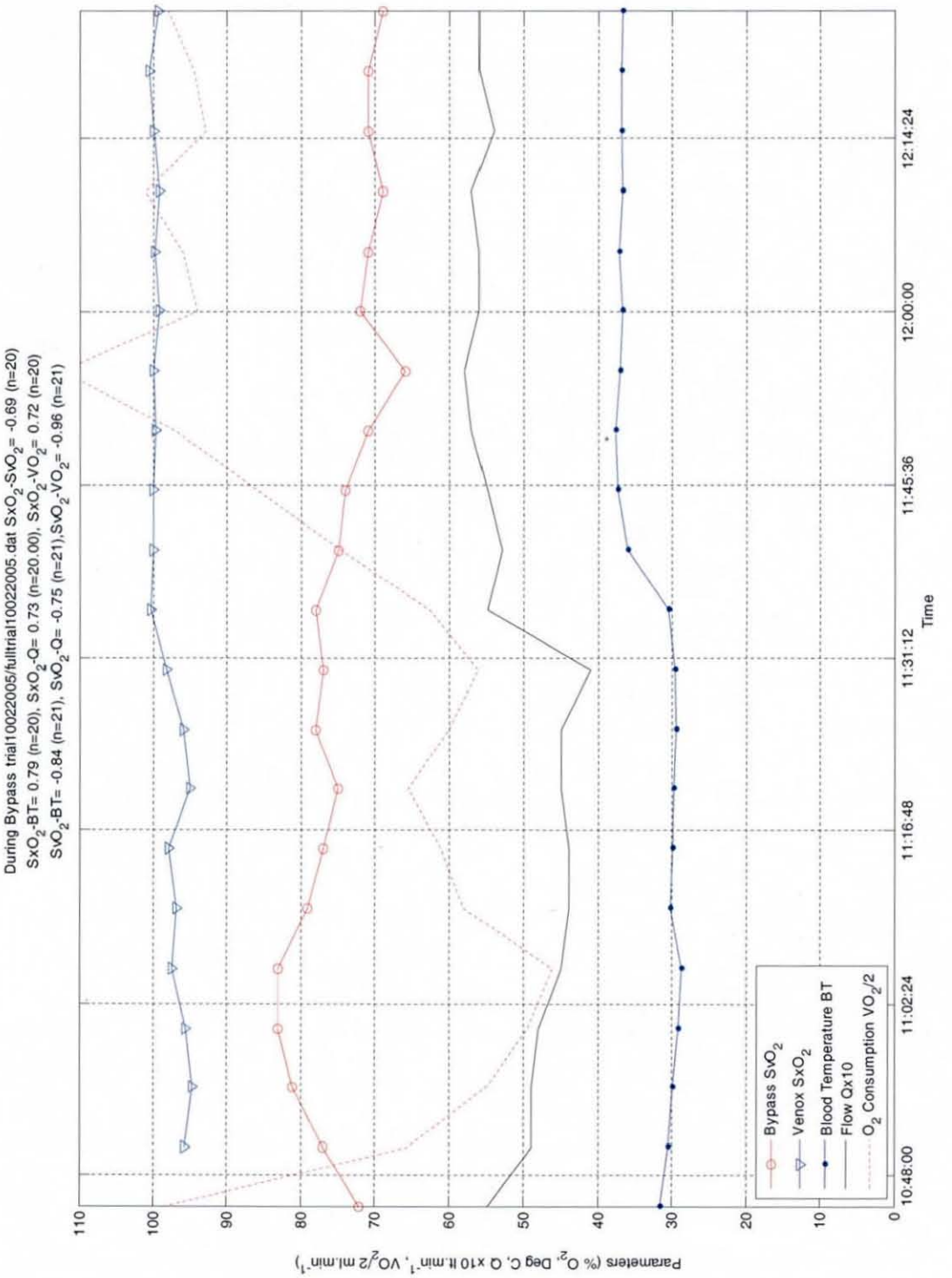

Figure I.19 – Clinical case study 19

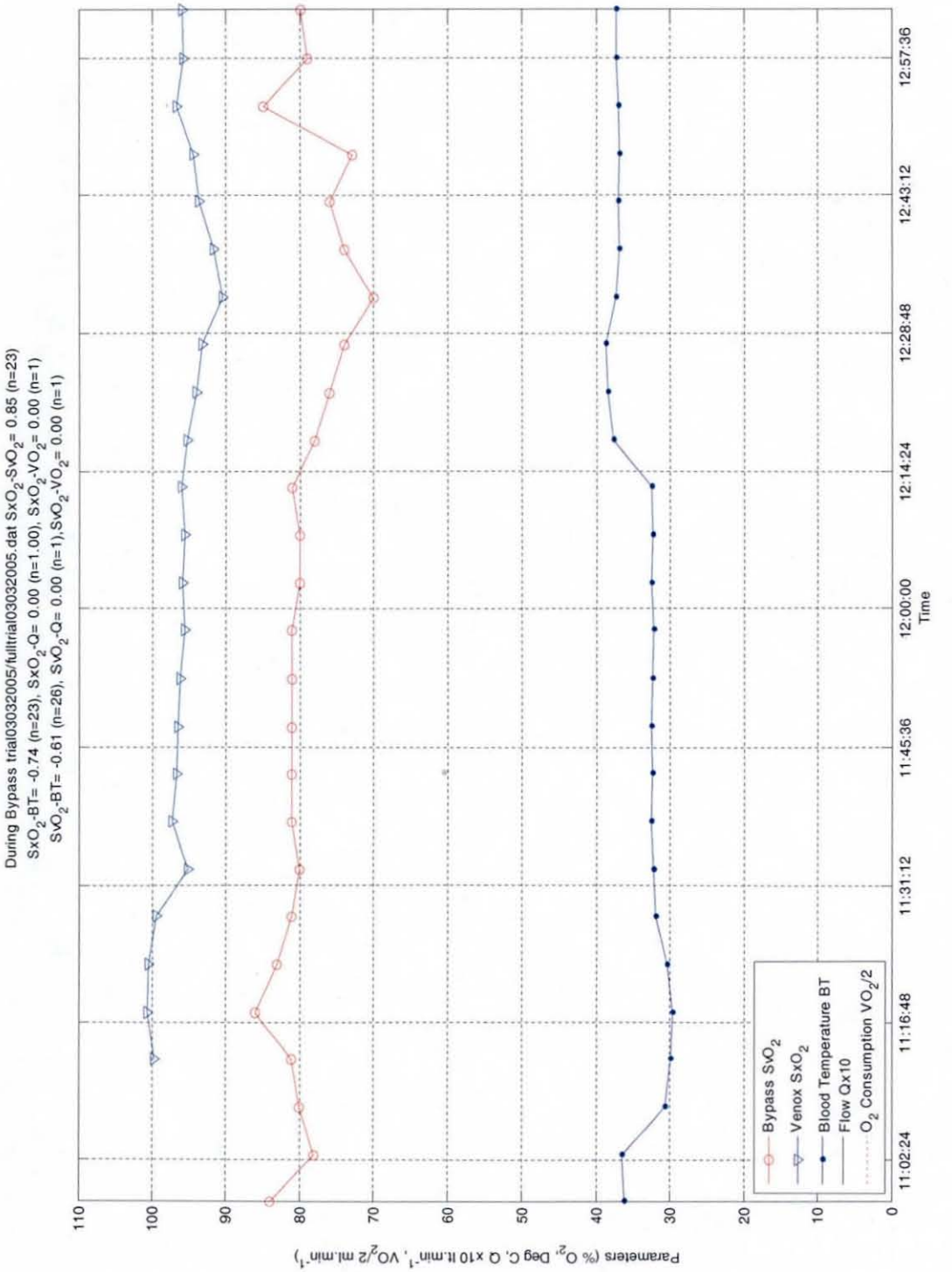

Figure I.20 – Clinical case study 20

APPENDIX

II. ELECTRONIC CIRCUITRY

This appendix presents the schematic diagrams of the pressure modulation controller, as well as the microcontroller code which provides all the functionality described in Chapter 4.

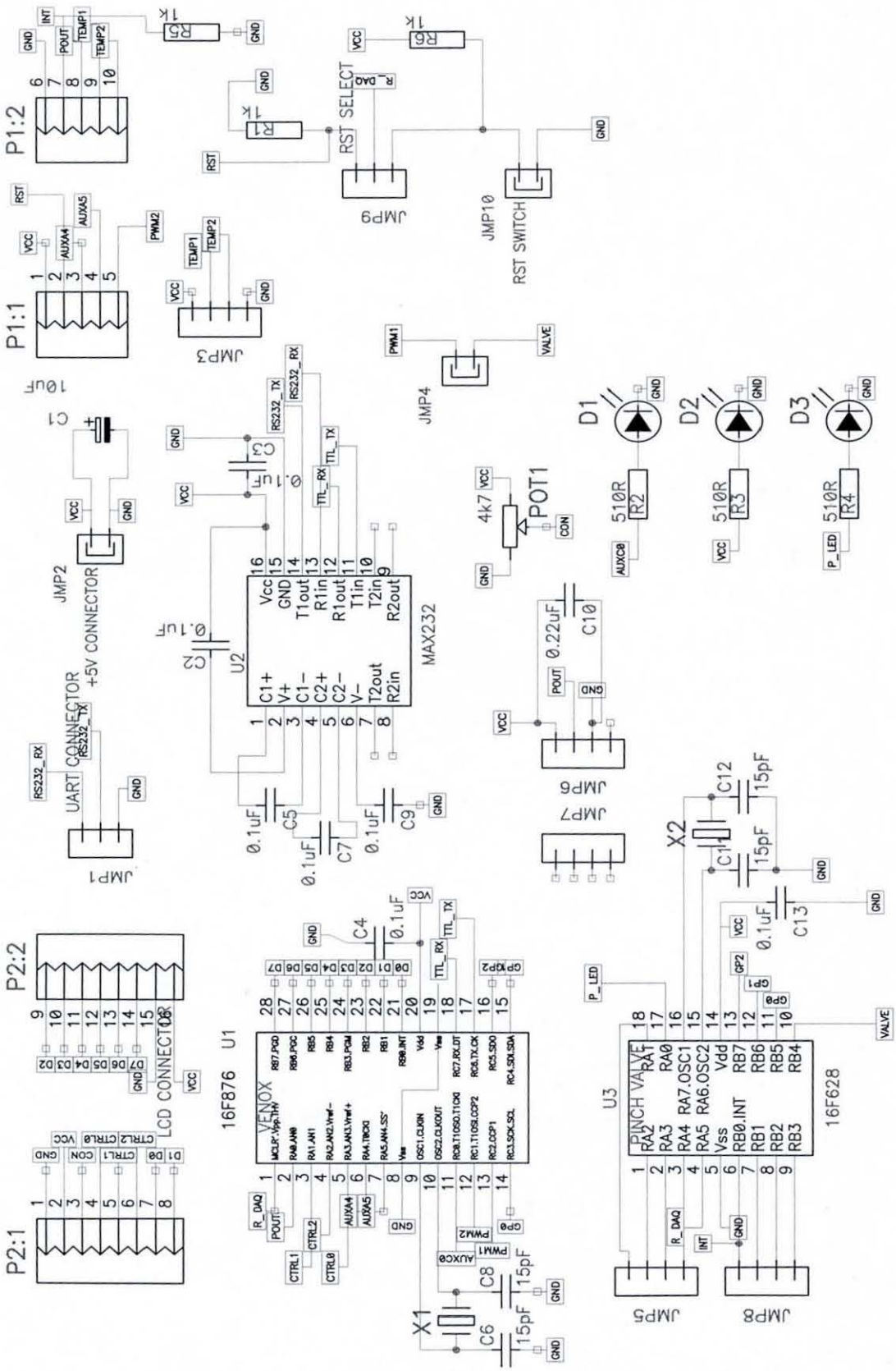

Figure II.1 – Pressure modulation controller board

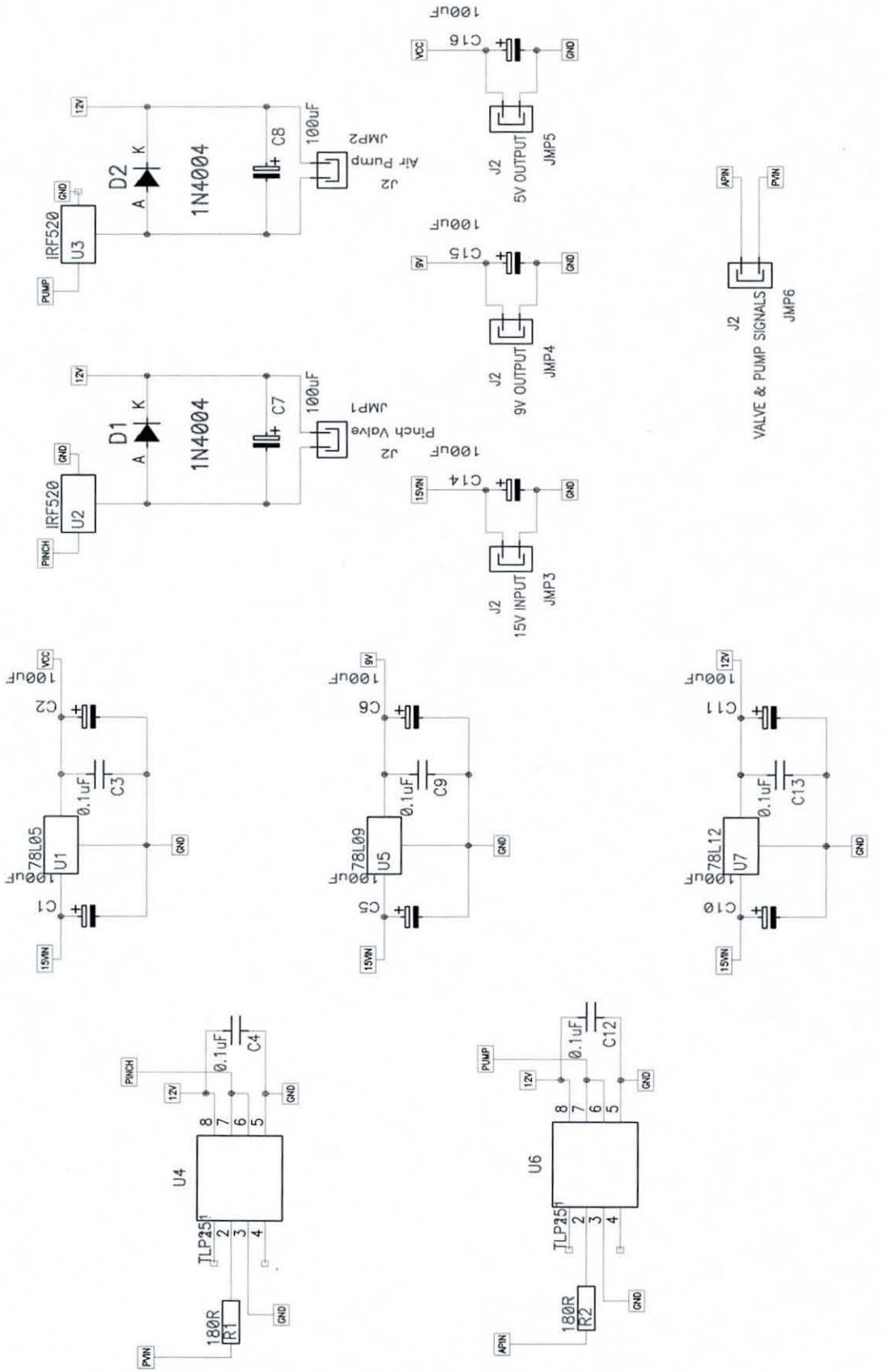

Figure II.2 – DC-DC converter and pump-valve drivers

```
;*****************************************************
;VENOX_BOARD - MICROCONTROLLER CODE FOR THE PRESSURE MODULATION
CONTROL BOARD, RUNNING ON MICROCHIP 16F876A @ 20MHz, FEATURING:
;-RS232 BI-DIRECTIONAL COMMUNICATION WITH PC
;-A/D CONVERSION OF THE PRESSURE SENSOR SIGNAL
;-MASTER CONTROL OF THE SLAVE MICROCONTROLLER (16F628) WHICH OPERATES
THE PINCH VALVE
;-DIRECT PUMP SPEED CONTROL
;-LCD SCREEN CONTROL
;-BOOTLOADER FOR ON-BOARD PROGRAMMING VIA USB
;*****************************************************

LIST    P=16F876A, R=DEC

#include "P16F876A.INC"

;*****************************************************
;CONFIGURE THE FUSES
;*****************************************************
__config _HS_OSC & _LVP_OFF & _WDT_OFF & _PWRTE_ON & _BODEN_ON

;*****************************************************
;DEFINE RESER VECTOR AND INTERRUPT SERVICE ROUTINE ;LOCATIONS
;*****************************************************
RESET_V         EQU  0x000
ISR_V           EQU  0x004
;*****************************************************
;ASSIGN NAMES TO SOME PORTS AND PINS
;*****************************************************
LCD_DATA        EQU     PORTB
LCD_DATA_TRIS   EQU     TRISB
LCD_CTRL        EQU     PORTA
LCD_RW          EQU     1
LCD_E           EQU     2
LCD_RS          EQU     3
;*****************************************************
;ASSIGN MEMORY ADDRESSES TO VARIABLES
;*****************************************************
LCD_LINE0       EQU     H'0000'
LCD_TEMP        EQU     H'0020'
DELAY           EQU     H'0021'
X_DELAY         EQU     H'0022'
TEMP            EQU     H'0023'
TEMP2           EQU     H'0024'
TEMPCHAR        EQU     H'0025'
TEMPREG         EQU     H'0026'
P_HI            EQU     H'0027'
P_LO            EQU     H'0028'
FLAG            EQU     H'0029'
;*****************************************************
;PROGRAM START
;*****************************************************
                ORG     RESET_V
                CLRF    PCLATH
                GOTO    START
;*****************************************************
;PERIPHERAL INTERRUPT ROUTINE
;*****************************************************
                ORG     ISR_V
                RETFIE
;*****************************************************
;INITIALISE PROCESSOR REGISTERS
;*****************************************************
START           CLRF    STATUS
                CLRF    INTCON
                CLRF    PORTA           ;CLEAR ALL PORTS
                CLRF    PORTB
                CLRF    PORTC
                MOVLW   0x081           ;10000001 A/D MODULE POWER UP
                MOVWF   ADCON0
                BSF     STATUS,RP0      ;SELECT BANK 1
                BCF     STATUS,RP1
                MOVLW   0x0CE           ;CONFIGURE A/D 11001110
                MOVWF   ADCON1          ;RA0 ANALOGUE, RES RIGHT JUST.
                                        ;TAD=FOSC/64 (110)
                MOVLW   0x0C0           ;ALL INTERRUPTS OFF, PEIE, GEIE ON
                MOVWF                   INTCON
                MOVLW   0x001           ;RA0 INPUT
                MOVWF   TRISA           ;RA7..1 OUTPUTS
                MOVLW   0x000           ;RB7..0 OUTPUTS
                MOVWF   TRISB
                MOVLW   0x080           ;ENABLE RX, ALL OTHER OUTPUTS
                MOVWF   TRISC
;*****************************************************
;SET BAUD RATE TO COMMUNICATE WITH THE PC
;BAUD RATE = 9600, NO PARITY, 1 STOP BIT
;*****************************************************
                MOVLW   H'0081'         ;DECIMAL 129(20MHz XTAL)
                MOVWF   SPBRG           ;BAUDRATE = 9600bps
                MOVLW   H'0024'         ;BRGH=1, TX ENABLED
                MOVWF   TXSTA
                BCF     STATUS,RP0      ;SELECT BANK 0
                MOVLW   H'0090'         ;ENABLE SERIAL PORT
                MOVWF   RCSTA           ;SET CONTINUOUS RECEIVE
                CLRF    PORTB
                CALL    HEXMAP          ;CONSTRUCT HEX-ASCII MAP
                GOTO    MAIN
;*****************************************************
;MAIN PROGRAM
;*****************************************************
MAIN            CALL    LCDINIT         ;INITIALIZE THE LCD
                CALL    INITPWM         ;INITIALIZE THE PWM GENERATOR
                CALL    LCDCLEAR        ;CLEAR THE LCD
                MOVLW   LCD_LINE0       ;MOVE CURSOR TO         LINE0
                CALL    LCDSDDA
                MOVLW   B'00110001'
                MOVWF   T1CON
                BSF     PORTC,0         ;SWITCH LED ON

MAIN2           ;CALL   PRESSURE        ;READ PRESSURE
                MOVLW   PR2
                MOVWF   FSR
                MOVF    INDF,W
                CALL    CONVERT
                BSF     PORTC,0
                CALL    RECEIVE         ;WAIT FOR CHARACTER INPUT
                BCF     PORTC,0
                GOTO    CHKR            ;GOTO CHECK CHARACTER

EXIT_IR         BCF     FLAG,0          ;CLEAR ERROR FLAG
                GOTO    MAIN2
;*****************************************************
;A/D CONVERSION OF THE PRESSURE SENSOR
;*****************************************************
PRESSURE        CALL    DELAY1
                CALL    DELAY1
                BSF     ADCON0,2        ;START CONVERSION
                BTFSC   ADCON0,2        ;IS IT DONE YET?
                GOTO    $-1             ;IF YES SKIP NEXT LINE
                MOVLW   H'0043'         ;POINT TO ADDRESS 0X043
                MOVWF   FSR
                MOVF    ADRESH,W        ;STORE HIGH NIBBLE
                MOVWF   INDF
                MOVWF   P_HI
                INCF    FSR,F           ;POINT TO ADDRESS 0X044
                BSF     STATUS,RP0      ;SELECT BANK 1
                MOVF    ADRESL,W        ;STORE LOWER NIBBLE
                BCF     STATUS,RP0      ;SELECT BANK 0
                MOVWF   INDF
                MOVWF   P_LO
                CALL    DELAY1          ;WAIT
                CALL    DELAY1
                RETURN                  ;RETURN
;*****************************************************
;DECIDE IF THE INCOMING PACKET IS
;A COMMAND (=) OR AN ENQUIRY (?)
;*****************************************************
CHKR            MOVF    RCREG,W
                MOVWF   TEMPCHAR        ;STORE INCOMING CHAR
                SUBLW   '?'
                BTFSC   STATUS,Z        ;IS IT A '?'
                GOTO    READ            ;YES GOTO READ VALUE
                MOVF    TEMPCHAR,W
                SUBLW   '='             ;IS IT A '='
                BTFSC   STATUS,Z
                GOTO    WRITE           ;YES GOTO WRITE NEW VALUE
                GOTO    EXIT_IR         ;NONE OF THEM, GO BACK
;*****************************************************
;INQUIRY PACKET DECODING. POINTS TO THE
;APPROPRIATE REGISTER TO SEND BACK TO PC
;*****************************************************
READ            CALL    RECEIVE         ;WAIT FOR NEXT CHAR AFTER ?
                MOVWF   TEMPCHAR        ;STORE
                SUBLW   '2'
                BTFSS   STATUS,Z        ;IS IT '2'? VENOX ID
                GOTO    EXIT_IR         ;NO, PACKET INVALID EXIT
                CALL    RECEIVE         ;YES, WAIT FOR NEXT CHAR
                MOVWF   TEMPCHAR        ;STORE CHARACTER
                SUBLW   0x00D           ;IS IT CARRIAGE RETURN?
                BTFSC   STATUS,Z        ;IF YES EXIT WITH ERROR
                GOTO    ERRMSG          ;SEND ERROR MESSAGE TO PC
                MOVF    TEMPCHAR,W      ;NOT CR, MOVE TO W
                MOVWF   FSR             ;POINT FSR TO CHAR VALUE
                SUBLW   'J'             ;IS THE CHAR =>'J' (ASCII)?
                BTFSS   STATUS,C        ;IF YES, REGISTER OUT OF RANGE
                GOTO    ERRMSG          ;EXIT WITH ERROR
                MOVLW   'A'             ;IS THE CHAR = OR AFTER 'A' (ASCII)
                SUBWF   FSR,W
                BTFSS   STATUS,C        ;IF YES, REGISTER IN RANGE
                GOTO    ERRMSG          ;IF NO, EXIT WITH ERROR
                CALL    RECEIVE         ;WAIT FOR NEXT CHAR
                SUBLW   H'000D'         ;IS IT CARRIAGE RETURN?
                BTFSS   STATUS,Z
                GOTO    $-3             ;NO, WAIT FOR NEXT CHAR
                MOVLW   '2'             ;YES, REPLY WITH REG VALUE
                CALL    SEND            ;SEND ID=2
                MOVF    FSR,W           ;COPY VALUE OF POINTER TO W
                CALL    SEND            ;SEND VALUE OF POINTER
                MOVLW   '.'             ;SEND '.'
                CALL    SEND
                MOVF    INDF,W          ;CONTENTS OF POINTER TO W
                CALL    CONVERT         ;CONVERT VALUE TO ASCII/SEND
                MOVLW   H'000D'
                CALL    SEND            ;SEND CARRIAGE RETURN
                GOTO    EXIT_IR         ;RETURN TO MAIN ROUTINE
;*****************************************************
;ERRMSG - SEND ERROR MESSAGE TO PC
;*****************************************************
ERRMSG          CALL    RECEIVE         ;WAIT FOR CARRIAGE RETURN
                SUBLW   H'000D'         ;BEFORE SENDING ERROR
                BTFSS   STATUS,Z
                GOTO    ERRMSG
ERRMSG1         MOVLW   '2'             ;SEND CHAR '2'
                CALL    SEND
                MOVLW   '.'             ;SEND CHAR '.'
                CALL    SEND
                MOVLW   'E'             ;SEND CHAR 'E'
                CALL    SEND
                MOVLW   'R'             ;SEND CHAR 'R'
                CALL    SEND
                MOVLW   'R'             ;SEND CHAR 'R'
                CALL    SEND
                MOVLW   H'000D'         ;SEND CARRIAGE RETURN
                CALL    SEND
                GOTO    EXIT_IR         ;RETURN TO MAIN ROUTINE
```

Figure II.3a – Master µController code part (a)

```
;*****************************************************************
;WRITE PACKET DECODING. POINTS TO THE
;APPROPRIATE REGISTER AND EXECUTES COMMAND
;*****************************************************************
;
WRITE   CALL    RECEIVE     ;READ CHARACTER
        MOVWF   TEMPCHAR
        SUBLW   '2'         ;IS IT ID=2?
        BTFSS   STATUS,Z
        GOTO    EXIT_IR     ;NO, IGNORE AND RETURN TO MAIN
        CALL    RECEIVE     ;YES, GET NEXT CHAR
        MOVWF   TEMPCHAR    ;STORE
        SUBLW   H'000D'     ;IS IT CARRIAGE RETURN?
        BTFSC   STATUS,Z
        GOTO    ERRMSG      ;YES, PACKET INCOMPLETE, ERROR
        MOVF    TEMPCHAR,W  ;NO, MOVE CHAR TO W
        MOVWF   FSR         ;POINT FSR TO VALUE OF CHAR
        MOVWF   TEMPREG
        SUBLW   'A'         ;IS IT 'A'?
        BTFSC   STATUS,Z
        GOTO    PUMP        ;YES, ADJUST PUMP SPEED
        MOVF    FSR,W
        SUBLW   'B'         ;IS IT 'B'?
        BTFSC   STATUS,Z
        GOTO    VALVE       ;YES, ADJUST VALVE FREQUENCY
        MOVF    FSR,W
        SUBLW   'E'         ;IS IT 'E'?
        BTFSC   STATUS,Z
        GOTO    LCDC        ;YES, SEND LCD COMMAND
        MOVF    FSR,W
        SUBLW   'F'         ;IS IT 'F'?
        BTFSC   STATUS,Z
        GOTO    LCDD        ;YES, SEND LCD DATA
        MOVF    FSR,W
        SUBLW   'G'         ;IS IT 'G'?
        BTFSC   STATUS,Z
        GOTO    USERCHAR    ;YES, SEND CUSTOM USER CHAR
        MOVF    FSR,W
        SUBLW   'H'         ;IS IT 'H'?
        BTFSC   STATUS,Z
;       GOTO    P_CTRL      ;YES, SET MAX PRESSURE (NOT USED)
        GOTO    MAIN2
        GOTO    ERRMSG      ;NONE OF THEM, RETURN ERROR
;*****************************************************************
;PUMP - EXECUTES THE COMMAND TO UPDATE THE PUMP SPEED
;*****************************************************************
PUMP    CALL    CHK1        ;READ NUMERICAL VALUE OF PACKET
        IORWF   TEMP,F      ;STORE BOTH CHARS IN SINGLE REG
        MOVF    TEMP,W      ;COPY THE TOTAL VALUE TO W
        MOVWF   INDF        ;AND THEN TO THE MEMORY
                            ;LOCATION FOR THE PUMP
        CALL    RECEIVE     ;WAIT FOR END OF PACKET (CR)
        SUBLW   H'000D'
        BTFSS   STATUS,Z
        GOTO    $-3
        BTFSC   FLAG,0      ;MAKE SURE THERE WERE NO ERRORS
        GOTO    ERRMSG
        MOVF    INDF,W      ;IF NO ERRORS, NEW PUMP SPEED IN W
        MOVWF   CCPR1L      ;CHANGE THE PWM DUTY CYCLE
        MOVLW   '2'         ;SEND CONFIRMATION OF EXECUTION
        CALL    SEND
        MOVF    FSR,W
        CALL    SEND
        MOVLW   ','
        CALL    SEND
        MOVLW   '0'
        CALL    SEND
        MOVF    CCPR1L,W    ;COPY NEW PUMP VALUE FROM PWM
        CALL    CONVERT     ; CONVERT TO ASCII CHARACTERS
        MOVLW   'O'
        CALL    SEND
        MOVLW   'K'
        CALL    SEND
        MOVLW   H'000D'
        CALL    SEND        ;END OF PACKET SENT
        GOTO    EXIT_IR     ;COMMAND COMPLETED, EXIT
;*****************************************************************
;VALVE - EXECUTES THE COMMAND TO UPDATE THE VALVE FREQUENCY
;*****************************************************************
VALVE   CALL    CHK1        ;READ NUMERICAL VALUE OF PACKET
        IORWF   TEMP,F      ;STORE BOTH CHARS IN A SINGLE REG
        MOVF    TEMP,W      ;COPY THE TOTAL VALUE TO W
        MOVWF   INDF        ;AND THEN TO THE MEMORY
                            ;LOCATION FOR THE VALVE
        CALL    RECEIVE     ;WAIT FOR END OF PACKET (CR)
        SUBLW   H'000D'
        BTFSS   STATUS,Z
        GOTO    $-3
        BTFSC   FLAG,0      ;MAKE SURE THERE WERE NO ERRORS
        GOTO    ERRMSG
        RLF     TEMP,F      ;ROTATE LEFT
        RLF     TEMP,F      ;ROTATE LEFT
        RLF     TEMP,F      ;ROTATE LEFT
        MOVF    PORTC,W     ;COPY PORTC VALUE
        ANDLW   B'11000111' ;DISCARD OLD VALVE VALUES
        IORWF   TEMP,W      ;ADD NEW VALVE VALUE TO PORTC
        MOVWF   PORTC       ;COPY UPDATED PORTC TO THE PORT
        MOVLW   '2'         ;SEND CONFIRMATION TO PC
        CALL    SEND
        MOVF    FSR,W
        CALL    SEND
        MOVLW   ','
        CALL    SEND
        MOVLW   '0'
        CALL    SEND
        MOVF    PORTC,W
        ANDLW   B'00111000' ;READ VALVE VALUE FROM PORT
        MOVWF   TEMP        ;IT WAS PROPERLY UPDATED
        RRF     TEMP,F      ;ROTATE RIGHT
        RRF     TEMP,F      ;ROTATE RIGHT
        RRF     TEMP,F      ;ROTATE RIGHT
        MOVF    TEMP,W      ;COPY RESULT TO W
        CALL    CONVERT     ;CONVERT HEX TO ASCII CHARS
        MOVLW   'O'
        CALL    SEND
        MOVLW   'K'
        CALL    SEND
        MOVLW   H'000D'
        CALL    SEND        ;END OF PACKET SENT
        GOTO    EXIT_IR
;*****************************************************************
;LCDC - EXECUTES THE COMMAND TO SEND COMMAND TO THE LCD SCREEN
;*****************************************************************
LCDC    CALL    CHK1        ;NUMERICAL VALUE OF PACKET
        IORWF   TEMP,F      ;STORE BOTH CHARS IN A REG
        MOVF    TEMP,W      ;COPY THE TOTAL VALUE TO W
        MOVWF   INDF        ;AND THEN TO THE MEMORY
                            ;LOCATION FOR THE LCD CMD
        CALL    RECEIVE     ;WAIT FOR END OF PACKET (CR)
        SUBLW   H'000D'
        BTFSS   STATUS,Z
        GOTO    $-3
        BTFSC   FLAG,0      ;MAKE SURE THERE WERE NO ERR
        GOTO    ERRMSG
        MOVF    INDF,W      ;MOVE COMMAND TO W
        CALL    LCDPUTCMD   ;SEND COMMAND TO LCD SCREEN
        MOVLW   '2'         ;SEND CONFIRMATION TO PC
        CALL    SEND
        MOVF    FSR,W
        CALL    SEND
        MOVLW   ','
        CALL    SEND
        MOVLW   '0'
        CALL    SEND
        MOVF    INDF,W      ;READ LCD CMD FROM MEM LOC
        CALL    CONVERT     ;CONVERT CMD TO ASCII CHARS
        MOVLW   'O'
        CALL    SEND
        MOVLW   'K'
        CALL    SEND
        MOVLW   H'000D'
        CALL    SEND        ;END OF PACKET SENT
        GOTO                EXIT_IR
;*****************************************************************
;LCDD - EXECUTES THE COMMAND TO SEND DATA TO THE LCD SCREEN
;*****************************************************************
LCDD    CALL    CHK1        ;NUMERICAL VALUE OF PACKET
        IORWF   TEMP,F      ;STORE BOTH CHARS IN A  REG
        MOVF    TEMP,W      ;COPY THE TOTAL VALUE TO W
        MOVWF   INDF        ;AND THEN TO THE MEMORY
                            ;LOCATION FOR THE LCD DATA
        CALL    RECEIVE
        SUBLW   H'000D'
        BTFSS   STATUS,Z
        GOTO    $-3
        BTFSC   FLAG,0      ;MAKE SURE THERE WERE NO ERR
        GOTO    ERRMSG
        MOVF    INDF,W      ;MOVE COMMAND TO W
        CALL    LCDPUTCHAR  ;SEND DATA TO THE LCD SCREEN
        MOVLW   '2'         ;SEND CONFIRMATION TO PC
        CALL    SEND
        MOVF    FSR,W
        CALL    SEND
        MOVLW   ','
        CALL    SEND
        MOVLW   '0'
        CALL    SEND
        MOVF    INDF,W      ;LCD DATA FROM MEMORY LOC
        CALL    CONVERT     ;CONVERT DATA TO ASCII CHARS
        MOVLW   'O'
        CALL    SEND
        MOVLW   'K'
        CALL    SEND
        MOVLW   H'000D'
        CALL    SEND        ;END OF PACKET SENT
        GOTO    EXIT_IR
;*****************************************************************
;USERCHAR - EXECUTES THE COMMAND TO SEND CUSTOM CHAR
;TO THE LCD SCREEN
;*****************************************************************
USERCHAR
        CALL    CHK1        ;NUMERICAL VALUE OF PACKET
        IORWF   TEMP,F      ;STORE BOTH CHARS IN A REG
        MOVF    TEMP,W      ;COPY THE TOTAL VALUE TO W
        MOVWF   INDF        ;AND THEN TO THE MEMORY
                            ;LOCATION FOR THE LCD DATA
        CALL    RECEIVE
        SUBLW   H'000D'
        BTFSS   STATUS,Z
        GOTO    $-3
        BTFSC   FLAG,0      ;MAKE SURE THERE WERE NO ERR
        GOTO    ERRMSG
        MOVF    INDF,W      ;MOVE COMMAND TO W
        CALL    LCDSCGA     ;SEND CUSTOM CHAR TO LCD SCR
        MOVLW   '2'         ;SEND CONFIRMATION TO PC
        CALL    SEND
        MOVF    FSR,W
        CALL    SEND
        MOVLW   ','
        CALL    SEND
        MOVLW   '0'
        CALL    SEND
        MOVF    INDF,W      ;CUSTOM CHAR FROM MEM LOC
        CALL    CONVERT     ;CONVERT DATA TO ASCII CHARS
        MOVLW   'O'
        CALL    SEND
        MOVLW   'K'
```

Figure II.3b – Master µController code part (b)

```
                CALL    SEND
                MOVLW   H'000D'
                CALL    SEND            ;END OF PACKET SENT
                GOTO                    EXIT_IR
;*****************************************************
;CHK1 - READ THE NUMERICAL VALUE WHICH COMES AFTER
;THE PARAMETER LETTER - E.G. =2A5B, READ '5B'
;*****************************************************
CHK1            CALL    RECEIVE         ;RECEIVE FIRST CHAR OF NUM VALUE
                MOVWF   TEMP            ;MOVE VALUE OF 1ST CHAR TO TEMP
                MOVWF   TEMPCHAR        ;MOVE  SAME VALUE TO TEMPCHAR
                SUBLW   H'000D'         ;IS IT CARRIAGE RETURN?
                BTFSC   STATUS,Z
                GOTO    ERRMSG1         ;IF YES, PACKET INCOMPLETE- ERROR
                MOVLW   H'0041'         ;MOVE HEX'41' (START OF ALPHABETIC
                                        ;CHARS) TO W
                SUBWF   TEMP,W          ;SUBTRACT W FROM TEMP
                BTFSS   STATUS,C        ;CHECK CARRY BIT STATUS, TO
                                        ;CHECK W>F OR W<=F
                GOTO    NUM1            ;IF TEMP<HEX'41', IT'S NOT A LETTER
                GOTO    CHAR1           ;IF TEMP=>HEX'41', IT'S NOT A NUMBER
CHK2            SWAPF   TEMP,1          ;SWAP LOW AND HIGH NIBBLES
                CALL    RECEIVE         ;RECEIVE NEXT CHARACTER
                MOVWF   TEMP2           ;STORE CHAR TO TEMP2
                MOVWF   TEMPCHAR        ;STORE CHAR TO TEMPCHAR
                SUBLW   H'000D'         ;IS IT CARRIAGE RETURN?
                BTFSC   STATUS,Z
                GOTO    ERRMSG1         ;YES, INCOMPLETE PACKET - ERROR
                MOVLW   H'0041'         ;MOVE HEX'41' (START OF ALPHABETIC
                                        ;CHARS) TO W
                SUBWF   TEMP2,0         ;SUBTRACT W FROM TEMP2
                BTFSS   STATUS,C        ;CHECK CARRY BIT STATUS, TO
                                        ;CHECK W>F OR W<F
                GOTO    NUM2            ;IF TEMP2<HEX'41', IT'S NOT A LETTER
                GOTO    CHAR2           ;IF TEMP2=>HEX'41', IT'S NOT NUMBER
CHAR1           MOVLW   H'0047'         ;MOVE HEX'47' IN W
                SUBWF   TEMP,W          ;SUBTRACT HEX'47' FROM TEMP
                BTFSS   STATUS,C        ;IS TEMP => OR < THAN W?
                GOTO    $+2             ;TEMP<W, CHARACTER BEFORE
                                        ;ASCII(H'47')
                GOTO    ERRMSG          ;TEMP=>W, CHARACTER EQUAL TO OR
                                        ;AFTER ASCII(H'47')
                MOVLW   H'0037'         ;MOVE HEX'37' TO W
                SUBWF   TEMP,F
                GOTO    CHK2
NUM1            MOVLW   H'003A'         ;TEMP NOT A LETTER, IS IT NUMBER?
                SUBWF   TEMP,W          ;SUBTRACT HEX'3A' FROM TEMP
                BTFSS   STATUS,C        ;IF TEMP>HEX'3A' NOT A NUMBER
                GOTO    $+2             ;TEMP<HEX'3A', PROBABLY A NUMBER
                GOTO    ERRMSG          ;TEMP>HEX'3A' NOT A NUMBER,ERROR
                MOVLW   H'0030'         ;MOVE HEX'30' TO W
                SUBWF   TEMP,F          ;SUBTRACT HEX'30' FROM TEMP
                BTFSS   STATUS,C        ;IF TEMP=>HEX'30' DEFINITELY NMBER
                GOTO    ERRMSG          ;IF TEMP<HEX'30', NOT NUMBER - ERR
                GOTO    CHK2            ;GOTO CHECK SECOND CHARACTER
CHAR2           MOVLW   H'0047'         ;MOVE HEX'47' IN W
                SUBWF   TEMP2,W         ;SUBTRACT HEX'47' FROM TEMP2
                BTFSS   STATUS,C        ;IS TEMP2 => OR < THAN W?
                GOTO    $+2             ;TEMP2<W, CHARACTER BEFORE
                                        ;ASCII(H'47')
                GOTO    ERRMSG          ;TEMP2=>W, CHARACTER EQUAL TO
                                        ;OR AFTER ASCII(H'47')
                MOVLW   H'0037'         ;MOVE HEX'37' TO W
                SUBWF   TEMP2,W
                RETURN
NUM2            MOVLW   H'003A'         ;TEMP2 NOT A LETTER, IS IT NUMBER?
                SUBWF   TEMP2,W         ;SUBTRACT HEX'3A' FROM TEMP2
                BTFSS   STATUS,C        ;IF TEMP2>HEX'3A' NOT A NUMBER
                GOTO    $+2             ;TEMP2<HEX'3A' PROBABLY NUMBER
                GOTO    ERRMSG          ;TEMP2>HEX'3A' NOT A NUMBER - ERR
                MOVLW   H'0030'         ;MOVE HEX'30' TO W
                SUBWF   TEMP2,F         ;SUBTRACT HEX'30' FROM TEMP2
                BTFSS   STATUS,C        ;IF TEMP2>HEX'30' DEFINITELY NMBER
                BSF     FLAG,0          ;SET BIT0 OF FLAG TO MARK ERROR
                MOVF    TEMP2,W
                RETURN                  ;RETURN
;*****************************************************
;HEXMAP - ROUTINE THAT CONSTRUCTS A TABLE WITH ALL
;POSSIBLE CHARACTERS IN HEX FORMAT (0-9 AND A-F)
;*****************************************************
HEXMAP          MOVLW   H'0054'         ;POINT TO MEMORY ADDRESS HEX'54'
                MOVWF   FSR
                MOVLW   H'0030'         ;HEX'30' IS ASCII CHAR '0'
                MOVWF   INDF            ;COPY TO MEMORY LOCATION HEX'54'
                INCF    FSR,1           ;INCREASE THE MEMORY POINTER TO
                                        ;HEX'54'+1
                MOVLW   H'0031'         ;HEX'31' IS ASCII CHAR '1'
                MOVWF   INDF
                INCF    FSR,1           ;INCREASE THE MEMORY POINTER + 1
                MOVLW   H'0032'         ;HEX'32' IS ASCII CHAR '2'
                MOVWF                   INDF
                INCF    FSR,1           ;INCREASE THE MEMORY POINTER + 1
                MOVLW   H'0033'         ;HEX'33' IS ASCII CHAR '3'
                MOVWF   INDF
                INCF    FSR,1           ;INCREASE THE MEMORY POINTER + 1
                MOVLW   H'0034'         ;HEX'34' IS ASCII CHAR '4'
                MOVWF   INDF
                INCF    FSR,1           ;INCREASE THE MEMORY POINTER + 1
                MOVLW   H'0035'         ;HEX'35' IS ASCII CHAR '5'
                MOVWF   INDF
                INCF    FSR,1           ;INCREASE THE MEMORY POINTER + 1
                MOVLW   H'0036'         ;HEX'36' IS ASCII CHAR '6'
                MOVWF   INDF
                INCF    FSR,1           ;INCREASE THE MEMORY POINTER + 1
                MOVLW   H'0037'         ;HEX'37' IS ASCII CHAR '7'
                MOVWF   INDF
                INCF    FSR,1           ;INCREASE THE MEMORY POINTER + 1
                MOVLW   H'0038'         ;HEX'38' IS ASCII CHAR '8'
                MOVWF   INDF
                INCF    FSR,1           ;INCREASE THE MEM POINTER + 1
                MOVLW   H'0039'         ;HEX'39' IS ASCII CHAR '9'
                MOVWF   INDF
                INCF    FSR,1           ;INCREASE THE MEM POINTER + 1
                MOVLW   H'0041'         ;HEX'41' IS ASCII CHAR 'A'
                MOVWF   INDF
                INCF    FSR,1           ;INCREASE THE MEM POINTER + 1
                MOVLW   H'0042'         ;HEX'42' IS ASCII CHAR 'B'
                MOVWF   INDF
                INCF    FSR,1           ;INCREASE THE MEM POINTER + 1
                MOVLW   H'0043'         ;HEX'43' IS ASCII CHAR 'C'
                MOVWF   INDF
                INCF    FSR,1           ;INCREASE THE MEM POINTER + 1
                MOVLW   H'0044'         ;HEX'44' IS ASCII CHAR 'D'
                MOVWF   INDF
                INCF    FSR,1           ;INCREASE THE MEM POINTER + 1
                MOVLW   H'0045'         ;HEX'45' IS ASCII CHAR 'E'
                MOVWF   INDF
                INCF    FSR,1           ;INCREASE THE MEM POINTER + 1
                MOVLW   H'0046'         ;HEX'46' IS ASCII CHAR 'F'
                MOVWF   INDF
                RETURN
;*****************************************************
;CONVERT - ROUTINE THAT INPUTS A VALUE AND OUTPUTS THE
;LOW AND HIGH NIBBLES SEQUENTIALLY FOR CONVERSION TO ASCII
;*****************************************************
CONVERT         MOVWF   TEMPCHAR        ;COPY VALUE TO TEMPCHAR
                SWAPF   TEMPCHAR,W      ;SWAP HIGH AND LOW NIBBLES
                ANDLW   H'000F'         ;KEEP ONLY THE MOST SIGNIF BITS
                MOVWF   TEMP2           ;COPY RESULT TO TEMP2
                MOVLW   H'0053'         ;SET THE MEMORY POINTER
                MOVWF   FSR             ;BEFORE THE START OF TABLE
                MOVLW   H'00FF'         ;COPY VALUE HEX'FF' TO W
                MOVWF   TEMP            ;COPY TO TEMP
                CALL    CH2HEX          ;CONVERT LOW NIBBLE INTO ASCII
                MOVF    TEMPCHAR,W      ;REPEAT THE ABOVE FOR THE LSB
                ANDLW   H'000F'
                MOVWF   TEMP2
                MOVLW   H'0053'
                MOVWF   FSR
                MOVLW   H'00FF'
                MOVWF   TEMP
                CALL    CH2HEX
                RETURN
;*****************************************************
;CH2HEX - ROUTINE THAT CONVERTS A HEX VALUE TO THE
;CORRESPONDING ASCII CHARACTER
;*****************************************************
CH2HEX          INCF    FSR,F           ;INCREASE THE MEM POINTER BY 1
                INCF    TEMP,F          ;SCAN ASCII TABLE FOR A MATCH
                MOVF    TEMP,W
                XORWF   TEMP2,W
                BTFSS   STATUS,Z
                GOTO    CH2HEX          ;NOT FOUND, CHECK NEXT CHAR
                MOVF    INDF,W          ;FOUND, COPY ASCII CHAR IN W
                CALL    SEND            ;SEND ASCII CHAR TO PC
                RETURN
;*****************************************************
;SEND - SEND A CHARACTER VIA RS232
;*****************************************************
SEND            MOVWF   TXREG           ;MOVE CHARACTER TO TX BUFFER
                NOP                     ;WAIT ONE CYCLE
                BTFSS   PIR1,TXIF       ;CHECK IF CHAR WAS READ BY PC
                GOTO    $-1             ;WAIT UNTIL DONE
                RETURN                  ;RETURN
;*****************************************************
;RECEIVE - RECEIVE A CHARACTER VIA RS232
;*****************************************************
RECEIVE         BTFSS   PIR1,RCIF       ;CHECK IF A CHAR IS PRESENT
                GOTO    $-1             ;KEEP CHECKING UNTIL DONE
                MOVF    RCREG,W         ;MOVE RECEIVED CHAR TO W
                BCF     PORTC,0
                RETURN                  ;RETURN
;*****************************************************
;INITPWM - INITIALISE THE PIC'S PWM MODULE AT 19.53kHz
;*****************************************************
INITPWM         BCF     STATUS,RP0      ;SELECT BANK 0
                BCF     STATUS,RP1
                MOVLW   H'0000'
                MOVWF   CCP2CON         ;DISABLE CCP2
                MOVF    CCP1CON,W       ;MOVE CCP1CON TO W
                ANDLW   H'00F0'         ;DISABLE CCP1 MODULE AND THEN
                IORLW   H'000C'         ;SET PWM MODE TO CCP1
                MOVWF   CCP1CON
                MOVLW   H'0000'         ;COPY HEX'00' TO W
                MOVWF   T2CON           ;SET TMR2 PRESCALER TO 1
                MOVLW   H'00FF'         ;COPY HEX'FF' TO W
                MOVWF   PR2             ;SET PWM f = 19531.25Hz
                BSF     T2CON,TMR2ON;START THE TIMER
                CLRF    CCPR1L          ;PWM OUTPUT OFF
                RETURN
;*****************************************************
;LCDINIT - INITIALISE THE LCD SCREEN
;*****************************************************
LCDINIT         CLRF    PORTA
                MOVLW   H'0023'
                CALL    X_DELAY500
                MOVLW   H'0038'
                CALL    LCDPUTCMD
                MOVLW   H'0000'
                CALL    LCDMODE
                CALL    LCDCLEAR
                MOVLW   H'0004'
                CALL    LCDMODE
                MOVLW   H'0002'
                CALL    LCDEMODE
                RETURN
```

Figure II.3c – Master µController code part (c)

```
;*****************************************************************
;LCDBUSY - CHECK FOR LCD SCREEN BUSY FLAG
;*****************************************************************
LCDBUSY         BSF     STATUS,RP0
                MOVLW   H'00FF'
                MOVWF   PORTB
                BCF     STATUS,RP0
                BCF     LCD_CTRL,LCD_RS
                BSF     LCD_CTRL,LCD_RW
                BSF     LCD_CTRL,LCD_E
                MOVF    LCD_DATA,W
                BCF     LCD_CTRL,LCD_E
                ANDLW   H'0080'
                BTFSS   STATUS,Z
                GOTO    LCDBUSY
LCDNOTBUSY      BCF     LCD_CTRL, LCD_RW
                BSF     STATUS,RP0
                MOVLW   H'0000'
                MOVWF   LCD_DATA_TRIS
                BCF     STATUS,RP0
                RETURN
;*****************************************************************
;LCDCLEAR - CLEAR THE LCD SCREEN
;*****************************************************************
LCDCLEAR        MOVLW   H'0001'
                CALL    LCDPUTCMD
                RETURN
;*****************************************************************
;LCDHOME - SEND THE CURSOR TO THE HOME POSITION
;*****************************************************************
LCDHOME         MOVLW   H'0002'
                CALL    LCDPUTCMD
                RETURN
;*****************************************************************
;LCDEMODE - LCD ENTRY MODE
;ENTRY MODE MUST BE STORED IN W BEFORE CALLING
;b0   : 0 = NO DISPLAY SHIFT, 1 = DISPLAY SHIFT
;b1   : 0 = AUTO DECREMENT, 1 = AUTO-INCREMENT
;b2-b7 : DON'T CARE
;*****************************************************************
LCDEMODE        ANDLW   H'0003'
                IORLW   H'0004'
                CALL    LCDPUTCMD
                RETURN
;*****************************************************************
;LCDDMODE - LCD ENTRY MODE
;ENTRY MODE MUST BE STORED IN W BEFORE CALLING
;b0   : 0 = CURSOR BLINK OFF, 1 = CURSOR BLINK ON (if b1 = 1)
;b1   : 0 = CURSOR OFF,  1 = CURSOR ON
;b2   : 0 = DISPLAY OFF, 1 = DISPLAY ON
;b3-b7 : DON'T CARE
;*****************************************************************
LCDDMODE        ANDLW   H'0007'
                IORLW   H'0008'
                CALL    LCDPUTCMD
                RETURN
;*****************************************************************
;LCDSCGA - SET CHARACTER GENERATOR RAM ADDRESS
;CGRAM MUST BE STORED IN W BEFORE CALLING
;b0-5  : REQUIRED CGRAM ADDRESS
;b3-b7 : DON'T CARE
;*****************************************************************
LCDSCGA         ANDLW   H'003F'
                IORLW   H'0040'
                CALL    LCDPUTCMD
                RETURN
;*****************************************************************
;LCDSDDA - SET DISPLAY DATA RAM ADDRESS
;DDRAM MUST BE STORED IN W BEFORE CALLING
;b0-6  : REQUIRED DDRAM ADDRESS
;b7    : DON'T CARE
;*****************************************************************
LCDSDDA         IORLW   H'0080'
                CALL    LCDPUTCMD
                RETURN
;*****************************************************************
;LCDGADDR - RETURNS ADDRESS COUNTER CONTENTS FOR DDRAM AND CGRAM
;ADDRESS IS RETURNED IN W
;*****************************************************************
LCDGADDR        BSF     STATUS,RP0
                MOVLW   H'00FF'
                MOVWF   LCD_DATA_TRIS
                BCF     STATUS,RP0
                BCF     LCD_CTRL,LCD_RS
                BSF     LCD_CTRL,LCD_RW
                BSF     LCD_CTRL,LCD_E
                MOVF    LCD_DATA,W
                BCF     LCD_CTRL,LCD_E
                ANDLW   H'007F'
                BCF     LCD_CTRL,LCD_RW
                BSF     STATUS,RP0
                MOVLW   H'0000'
                MOVWF   LCD_DATA_TRIS
                BCF     STATUS,RP0
                RETURN
;*****************************************************************
;LCDPUTCHAR - SEND CHARACTER TO LCD SCREEN
;CHARACTER MUST BE STORED IN W BEFORE CALL
;*****************************************************************
LCDPUTCHAR      MOVWF   LCD_TEMP
                CALL    LCDBUSY
                BCF     LCD_CTRL, LCD_RW
                BSF     LCD_CTRL, LCD_RS
                BSF     LCD_CTRL, LCD_E
                MOVF    LCD_TEMP,W
                MOVWF   LCD_DATA
                BCF                     LCD_CTRL, LCD_E
                RETURN
;*****************************************************************
;LCDPUTCMD - SEND COMMAND TO LCD SCREEN
;COMMAND MUST BE STORED IN W BEFORE CALL
;*****************************************************************
LCDPUTCMD       MOVWF   LCD_TEMP
                CALL    LCDBUSY
                BCF     LCD_CTRL,LCD_RW
                BCF     LCD_CTRL,LCD_RS
                BSF     LCD_CTRL,LCD_E
                MOVF    LCD_TEMP,W
                MOVWF   LCD_DATA
                BCF     LCD_CTRL,LCD_E
                RETURN
;*****************************************************************
;DELAY500 - 500us delay
;*****************************************************************
DELAY500        MOVLW   H'00A5'
                MOVWF   DELAY
                DECFSZ  DELAY,F
                GOTO    $-1
                RETURN
;*****************************************************************
;X_DELAY500 - MULTIPLE DELAY OF 500us * W REG
;*****************************************************************
X_DELAY500      MOVWF   X_DELAY
                CALL    DELAY500
                DECFSZ  X_DELAY,1
                GOTO    $-2
                RETURN
;*****************************************************************
;DELAY1 - SHORT DELAY OF 10CYCLES + CALL + RETURN
;*****************************************************************
DELAY1          NOP
                NOP
                NOP
                NOP
                NOP
                NOP
                NOP
                NOP
                NOP
                NOP
                RETURN
END
;*****************************************************************
;END OF LISTING
;*****************************************************************
```

Figure II.3d – Master µController code part (d)

```
;*****************************************
;VALVE - MICROCONTROLLER CODE FOR THE PRESSURE MODULATION#
;BOARD, RUNNING ON MICROCHIP 16F628 @ 20MHz, WHICH EXCLUSIVELY
;DRIVES THE PINCH VALVE. THIS IS THE 'SLAVE' MICROCONTROLLER
;OF THE CONTROL BOARD WHICH IS CONFIGURED BY THE MASTER
;MICROCONTROLLER IN TERMS OF SWITCHING SPEED, AS DESCRIBED IN
;CHAPTER 3.
;*****************************************

LIST    P=16F628

#include "P16F628.INC"

;*****************************************
;CONFIGURE THE FUSES
;*****************************************
__config _CP_OFF & _WDT_OFF & _PWRTE_ON & _BODEN_OFF & _HS_OSC &
_MCLRE_ON & _LVP_OFF

;*****************************************
;DEFINE RESET VECTOR AND INTERRUPT SERVICE ROUTINE LOCATIONS
;*****************************************
RESET_V         EQU     0x000
ISR_V           EQU     0x004

;*****************************************
;ASSIGN MEMORY ADDRESSES TO VARIABLES
;*****************************************
TEMP0           EQU     0x020
TEMP1           EQU     0x021
TEMP2           EQU     0x022
delaycnt2       EQU     0x023
delaycnt        EQU     0x024
;*****************************************
;PROGRAM START
;*****************************************
                ORG     RESET_V
                CLRF    PCLATH
                GOTO    START
;*****************************************
;PERIPHERAL INTERRUPT ROUTINE
;*****************************************
                ORG     ISR_V
                RETFIE
;*****************************************
;INITIALISE PROCESSOR
;*****************************************
START           CLRF    PORTA           ;CLEAR ALL PORTS
                CLRF    PORTB
                BCF     STATUS, RP1     ;SELECT BANK0
                BCF     STATUS, RP0
                MOVLW   0x007
                MOVWF   CMCON           ;SWITCH OFF ANALOGUE INPUTS
                BSF     STATUS,RP0      ;SELECT BANK 1
                MOVLW   b'100000'
                MOVWF   TRISA           ;RA5 INPUT
                MOVLW   b'11100000'     ;RB7..5 INPUTS
                MOVWF   TRISB
                MOVLW   0x000
                MOVWF   OPTION_REG      ;CLEAR OPTION REGISTER
                MOVWF   INTCON          ;DISABLE INTERRUPTS
                BCF     STATUS,RP0      ;SELECT BANK 0
;*****************************************
;MAIN PROGRAM
;*****************************************
MAIN            CLRF    TEMP0           ;CLEAR VARIABLES
                CLRF    TEMP1
                CLRF    TEMP2
                CLRF    delaycnt2
                CLRF    delaycnt
                GOTO    READPORT        ; READ FRENQUENCY SELECTION BITS
;*****************************************
;BASEDELAY - VALVE OPERATES BETWEEN 8.0 AND 6.45Hz
;A BASIC DELAY OF 0.0625002Hz BETWEEN ON AND OFF
;STATES GIVES f=8Hz. 1/(2*0.0625s) = 8Hz
;*****************************************
BASEDELAY       MOVLW   D'2'
                MOVWF   TEMP2
                MOVLW   D'151'
                MOVWF   TEMP1
                MOVLW   D'211'
                MOVWF   TEMP0
                DECFSZ  TEMP0, f
                GOTO    $-1
                DECFSZ  TEMP1, f
                GOTO    $-3
                DECFSZ  TEMP2, f
                GOTO    $-5
                RETURN
;*****************************************
;MOREDELAY - IN ORDER TO ACHIEVE LOWER FREQUENCIES
;MORE DELAY IS INTRODUCED AFTER THE BASEDELAY DEPENDING
;ON THE FREQUENCY CONFIGURATION BITS (TABLE 3.2 - CHAPTER 3)
;AN ADDITIONAL DELAY OF 0.0025006s FOR EACH ADDITIONAL BIT
;INCREASES THE PERIOD OF MODULATION BY 2*0.0025006s = 0.005012s
;THEREFORE DECREASING THE FREQUENCY OF MODULATION (f=1/T)
;*****************************************
MOREDELAY       MOVLW   D'17'
                MOVWF   TEMP1
                MOVLW   D'58'
                MOVWF   TEMP0
                DECFSZ  TEMP0, f
                GOTO    $-1
                DECFSZ  TEMP1, f
                GOTO    $-3
                RETURN

;*****************************************
;READPORT - READS PORTS RB7..RB5 WHICH ARE THE FREQUENCY
;CONFIGURATION BITS, SET BY THE MASTER MICROCONTROLLER
;AS IN TABLE 3.2, CHAPTER 3. THE PORT VALUE IS ROTATED
;FIVE TIMES TO BRING THE BITS IN THE LSB POSITIONS AND
;SUBSEQUENTLY LOADED ON A COUNTER WHICH ADDS EXTRA DELAY
;TO THE VALVE MODE (WHETHER ON OR OFF) BY CALLING FUNCTION
;MOREDELAY
;*****************************************
READPORT        MOVF    PORTB, W        ;COPY VALUE OF PORT B
                ANDLW   0xE0            ;KEEP THE THREE MSB
                MOVWF   delaycnt        ;COPY TO delaycnt
                RRF     delaycnt, f     ;ROTATE FIVE TIMES TO
                RRF     delaycnt, f     ;BRING THE THREE MSBs
                RRF     delaycnt, f     ;TO THE THREE LSBs
                RRF     delaycnt, f
                RRF     delaycnt, W
                ANDLW   0x07            ;DISCARD ANY CARRY BITS
                MOVWF   delaycnt        ;COPY VALUE TO delaycnt
                MOVWF   delaycnt2       ;AND TO delaycnt2
                BTFSC   delaycnt, 0     ;TEST LSB
                GOTO    SWITCHON        ;IF SET MEANS SWITCH ON VALVE
                BTFSC   delaycnt, 1     ;IF NOT SET, CHECK 2ND LSB
                GOTO    SWITCHON        ;IF SET, SWITCH ON VALVE
                BTFSC   delaycnt, 2     ;IN NOT SET, CHECK 3RD LSB
                GOTO    SWITCHON        ;IF SET SWITCH ON
                GOTO    READPORT        ;NONE IS SET, VALVE STAYS OFF

;*****************************************
;SWITCHON - SWITCHES ON THE VALVE AND KEEPS IT OPEN
;FOR t=BASEDELAY + (configuration_bits)*MOREDELAY
;IF configuration_bits=001 THEN f = 8Hz
;IF configuration_bits=111 THEN f = 6.45Hz
;*****************************************
SWITCHON        BSF     PORTB, 4        ;OPEN VALVE
                BSF     PORTA, 0        ;SWITCH ON LED
                CALL    BASEDELAY       ;WAIT 1*BASEDELAY
                DECFSZ  delaycnt, f     ;DECREASE THE COUNTER OF
                                        ;MOREDELAY
                CALL    MOREDELAY       ;AND CALL MOREDELAY

;*****************************************
;SWITCHON - SWITCHES OFF THE VALVE AND KEEPS IT CLOSED
;FOR t=BASEDELAY + (configuration_bits)*MOREDELAY
;IF configuration_bits=001 THEN f = 8Hz
;IF configuration_bits=111 THEN f = 6.45Hz
;*****************************************
SWITCHOFF       BCF     PORTB, 4        ;CLOSE VALVE
                BCF     PORTA, 0        ;SWITCH OFF LED
                CALL    BASEDELAY       ;WAIT 1*BASEDELAY
                DECFSZ  elaycnt2, f     ;DECREASE THE COUNTER OF
                                        ;DELAY
                CALL    MOREDELAY       ;CALL MOREDELAY
                GOTO    READPORT        ;CYCLE FINISHED, GO BACK AND ;
                                        ;CHECK CONFIGURATION BITS
END
```

Figure II.4 – Slave µController code

APPENDIX

III. ETHICAL APPROVALS

This appendix presents the letters which confirm that ethical approval has been obtained from the relevant Ethics Committees.

Leicestershire NHS
Health Authority

Melanie Sursham
Direct Dial 0116 258 8610

Gwendolen Road
Leicester
LE5 4QF

Tel: 0116 2731173
Fax: 0116 2588577
DX 709470 Leicester 12

10 September 2001

Mr T Spyt
Consultant Cardiothoracic Surgeon
Glenfield Hospital

19 SEP 2001

Dear Mr Spyt

Non Invasive Measurement of Changes in Peripheral Perfusion during Cardiac Surgery and its Relation to Cardiac Function – our ref no 6416

Further to your application dated 20 June, you will be pleased to know that the Leicestershire Research Ethics Committee at its meeting held on the 7 September 2001 approved your application to undertake the above-mentioned research.

The Committee wondered if patients would be randomised to either hypothermic or normothermic cardiopulmonary bypass. It was assumed that no randomisation was involved as there is no mention of it in the application or protocol.

The Committee felt that the patient information was too brief and should be revised to be more patient friendly and include more detail of the rationale, methods/design of the study. It was assumed that clinical management would be standard as for current practice. The collection of data was additional. 'Essentially' in question 2 should be removed. Perhaps you would let me have a revised information sheet for further consideration.

Your attention is drawn to the attached paper which reminds the researcher of information that needs to be observed when Ethics Committee approval is given.

Yours sincerely

P G Rabey
Chairman
Leicestershire Research Ethics Committee
(NB All communications relating to Leicestershire Research Ethics Committee must be sent to the Committee Secretariat at Leicestershire Health Authority. If, however, your original application was submitted through a Trust Research & Development Office, then any response or further correspondence must be submitted in the same way.)

Figure III.1 – Clinical feasibility study approval letter

Ref No: R07-P12

LOUGHBOROUGH UNIVERSITY
ETHICAL ADVISORY COMMITTEE

RESEARCH PROPOSAL
INVOLVING HUMAN PARTICIPANTS

Title: Assessment of peripheral venous oxygen changes during arterio-venous occlusion using new non-invasive oximetry system (Venox)

Applicant: Dr S Hu, Mr A Echiadis

Department: Electronic and Electrical Engineering

Date of clearance: 13 February 2007

Comments of the Committee:

The Committee agreed to issue clearance to proceed subject to the following conditions:

- The Committee expressed concern that the high level of arm cuff pressure to be applied could cause significant discomfort and bruising. The investigators were asked to provide additional information to justify the levels of pressure involved in the context of the research, and to establish that this was standard practice. The Committee noted also that participants would be unlikely to understand what "twice your arterial systolic blood pressure" actually meant in practice, and noted that the Participant Information sheet should be amended to explain this more clearly in layman's terms.
- That the investigators noted that the University's Code of Practice on Persons Having Contact with Human Body Fluids had been replaced with new Health and Safety Policies on Blood Borne Viruses and Pathogens (excluding Blood Borne Viruses). The new policies were available on the Committee's web-pages.
- That full contact details, including telephone numbers, of the investigators be included on the Participant Information Sheet.
- That question 4 of the Health Screen Questionnaire was removed, as it was intended for use in proposals which involved participants undertaking exercise and was not appropriate in this context.

Figure III.2 – Venous oxygen de-saturation study approval letter